

**BETWEEN ISLANDS: AN OVERVIEW OF
OBSIDIAN PATHS IN THE WESTERN
MEDITERRANEAN
(CORSICA, MIDDLE NEOLITHIC)**

MARIE ORANGE

M.Sc - Science applied to Archaeology

A thesis submitted in fulfilment of the requirements of the degree of
Doctor of Philosophy

Southern Cross GeoScience
Southern Cross University Lismore NSW Australia
6th of December 2016

Thesis Declaration

I certify that the work presented in this thesis is, to the best of my knowledge and belief, original, except as acknowledged in the text, and that the material has not been submitted, either in whole or in part, for a degree at this or any other university.

I acknowledge that I have read and understood the University's rules, requirements, procedures and policy relating to my higher degree research award and to my thesis. I certify that I have complied with the rules, requirements, procedures and policy of the University (as they may be from time to time).

Name: Marie Orange

Signature:

Date: 6th of December 2016

Abstract

This research project focuses on the reconstruction of obsidian economies in Middle Neolithic settlements (5th-4th millennium B.C.) from Corsica (Western Mediterranean area). Considered as a 'marker' of the Neolithisation process, this raw material allows direct insight into population movements and human contacts (exchange, trade patterns), technical know-how, and ultimately on the diffusion mode of cultural models. The present work follows a long tradition of obsidian sourcing studies while integrating the latest trends of the discipline adopted by our research group.

Relying on the exhaustive and non-destructive analysis of the obsidian assemblages, our approach allows the extraction of as much information as possible from the artefacts. Such a strategy depends on the combined use of several analytical techniques, such ED-XRF, pXRF, PIXE, SEM-EDS, and LA-ICP-MS to allow the geochemical characterisation of every artefact regardless of its size, shape, or surface state.

The outcomes of this research will provide new insights into local obsidian consumption patterns that will help deepen our understanding of the Neolithic communities of the Western Mediterranean area.

Acknowledgments

Personal acknowledgements

This project stems from the research initiated by the late **G rard Poupeau** in the 1990s and carried on by **Fran ois-Xavier Le Bourdonnec** at the IRAMAT-CRP2A. Embedded in different multidisciplinary research projects relying on strong international collaborations, the work presented here distils and furthers the research undertaken in the last 15 years, to add to our general knowledge of the Prehistoric communities in the Mediterranean area. I am very grateful to have been integrated as part of this diversified research group.

Among our collaborators I would like to thank **Ludovic Bellot-Gurlet**, **Carlo Lugli **, **Andr  D'Anna**, as well as **Jean-Michel Bontempi**, **C line Bressy-Leandri**, **St phan Dubernet**, **Fran oise Lorenzi**, **Sylvain Mazet**, **Henri Marchesi**, **Jos phine Tuquoi**, **Elsa Perruchini**, and **Pascal Tramoni**.

I am grateful to **Southern Cross University** and **Southern Cross GeoScience** for allowing me to undertake this postgraduate project. I am very thankful to have had the opportunity to work in such a privileged environment.

I am most indebted to my supervisors at Southern Cross University, **Renaud Joannes-Boyau** and **Anja Scheffers** for their priceless guidance and support along the way.

To the staff at Southern Cross GeoScience I would like to express my deepest gratitude for the warm welcome and the constant help through the years: **Laurel Giles**, **Ellen Moon**, **Mark Rosicky**, **Scott Johnston**, **Chrisy Clay**, **Matthew Tonge**, **Crystal Maher**, **Diane Fyfe**, **Nigel Dawson**, **Yen Lin Ho**, **Michelle Bush**, **Girish Choppala**, **Chamindra Vithana**, **Matt Veness**, **Andrew Rose**, **Ed Burton**, **Ros Hagan**, **Nadia**

Toppler, Nick Ward, and many others. The numerous morning cakes from Henry's are all the comfort a student needs... I am also grateful to **Hanabeth Luke** for providing me with the opportunity to further my teaching experience through the Science in Society unit.

To the students at SCGS, thank you for your friendship and your help in time of need. I especially want to express my gratitude to **Niloofar Karimian, Hanieh Tohidi-Farid, Stan Kinis**, and **Sai Na**, as well as **Valerie Schoepfer** for her many revisions of my papers, and **Jonathan Avaro** for his constant help.

To the staff of the School of Environment, Science, and Engineering, I would like to thank **Lachlan Yee** for giving me the opportunity to help with the Chemistry unit and for the precious life advices, **Maxine Dawes** for her help with the SEM-EDS, **Debra Stokes** for the obsidian samples, and also **Paul Kelly, Malcolm Clark, John Arthur**, and **Barbara Harrison**.

I am most grateful to **Pierre Guibert**, former director of the IRAMAT-CRP2A, for welcoming me several times in his research centre. Amongst the CRP2A staff I would like to express my gratitude to **Yannick Lefrais** for his help with the SEM-EDS, **Brigitte Spiteri** for her precious help with the geological sample preparation, as well as to **Claude Ney, Pierre Selva**, and **Pierre Machut** for their support.

I would also like to thank **Tristan Carter** from the McMaster University in Hamilton (Canada) for passing on his passion for archaeology, his mentorship during my masters' degree as well as for the opportunities he created for me.

A heartfelt thanks to **Frédéric Abbès** for his precious support since my masters' degree and along the way, as a mentor and as a friend. The times spent at Jalès were deeply inspiring.

For giving me the passion of obsidian, his constant help, support, energy, and friendship, I would like to express my deepest gratitude to **François-Xavier Le Bourdonnec**. As my mentor and external supervisor of this Ph.D. he kept me on the right path and helped me get where I am today. For that I will always be in his debt.

To my family and friends, thank you for your kindness, help, and encouragements. I could not have done it without all of you. A special thanks to my dear friends **Laurel**, **Ellen**, and **Ruth** for helping me make it to the finish line.

My deepest gratitude finally goes to my mum **Sylvie**, and my husband **Trent**, for always loving me and supporting me through thick and thin.

Funding acknowledgements

This Ph.D. project was funded by a Postgraduate scholarship supported by Southern Cross University as well as an Australian Research Council discovery grant [DP140100919]. It was also supported by Southern Cross GeoScience.

Part of this project has been financially supported by the Conseil Régional d'Aquitaine, the ANR (French National Research Agency; n°ANR-10-LABX-52), and the Université Bordeaux Montaigne PSE (Politique Scientifique d'Établissement). Part of the PIXE measures at AGLAE were funded by the Eu-Artech (ref. 06-05) and Charisma (ref 10-21) European programs.

List of publications included in the thesis

The publications included as part of this thesis are fully integrated to the manuscript as per the guidelines provided by Southern Cross University. The publications already available online have also been included in their final form in Appendices K and L.

Orange, M., Le Bourdonnec, F.-X., Bellot-Gurlet, L. *in press* 1. Obsidian provenance analysis in Archaeology: 50 years of methodological developments. In: Chapoulie, R., Sepulveda, M., Wright, V. (Eds.), *Manual de Arqueometria*. IFEA editions, Lima, Peru.

Orange, M., Le Bourdonnec, F.-X., Bellot-Gurlet, L., Lugliè, C., Dubernet, S., Bressy-Leandri, C., Scheffers, A., Joannes-Boyau, R., *in press* 2. On sourcing obsidian assemblages from the Mediterranean area: analytical strategies for their exhaustive geochemical characterisation, *Journal of Archaeological Science: Reports*.

See Appendix K.

Orange, M., Le Bourdonnec, F.-X., Scheffers, A., Joannes-Boyau, R. 2016. Sourcing obsidian: a new optimized LA-ICP-MS protocol. *Science and Technology of Archaeological Research*, 2(2), 192-202.

See Appendix L.

Orange, M., Le Bourdonnec, F.-X., D'Anna, A., Tramoni, P., Lugliè, C., Bellot-Gurlet, L., Scheffers, A., Marchesi, H., Guendon, J.-L., Joannes-Boyau, R. *submitted for publication* (journal *Geoarchaeology*). Obsidian economy on the Cauria plateau (South Corsica, Middle Neolithic): new evidence from Renaghju and I Stantari.

Contribution statements

Conception and design MO (85 %), FXLB (10 %), RJB (5 %), AS (5 %)

Analyses MO (85 %), FXLB (15 %)

Data processing and interpretation MO (90 %), FXLB (5 %), LBG (3 %), RJB (2 %)

Thesis writing MO (100 %)

Publication writing MO (80 %), FXLB (3 %), LBG (3 %), CL (3 %), ADA (3 %), RJB (2 %), SD (1 %), CBL (1 %), PT (1 %), HM (1 %), JLG (1 %), AS (1 %)

MO (Marie Orange), RJB (Renaud Joannes-Boyau), AS (Anja Scheffers), FXLB (François-Xavier Le Bourdonnec), LBG (Ludovic Bellor-Gurlet), CL (Carlo Lugliè), ADA (André D'Anna), SD (Stéphan Dubernet), CBL (Céline Bressy-Leandri), PT (Pascal Tramoni), HM (Henri Marchesi), JLG (Jean-Louis Guendon).

Authors' declarations

I, Marie Orange, the author of this thesis, certify that the contributors and conflicts of interest statements included in this thesis are correct and have been approved by all contributors.

Marie Orange

Signature:

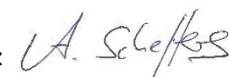


Date: 15/07/16

I agree with the contents of the thesis, to be listed as a contributor, and to the conflicts of interest statements included in this thesis. I have had access to all the data in this study and accept responsibility for its validity.

Pr. Anja Scheffers

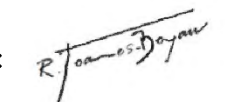
Signature:



Date: 15/07/16

Dr. Renaud Joannes-Boyau

Signature:



Date: 15/07/16

A/Pr. François-Xavier Le Bourdonnec

Signature:



Date: 15/07/16

Signed statements from each of the following contributors are included in Appendix A:

Pr. Ludovic Bellot-Gurlet (LBG)

A/Pr. Carlo Lugliè (CL)

Dr. Stéphan Dubernet (SD)

Dr. André D'Anna (ADA)

Mr. Pascal Tramoni (PT)

Dr. Céline Bressy-Leandri (CBL)

Mr. Henri Marchesi (HM)

Dr. Jean-Louis Guendon (JLG)

Table of Contents

<i>Thesis Declaration</i>	<i>I</i>
<i>Abstract</i>	<i>III</i>
<i>Personal Acknowledgments</i>	<i>V</i>
<i>Funding Acknowledgments</i>	<i>VII</i>
<i>List of publications included in the thesis</i>	<i>IX</i>
<i>Contribution statements</i>	<i>XI</i>
<i>Authors' declarations</i>	<i>XIII</i>
<i>List of Abbreviations</i>	<i>vii</i>
<i>List of Figures</i>	<i>xi</i>
<i>List of Tables</i>	<i>xxi</i>
<i>List of Appendices</i>	<i>xxv</i>
<i>Foreword</i>	<i>1</i>
<i>References</i>	<i>199</i>
<i>Appendices</i>	<i>233</i>
PART I – Obsidian sourcing in the Western Mediterranean: an overview	5
Chapter 1: Introduction	7
1.1. General framework.....	7
1.2. Research problem investigated.....	11
1.3. Overall objective and aims of the research.....	14
1.4. Research design.....	15
1.5. Research limitations.....	17

Chapter 2: Background and research context.....	19
2.1. Obsidian, an ‘ideal’ material for sourcing studies.....	19
2.2. Geochemistry of obsidian.....	20
2.3. Significance of provenance studies and concept of ‘source’.....	22
2.3.1. The significance of provenance studies.....	22
2.3.2. The concept of ‘source’.....	24
2.4. Obsidian sources in the Western Mediterranean.....	25
2.4.1. Sardinia.....	27
2.4.2. Lipari.....	29
2.4.3. Palmarola.....	30
2.4.4. Pantelleria.....	31
2.5. Obsidian diffusion in the Western Mediterranean during the Neolithic: current state of the research.....	33
2.5.1. The Western Mediterranean context.....	33
2.5.2. Sardinia and Corsica.....	35
2.6. Research projects and collaborations.....	37
2.6.1. The Cauria plateau, Corsica: Renaghju and I Stantari.....	39
2.6.2. The Abri des Castelli.....	44
2.6.3. A Guaita.....	45
Chapter 3: A long tradition of obsidian sourcing: review of the literature.....	49
3.1. The beginning of a discipline.....	49
3.2. On the road to success: an expanding range of methods.....	52
3.3. Searching for alternative methods.....	54
3.4. Towards new analytical strategies.....	55
PART II – Towards an exhaustive characterisation of obsidian assemblages: analytical strategies and enhanced protocols.....	59

Chapter 4: Analytical strategies 61

On sourcing obsidian assemblages from the Mediterranean area: analytical strategies for their exhaustive geochemical characterisation 63

4.1. Introduction..... 65

4.2. Geographical and Archaeological framework 66

4.3. Methods available within our research group 69

 4.3.1. Visual characterisation 69

 4.3.2. SEM-EDS 70

 4.3.3. Bench top ED-XRF 75

 4.3.4. Portable XRF 78

 4.3.5. IBA-PIXE 81

 4.3.6. LA-ICP-MS 86

4.4. Discussion 90

4.5. Conclusions..... 94

Chapter 5: Improving LA-ICP-MS protocol for obsidian sourcing studies 99

Sourcing obsidian: a new optimised LA-ICP-MS protocol..... 101

5.1. Introduction..... 103

5.2. Instrumentation and protocols 105

 5.2.1. Instrumentation..... 105

 5.2.2. V1 and V2 protocols..... 105

 5.2.3. Laser ablation parameters..... 107

5.3. Results and discussion 108

 5.3.1. Sensitivity: V1 vs. V2 protocol..... 108

 5.3.2. Reliability of the V2 protocol 109

 5.3.3. Application to obsidian sourcing studies in the Western Mediterranean 116

5.4. Conclusions..... 123

**PART III – Archaeological challenges in the Western Mediterranean:
application of the analytical strategies in Neolithic Corsica 127**

Chapter 6: The Cauria plateau.....129

Obsidian economy on the Cauria plateau (South Corsica, Middle Neolithic): new evidence from Renaghju and I Stantari 131

6.1. Archaeological background and lithic industries 135

6.1.1. The Cauria plateau 135

6.1.2. Renaghju 139

6.1.3. I Stantari..... 143

6.2. Obsidian sourcing 149

6.2.1. Analytical protocols and sampling..... 149

6.2.2. Sourcing results..... 152

6.3. Outcomes, Discussion, and Conclusions 156

Chapter 7: The Abri des Castelli site.....165

7.1. The Abri des Castelli site: context and lithic industries 165

7.1.1. General context 165

7.1.2. Lithic industries..... 167

7.2. Sourcing obsidian from the Castelli shelter: previous analyses and analytical strategy 170

7.2.1. Previous sourcing campaigns..... 170

7.2.2. Analytical strategy..... 170

7.3. ED-XRF analyses..... 171

7.3.1. Protocol..... 171

7.3.2. Results 171

7.4. LA-ICP-MS analyses 173

7.4.1. Protocol..... 173

7.4.2. Results	173
7.5. Discussion and conclusions	175
7.5.1. General obsidian economy of the site.....	175
7.5.2. Comparison between the 5 th and 4 th millenia B.C.	176
7.5.3. Comparison with the obsidian economy of other archaeological sites	178
7.6. Further studies.....	179
Chapter 8: A Guaita.....	181
8.1. The A Guaita archaeological site.....	181
8.1.1. General context	181
8.1.2. Lithic industries.....	183
8.2. Sourcing obsidian from A Guaita: previous analyses and analytical strategy... 184	
8.2.1. Previous sourcing campaigns	184
8.2.2. Analytical strategy.....	185
8.3. ED-XRF analyses.....	186
8.3.1. Protocol.....	186
8.3.2. Results	186
8.4. LA-ICP-MS analyses	188
8.4.1. Protocol.....	188
8.4.2. Results	188
8.5. Discussion and conclusions	190
General conclusions	193

List of Abbreviations

AGLAE	Accélérateur Grand Louvre d'Analyses Elémentaires
AIFIRA	Applications Interdisciplinaires de Faisceaux d'Ions en Région Aquitaine
alr	Additive log-ratio transformation
ANR	Agence Nationale de la Recherche
ARC	Australian Research Council
B.C.	Before Christ
BCR	Basalt, Columbia River
B.P.	Before Present
C2RMF	Centre de Recherche et de Restauration des Musées de France
CEA	Commissariat à l'Énergie Atomique
CENBG	Centre Etudes Nucléaires de Bordeaux Gradignan
CEPAM	Cultures et Environnements Préhistoire, Antiquité, Moyen Âge
clr	Centred log-ratio transformation
CNRS	Centre National de la Recherche Scientifique (France)
CRA	Conseil Régional d'Aquitaine
ED-XRF	Energy Dispersive – X-Ray Fluorescence
EN	Early Neolithic

ESI	Electro Scientific Industries, Inc.
ESRI	Environmental Systems Research Institute, Inc.
GeoRem	Geochemical and Environmental Reference Materials
IBA	Ion Beam Analysis
IFEA	Instituto Francés de Estudios Andinos
IRAMAT-CRP2A	Institut de recherche sur les Archéomatériaux – Centre de Recherche en Physique Appliquée à l’Archéologie
LabEx	Laboratoire d’Excellence
LA-ICP-MS	Laser Ablation – Inductively Coupled Plasma – Mass Spectrometry
LAPA	Laboratoire Archéomatériaux et Prévision de l’Altération
LaScArBx	LabEx Sciences Archéologiques de Bordeaux
LN	Late Neolithic
MN	Middle Neolithic
Nd:YAG	Neodymium-doped Yttrium Aluminium Garnet
NIST	National Institute of Standards and Technology
NOAA	National Oceanic & Atmospheric Administration
PCR	Project Collectif de Recherche
PIGE/PIGME	Particle Induced Gamma-Ray Emission
PIXE	Particle Induced X-Ray Emission

pXRF	portable X-Ray Fluorescence
RGM	Rhyolite, Glass Mountain
SAS	Statistical Analysis Software, Inc.
SCGS	Southern Cross GeoScience
SCU	Southern Cross University
SDD	Silicon Drift Detector
SEM-EDS	Scanning Electron Microscope – Energy Dispersive Spectrometry
SOLARIS	Southern CrOss Laser-Ablation Research InStrument
SQUID	Superconducting QUantum Interference Device
UMR	Unité Mixte de Recherche
USGS	United States Geological Survey

List of Figures

Chapter 1

- Figure 1.1.** Operational sequence, or *chaîne opératoire* - conceptual representation. Adapted from Tykot, 2002a..... 9
- Figure 1.2.** Foliated piece, Sardinian obsidian, Final Neolithic (4th millennium B.C.). Photography: courtesy of Carlo Lugliè.....9
- Figure 1.3.** Map indicating the location of the main obsidian sources of the Western Mediterranean area, the archaeological settlements studied in this research project (Renaghju, I Stantari, Abri des Castelli, and A Guaita), and other archaeological sites mentioned in the text. Maps created with ArcGIS® software by Esri. ArcGIS® and ArcMap™ are the intellectual property of Esri and are used herein under license. Copyright © Esri. All rights reserved. For more information about Esri® software, please visit www.esri.com. Sources: Esri, USGS, NOAA13

Chapter 2

- Figure 2.1.** Map showing the location of the main obsidian sources of the peri-Mediterranean area 25
- Figure 2.2.** Location of the Sardinian obsidian source of the Monte Arci (left) and detail of the SA, SB1, SB2, and SC obsidian flows (right). Adapted from Lugliè *et al.*, 2006..... 28
- Figure 2.3.** Map of the Lipari island, indicating the location of the main obsidian outcrops (*Acquacalda, Roche Rosse, Gabelotto, and Forgia Vecchia*). Adapted from Pichler, 1980... 30

Figure 2.4. Map of the Palmarola island, indicating the location of the main obsidian outcrops (*Monte Tramontana, San Silverio, Punta Vardella*). Adapted from Tykot *et al.*, 2005 and Cadoux *et al.*, 200531

Figure 2.5. Map of the Pantelleria island, indicating the location of the main obsidian outcrops (*Lago di Venere, Gelkhamar, Grotta Fromaggio, Salto de la Vecchia, and Balata dei Turchi*). Adapted from Civetta *et al.*, 198432

Figure 2.6. Statue-menhirs of I Stantari (from left to right: M5, M4, M2, and M1). ©A. D’Anna. D’Anna, 201340

Figure 2.7. The Abri des Castelli site. ©S. Mazet. Mazet, Dir., 201144

Chapter 4

Figure 4.1. Map of the main obsidian sources of the Western Mediterranean and Aegean areas: Sardinia (Monte Arci: SA, SB1, SB2, SC), Pantelleria (Balata dei Turchi, Lago di Venere), Lipari, Palmarola, Melos, and Yali.....67

Figure 4.2. Comparison of the $\log(\text{SiO}_2/\text{Al}_2\text{O}_3)$ and $\log(\text{CaO}/\text{Al}_2\text{O}_3)$ ratios obtained by SEM-EDS (IRAMAT-CRP2A) for 175 geological samples from the Mediterranean area (90 % density ellipses). Analyses conducted at the IRAMAT-CRP2A (France); see Le Bourdonnec *et al.*, 201072

Figure 4.3. Discriminant analysis achieved with the JMP software (SAS Inc. 2012) after additive log-ratio (alr) transformation of the Na_2O , Al_2O_3 , SiO_2 , K_2O , and CaO contents (common denominator for alr: Fe_2O_3) obtained by SEM-EDS on 80 geological samples from the Monte Arci (SA, SB1, SB2 and SC subtypes). The ellipses represent the 95 % confidence region to contain the true mean of each geological sample group. $F1 = - 2.035 \text{Na}_2\text{O} - 80.102 \text{Al}_2\text{O}_3 + 93.578 \text{SiO}_2 - 3.356 \text{K}_2\text{O} - 5.864 \text{CaO}$; $F2 = 46.597 \text{Na}_2\text{O} -$

118.527 Al₂O₃ - 3.385 SiO₂ + 72.787 K₂O + 10.778 CaO. Analyses conducted at the IRAMAT-CRP2A (France); see Le Bourdonnec *et al.*, 2010 73

Figure 4.4. Discriminant analysis achieved with the JMP software (SAS Inc. 2012) after alr transformation of the Na₂O, Al₂O₃, SiO₂, K₂O, and CaO contents (common denominator for alr: Fe₂O₃) obtained by SEM-EDS on 80 geological samples from the Monte Arci [SA, SB1, SB2 and SC subtypes] (Le Bourdonnec *et al.*, 2010) and 223 archaeological samples from Neolithic sites situated in Corsica (Le Bourdonnec *et al.*, 2006, 2010, 2014, 2015b, and unpublished data). The ellipses represent the 95 % confidence region containing the true mean of each geological sample group. F1 = - 2.035 Na₂O – 80.102 Al₂O₃+ 93.578 SiO₂ – 3.356 K₂O – 5.864 CaO; F2 = 46.597 Na₂O – 118.527 Al₂O₃ - 3.385 SiO₂ + 72.787 K₂O + 10.778 CaO. Analyses conducted at the IRAMAT-CRP2A (France)..... 74

Figure 4.5. Principal Component Analysis conducted with the JMP software (SAS Inc. 2012) after clr transformation of the MnO, Fe₂O₃, Zn, Ga, Rb, Sr, Y, and Zr contents obtained by ED-XRF (IRAMAT-CRP2A) on 24 geological samples from the Western Mediterranean area. 99 % density ellipses. Data published in Lugliè *et al.*, 2014, and unpublished data 76

Figure 4.6. Principal Component Analysis conducted with the JMP software (SAS Inc. 2012) after clr transformation of the MnO, Fe₂O₃, Zn, Ga, Rb, Sr, Y, and Zr contents obtained by ED-XRF (IRAMAT-CRP2A) on 24 geological samples (Western Mediterranean) and 703 archaeological samples (from Corsica, Sardinia, Southern France, and Northern Italy; Neolithic period). 99 % density ellipses. Data published in Lugliè *et al.*, 2014, and unpublished data 77

Figure 4.7. Comparison of the log(Zn/Sr) and log(Rb/Sr) ratios obtained by pXRF for 41 geological samples from the Western Mediterranean area. 99 % density ellipses. Non-destructive analysis conducted with a Niton XL3 Series analyser pXRF (RX tube: 50 kV;

detector: Si-PIN), as part of the program-test LAPA (CEA/CNRS-IRAMAT UMR 5060 CNRS). Data published in Le Bourdonnec *et al.*, 2015b79

Figure 4.8. Comparison of the $\log(\text{Zn}/\text{Sr})$ and $\log(\text{Rb}/\text{Sr})$ ratios obtained by pXRF for 41 geological samples from the Western Mediterranean area (Le Bourdonnec *et al.*, 2015b) and 343 archaeological samples from Corsica (unpublished data). 99 % density ellipses. Non-destructive analysis conducted with a Niton XL3 Series analyser pXRF (RX tube: 50 kV; detector: Si-PIN), as part of the program-test LAPA (CEA/CNRS-IRAMAT UMR 5060 CNRS)80

Figure 4.9. Comparison of the $\log(\text{Rb}/\text{Zn})$ and $\log(\text{MnO}/\text{Zn})$ ratios obtained by PIXE (CENBG, AIFIRA) for 55 geological samples from the Western Mediterranean area (see Lugliè *et al.*, 2007, 2008a, 2009; Mulazzani *et al.*, 2010; Poupeau *et al.*, 2000). 99 % density ellipses. Data published in Lugliè *et al.*, 2007, 2008a, 2009; Mulazzani *et al.*, 2010; Poupeau *et al.*, 200082

Figure 4.10. Comparison of the $\log(\text{Rb}/\text{Zr})$ and $\log(\text{Zn}/\text{Zr})$ ratios obtained by PIXE (CENBG, AIFIRA) for 44 geological samples from the Western Mediterranean area; focus on the sources of Sardinia (Monte Arci: SA, SB1, SB2, SC), Lipari, and Palmarola. 99 % density ellipses. Data published in Lugliè *et al.*, 2007, 2008a, 2009; Mulazzani *et al.*, 2010; Poupeau *et al.*, 200083

Figure 4.11. Comparison of the $\log(\text{Rb}/\text{Zn})$ and $\log(\text{MnO}/\text{Zn})$ ratios obtained by PIXE (CENBG, AIFIRA) for 55 geological samples from the Western Mediterranean area (see Lugliè *et al.*, 2007, 2008a, 2009; Mulazzani *et al.*, 2010; Poupeau *et al.*, 2000) and 675 archaeological samples from Sardinia, Southern France, Corsica, and Tunisia. 99 % density ellipses. Bressy *et al.*, 2008; Le Bourdonnec, 2007; Le Bourdonnec *et al.*, 2010, 2015a, 2015b; Lugliè *et al.*, 2007, 2008b, 2008a, 2009; Poupeau *et al.*, 2000; and unpublished data.84

Figure 4.12. Comparison of the $\log(\text{Rb}/\text{Zr})$ and $\log(\text{Zn}/\text{Zr})$ ratios obtained by PIXE (CENBG, AIFIRA) for 44 geological samples (99 % density ellipses) (Lugliè *et al.*, 2007, 2008a, 2009 ; Poupeau *et al.*, 2000) and 626 archaeological samples (Bressy *et al.*, 2008; Le Bourdonnec 2007; Le Bourdonnec *et al.*, 2010, 2015b; Lugliè *et al.*, 2007, 2008b, 2008a, 2009; Poupeau *et al.*, 2000 and unpublished data) 85

Figure 4.13. Comparison of the $\log(^{133}\text{Cs}/^{93}\text{Nb})$ and $\log(^{88}\text{Sr}/^{93}\text{Nb})$ ratios obtained by LA-ICP-MS (SOLARIS, SCU) for 175 geological samples from the Western Mediterranean and the Aegean area. 99 % density ellipses. Orange *et al.*, 2016 (**Chapter 5**) 88

Figure 4.14. Comparison of the $\log(^{133}\text{Cs}/^{93}\text{Nb})$ and $\log(^{88}\text{Sr}/^{93}\text{Nb})$ ratios obtained by LA-ICP-MS (SOLARIS, SCU) for 175 geological samples from the Western Mediterranean and the Aegean area (Orange *et al.*, 2016 [**Chapter 5**]) and 538 archaeological samples (Neolithic levels, Corsica). 99 % density ellipses 89

Figure 4.15. Concept and unfolding of the analytical strategy for obsidian sourcing studies 91

Chapter 5

Figure 5.1. Evolution of the ^{66}Zn , ^{88}Sr , ^{133}Cs , ^{137}Ba and ^{146}Nd contents on the NIST SRM 613 international standard over 5 months (23 measures represented). Data obtained by LA-ICP-MS with V2 protocol. The dotted lines represent the $\pm 2\sigma$ dispersion114

Figure 5.2. Map of the main obsidian sources in the Mediterranean area: Monte Arci (Sardinia), Lipari, Palmarola, Pantelleria, Yali, Melos, Antiparos, and the Carpathians .117

Figure 5.3. Comparison of $\log(^{133}\text{Cs}/^{93}\text{Nb})$ and the $\log(^{88}\text{Sr}/^{93}\text{Nb})$ ratios obtained by LA-ICP-MS (V2 protocol) on 200 geological samples from the Mediterranean region118

Figure 5.4. Comparison of $\log(^{133}\text{Cs}/^{93}\text{Nb})$ and the $\log(^{88}\text{Sr}/^{93}\text{Nb})$ ratios obtained by LA-ICP-MS (V2 protocol) on 200 geological samples from the Mediterranean region and 538 Neolithic archaeological samples from the Tyrrhenian area..... 119

Figure 5.5. Dispersion of measurements for the ^{88}Sr and ^{93}Nb isotopes for the SA (n=21), SB1 (n=17), SB2 (n=18), and SC (n=26) obsidian source samples (Sardinia): comparison between exhaustive (V1) and optimized (V2) protocols. For each protocol and each source, the boxplot summarizes the minimum and maximum values (whiskers), the 25 and 75 % quantiles (lower and upper limits of the boxplot) and the median value (central line within the boxplot)..... 120

Chapter 6

Figure 6.1. Stone alignments of the Renaghju (left) and I Stantari (right) sites 134

Figure 6.2. General map of the Mediterranean area displaying the main obsidian sources of the Western Mediterranean (Monte Arci [SA, SB1, SB2, SC], Lipari, Palmarola, Pantelleria) and the Aegean (Melos, Yali, Antiparos) 135

Figure 6.3. Location of the Cauria plateau and the main archaeological sites cited in the text 136

Figure 6.4. Stratigraphic profiles #3, #1, and #18 of the Renaghju archaeological site.. 140

Figure 6.5. Renaghju, Neolithic monument: spatial distribution of the menhirs (upright and lying), stone slabs, and gabbro blocks 142

Figure 6.6. Ceramics from Corsica – Middle Neolithic I (Curasian, punched, Bonuighinu). 1: Renaghju, Sartene, Cauria plateau. 2: Lecci, San Ciprianu. 3-6: Murtuli, Sartene. Drawings by Pascal Tramoni..... 143

Figure 6.7. Examples of obsidian artefacts from the Renaghju phase 3 and I Stantari assemblages.....	144
Figure 6.8. Stratigraphic profiles of the I Stantari site. A: Profile #6 (2002), West-East, H to N, 15 to 16. B: Profile #8 (2005), South-North, M to N, 3 to 10. C: Profile #9 (2003, 2007), K to P, 19 to 20	146
Figure 6.9. I Stantari-Stazzona structure: general disposition of the monoliths (left). I Stantari, Neolithic monument: spatial distribution of the monoliths (right)	147
Figure 6.10. Comparison of the $\log(^{133}\text{Cs}/^{93}\text{Nb})$ and $\log(^{90}\text{Zr}/^{93}\text{Nb})$ ratios obtained by LA-ICP-MS on 111 artefacts from the Renaghju phase 3 (MN) assemblage and 200 geological samples from the Mediterranean area (Monte Arci [SA, SB1, SB2, SC], Lipari, Palmarola, Melos, Yali, and Antiparos). 90 % normal density ellipses. For reasons of clarity, the sources of Pantelleria (Balata dei Turchi and Lago di Venere) and the Carpathians are not represented in the graph	154
Figure 6.11. Comparison of the $\log(^{133}\text{Cs}/^{93}\text{Nb})$ and $\log(^{90}\text{Zr}/^{93}\text{Nb})$ ratios obtained by LA-ICP-MS on 95 artefacts from the I Stantari phase 1 (MN) assemblage and 200 geological samples from the Mediterranean area (Monte Arci [SA, SB1, SB2, SC], Lipari, Palmarola, Melos, Yali, and Antiparos). 90 % normal density ellipses. For reasons of clarity, the sources of Pantelleria (Balata dei Turchi and Lago di Venere) and the Carpathians are not represented in the graph	156
Figure 6.12. Bar charts (100 % stacked columns) comparing the obsidian consumption revealed at Renaghju phase 1 (EN), Renaghju phase 3 (MN), and I Stantari phase 1 (MN). N/A: artefacts non-attributed to a specific obsidian source.....	160

Chapter 7

Figure 7.1. The Abri des Castelli – view from the north-east. ©N. Marini. Mazet, Dir. 2011..... 165

Figure 7.2. The Castelli plateau – view from the south-west. ©S. Mazet. Mazet, Dir. 2011 166

Figure 7.3. Stratigraphy of the Abri des Castelli site. Southwest-Northeast cross-section (left) and Northwest-Southeast cross-section (right). Source: Mazet, Dir., 2011 168

Figure 7.4. Comparison of the $\log(\text{Sr}/\text{Rb})$ and $\log(\text{Zn}/\text{Rb})$ ratios obtained by ED-XRF on 114 artefacts from the Abri des Castelli site and 24 geological samples from the Western Mediterranean area (Sardinia [SA, SB1, SB2, SC], Lipari, and Palmarola) 172

Figure 7.5. Comparison of the $\log(^{133}\text{Cs}/^{93}\text{Nb})$ and $\log(^{88}\text{Sr}/^{93}\text{Nb})$ ratios obtained by LA-ICP-MS on 328 artefacts from the Abri des Castelli site and 153 geological samples from the Mediterranean area (Sardinia [SA, SB1, SB2, SC], Lipari, Palmarola, Melos, Yali, Antiparos, and the Carpathian sources). For reasons of clarity, the sources of Pantelleria (Balata dei Turchi and Lago di Venere) are not represented..... 174

Figure 7.6. Obsidian source proportions per occupation period at the Abri des Castelli site. N/A indicates the percentage of artefacts that we were not able to attribute with the characterisation methods applied 178

Chapter 8

Figure 8.1. View of the A Guaita site from Centuri (Cap Corse). The arrow indicates the location of the upper terrace of the site. ©F. Lorenzi. Adapted from Lorenzi, 2011a 181

Figure 8.2. *Ceramica cardiale* (1-4) and *ceramica a line incise* (5, 6) elements from the A Guaita site. Technical drawing by F. Lorenzi. Adapted from Lorenzi, 2011b.....183

Figure 8.3. Obsidian borer from the A Guaita site: photography (left) and technical drawing (centre). Obsidian armature *à tranchant transversal* (right). Photography: ©N. Mattei – from Lorenzi, 2011a. Drawing by F. Lorenzi, from Lorenzi, 2011b.....184

Figure 8.4. Comparison of the $\log(\text{Sr/Rb})$ and $\log(\text{Zn/Rb})$ ratios obtained by ED-XRF on 161 artefacts from A Guaita and 24 geological samples from the Western Mediterranean area (Sardinia [SA, SB1, SB2, SC], Lipari, and Palmarola).....187

Figure 8.5. Comparison of the $\log(^{133}\text{Cs}/^{93}\text{Nb})$ and $\log(^{88}\text{Sr}/^{93}\text{Nb})$ ratios obtained by LA-ICP-MS on 4 artefacts from A Guaita and 153 geological samples from the Mediterranean area (Sardinia [SA, SB1, SB2, SC], Lipari, Palmarola, Melos, Yali, Antiparos, and the Carpathian sources). For reasons of clarity, the sources of Pantelleria (Balata dei Turchi and Lago di Venere) are not represented189

Figure 8.6. Obsidian source proportions at A Guaita. N/A indicates the percentage of artefacts that we were not able to attribute with the characterisation methods applied...191

List of Tables

Chapter 2

Table 2.1. Summary of the main obsidian sources and outcrops of the Western Mediterranean area and their denomination..... 26

Table 2.2. Synoptic description of the SA, SB1, SB2, and SC Sardinian obsidian types. Table adapted from Tykot, 1996..... 27

Chapter 3

Table 3.1. Summary of the main characterisation and dating methods applied to the obsidian material 51

Chapter 4

Table 4.1. Summary table relating the number of archaeological samples (artefacts) analysed with each sourcing method available within our research group, *i.e.* visual characterisation, SEM-EDS, ED-XRF, pXRF, PIXE, and LA-ICP-MS..... 93

Chapter 5

Table 5.1. LA-ICP-MS instrumental parameters for the V1 and V2 protocols 106

Table 5.2. Comparison of the raw counts and sensitivity results for ^{66}Zn , ^{85}Rb , ^{88}Sr , ^{89}Y , ^{90}Zr , ^{93}Nb , ^{133}Cs , ^{137}Ba , ^{146}Nd , ^{147}Sm , ^{208}Pb , ^{232}Th , and ^{238}U between the V1 and V2

protocols. Certified concentrations: GeoRem. The number of rows [Nb rows] indicates the number of measurements obtained within a single ablation line, after statistical treatment with removal of the outliers with JMP statistical software (SAS)..... 109

Table 5.3. Comparison of the ^{45}Sc , ^{66}Zn , ^{85}Rb , ^{88}Sr , ^{89}Y , ^{90}Zr , ^{93}Nb , ^{133}Cs , ^{137}Ba , ^{146}Nd , ^{147}Sm , ^{208}Pb , ^{232}Th , and ^{238}U contents with uncertainty (± 1 standard deviation) obtained on the NIST SRM 613 standard between the V2 protocol (total number of measurements = 50) and the reference values recommended by the NIST and the GeoRem database. The concentrations obtained for each isotope (with the exception of ^{45}Sc , unassessed with the V1 protocol) and corresponding relative error are also compared between the V1 and V2 protocol for the same number of measurements (n=8). Relative error (Rel. err.) calculated in comparison with the GeoRem reference values. Concentrations (Conc.) are in ppm 111

Table 5.4. Comparison of the standard error of the mean (Std. err. mean) obtained on the NIST SRM 613 international standard for the 13 isotopes common to the V1 and V2 protocols (^{66}Zn , ^{85}Rb , ^{88}Sr , ^{89}Y , ^{90}Zr , ^{93}Nb , ^{133}Cs , ^{137}Ba , ^{146}Nd , ^{147}Sm , ^{208}Pb , ^{232}Th , and ^{238}U). Average contents (Ave.) and standard deviations (Std. dev.) obtained on 8 measurements. Contents are in ppm..... 113

Table 5.5. Comparison of the ^{45}Sc , ^{66}Zn , ^{85}Rb , ^{88}Sr , ^{89}Y , ^{90}Zr , ^{93}Nb , ^{133}Cs , ^{137}Ba , ^{146}Nd , ^{147}Sm , ^{208}Pb , ^{232}Th , and ^{238}U contents and uncertainties (± 1 standard deviation) obtained on basalt USGS standard BCR-2G (glass) in a previous LA-ICP-MS study (Barca *et al.*, 2007), this study, and the reference values recommended by the USGS and the GeoRem database. The relative error (Rel. error) is calculated in comparison with reference values of the GeoRem database. In bold: isotopes for which this study achieves a higher accuracy compared to a previous LA-ICP-MS study (Barca *et al.*, 2007). Contents are in ppm..... 115

Table 5.6. Comparison of the average ^{85}Rb , ^{88}Sr , ^{89}Y , ^{90}Zr , ^{93}Nb , and ^{137}Ba contents and uncertainties (± 1 standard deviation) for the SA, SB1, SB2, and SC sub-types obtained in this study and previous studies (Tykot, 1995, Barca *et al.*, 2007, De Francesco *et al.*, 2008, Le Bourdonnec *et al.*, 2011). Contents are in ppm..... 122

Chapter 6

Table 6.1. Ablation parameters adopted for the LA-ICP-MS analyses conducted on the archaeological samples at SOLARIS (SCU, Australia). The ablation parameters used for the geological samples can be found in Orange *et al.*, 2016, along with the analytical protocol developed (**Chapter 5**) 150

Table 6.2. Comparison of the ^{45}Sc , ^{66}Zn , ^{85}Rb , ^{88}Sr , ^{89}Y , ^{90}Zr , ^{93}Nb , ^{133}Cs , ^{137}Ba , ^{146}Nd , ^{147}Sm , ^{208}Pb , ^{232}Th , and ^{238}U contents with uncertainty (± 1 standard deviation) obtained on the NIST SRM 613 standard during this study (16 measurements over 8 runs) and the reference values recommended by the NIST and the GeoRem database. Relative error calculated in comparison with the GeoRem reference values. Concentrations are in ppm 151

Table 6.3. Number of artefacts – and proportions within the complete assemblage – attributed to each source for the Renaghju and I Stantari Middle Neolithic..... 153

Chapter 7

Table 7.1. Summary table of the different raw materials present at the Abri des Castelli site 169

Table 7.2. Summary table of the different obsidian sources used on the Abri des Castelli settlement, their proportions, and the number of artefacts characterised by each analytical method. N/A indicates the number of artefacts that we were not able to attribute with the characterisation methods applied 176

Table 7.3. Obsidian sourcing results for the Abri des Castelli assemblage: source proportions and unattributed artefacts by occupation period (4th and 5th millennium B.C.). N/A indicates the number of artefacts that we were not able to attribute with the characterisation methods applied, and Unav. the artefacts that were unavailable for analysis and are yet to be characterised 177

Chapter 8

Table 8.1. Summary of the A Guaita obsidian artefacts attributions (n=140) after SEM-EDS and PIXE analyses. Adapted from Le Bourdonnec *et al.*, 2014..... 185

Table 8.2. Summary table of the different obsidian sources used at A Guaita, their proportions, and the number of artefacts characterised by each analytical method .. 190

List of Appendices

Appendix A: Co-authors' contribution statements.....	235
Appendix B1: Identification of the geological samples from the Mediterranean area included in the geological database. With the exception of the Antiparos (Carter and Contreras, 2012) and Palmarola samples (PSE mission 2013), the geological samples have been transferred to Dr. Gérard Poupeau in the framework of the research led at the IRAMAT-CRP2A, and more particularly the Ph.D. projects of Dr. Mathieu Duttine (2005) and Dr. François-Xavier Le Bourdonnec (2007).....	255
Appendix B2: Identification and geo-referencing of the 44 geological samples from the Monte Arci massif (Sardinia) obtained in 2002. Table adapted from Lugliè, 2006. Source attributions obtained by LA-ICP-MS as part of this study	267
Appendix B3: Scans of the resins and identification of the geological samples embedded	271
Appendix C: Polishing protocol adopted for the samples embedded in epoxy resin. Protocol developed at the IRAMAT-CRP2A for automated polishing on Mecatech 334 (PRESI)	281
Appendix D: LA-ICP-MS results obtained on 200 geological samples from the Mediterranean area (Tyrrhenian Sea and Aegean) and the Carpathians: Sardinia (SA, SB1, SB2, and SC), Lipari, Palmarola, Pantelleria (Lago di Venere and Balata dei Turchi), Melos, Yali, Antiparos, and Carpathians. Number of rows [Nb rows] indicates the number of measurements obtained within a single ablation line, after statistical treatment with removal of the outliers with JMP statistical software (SAS); the results	

displayed for each isotope represent the average concentration (in ppm) for the corresponding number of ‘rows’283

Appendix E: Proposed chronology and associated cultural facies for the Neolithic of Corsica and Sardinia. Data adapted from Soula, 2012297

Appendix F: LA-ICP-MS data obtained on the NIST 613 international standard. 50 measurements acquired at the start and end of 25 runs. Number of rows [Nb rows] indicates the number of measurements obtained within a single ablation line, after statistical treatment with removal of the outliers with JMP statistical software (SAS); the results displayed for each isotope represent the average concentration (in ppm) for the corresponding number of ‘rows’299

Appendix G: LA-ICP-MS data obtained on the BCR-2G (glass) international standard; 4 measurements acquired. Number of rows [Nb rows] indicates the number of measurements obtained within a single ablation line, after statistical treatment with removal of the outliers with JMP statistical software (SAS); the results displayed for each isotope represent the average concentration (in ppm) for the corresponding number of ‘rows’303

Appendix H1: LA-ICP-MS data obtained on 112 artefacts of Renaghju phase 3. Analyses conducted at the SOLARIS laboratory (Southern Cross University). Number of rows [Nb rows] indicates the number of measurements obtained within a single ablation line, after statistical treatment with removal of the outliers with JMP statistical software (SAS); the results displayed for each isotope represent the average concentration (in ppm) for the corresponding number of ‘rows’. N/A: artefacts non-attributed to a specific obsidian source305

Appendix H2: LA-ICP-MS data obtained on 99 artefacts of I Stantari phase 1. Analyses conducted at the SOLARIS laboratory (Southern Cross University). Number

of rows [Nb rows] indicates the number of measurements obtained within a single ablation line, after statistical treatment with removal of the outliers with JMP statistical software (SAS); the results displayed for each isotope represent the average concentration (in ppm) for the corresponding number of ‘rows’. N/A: artefacts non-attributed to a specific obsidian source311

Appendix I1: ED-XRF data obtained on 122 artefacts from the Abri des Castelli. Analyses conducted at the IRAMAT-CRP2A. N/A: artefacts non-attributed to a specific obsidian source. Concentrations are in ppm317

Appendix I2: LA-ICP-MS data obtained on 344 artefacts of the Abri des Castelli. Analyses conducted at the SOLARIS laboratory (Southern Cross University). N/A: artefacts non-attributed to a specific obsidian source. Concentrations are in ppm .325

Appendix J1: ED-XRF data obtained on 122 artefacts from A Guaita. Analyses conducted at the IRAMAT-CRP2A. Concentrations are in ppm343

Appendix J2: LA-ICP-MS data obtained on 6 artefacts of A Guaita. Analyses conducted at the SOLARIS laboratory (Southern Cross University). Number of rows [Nb rows] indicates the number of measurements obtained within a single ablation line, after statistical treatment with removal of the outliers with JMP statistical software (SAS); the results displayed for each isotope represent the average concentrations (in ppm) for the corresponding number of ‘rows’. N/A: artefacts non-attributed to a specific obsidian source351

Appendix K: Published manuscript – available online: Orange, M., Le Bourdonnec, F.-X., Bellot-Gurlet, L., Lugliè, C., Dubernet, S., Bressy-Leandri, C., Scheffers, A., Joannes-Boyau, R. *in press* 2. On sourcing obsidian assemblages from the Mediterranean area: analytical strategies for their exhaustive geochemical characterisation, *Journal of Archaeological Science: Reports*353

Appendix L: Published manuscript: Orange, M., Le Bourdonnec, F.-X., Scheffers, A., Joannes-Boyau, R. 2016. Sourcing obsidian: a new optimized LA-ICP-MS protocol. *Science and Technology of Archaeological Research*, 2(2), 191-202 365

Foreword

The present thesis has been organised around several publications, following the course and design of this research project.

Part I presents an introduction to this work (**Chapter 1**), the background and general research context of this project (**Chapter 2**), and a review of the literature (**Chapter 3**). **Chapter 2** includes more precisely: (i) a presentation of the obsidian material on a geochemical level, (ii) a description of the main obsidian sources of the Western Mediterranean area, (iii) a review of the current state of the archaeological research on obsidian economies in the area, and (iv) an introduction to the archaeological sites selected for the case studies. **Chapter 3** was originally conceived as book chapter, written for an Archaeometry¹ manual destined for Peruvian undergraduate students. It introduces the history of obsidian sourcing as a discipline, through the diverse analytical techniques that can be applied to the obsidian material in archaeological studies. The publication of this manual is scheduled for 2016 by the IFEA Lima editions under the title ‘Manual de Arqueometria’ (Editors: R. Chapoulie, M. Sepulveda, V. Wright).

Part II focuses on the methodologies and protocols adopted in this work. **Chapter 4** includes a scientific publication entitled ‘*On sourcing obsidian assemblages from the Mediterranean area: analytical strategies for their exhaustive geochemical characterisation*’. This paper, presented at the GeoMedislands conference held in Cargèse (Corsica) on the 30th June – 2nd July 2015, was invited for submission in the GeoMedislands special issue of the *Journal of Archaeological Research: Reports*. Submitted in February 2016, it was accepted with minor revisions, and published online on the 14th of June 2016

¹ Archaeometry, or Archaeological Science, is the use of scientific disciplines such as physics, chemistry, or mathematics for the study of archaeological artefacts, materials, or data.

([doi:10.1016/j.jasrep.2016.06.002](https://doi.org/10.1016/j.jasrep.2016.06.002); Appendix K). It describes the different sourcing methods accessible to our research group (visual characterisation, ED-XRF, SEM-EDS, PIXE, pXRF, and LA-ICP-MS) as well as the analytical strategies we developed and adopted for obsidian sourcing studies. It summarises and furthers the work initiated by the late Dr. Gérard Poupeau. **Chapter 5** is dedicated to the presentation of a LA-ICP-MS obsidian sourcing protocol developed during this Ph.D. project. This enhanced protocol aims to optimise the analyses for the sourcing (or ‘fingerprinting’) of obsidian artefacts from the Western Mediterranean. This work was conducted at the SOLARIS laboratory (Southern Cross University) exclusively during the duration of this Ph.D. research project. The results have been submitted for publication in the ‘*STAR: Science and Technology of Archaeological Research*’ journal under the title ‘*Sourcing obsidian in Archaeology: a new optimised LA-ICP-MS protocol*’; the manuscript was accepted for publication on the 27th of July 2016 and published online on the 3rd of October 2016 ([doi:10.1080/20548923.2016.1236516](https://doi.org/10.1080/20548923.2016.1236516); Appendix L).

Part III concerns the application of our research process (*i.e.* the analytical strategy) to obsidian assemblages originating from the Middle Neolithic levels of Corsican sites. The first study case (**Chapter 6**) involves a comparison of the obsidian economies from the Middle Neolithic levels of two sites situated on the Cauria plateau (South-western Corsica). It was submitted for publication in the journal *Geoarchaeology* under the title ‘*Obsidian economy on the Cauria plateau (South Corsica, Middle Neolithic): new evidence from Renaghju and I Stantari*’, and is currently under review. The second study case (**Chapter 7**) investigates obsidian consumption patterns at the Abri des Castelli (or ‘Castelli shelter’) a high altitude site dated from the Middle Neolithic (Mazet *et al.*, 2014). The third study case is presented in **Chapter 8** and concerns the obsidian assemblage of A Guaita (Northern Corsica).

Finally, the general conclusions summarise the present work and deliver the first insights given by these three study cases, as well as highlighting the further studies and research project that will need to be initiated in order to deepen our understanding of Corsican Neolithic populations. Complementary research projects already underway are also briefly described in this chapter.

This thesis follows the guidelines of Southern Cross University for incorporating publications. It contains papers that have been either (i) peer reviewed and accepted for publication (Chapters 3, 4, and 5), (ii) submitted for publication (Chapter 6), or (iii) intended for submission in a peer-reviewed journal. This specific format made some repetitions inevitable.

PART I

-

OBSIDIAN SOURCING STUDIES IN THE WESTERN
MEDITERRANEAN: AN OVERVIEW

Chapter 1

Introduction

1.1. General framework

The study of Prehistoric populations, *i.e.* preceding the invention of writing, has always constituted a challenge to archaeologists. Without written records, understanding such cultures remains a difficult task, necessarily relying on the sites' characteristics (*e.g.* stratigraphy, structure, organisation) as well as on the various types of objects excavated, be it natural remains (human, zoological, or botanical), artefacts (*e.g.* stone or metal tools and weapons, ceramics, metal objects), or features (hearths, constructions, grave sites, *inter alia*). By using a multidisciplinary approach combining archaeology, geology, geochemistry, and biology, these vestiges can be thoroughly investigated and hopefully interpreted to gain a better insight into these communities' identities, cultures and evolutions.

Among these clues, stone artefacts are frequently unearthed. Their examination can deliver many different levels of information (see *e.g.* Perlès, 1992), via the reconstitution of all stages of production and utilisation, *i.e.* from the acquisition of the raw material at the source to the disposal of the used/broken object (Bar Yosef *et al.*, 1992:511; see also Pelegrin, 2015). The reconstruction of this entire 'operational sequence' (or '*chaîne opératoire*', Leroi-Gourhan, 1943; see **Figure 1.1**) indeed allows the contextualisation of the artefacts, and therefore to extract from them as much information as possible. First, through the identification and sourcing of the raw material one can reveal what knowledge a specific group of humans had of their environment (location of the sources, how and when to access them; see *e.g.* Barge and Chataigner, 2003) and, consequently, how they interacted with it (*e.g.* mobility, seasonality/regularity of the expeditions to the

sources, procurement patterns (*cf. e.g.* Wilson, 2007) and transportation effort associated – see *e.g.* Cessford and Carter, 2005).

The manufacturing process itself can shed light on technical know-how and psychomotor skills (Inizan *et al.*, 1995); once compared between different periods and/or communities, it can also show how these skills evolved and were transmitted from generation to generation or between different groups. The mere type of the object exhumed can inform on contacts between populations (transfer of typological trends and specific techniques) and, when combined to use-wear analyses (see *e.g.* Setzer and Tykot, 2010; Kononenko *et al.*, 2015), reveal which type of food (*e.g.* grains, plants, meat, poultry, seafood) or what kind of material was being processed (bone, antler, wood, stone, *etc.*). These are precious clues in the study of prehistoric cultures, and can help to reconstruct their entire lifestyle (diets, crafts, survival strategies *inter alia*).

One of the most enlightening lithic raw materials is undeniably obsidian. This volcanic glass, generally of a black colour, has indeed numerous advantages over other types of rocks used for the lithic industries, such as flint, chert, quartz, or rhyolite (Clark, 1981; Glascock *et al.*, 1998). Due to its glassy texture, it records particularly well the scars of the manufacturing process mentioned earlier, which provides valuable clues about the knapping technique and the different gestures involved.

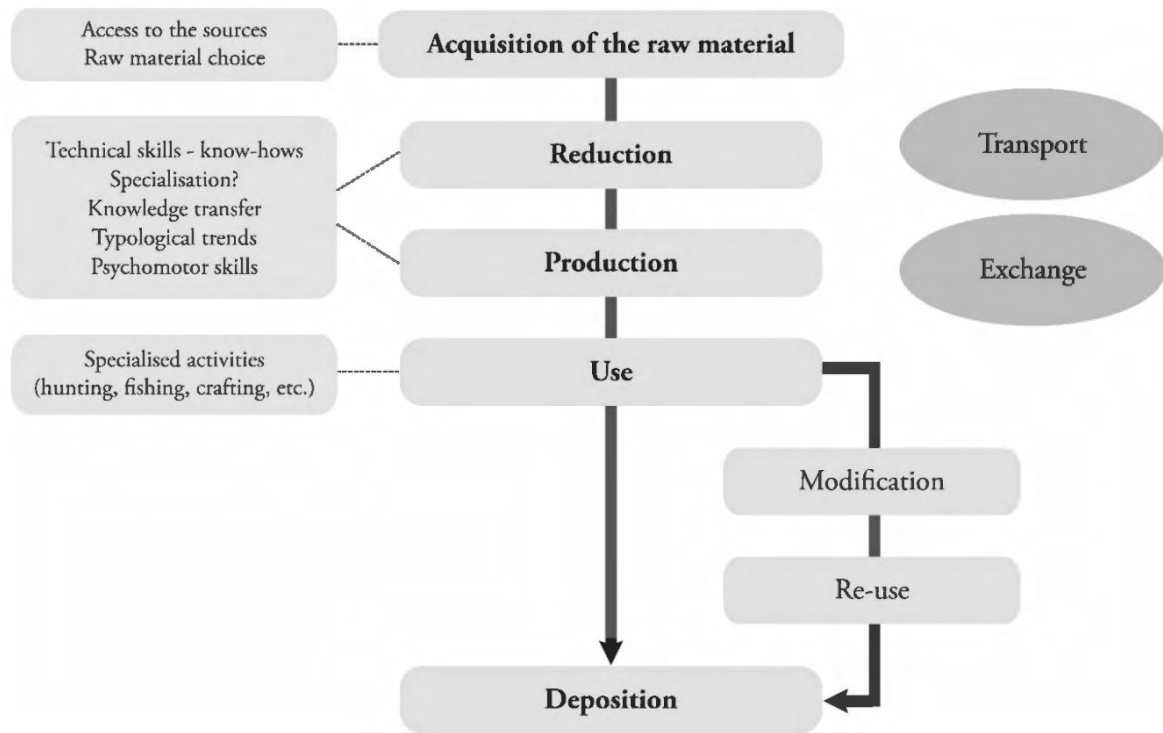


Figure 1.1. Operational sequence, or *chaîne opératoire* - conceptual representation. Adapted from Tykot, 2002a.



Figure 1.2. Foliated piece, Sardinian obsidian, Final Neolithic (4th millennium B.C.). Photography: courtesy of Carlo Lugliè.

Obsidian's nature also gives it excellent flaking qualities as well as an exceptionally sharp edge, which is ideal for tools and weapons (**Figure 1.2**). It has been used in a large number of sites and contexts, although in some areas its exploitation has been limited in time. In the Western Mediterranean area, for example, the use of obsidian spread along with the neolithisation process (the major shift from hunting and gathering to farming and herding), for which it became a real 'indicator' (Lugliè, 2009:214), and then gradually disappeared with the appearance of copper industries during the Chalcolithic period. Its fragility, as a volcanic glass, also meant that those tools and weapons had to be replaced quite frequently; the quantity of objects thus produced allows us to recover consumption patterns as well as typological/technological trends and evolutions.

The relative scarcity of obsidian sources has made it an 'exotic' or even 'precious' material in many contexts (Poupeau *et al.*, 2009:193; see also Guilaine and Vaquer, 1994; Lugliè, 2009; Tykot, 2011; Ebert *et al.*, 2015 *inter alia*), sometimes preferred over the local alternatives, raising the possibility of a potential 'symbolic' value (see Saunders, 2001; Cauvin, 1998). Some obsidians have therefore travelled over hundreds (*e.g.* Perreault *et al.*, 2016; Burley *et al.*, 2011) or even thousands of kilometres (Sand and Sheppard, 2000; Ambrose *et al.*, 2009), either by direct procurement or via exchange and/or trade.

Reconstructing the "*mechanisms by which [obsidian] was procured*" (Freund, 2013:5) is of great significance for the reconstruction of cultural interactions. The circulation of this raw material can be investigated on a geochemical level, as each obsidian source has its own chemical signature, also called 'fingerprint' (Düring and Gratuze, 2013:173). When an obsidian artefact is recovered from an archaeological site, its composition can be analysed and hopefully matched with a specific geological source, hence revealing its origin. Once coupled to the technological and typological evidences, one can attempt a reconstitution of the overall obsidian economy of a specific site for the period considered, for example through the reconstruction of the aforementioned 'operational sequence'.

Synchronic and diachronic comparisons can consequently be made to gain a better view of the ‘bigger picture’, *i.e.* the broader archaeological context.

1.2. Research problem investigated

This research project follows the long tradition of obsidian sourcing studies in Archaeology. Drawing the lessons from more than 60 years of research, during which the discipline has experienced diverse transformations (see **Chapter 3**), the research presented here reflects the latest trends adopted by our research group.

It particularly focuses on the obsidian economies of Neolithic populations from the Western Mediterranean (**Figure 1.3**). More specifically, the sites considered are located in Corsica, an island south of France, for which we investigated the Middle Neolithic occupation levels (5th millennium B.C.). Rich in many Neolithic settlements, this region has been studied for more than a century (see *e.g.* Mérimée, 1840; Grosjean, 1955; Camps, 1988), and yet our knowledge of this specific period is still incomplete. Reconstructing the diffusion patterns of a specific material like obsidian can help bridge the existing gaps, through the elaboration of ‘interpretative models’ defining exchange networks and contacts between culturally distinct populations (Lugliè, 2009:213).

Nevertheless, even if obsidian studies can bring a large range of information on a past community, some methodological issues still have to be addressed. Victim of its success, the sourcing of obsidian has indeed been a springboard for the development of analytical methods and their application to archaeological materials (see **Chapter 2**). This triggered a pursuit for a ‘universal’ sourcing technique (Francaviglia, 1984), which in turn led to the production of decontextualized and heterogeneous data on diverse sites, especially when such sourcing studies were conducted for their own purposes (*e.g.* not embedded in a larger archaeological research question or at least integrated to the typo-technological data of the artefacts).

Selective/restrictive archaeological sampling (see *e.g.* Quarta *et al.*, 2011) is also a major problem, as it can hamper the detection of unusual consumption patterns, sometimes represented by a unique artefact within a whole assemblage (see *e.g.* Summerhayes *et al.*, 1998; Carter *et al.*, 2013; Le Bourdonnec *et al.*, 2015a), or also produce “*bias interpretations about the extent of residential mobility and/or trade patterns because more distant sources will be underrepresented*” (Eerkens *et al.*, 2007:585). This also constitutes a problem for the geochemical characterisation of the sources, where a limited sampling can lead to errors in the attribution of the artefacts to a specific origin (Shackley, 1998).

Altogether, these issues dramatically prevent the accurate reconstruction of the overall obsidian economy of an archaeological site. Therefore, only studies conducted on well-dated and complete assemblages and integrating typological and technological data to the sourcing results can help fill the knowledge gaps (Tykot and Ammerman, 1997; Tykot, 2004:428; Le Bourdonnec *et al.*, 2011:267). As Farr (2006) recently recommended, the “[*studies*] must go beyond the materials [*and*] refocus upon the people and the actions which led to the movement of the artefacts”. Such an approach, described in **Chapter 4**, has been adopted by our research group and applied to several geographical areas (*cf. e.g.* Lugliè *et al.*, 2006; Orange *et al.*, 2013; Le Bourdonnec *et al.*, 2015a). It is here initiated for the distinct research projects investigating three distinct archaeological sites (Chapters 6, 7, and 8), for which we present new sourcing data. These projects will reach their completion (*i.e.* the full integration of the sourcing results to the archaeological data) in the near future (see 1.5 ‘Research limitations’).

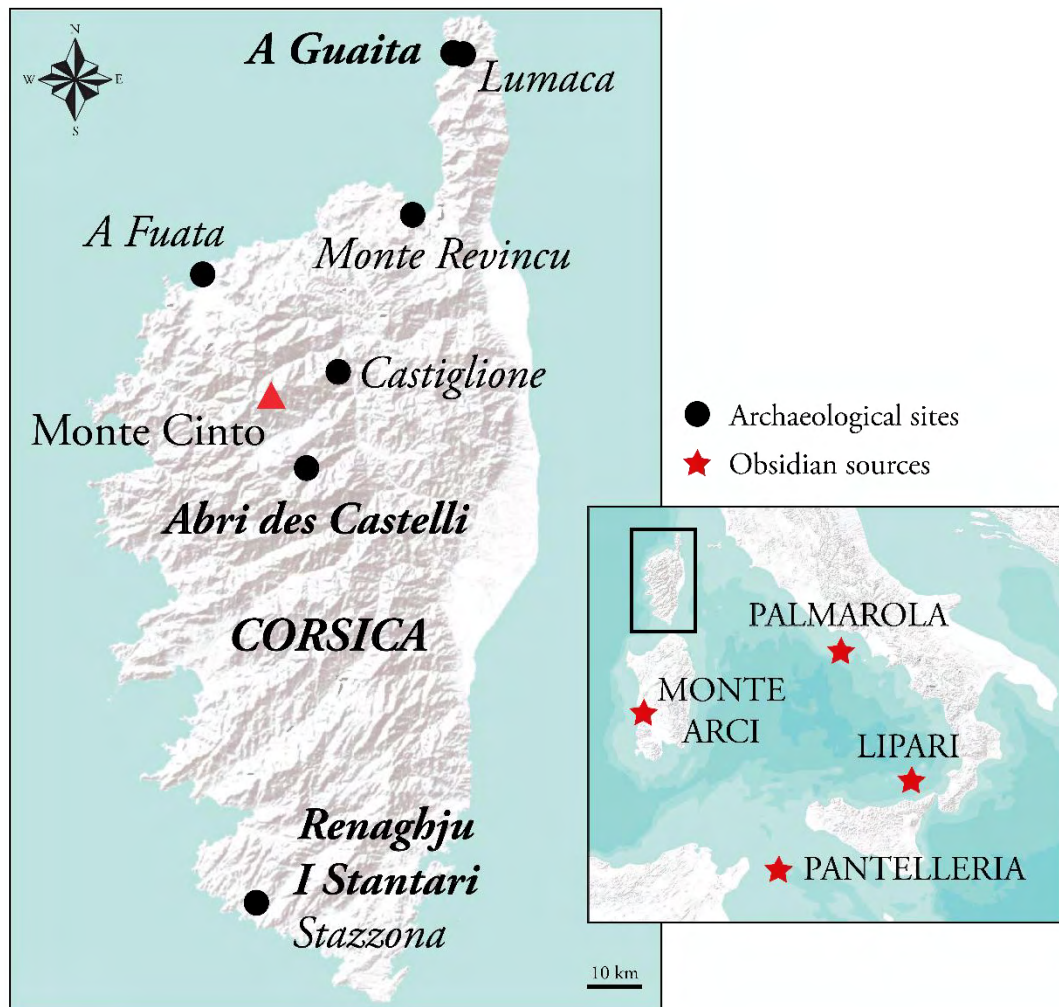


Figure 1.3. Map indicating the location of the main obsidian sources of the Western Mediterranean area, the archaeological settlements studied in this research project (Renaghju, I Stantari, Abri des Castelli, and A Guaita), and other archaeological sites mentioned in the text. Maps created with ArcGIS® software by Esri. ArcGIS® and ArcMap™ are the intellectual property of Esri and are used herein under license. Copyright © Esri. All rights reserved. For more information about Esri® software, please visit www.esri.com. Sources: Esri, USGS, NOAA.

1.3. Overall objective and aims of the research

The overall objective of our research is to contribute to the reconstruction of a ‘general picture’ of the obsidian economy in the Western Mediterranean area during the Neolithic (*ca.* 6000-2500 B.C., Guilaine, 2005), through the study of obsidian artefacts associated with specific communities in place during this period. To reach this goal, four overarching aims are systematically pursued:

- ✓ **To produce new and comparable data on the obsidian economy of the Western Mediterranean area for the Middle Neolithic**, through the exhaustive and non-destructive (or virtually² non-destructive) analysis of the selected assemblages;
- ✓ **To contextualise the sourcing results** by integrating them to the data obtained on the typological and technological characteristics of the artefacts;
- ✓ **To obtain synchronic and diachronic perspectives** by comparing the data of the different sites and periods (by referring to previous studies for the later);
- ✓ **To draw conclusions** on the obsidian economies of the Neolithic settlements studied at site level, then on a broader regional context.

The information obtained with this type of study can then be coupled to other aspects of archaeology, to understand past societies as a whole through their different features such as economy, religion and beliefs, social organisation, exchange networks, interactions between different communities, human/environment interactions, lifestyles,

² The ablation performed is invisible to the naked eye (between 20 and 200 µm width) and keeps the artefact ‘whole’, thus not compromising any further investigation of the artefact (*i.e.* typo-technological or use-wear study, complementary geochemical analyses).

seasonality, hierarchies, cognitive aspects, technical know-how – all of the characteristics that embody a community's identity.

The present Ph.D. project, conducted in three years, primarily focuses on the achievement of the first of the aims described above, *i.e.* the production of new and comparable data on the obsidian economy of Western Mediterranean archaeological sites.

1.4. Research design

To achieve this specific aim, several important steps were designed:

- ✓ A review of the methods available and of their potential for sourcing obsidian artefacts recovered from the Western Mediterranean area (see **Chapter 3**). This step led us (i) to reconsider the traditional Laser-Ablation Inductively-Coupled-Plasma Mass-Spectrometer [LA-ICP-MS] analytical protocols for the obsidian material and (ii) to develop an optimised version, taking into account previous research techniques (Speakman and Neff, 2005) that, despite their proven efficiency, are rarely applied in obsidian sourcing studies (although see *e.g.* Tabares *et al.*, 2005; Glascock *et al.*, 2005; Speakman *et al.*, 2007);
- ✓ The constitution of a geological database, involving an extensive sampling of the obsidian sources from the Western Mediterranean area, and their geochemical characterisation with the different analytical techniques at our disposal, *i.e.* SEM-EDS and LA-ICP-MS. Geological data for the other available methods (PIXE, pXRF, ED-XRF) were collected from earlier studies conducted by our research group (see Poupeau *et al.*, 2000; Lugliè *et al.*, 2007, 2008, 2009; Mulazzani *et al.*, 2010). Some of the archaeological assemblages have been, depending on a number of factors (see **Chapter 4**), analysed by different and/or several methods.

However, only the results obtained with a specific method can be compared to one another, hence the need to analyse the geological samples in the current study with several techniques, to allow accurate comparisons with the archaeological assemblages;

- ✓ The selection of assemblages excavated from well-dated and well-documented Corsican archaeological settlements from the Neolithic period (5th millennium) and the creation of multidisciplinary research projects/teams for their study;
- ✓ The elaboration, for each assemblage, of a tailored analytical strategy relying on the complementarity of the available methods, to allow the exhaustive geochemical sourcing of each artefact regardless of their size, thickness, or geometrical shape (limiting factors for most methods);
- ✓ The comparison and matching of the geochemical ‘fingerprint’ of the artefacts to those of the geological samples from our database to propose a possible origin;

Once the results of the aforementioned steps are put together, the integration of the sourcing results with the information brought by the technological and typological characteristics of the artefacts will be attempted, in collaboration with the Archaeologist/Lithic expert, and as part of the broader context of the multi-disciplinary research projects initiated within this Ph.D. dissertation. Subsequently, a comparison between the different periods of the sites studied (diachronic perspective), and in between the same period of different sites (synchronic perspective) will be achieved.

It is only with such information that we will be able to endeavour, once these larger projects reach their completion, to understand how the obsidian material was apprehended and distributed by these prehistoric communities, which will ultimately allow larger conclusions to be drawn on their lifestyles.

1.5. Research limitations

While we insist in this thesis on the necessity to couple the provenance results to the typo-technological data and the broader archaeological context, the present work only focuses – as mentioned above – on the first steps inherent to each research project pursued by our research group, *i.e.* the adoption of an analytical strategy tailored to the archaeological assemblage, the validation of the methods (assessment of the reliability and validity when necessary), and the production of precise and accurate results while pursuing the exhaustive characterisation of the assemblage under study. The following steps are long-term collaborative processes, and are still ongoing to this day. For example, the integration of the sourcing results to the typo-technological data, which involves a thorough discussion of the results with the specialists involved (archaeologist, lithic expert), is a lengthy process, and therefore could not be included in this three-year Ph.D. project timeline. This type of limitation is inherent to research projects involving a large number of specialists spread in different universities and, ultimately, different countries/continents.

This thesis therefore represents part of a larger research project (*cf.* 1.3. ‘Overall objective and aims of the research’), while laying the foundations of several collaborations for multi-disciplinary projects. It delivers some important outcomes, adding significant information to the existing knowledge.

Chapter 2

Background and Research context

2.1. Obsidian, an ‘ideal’ material for sourcing studies

The success of obsidian sourcing studies in Archaeology relies on several of its characteristics mentioned earlier, mainly (i) its glassy texture - which records the scars of the fabrication process, and (ii) its presence on a large number of sites and contexts. Moreover, the fragility of this glassy material renders the manufactured objects delicate enough to necessitate a regular replacement, therefore placing them in the category of ‘consumption goods’. The production of such a significant amount of objects thus allows us to determine typological trends and evolutions present within an assemblage, and ultimately to replace it within a broader chrono-cultural context.

Also mentioned earlier is its main archaeometric interest, *i.e.* the uniqueness of each source’s geochemical composition. Obsidians of a singular magma flow will indeed be characterised by a very specific ‘fingerprint’, and the differences in composition within it will be relatively insignificant, or at least much smaller than between separate sources (Glascok *et al.*, 1998). These differences in composition normally observed between different flows is what makes provenance studies possible: by allowing us to geochemically characterise every one of them with precision, we are normally able to match an artefact’s fingerprint to a particular source, and thus propose an origin for the raw material used for its fabrication.

2.2. Geochemistry of obsidian

The obsidian material is originating from a felsic – or acidic – magma, which has the highest silica content of all magmas (more than 66 %, and generally between 65 and 75 % in obsidian, Pollard and Heron, 2008:77). This high SiO₂ content gives it a high viscosity, *i.e.* 10⁴ to 10⁶ poises at 1200°C; as a comparison, basalts will generally have a viscosity of 300 to 600 poises at same temperature (Gourgaud, 1998:16).

Obsidian is thus a rhyolitic glass (granitic composition), which has gone through the highest level of differentiation³. It is therefore the most ‘evolved’ type of magma, generally enriched in sodium, potassium, and silica, but depleted in calcium and magnesium (Le Bourdonnec, 2007:9). As a relatively anhydrous material, obsidian generally contains less than 3 % of water (Zhang, 1999:494); nevertheless, a partial hydration can be induced over time and produce inclusions of perlite (up to 5 % H₂O, Zielinski *et al.*, 1977:426).

Obsidian has originally been classified into three types, *i.e.* peraluminous, meta-aluminous or peralkaline, depending on the molecular proportions of CaO, (Na₂O + K₂O) and Al₂O₃ (MacDonald *et al.*, 1992:14-16):

- Peraluminous: $Al_2O_3 \geq CaO + (Na_2O + K_2O)$
- Meta-aluminous: $(Na_2O + K_2O) < Al_2O_3 < CaO + (Na_2O + K_2O)$
- Peralkaline: $(Na_2O + K_2O) \leq Al_2O_3$

Besides silica, the average amount of major and minor elements in obsidian are as follows (Le Bourdonnec, 2007:9): Al₂O₃ 10-15 %, Na₂O 3-5 %, K₂O 1-5 %, and Fe₂O₃ 1-3 % (up to 9 % for some peralkaline obsidians). Trace elements (less than 1 %) present in

³ Steps leading to the formation of chemically different types of rocks from the same original magma, *e.g.* fractional crystallisation; see Bowen, 1928; Thompson, 1972.

obsidian are essentially zinc, gallium, rubidium, strontium, yttrium, zirconium, niobium, barium, and thorium. Some sources can be distinguished simply by relying on the differences in major and minor elements contents (see *e.g.* Le Bourdonnec *et al.*, 2006), however it is often necessary to measure and compare the amount of trace elements, especially in regions where the geochemical composition of the sources can be relatively similar (*e.g.* Near East area, see Binder *et al.*, 2011).

Due to its formation by a rapid cooling of the magma, obsidian presents almost no crystals (Gourgaud, 1998:18), although some inclusions (nanocrystals, microcrystals, phenocrysts) can sometimes be present. They often are the result of ‘contaminations’ occurring by corruption via the environment, or originate from high pressures arising with the final stages of magma formation (*e.g.* for quartz phenocrysts, MacDonald *et al.*, 1992:17). Obsidian can sometimes present some ‘banding’ resulting from (i) the succession and superposition of different crystallisation levels flows, or (ii) magma brecciation, welding, and fragmentation processes (Gonnermann and Manga, 2005:145). The composition in major elements can be altered during the phases of magma mixing (Bowman *et al.*, 1973; MacDonald *et al.*, 1992:48; Hughes and Smith, 1993:83-84), and further post-eruptive alterations such as surficial or hydrothermal alteration (see MacDonald *et al.*, 1992) can also arise over time.

The complexity of the obsidians’ genesis therefore necessitates caution when undertaking obsidian sourcing campaigns. If obsidian is a rather ‘homogeneous’ material in most cases, intrasource chemical variability can nevertheless occur in some contexts and tamper with the sourcing outcomes (see Shackley, 1994, 1998; Hughes and Smith, 1993:81-83 *inter alia*). Such a possibility consequently calls for “*more intensive and extensive sampling* [of the sources]” (Shackley, 1998:89) in certain geographical areas, including field investigations to extend our knowledge of the different outcrops. This has as already been undertaken – or at least initiated – in diverse regions (see *e.g.*

Poidevin, 1998; Lugliè *et al.*, 2006; Cherry *et al.*, 2008; Binder *et al.*, 2011; Carter and Contreras, 2012; Speakman *et al.*, 2005).

2.3. Significance of provenance studies and concept of ‘source’

2.3.1. *The significance of provenance studies*

Researching the origin of archaeological objects through their physical or chemical similarities with geological samples is not a recent endeavour. The concept appears in Europe during the 19th century, and was mostly initiated by mineralogists and chemists such as Gobel, Damour, or Helm (Harbottle, 1982:14; Caley, 1951, 1967). Interested in different materials – respectively brass, jadeite, and amber – they reveal the usefulness of chemistry for archaeology purposes and thus lay the foundations of what later became a full-fledged discipline: ‘Archaeometry’ or ‘Science applied to Archaeology’.

Provenance studies then flourished to attain the success it is today, and due to the significant technological advances accomplished since then, an increasing number of archaeological materials can now be ‘sourced’. Following the multiplication of this type of study, Harbottle (1982:15) however draws our attention on an important consideration, *i.e.* the necessity for archaeologists to understand that sourcing studies cannot categorically confirm an artefact’s origin/source, but only propose its possible attribution to a specific source:

“Archaeologists love the term sourcing, with its upbeat, positive thrust – that you analyse or examine an artifact and, by comparison with material of known origin, ‘source’ it. In point of fact, with a very few exceptions, you cannot unequivocally source anything. What you can do is characterize the object, or better, groups of similar objects found in a site or archaeological zone by mineralogical, thermoluminescent,

density, hardness, chemical, and other tests, and also characterize the equivalent source material, if they are available, and look for similarities to generate attributions.”

This recommendation ultimately relies on a crucial concept when conducting sourcing campaigns, which is the contextualisation of (i) the artefacts analysed within their archaeological and special context and environment, and (ii) the analyses themselves, as expressed here again by Harbottle (1982:17):

“[...] the physical scientist must warn the archaeologist that chemical characterization and indeed all other physical methods are not panaceas. They will not, in general, supply information that is very meaningful unless they are projected against an extensive analytical and archaeological background. As an adjunct, however, they can often supply decisive hard data for hypothesis testing in the form of probabilistic statements. Another thing that they can do is to suggest unexpected connections, and from this allow the archaeologist to generate new hypotheses.”

If not properly contextualised, our geochemical analyses are as a result stripped of their full meaning and potential. Thus, they should not be conducted for the sole purpose of the sourcing itself but rather embedded in a larger archaeological research question.

Following the popular ‘provenance postulate’ defined for the first time in Weigand *et alii* (1977) and more recently reformulated by Neff, who states that « *Sourcing is possible as long as there exists some qualitative or quantitative chemical or mineralogical difference between natural sources that exceed the qualitative variation within each source* » (Neff, 2000:107-108), the obsidian material – with its fingerprint unique to each source - is hence considered as an ‘ideal’ material for sourcing studies in archaeology (Glascock, 1998:2).

2.3.2. *The concept of 'source'*

As reported above, the concept of 'source' has been previously discussed by many authors and is still under debate today (Harbottle, 1982; Neff, 1998; Green, 1998; Hughes and Lees, 1991, Hughes, 1998; Shackley, 2008; Nazarovff *et al.*; 2010; Lugliè *et al.*, 2006; Frahm, 2012a *inter alia*). Its definition, as for the term of 'provenance', is indeed not always clear or not always given the same meaning depending on who employs it. For many scholars, it is the 'ultimate starting point' (Harbottle, 1982:16) where a material is obtained by the human, which in our case is the specific obsidian 'outcrop' where the raw material has been collected. However, this implies a spatial dimension, *i.e.* a notion of 'geographical origin' that we are actually unable to determine. Indeed, the sourcing of obsidians mostly relies on their geochemical characterisation and, as explained by Hughes (1998:104) and demonstrated in several cases (see *e.g.* Lugliè *et al.*, 2006), a geochemical composition does not always corresponds to a unique specific geographical position, where several distinct flows can sometimes be represented. As observed by Le Bourdonnec (2007:16), the precise procurement location might also have been transformed by natural (recovered by sediments or by new eruption material) or anthropological (*e.g.* exhaustive exploitation of the source) phenomena. Therefore, finding that 'ultimate *geographical* starting point' (*i.e.* the precise procurement location) is so far somewhat impossible, and the attributions that are reached in obsidian sourcing studies only ascertain which sources the fingerprints obtained did not match, as one cannot be completely sure that all the sources have yet been discovered and analysed (see discussion in Ward, 1974).

Taking into consideration these concerns, the term of 'source' is used in the present dissertation, in the sense of the geochemical group/type as defined by the analyses.

2.4. Obsidian sources in the Western Mediterranean

In the Western Mediterranean (*cf.* **Figure 2.1**), the main sources are situated on the islands of Sardinia (Monte Arci massif), Lipari, Palmarola, and Pantelleria (see summary in **Table 2.1**). The geological database for this research project (refer to **Appendices B1, B2 and B3**) includes geological samples from these locations, as well as geological samples from the further sources of the Aegean (Carter and Contreras, 2012; Milić, 2014) and the Carpathians (Bigazzi *et al.*, 1990; Oddone *et al.*, 1999) taken as reference points. If the use of these sources has not previously been documented in Corsican or even Sardinian archaeological sites, we consider their inclusion in our database as a necessary precaution.

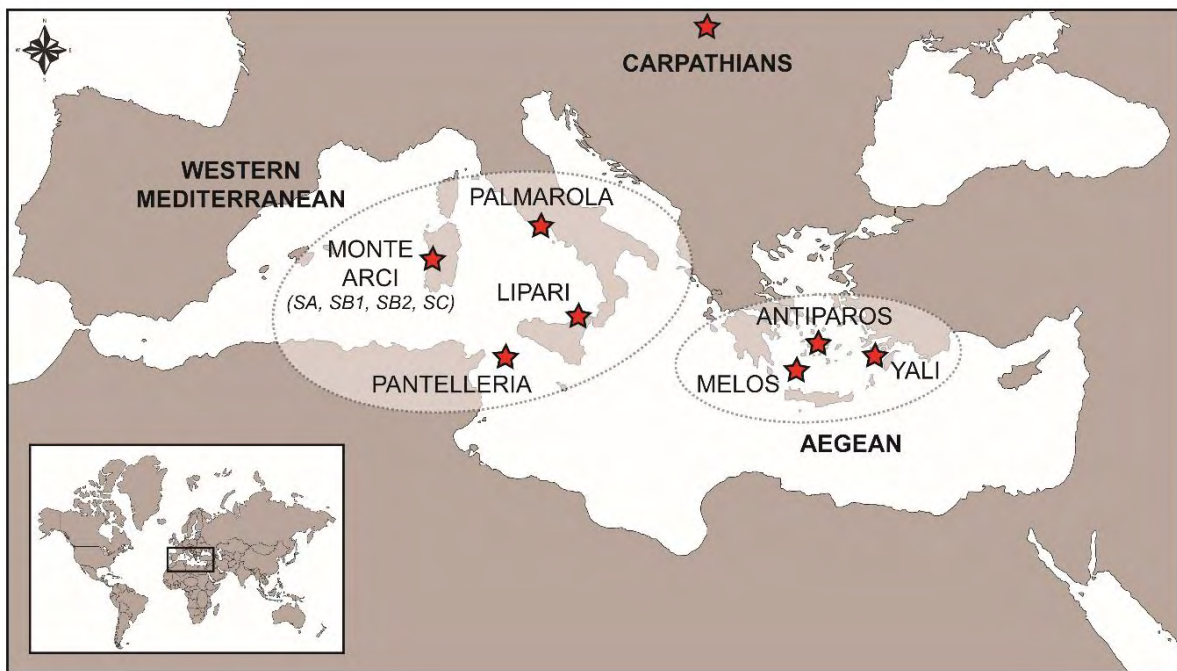


Figure 2.1. Map showing the location of the main obsidian sources of the peri-Mediterranean area.

Every geological sample collected for our geological database and destined for analysis was embedded in an epoxy resin to (i) ensure the availability of a fresh, polished surface

for geochemical analysis, and (ii) facilitate their transport, handling, cleaning, and conservation. The polishing of the samples embedded in resins was achieved at the IRAMAT-CRP2A laboratory with a PRESI Mecatech 334 polishing machine. The polishing protocol followed is described in **Appendix C**.

Here we locate and briefly describe the main Western Mediterranean sources and some of their characteristics.

Table 2.1. Summary of the main obsidian sources and outcrops of the Western Mediterranean area and their denomination.

SOURCE	OUTCROPS
LIPARI	<i>Forgia Vecchia</i> <i>Rocche Rosse</i> <i>Vallone Gabellotto</i> <i>Acquacalda</i>
PALMAROLA	<i>Monte Tramontana</i> <i>Punta Vardella</i> <i>San Silverio</i>
PANTELLERIA	<i>Balata dei Turchi</i> <i>Lago di Venere</i> <i>Salto de la Vecchia</i> <i>Grotta Fromaggio</i> <i>Gelkhamar</i>
SARDINIA (MONTE ARCI)	<i>Conca'e Cannas</i> SA type
	<i>Uras</i>
	<i>Su Paris de Monte Bingias</i>
	<i>Bruncu Perda Crobina</i> SB1 type
	<i>Seddai</i>
	<i>Cucru Is Abis</i>
	<i>Punta Su Zippiri</i>
	<i>Cuccuru Porcufurau</i> SB2 type
<i>Punta Nicola Pani</i>	
<i>Monte Sparau</i>	
<i>Punta Pizzighinu</i> SC type	
<i>Perdas Urias</i>	

2.4.1. Sardinia

With an area of about 25 000 km² (Tykot, 2002a), Sardinia is the biggest island of the Mediterranean presenting obsidian, which was produced by the *Monte Arci* volcanic complex (**Figure 2.2**; Lugliè *et al.*, 2006). Spread across an area of about 25 km long by 8 km wide (Tykot, 1995) and formed during the late Tertiary⁴, the Monte Arci presents three main obsidian flows: SA, SB, and SC (Hallam *et al.*, 1976). Further distinctions can be made within the SB (SB1a, SB1b, SB1c; Tykot, 1995) and the SC groups (SC1, SC2; Tykot, 1995), but only SA, SB1, SB2, and SC (see details in **Table 2.1**; Le Bourdonnec, 2007) are considered to be of archaeological significance (Tykot, 1996). The Sardinian obsidian is generally black, translucent to opaque, and sometimes presenting grey bands (SC). A further description of the different Monte Arci types can be found elsewhere (Tykot, 2002b:4). We report in **Table 2.2** a synoptic description of the SA, SB1, SB2, and SC types adapted from Tykot (1996).

Table 2.2. Synthetic description of the SA, SB1, SB2, and SC Sardinian obsidian types. Adapted from Tykot, 1996.

TYPE	TRANSLUCENCY	REFLECTIVITY	VISUAL CHARACTERISTICS
SA	4	4	Visible microlites, flow banding
SB1	1.5-2	2-3	Usually indistinguishable from SC
SB2	2.5-5	4-4.5	Quite variable, phenocrysts
SC	1	3-4	Frequent surface banding

⁴ Pliocene epoch, *i.e.* from 5.3 to 1.8 million years ago, see K-Ar datings in Di Paola *et al.*, 1975.

For this research project, a selection of 80 geological samples from the Monte Arci (SA: 21; SB1: 15; SB2: 18; SC: 26) were included in our geological database and characterised by LA-ICP-MS. The results are reported in **Appendix D**. Part of these samples (n=44) are issued from the fieldwork conducted for a previous study focusing on the mapping of the Monte Arci primary and secondary obsidian flows (Lugliè *et al.*, 2006), where an area of about 400 km² centred on the Monte Arci was “*systematically prospected and sampled*” (*Ibid.*:999). These samples were obtained in 2002 and are geo-referenced (see **Appendix B2**; Lugliè, 2006; Le Bourdonnec, 2007:Annexe A1). The remaining source samples (n=36) from the Monte Arci have been transferred to Dr. Gérard Poupeau in the framework of the research led at the IRAMAT-CRP2A – more particularly the Ph.D. projects of Dr. Mathieu Duttine (2005) and Dr. François-Xavier Le Bourdonnec (2007). The origin of each sample is specified in **Appendix B1**.

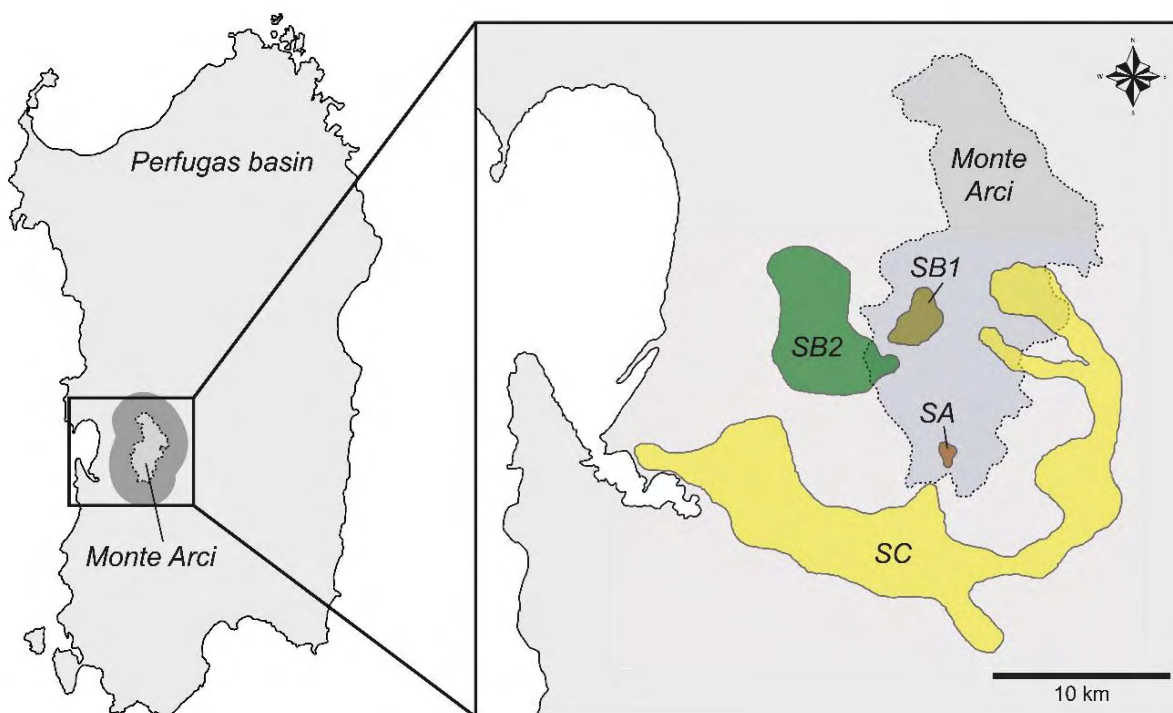


Figure 2.2. Location of the Sardinian obsidian source of the Monte Arci (left) and detail of the SA, SB1, SB2, and SC obsidian flows (right). Adapted from Lugliè *et al.*, 2006.

2.4.2. Lipari

The island of Lipari (**Figure 2.3**) is situated about 30 km to the north-eastern coast of Sicily, in the Mediterranean Sea. This island was first formed around 150 000 BP (Tykot, 1995), and has an area of approximately 38 km². Several obsidian flows are present on Lipari: *Forgia Vecchia*, *Rocche Rosse*, *Gabellotto*, and *Acquacalda*. The *Forgia Vecchia* and *Rocche Rosse* flows are dated from the historic period (Cortese *et al.*, 1986) and thus cannot have been used by the prehistoric people. The other flows – *Gabellotto* and *Acquacalda* – are however more ancient, *e.g.* 4800-13000 B.P. for the former (radiocarbon dating, see *e.g.* Pichler, 1980). The obsidian found in Lipari can be either black and shiny with excellent flaking qualities (Tykot, 1996), or grey-banded with often many spherulites (Tykot, 2002b; Ammerman, 1979). A selection of 7 geological samples from Lipari, acquired from the IRAMAT-CRP2A, was included in our geological database for analysis (see LA-ICP-MS results in **Appendix D**).

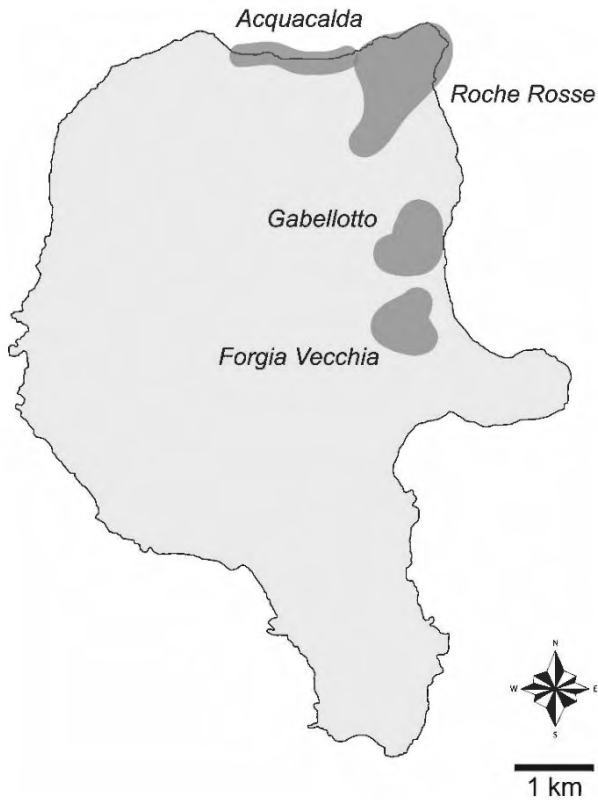
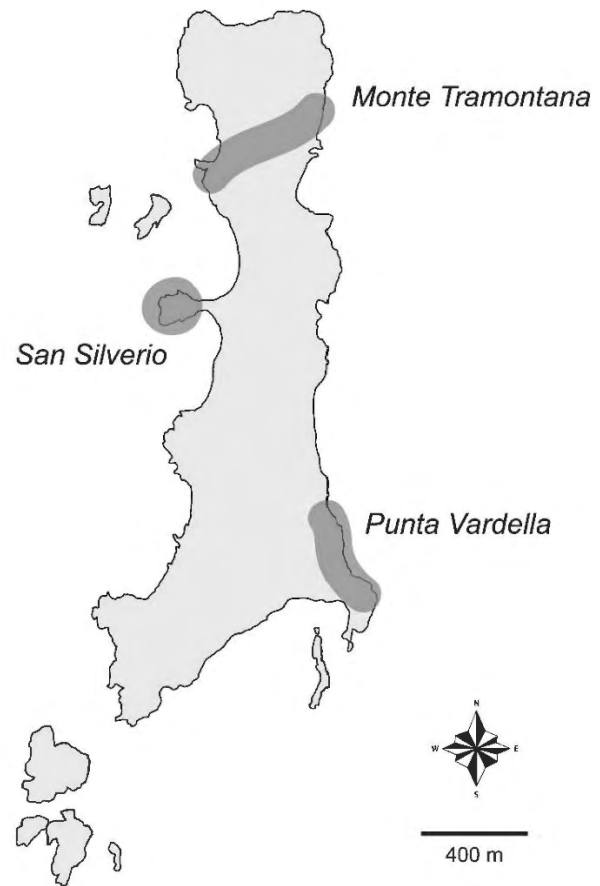


Figure 2.3. Map of the Lipari island, indicating the location of the main obsidian outcrops (*Acquacalda*, *Roche Rosse*, *Gabellotto*, and *Forgia Vecchia*). Adapted from Pichler, 1980.

2.4.3. Palmarola

Situated east of Naples (Italy), the Pontine island of Palmarola (**Figure 2.4**) was formed during the Early Pleistocene, between 1.64 ± 0.02 and 1.52 ± 0.02 million years ago (Cadoux *et al.*, 2005). Although its area is restricted to *ca.* 3 km², the obsidian is present in three different locations: one primary source to the south of the *Monte Tramontana* (Francaviglia, 1984; Acquafredda *et al.*, 1999), and two secondary deposits in *Punta Vardella* (Buchner, 1949; Tykot, 2002a, Tykot *et al.*, 2005) and near San Silverio, although the latter does not seem to be of sufficient quality for knapping (“*devitrified obsidian of unworkable quality*”, Tykot, 2002a:II4.6.5). The Palmarola obsidian can be grey or black, without inclusions, and most often opaque, although transparent varieties can be found in *Punta Vardella* (Le Bourdonnec, 2007:40). As for the source of Lipari, we selected a total of 7 geological samples from Palmarola for analysis (see LA-ICP-MS results in **Appendix D**).

Figure 2.4. Map of the Palmarola island, indicating the location of the main obsidian outcrops (*Monte Tramontana*, *San Silverio*, *Punta Vardella*). Adapted from Tykot *et al.*, 2005 and Cadoux *et al.*, 2005.



2.4.4. Pantelleria

Located in the Strait of Sicily (between Sicily and Tunisia), Pantelleria (**Figure 2.5**) is a rather small island of about 83 km² (White *et al.*, 2009). The large dome of *Montagna Grande*, formed approximately 50 000 years ago (Civetta *et al.*, 1984), has produced peralkaline (rich in iron) obsidians, named ‘pantellerites’ (Foerstner, 1881) or ‘hyalo-pantellerites’ for its glassy variant (Washington, 1913). Several exploitable sources are recognised: *Balata dei Turchi*, *Lago di Venere*, and *Salto de la Vecchia*. The sources of *Grotta Fromaggio* (Tykot, 1995) and *Gelkhamar* (Civetta *et al.*, 1988) do not seem to have produced obsidian of a suitable quality to have been used by the prehistoric people.

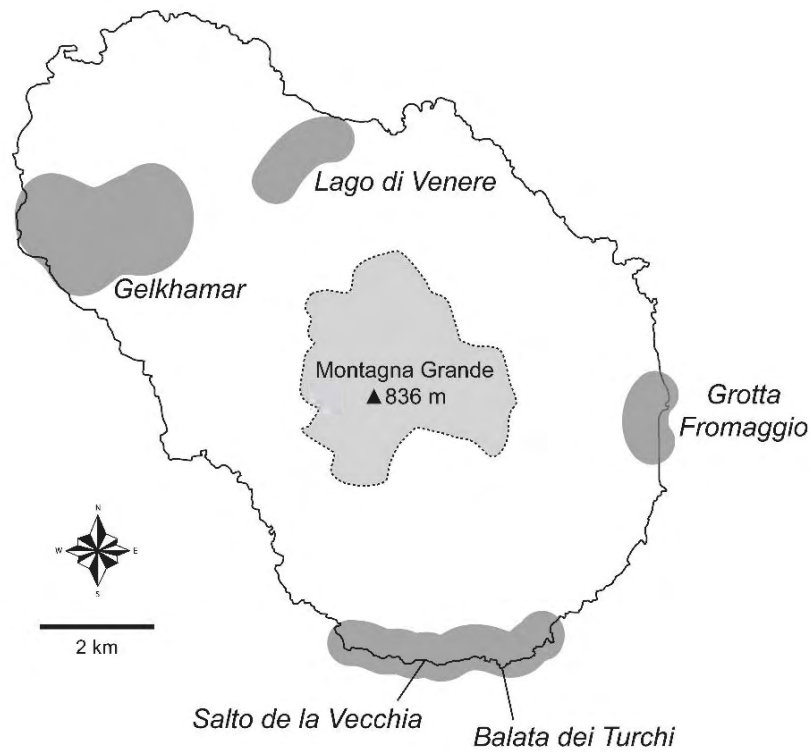


Figure 2.5. Map of the Pantelleria island, indicating the location of the main obsidian outcrops (*Lago di Venere*, *Gelkhamar*, *Grotta Fromaggio*, *Salto de la Vecchia*, and *Balata dei Turchi*). Adapted from Civetta *et al.*, 1984.

Visually speaking, the Pantelleria obsidian can be translucent and green, white-banded (*Balata dei Turchi*), or opaque with metallic reflections (*Lago di Venere*; Tufano, 2005). A selection of 48 geological samples from Pantelleria was added to our geological database and analysed by LA-ICP-MS (*Balata dei Turchi* type: 25; *Lago di Venere* type: 23). The results are reported in **Appendix D**.

2.5. Obsidian diffusion in the Western Mediterranean during the Neolithic: current state of the research

If our knowledge of the Western Mediterranean obsidian sources is now relatively extensive due to the investigations conducted more or less recently (Tykot, 1997; Meloni *et al.*, 2007; Bigazzi *et al.*, 2005; Lugliè *et al.*, 2006), our understanding of its diffusion and consumption modes is still quite incomplete. First conclusions have nevertheless been provided in previous studies (see *e.g.* Ammerman and Andrefsky, 1982; Binder and Courtin, 1994; Guilaine and Vaquer, 1994; Tykot, 1996; Vaquer, 2006, 2007; Pessina and Radi, 2006; Radi and Bovenzi, 2007; Poupeau *et al.*, 2010a; Lugliè, 2012; Binder *et al.*, 2012), attempting to give a general ‘temporary’ overview of the obsidian diffusion phenomenon despite the lack and heterogeneity of the data (Lugliè, 2009), and eventually guiding future research studies.

2.5.1. *The Western Mediterranean context*

The use of obsidian as lithic raw material emerges in the Western Mediterranean area with the Neolithic ‘revolution’ (Childe, 1925), a process witnessing the transition from communities relying on hunting and gathering the food to populations practicing farming and herding. It is essentially restricted to the Neolithic period timeframe, to the exception of two artefacts presumably attributed to the earlier Mesolithic period in Northern Italy and Sicily (*e.g.* Tykot, 2002a). This rare occurrence is however not completely surprising if we consider that seafaring could have appeared much earlier than the Neolithic transition, thus enabling the movement of materials between the Mediterranean islands (see Ammerman, 2010). Nonetheless, the use of obsidian faded during the Chalcolithic period (or ‘Copper Age’, 3rd millennium B.C.), with the “*decline of long-distance Neolithic exchange networks*” (Freund, 2014:242).

Obsidian in the Western Mediterranean has mainly been circulating within a ‘diffusion cell’ (Le Bourdonnec *et al.*, 2010:100), which means that the communities preferentially used the obsidian from the sources of the surrounding area (Sardinia, Lipari, Palmarola, Pantelleria). Only in rare occasions other sources exterior to the Western Mediterranean have been found on the sites excavated in the area (Poupeau *et al.*, 2010a:185-186). Such unusual findings constitute nonetheless a significant clue, revealing rather sporadic ‘interregional’ contacts. Inside this broader ‘diffusion cell’, defined at the scale of the Western Mediterranean, different ‘exchange networks’ can be observed (Le Bourdonnec *et al.*, 2011). For example, obsidian from Lipari has mainly diffused towards the Italian peninsula (Vaquer, 2007; Lugliè, 2009 *inter alia*), while during the Middle and Late Neolithic Corsica and Sardinia are forming a ‘complex’ (Le Bourdonnec *et al.*, 2011:266) for which the obsidian diffusion patterns seem to be different than between the source-islands and the European continent (France, Italy, Spain, *etc.*; Poupeau *et al.*, 2010a).

Nevertheless, the use of other Western Mediterranean sources in Corsican sites has occasionally been reported: so far, four artefacts from Palmarola were found in Corsica (Castiglione, Salotti *et al.*, 2000; A Guaita, Le Bourdonnec *et al.*, 2014; Renaghju, Le Bourdonnec *et al.*, 2015a), as well as two artefacts originating from Lipari (A Fuata, Le Bourdonnec *et al.*, 2010). Those artefacts may have been introduced via Tuscan coastal groups (Le Bourdonnec *et al.*, 2015a:459).

In France, the obsidian procurement patterns differ considerably from those observed on the Sardinian and Corsica islands, as reported in a general review recently published (Binder *et al.*, 2012). This raw material is indeed present from the beginning of the 6th millennium B.C. but emanates exclusively from Palmarola. Absent from the sites of the second half of the 6th millennium B.C., it then reappears on the continent but, this time, is solely originating from Lipari. It is only from the *Chasséen* period onwards (4th

millennium B.C.) that the Monte Arci obsidians became strongly predominant (mostly SA type), to then witness the rarefaction of the use of obsidians altogether. The preference for the SA type in the *Chasséen* cultures has been linked to the reduction mode itself (*i.e.* pressure technique – observed on the flint industry of these sites) which requires highly skilled specialists (see Perlès, 2001; Astruc *et al.*, 2007) as well as a very homogeneous and high quality material. This is the case of the Bedoulian flint exploited on the Terres Longues *Chasséen* settlement (Léa *et al.*, 2010) and of the SA type obsidian (Lugliè, 2012:178), both used for the production of bladelets. Specialised manufacturing centres such as Terres Longues, where the obsidian was imported in the form of decorticated cores reduced on-site, may have been acting as ‘redistribution centres’ (Lugliè, 2012; Léa *et al.*, 2010) to diffuse obsidian and flint end-products to sites located further in France or even Spain (Binder *et al.*, 2012; Gibaja *et al.*, 2013; Terradas *et al.*, 2013).

2.5.2. *Sardinia and Corsica*

As mentioned above, at a certain point the Sardinian and Corsican islands likely functioned as a singular ‘complex’, *i.e.* they were embedded in the same obsidian exchange network and sharing cultural similarities, especially during the Middle and Late Neolithic periods (Tykot, 2002b; see also **Appendix E** for a proposed chronology of the Neolithic in Corsica and Sardinia). This could be due to the proximity of the two islands, only separated by the strait of Bonifaccio (11 kilometres long) and/or to the fact that, even if quartz and rhyolite were present in Corsica and used for the production of tools, their poor knapping potential lead prehistoric populations to rely on Sardinia’s resources to provide good quality lithic raw materials such as flint and obsidian (Le Bourdonnec *et al.*, 2011).

Early Neolithic

Integrated studies conducted on several sites from the Early Neolithic period (6th millennium B.C.) revealed a general tendency regarding the obsidian economy of the area (Sardinia, Corsica, Tyrrhenian region; Lugliè *et al.*, 2008). Regarding the origin of the artefacts the SA, SB2, and SC obsidian types (Monte Arci, Sardinia) were generally preferred over the other sources (Lipari, Palmarola, Pantelleria). SB1 type obsidians were only seldom used (see *e.g.* Lugliè *et al.*, 2008), probably due to their lower knapping qualities compared to the other types.

The procurement patterns and reduction strategies also seem to follow the same trends (Le Bourdonnec *et al.*, 2015a), *i.e.* a preference for rather small nodules to exploit as support (for example in the form of pebbles, completely unworked or partially prepared) rather than larger nodules (although available from the sources) with a high level of core exploitation and a low level of tool standardisation (mainly flake tools, with a subsidiary blade/bladelet production; *Ibid.*). The choice of smaller nodules over larger ones has so far been interpreted as a “*culturally-orientated choice*” (Lugliè *et al.*, 2008:256) rather than the result of natural constraints (Lugliè *et al.*, 2009:214), implying a minimal effort (Lugliè, 2012). In relation, a possible role of ‘filter’ for the populations settled near the sources has been suggested (Lugliè *et al.*, 2008:256).

Middle Neolithic

The Middle Neolithic period seems to hint towards a consolidation of the exchange networks in place previously, with a “*progressive emergence of a specialized production*” (Lugliè, 2012:177). This results in an increase of blade/bladelets products as well as the use of the pressure technique (*Ibid.*). In Sardinia this period is marked by the Bonu Ighinu culture (4700-4000 B.C.), which echoes in Corsica during the Middle Neolithic

(4900-3900/3800 B.C.; Soula, 2012) through diverse settlements of (*e.g.* Renaghju phase 1, D'Anna *et al.*, 2001). However, the small number of Middle Neolithic sites studied both in Sardinia and Corsica does not allow further assumptions on the obsidian phenomenon for this period.

Late Neolithic

At the end of the Middle Neolithic and the beginning of the Late Neolithic, identified by the Ozieri culture in Sardinia (4000-3200 B.C.; Tykot, 2002a) and the Basien and Monte Grossu cultures in Corsica (Soula, 2012), the obsidian consumption patterns see a significant evolution. This shift is primarily characterised by an important increase in the production rates and a more 'organised' management of the source, with the establishment of workshops directly at the obsidian outcrops - mainly SA and SC at the Monte Arci source (Lugliè *et al.*, 2006). This is corroborated by the prevalence of SA and SC type obsidians on a variety of settlements in Corsica, Italy (Lugliè, 2012; Freund and Batist, 2014), and in southern France, where Sardinian obsidian only just appeared (Binder *et al.*, 2012).

2.6. Research projects and collaborations

Recently, the research conducted in the Western Mediterranean area tends to set an example regarding the different 'good' practices to adopt while undertaking obsidian sourcing campaigns, as well as the priorities on which to concentrate. The necessity to produce a 'high resolution picture' (Tykot, 2002b:10) of obsidian exploitation and diffusion patterns is for example increasingly recognised (Freund *et al.*, 2015). As discussed earlier, this involves conducting exhaustive and non-destructive analyses on well documented assemblages (Le Bourdonnec *et al.*, 2011:267), which should in turn

be contextualised with the reconstruction of the *chaîne opératoire* (cf. **Figure 1.1**) and compared with data from other periods and other sites (see **Chapter 1**). Only this type of approach will allow us to capture the complexity of obsidian trade, exchange, and consumption patterns in place during the Neolithic.

The larger research project in which this Ph.D. is embedded aims to follow such a perspective, and also to further the work conducted within a larger research group – initiated by Dr. Gérard Poupeau – composed of several specialists in Archaeology, Geochemistry, and Geoarchaeology. The research on obsidian economies in Neolithic Corsica from which this work originates was chiefly initiated by Dr. François-Xavier Le Bourdonnec in his Ph.D. dissertation (Le Bourdonnec, 2007), and was the fruit of a collaboration with several specialists. As a co-supervisor of the present Ph.D. project, Dr. Le Bourdonnec has strongly supported this study, in a common effort to bring new data on the obsidian procurement and consumption patterns in Neolithic Corsica.

The researchers and students mainly involved in this work are:

- Gérard Poupeau[†], *UMR 7194, Département de Préhistoire, Muséum National d'Histoire Naturelle, Paris, France*
- Ludovic Bellot-Gurlet, *Sorbonne Université, UPMC Université Paris 6, MONARIS "de la Molécule aux Nano-objets : Réactivité, Interactions et Spectroscopies", UMR 8233, UPMC-CNRS Paris, France*
- Carlo Lugliè, *Dipartimento di Scienze Archeologiche e Storico-Artistiche, Università di Cagliari, Cagliari, Italy*
- André D'Anna, *LAMPEA, UMR 7269, CNRS, MCC, MMSH, Aix-Marseille Université, Aix-en-Provence, France*
- Pascal Tramoni, *INRAP Méditerranée, France*
- Sylvain Mazet, *INRAP Grand Ouest, France*

- Jean-Michel Bontempi, *Musée d'Archéologie d'Aléria Jérôme Carcopino, France*
- Françoise Lorenzi, *Université de Corse, CNRS UMR 6240 LISA, Campus Mariani, Corte, France; Association pour la Promotion de l'Archéologie Universitaire Corse (APAUC), Département d'Archéologie, Université de Corse, Corte, Corse*
- Céline Bressy-Leandri, *DRAC/SRA de Corse, Ajaccio, France*
- Henri Marchesi, *DRAC/SRA de Languedoc-Roussillon, Montpellier, France*
- Stéphan Dubernet, *IRAMAT-CRP2A, UMR 5060 CNRS - Université Bordeaux Montaigne, Pessac, France*
- Joséphine Tuquoi, *IRAMAT-CRP2A, UMR 5060 CNRS - Université Bordeaux Montaigne, Pessac, France*
- Elsa Perruchini, *IRAMAT-CRP2A, UMR 5060 CNRS - Université Bordeaux Montaigne, Pessac, France*
- Pierre Machut, *IRAMAT-CRP2A, UMR 5060 CNRS - Université Bordeaux Montaigne, Pessac, France*

2.6.1. *The Cauria plateau, Corsica: Renaghju and I Stantari*

The first case study within this research project was led on two Corsican Middle Neolithic settlements, Renaghju and I Stantari. Located on the Cauria plateau, south of Sartène (**Figure 1.3**), both sites are famous for their stone alignments (see **Figure 2.6**) and were thus reported as early as the 19th century (Mérimée, 1840). Described later on by Adrien de Mortillet (1893), the excavations only started during the second half of the 20th century under the supervision of Roger Grosjean (I Stantari: Grosjean, 1964, 1968; Renaghju: Liégeois, 1975; Jehasse, 1976). They mainly concerned the western and north-western part of the stone alignments, which they aimed to redress (D'Anna, Dir., 2009).

A larger operation has since been directed by André D'Anna and Henri Marchesi within a PCR⁵ focusing on the '*Statues-menhirs, Menhirs et Mégalithisme de la Corse*' (Statues-menhirs, Menhirs, and Megalithism in Corsica), and involving several steps: preliminary prospections in 1994, and excavation campaigns led in 1995 and 1997-2000 in Renaghju (D'Anna, Dir., 2009). They were mainly followed by the excavation campaigns led on the I Stantari site (2001-2009) and the Stazzona structure (2006-2011).



Figure 2.6. Statue-menhirs of I Stantari (from left to right: M5, M4, M2, and M1).
©A. D'Anna. D'Anna, 2013.

⁵ *Projet Collectif de Recherche (Ministère de la Culture en France) / Collective Research Project (Ministry of Culture in France).*

Renaghju

The study of Renaghju's stratigraphy (see **Chapter 6**) revealed an occupation period lasting from the Neolithic to modern times, and divided into 6 different phases (D'Anna, Dir., 2009):

- Phase 1 corresponds to an Early Neolithic occupation ('Cardial' EN) dated from 5600-5000 B.C. (D'Anna *et al.*, 2007);
- Phase 2 reveals a period of abandonment of the site, occurring at the end of the Early Neolithic and eventually linked to climatic changes. The stratigraphy of this level is strongly disturbed by the implantation of standing stones during the following occupation phase;
- Phase 3 sees the erection of the first megalithic monument, *ca.* 4500-4400 B.C. (D'Anna, Dir., 2009:58), which corresponds to the Middle Neolithic period;
- Phase 4 reveals a second megalithic monument, probably implanted at the end of the Late Neolithic period or the beginning of the Bronze Age (estimated date: 2300-2000 B.C., D'Anna *et al.*, 2007);
- Phase 5 is a post-megalithic occupation phase, and lasts from Antiquity to Modern times (D'Anna *et al.*, 2001);
- Phase 6 mainly shows modern perturbations of the site caused by the early excavation campaigns led by Roger Grosjean in 1975, as well as tourist activity.

A total of 5806 lithic artefacts have been unearthed during the excavations. Several raw materials are represented: two available locally (quartz and rhyolite) and two exogenous (chert and obsidian). The quartz has presumably been collected in the outcrops surrounding the site, within a few hundred meters (Bressy *et al.*, 2003:196). The rhyolite originated from a nearby source located on the Pastini plateau, only about 2.5 km of

Renaghju (Bressy *et al.*, 2003, 2008). The closest sources for both allochthonous materials – chert and obsidian – are located in Sardinia. A petrographic study (Bressy, 2002) seems to confirm that the chert was obtained from the Perfugas basin, located in Northern Sardinia (*cf.* **Figure 2.2**).

Regarding the obsidian industry, so far only part of the Phase 1 (Cardial Early Neolithic) assemblage has been studied as part of a sourcing campaign (Bressy *et al.*, 2003, 2008, Le Bourdonnec *et al.*, 2015a). Among the 622 artefacts sourced by visual characterisation (n=348), PIXE (n=250), and SEM-EDS (n=24), the majority matched the Sardinian sources of the Monte Arci, with a prevalence of the SA type (45.3 % of the assemblage) over SB2 (35.4 %) and SC (19.1 %), while the SB1 type is completely absent. Only one artefact was attributed to the furthest source of Palmarola. This consumption pattern follows what has been generally observed for this period in the area, be it for the origin of the obsidian raw materials used for manufacturing the objects or the way in which they were exploited (Le Bourdonnec *et al.*, 2015a). As mentioned earlier, the sporadic use of sources other than Sardinia is relatively uncommon but has been reported in a few cases (Salotti *et al.*, 2000; Le Bourdonnec *et al.*, 2010, 2014, 2015).

The present research project has focused on the Phase 3 (Middle Neolithic) obsidian assemblage, gathering a total of 112 artefacts. The intrinsic characteristics of these artefacts (thickness, dimensions, surface state) has been taken into consideration for the establishment of a tailored analytical strategy to allow the sourcing of the complete assemblage (*cf.* **Chapter 4**). In this case, the artefacts were generally of an irregular shape and small dimensions (< 1 cm diameter), often presenting surface alterations. We thus opted for LA-ICP-MS analyses, conducted at the SOLARIS laboratory in Southern Cross University (Australia) to allow the fast and virtually non-destructive characterisation of every artefact.

I Stantari

The I Stantari site is located only 400 meters from Renaghju, on the Cauria plateau. The excavations campaigns (2001-2009) revealed here again a rather long and complex occupation sequence, from the Middle Neolithic to modern times (D'Anna *et al.*, 2014). The first standing stones appear in the phase 1 occupation level and seem to have been elevated during the same period as those of Renaghju, *i.e.* 4600-4300 B.C. (D'Anna, 2011). Further comparisons can be made between the phase 2 of I Stantari and the phase 4 of Renaghju, the former being dated from the Early Bronze Age, *i.e.* 3315±55 B.P. (Poz 22818:1687-1510 cal. B.C. [2σ]; D'Anna *et al.*, 2014: 315). The phase 3 corresponds to the Middle Bronze Age (3045±35 B.P. – Poz-16680: 1410-1212 cal. B.C. [2σ]; *Ibid.*) and seems partly contemporary to the Stazzona structure. Phases 4 (2945±30 B.P. – Poz-21143: 1265-1048 cal. B.C. [2σ]; *Ibid.*) and 5 (2720±45 B.P. – Ly-12024: 974-802 cal. B.C. [2σ]; *Ibid.*) correspond to the Late Bronze Age, while phase 6 has provided dates matching the Iron Age (2120±110 B.P. – Gif-1397: 395 cal. B.C.-77 cal. A.D. [2σ]; *Ibid.*).

The chrono-cultural similarities between the phase 1 of I Stantari and the phase 3 of Renaghju motivated their selection for study and comparison in the present research project.

The lithic material uncovered for the phase 1 occupation level of I Stantari is mostly made of obsidian, constituting 60 % of the assemblage. Quartz and chert represent the rest (D'Anna *et al.*, 2006). The obsidian artefacts from I Stantari (n=99, all phases combined) have not previously been the object of sourcing studies.

2.6.2. *The Abri des Castelli*

The second research project embedded into this Ph.D. study concerns the Castelli rock shelter, or ‘Abri des Castelli’ (Figure 2.7). Located in northern Corsica (*cf.* Figure 1.3), this site culminates at 2140 metres above sea level, and has a surface of about 7m². The three excavation campaigns led in 2008, 2009, and 2010 under the direction of Sylvain Mazet and Jean-Michel Bontempi (see Mazet, *Dir.*, 2011) have revealed three occupation levels, one affiliated to the Early Neolithic (6th millennium B.C.), and two affiliated to the Middle Neolithic (5th and 4th millenia B.C.).

A total of 7786 lithic artefacts have thus far been unearthed from the Middle Neolithic occupation levels. They are mainly made of rhyolite (6563 artefacts, *ca.* 84 % of the total assemblage) originating from the nearby outcrop situated some 250 metres from the site (Mazet, *Dir.*, 2011:49). The rest of the assemblage is constituted of obsidian (620 artefacts; *ca.* 8 %), quartz (588 artefacts, *ca.* 8 %), or more rarely chert (15 artefacts).



Figure 2.7. The Abri des Castelli site. ©S. Mazet. Mazet, *Dir.*, 2011.

A first characterisation campaign was achieved by SEM-EDS at the IRAMAT-CRP2A on part of the Abri des Castelli obsidian assemblage (56 artefacts) and revealed a Sardinian origin (SA, SB2, and SC types only). Complementary non-destructive analyses were conducted by PIXE on 18 artefacts at the CENBG (Gradignan, France) and attributed the samples to the same sources.

Within the present research project, we endeavoured to geochemically characterise the remaining artefacts available for analysis (*cf.* Chapter 7).

2.6.3. *A Guaita*

The last case study of this research project concerns the archaeological site of A Guaita, located in northern Corsica (Cap Corse). This coastal settlement has been excavated under the direction of Françoise Lorenzi (APAUC, Université de Corse) between 2004 and 2013. So far the first Corsican site to have delivered ceramics issued from both *ceramica cardiale* and *ceramica lineare* facies (see *e.g.* Tozzi and Weiss, 2001; Grifoni Cremonesi, 2012), representative of two chrono-cultural trends of the Early Neolithic – Tuscany and Latium – A Guaita is of prime importance to understand the neolithisation of the Corsican island (Lorenzi, 2011a). Its occupation sequence spreads from the second half of the 6th millennium B.C. (Early Neolithic) to the first half of the 4th millennium B.C. (Late Neolithic; *cf.* Lorenzi, 2011a; Gabriele and Lorenzi, 2014).

The lithic industry of the site involves raw materials obtained locally (rhyolite, quartz) or imported (flint, obsidian, jasper). They all appear to have been reduced on the site, as attested by the presence of debitage by-products for each geological material used (Le Bourdonnec *et al.*, 2014:322).

Between 2009 and 2014, a first research project led by Dr. Le Bourdonnec and Dr. Poupeau in collaboration with Françoise Lorenzi, Jean Sicurani, and Pierre Machut achieved the geochemical characterisation of 140 obsidian artefacts excavated from the A Guaita settlement, all periods combined (Le Bourdonnec *et al.*, 2014). This study was conducted following a precise analytical strategy, aiming at the exhaustive characterisation of the available assemblage. Involving SEM-EDS and PIXE techniques, it revealed the use of the Sardinian obsidian sources, but also of the obsidian of the Palmarola island (n=2; *Ibid.*).

As part of the present research project and in the similar objective to analyse the A Guaita assemblage exhaustively, a further 161 artefacts have been analysed in 2014. Excavated between 2006 and 2013, they originated from the layers 1, 2a, 2b, and 3 of the site. The results of this study are presented in **Chapter 8**.

Chapter 3

A long tradition of obsidian sourcing: review of the literature

The content of this chapter is part of the 'Manual de Arqueometria' designed for undergraduate students in Peru. This manual involves the participation of 25 authors and will be published in both printed (IFEA Lima Editions) and digital form in 2016. Editors: Rémy Chapoulie (IRAMAT-CRP2A, LabEx Sciences Archéologiques de Bordeaux), Marcela Sepulveda (Universidad d'Arica, Chili), and Véronique Wright (IFEA).

Obsidian is one of the most important lithic materials for the reconstruction of the past populations' lifestyles. The study of its geological origin, part of a long tradition, resulted in the use of a multiplicity of analytical methods for its sourcing, being elementary, structural or for example relying on its macroscopic characteristics. This chapter is aimed to present the variety of methods developed along the years, and to provide an overview of the techniques used nowadays for the analysis of obsidians in Archaeology.

3.1. The beginning of a discipline

Obsidian provenance studies in Archaeology are issued from a long tradition, due to the key role of this lithic material in the study of past communities (Poupeau *et al.*, 2014). Present on a large number of Prehistoric settlements, its geochemical 'fingerprint' -

virtually indestructible and unique to each outcrop – allows the identification of the geological origin of artefacts potentially excavated from the archaeological sites. Depending on the data collected, it then becomes possible to retrace the circulation and consumption pattern of this semi-precious material. Once coupled to the typotechnological data revealing the type of object and placing it in an operational sequence (*cf.* **Chapter 1**; see also Leroi-Gourhan, 1971), provenance results help us better understand (a) human interactions with the obsidian material and its sources, (b) interactions between different communities, and (c) these populations' economic, social, and cognitive evolutions (Lugliè, 2012; Freund, 2013; Carter, 2014).

If previous studies have already reported the interest of obsidian within the broader archaeological research questions (Hamilton, 1842; Ordonez, 1892 *i.a.*), the real 'success' of this discipline probably begins with the founding study led by Cann and Renfrew in the early 1960s (Cann and Renfrew, 1964), in which they introduce the use of the sources' geochemical composition to try to deduce the artefacts' origin.

Including up to 25 obsidian sources of the Mediterranean as well as a few archaeological objects, they adopted Optical Emission Spectroscopy [OES] as an analytical technique to differentiate between the numerous sources of the area. Although the geological and archaeological sampling conducted in this study was rather restricted, the authors lay the foundations of the discipline, which met a considerable success in archaeometric studies in the following decades (Williams-Thorpe, 1995).

A multitude of elementary and structural methods have since then been developed and applied to the obsidian material in the framework of provenance studies conducted on archaeological samples (see **Table 3.1**). The majority of these methods are presented below.

Table 3.1. Summary of the main characterisation and dating methods applied to the obsidian material.

Method type	Method	Acronym	Sampling	Elements / Parameters assessed	Analysis type
Elementary	Inductively Coupled Plasma - Atomic Emission Spectroscopy	ICP-AES	10-20mg	Major, minor, and trace elements	Bulk
	Inductively Coupled Plasma - Mass Spectrometry	ICP-MS	< 20 mg	Major, minor, trace, and ultratrace elements	
	Neutron Activation Analysis	NAA	100 mg	Major, minor, and trace elements	
	Laser Ablation - Inductively Coupled Plasma - Mass Spectrometry	LA-ICP-MS	< 10 ⁻⁴ mm ³	Major, minor, trace, and ultratrace elements	Surface
	Electron Microprobe – Wavelength Dispersive Spectrometry	EMP-WDS	A few mm ²	Major and minor elements	
	Scanning Electron Microscope – Energy Dispersive Spectrometry	SEM-EDS	A few mm ²	Major and minor elements	
	Energy Dispersive – X-Ray Fluorescence	ED-XRF	Strictly non-destructive	Major, minor, and trace elements	
	Wavelength Dispersive – X-Ray Fluorescence	WD-XRF		Major, minor, and trace elements	
	Portable Energy Dispersive X-Ray Fluorescence	pXRF		Major, minor, and trace elements	
	Particle Induced X-ray Emission Particle Induced γ -ray Emission	PIXE PIGE/PIGME		Major, minor, and trace elements	
Structural	Raman Spectroscopy	Raman	Strictly non-destructive	Spectrum shape and level of depolymerisation of the silicate network	Bulk or local
	Electron Spin Resonance Spectroscopy	ESR	< 10 mg	Nature and relative abundance of paramagnetic and ferromagnetic species	Bulk
	⁵⁷ Fe Mössbauer Spectroscopy	Mössbauer	250 mg	Hyperfine structures, Fe ²⁺ /Fe ³⁺ ratio, presence of a magnetic component	
Magnetic properties	Superconducting Quantum Interference Devices Magnetometry	SQUID	30 mg	Coercive force, magnetic susceptibility, remanent and saturation magnetization	
Dating	Fission Track dating	TF	A few mm ²	Geological age	Bulk
	⁴⁰ Ar/ ³⁹ Ar dating	⁴⁰ Ar/ ³⁹ Ar	40-140 mg		

3.2. On the road to success: an expanding range of methods

Following the work of Cann and Renfrew, obsidian provenance studies spread rapidly, fostering the development of new analysis techniques. Some already appeared at the end of the 1960s such as X-Ray Fluorescence Spectrometry [XRF] (Parks and Tieh, 1966) or Neutron Activation Analysis [NAA] (Gordus *et al.*, 1968). Allowing the non-destructive analysis of smaller samples, the latter is used to characterise the sources of the Western Mediterranean (Hallam *et al.*, 1976) and Meso-America (Vogt *et al.*, 1982), or more recently the Russian and Japanese sources (Glascock *et al.*, 2011; Kuzmin *et al.*, 2013 respectively). NAA however remains a slow method, requiring several weeks to obtain a chemical composition, and necessitating access to a nuclear reactor. It nonetheless offers various advantages such as the possibility to measure a large number of elements as well as the production of highly precise and accurate results (Kuzmin and Glascock, 2014:87). It has therefore been used in numerous studies (Ammerman *et al.*, 1990; Ambroz *et al.*, 2001, *i.a.*) and continues nowadays (Kuzmin *et al.*, 2013; Izuho *et al.*, 2014 *inter alia*). The XRF technique has had a belated but undeniable success (Shackley, 1995, 2011) thanks to its accessibility and swiftness of analysis in both its energy dispersive (Hall and Kimura, 2002; Freund, 2014; Lugliè *et al.*, 2014) and wavelength dispersive versions (Nadooshan *et al.*, 2007; De Francesco *et al.*, 2011).

The succeeding decades saw the deployment of an even larger number of methods to characterise obsidian, in accordance with the evolution of the techniques themselves. Ion beam analyses (PIXE-PIGME [Particle-Induced X-ray Emission, Particle-Induced Gamma-ray Emission]) then emerge and quickly prove their utility in the broader fields of art and archaeology (Malmqvist, 2004; Beck, 2014). Employed from the end of the 1970s onwards to obsidian in the Pacific (Coote *et al.*, 1972; Duerden *et al.*, 1980; Neve *et al.*, 1994) they consecutively spread to the South American continent (Bellot-Gurlet *et al.*, 1999), the Near East (Poupeau *et al.*, 2010b; Carter *et al.*, 2011), and the Western

Mediterranean (Poupeau *et al.*, 2000; Le Bourdonnec *et al.*, 2015a). Offering two non-invasive analytical alternatives – nuclear microprobe or external micro-beam (see Le Bourdonnec *et al.*, 2005), it allows the measurement of more than 15 major and minor elements. For the archaeological samples presenting larger dimensions (see Le Bourdonnec *et al.*, 2011), the possibility to use an external micro-beam set-up is a significant advantage over the other available methods.

The search for analytical techniques permitting the assessment of a large number of elements in a limited amount of time, without compromising precision or accuracy, also motivated the use of a ‘virtually’ non-destructive method, the ICP-MS (Inductively Coupled Plasma – Mass Spectrometry; Bellot-Gurlet *et al.*, 2005). Combined with laser ablation [LA], this technique was developed for the sourcing of obsidian (Gratuze *et al.*, 1999; Barca *et al.*, 2007), indeed bringing the combined assets of a micro-sampling protocol invisible to the naked eye (the ablation varies between 20 µm and 200 µm of diameter, see Gratuze *et al.*, 2001:645) with the possibility to measure more than 30 elements (Speakman and Neff, 2005).

In parallel with the ‘quest’ for increasingly sophisticated techniques rises a renewed interest for ‘simpler’ and more accessible methods. Acquafredda *et alii* (1999, 2004) thus introduced the use of Scanning Electron Microscopy coupled to Energy-Dispersive Spectrometry [SEM-EDS]. When used destructively on polished sections (to circumvent any surface alterations), it allows one to clearly distinguish the different sources of the Western Mediterranean area (Le Bourdonnec *et al.*, 2006, 2010), where it has mainly been applied. The SEM-EDS is also useful in the Near East (Keller and Seifried, 1990; Delerue, 2007), where it enables, for example, the discrimination between the Nemrut Dağ and Bingöl A, since it is able to measure aluminium, which is essential in this case and delicate to assay with other methods (Chataigner, 1994; Frahm, 2012b ; Orange *et al.*, 2013).

3.3. Searching for alternative methods

The search for 'simpler' methods introduced a growing interest for non-instrumental techniques. Several studies have for example demonstrated the advantages of visual characterisation (Tykot and Ammerman, 1997; Lugliè *et al.*, 2007, 2008), used as an alternative to geochemical analyses. The benefit of this method indeed lies in its simplicity: it only necessitates an experienced eye, trained to recognise the different macroscopic facies specific to the obsidian sources of a given geographical area, to obtain very satisfying provenance results (up to 97 % success in some cases, see *e.g.* Milić *et al.*, 2013). The number of samples that need to be analysed geochemically can thus be considerably reduced (*e.g.* Le Bourdonnec *et al.*, 2014 *inter alia*).

Further alternate methods have been tested, such as the identification of microphenocrysts (anorthoclase, apatite, magnetite, olivine, *etc.*). Despite the fact that this technique allows one to distinguish the main obsidian sources of the Mediterranean area (Acquafredda *et al.*, 1999; Acquafredda and Muntoni, 2008) and bring complementary discrimination information (see Robin *et al.*, 2015), it has not spread further.

The structural properties of obsidian have also been exploited through the use of Raman spectroscopy. Offering a strictly non-destructive approach, this technique is based on the structural differences between glasses (such as obsidian) in function of their chemistry and thermal history. Nowadays considered to be a complementary technique to the most common ones, its efficacy has been proved for the sources of the Mediterranean (Bellot-Gurlet *et al.*, 2004) and the Pacific (Carter *et al.*, 2009).

Fission-track dating, developed in the 1970s (Bigazzi *et al.*, 1971), allows the determination of obsidians' formation age and hence differentiate the sources (or flows) dating from different periods. This approach necessitates a substantial amount of matter

and is a cumbersome process, but can nevertheless complement other techniques when those are insufficient to differentiate the sources. It is for example the case for some Anatolian and Ecuatorial obsidians (Bellot-Gurlet *et al.*, 1999). We should also mention additional techniques like Argon-Argon dating (or $^{40}\text{Ar}/^{39}\text{Ar}$) aiming to date the formation of obsidians, either for sourcing purposes or for documenting the history of volcanic massifs having produced obsidian (Chataigner *et al.*, 1998; Vogel *et al.*, 2006; Le Bourdonnec *et al.*, 2012).

Mössbauer spectroscopy and Electron Spin Resonance [ESR] techniques were developed in the 1980s. The latter is demonstrated as very efficient in Equator and in the Mediterranean area (Duttine *et al.*, 2003; Duttine *et al.*, 2009). Mössbauer spectroscopy is however very demanding in material (necessitates ≈ 250 mg of the sample for measurement, see Poupeau *et al.*, 2007:82) and is limited by the low amount of iron in obsidians – rarely over 10 %, which extends the measuring time.

The impulse to improve the geographical resolution of provenance analyses also led some researchers to turn towards the magnetic properties of obsidian. Previously contemplated as an alternative to more common characterisation methods (McDougall *et al.*, 1983; Chavez-Rivas *et al.*, 1991; Stewart *et al.*, 2003; Zanella *et al.*, 2012), they offer several advantages (fast and low-cost semi-destructive analysis, potentially portable, see Frahm and Feinberg, 2013:3706) but also uncertain results. Recently revisited (Frahm and Feinberg, 2013; Frahm *et al.*, 2014a), they could eventually offer an alternative to geochemical analyses.

3.4. Towards new analytical strategies

Since the beginning of the 1980s Francaviglia pinpoints the lack of comparability in the analyses previously conducted, emphasizing the fact that the search for a ‘universal’

technique (Francaviglia, 1984:311) induced the production of a large amount of rarely comparable results (Glascock *et al.*, 1998:21). The homogeneity, validity, and reliability of the data obtained by the different laboratories is hence questioned, and sparked a debate still alive today (see *e.g.* Hancock and Carter, 2010). Francaviglia was also the first to underline the lack of statistical significance in previous studies, where only a handful of samples are at times taken into consideration to define an obsidian geological source (Francaviglia, 1984:311). He thus laid down the two major issues in obsidian sourcing, still challenging contemporary provenance studies. Arguing that the choice of the technique is less important than the choice of the elements to measure, he concludes that an ‘ideal’ method for obsidians’ geochemical characterisation does not exist, as Shackley later reaffirmed (1998:7).

This awareness generated the development of new lines of reflection within the discipline. Two main observations are still relevant today: (a) the necessity to promote multidisciplinary approaches to better meet the archaeological challenges and, (b) the development of analytical strategies involving complementary techniques to enable the non-destructive characterisation of complete assemblages to precisely document the operational sequences (Poupeau *et al.*, 2010a; Lugliè, 2012). The importance of a single artefact’s origin has indeed already been emphasised in previous studies (see *e.g.* Carter *et al.*, 2013; Orange *et al.*, 2013).

The method’s selection depends on several factors, mentioned earlier: cost, access to the relevant infrastructure, timeliness of the analysis, elements to measure (related to the possible sources), or limitations imposed by the samples themselves such as size, geometry, surface state, and availability for analyses in the laboratory (which requires a temporary withdrawal from the museum or even country where they are stored). This type of multidisciplinary project adopting an analytical strategy tailored to the assemblage under study has already been applied in several geographical areas, such as

the Western Mediterranean (Le Bourdonnec *et al.*, 2014) and the Near East (Poupeau *et al.*, 2010b; Orange *et al.*, 2013).

The development of techniques permitting an in situ geochemical characterisation such as portable XRF [pXRF] (Goodale *et al.*, 2012; Frahm and Doonan, 2013) also contributes to the metamorphosis of obsidian provenance studies, although the protocols involved are still under debate today (Speakman and Shackley, 2013; Frahm, 2013). Its use is nevertheless widespread and has gained application in almost every region undergoing obsidian provenance projects: Asia (Jia *et al.*, 2010; Neri *et al.*, 2015), Aegean (Milić, 2014), Central America (Millhauser *et al.*, 2011, 2015), Near East (Frahm *et al.*, 2014b), Pacific (Sheppard *et al.*, 2011; McCoy *et al.*, 2014), South America (Nazaroff *et al.*, 2010), Western Mediterranean (Freund *et al.*, 2015) *inter alia*.

Finally, research should further continue in several geographical areas with the multiplication of source sample analyses to better recognise and define the different outcrops (Lugliè *et al.*, 2006; Reepmeyer *et al.*, 2011; Binder *et al.*, 2011; Chataigner *et al.*, 2013; also see the GeObs project: <https://geobs.univ-rouen.fr>) or discover new ones (Burger and Glascock, 2002; Summerhayes *et al.*, 2014 *inter alia*). The use of databases integrating (a) precise geo-referencing data with an environmental contextualisation of the outcrops and, (b) information on the typological and technological attributes of the artefacts will allow the assimilation of the various facets of a provenance study, to enable the interpretation of the raw materials' circulation and the lifeways of past populations.

PART II

-

TOWARDS AN EXHAUSTIVE CHARACTERISATION OF OBSIDIAN ASSEMBLAGES: ANALYTICAL STRATEGIES AND ENHANCED PROTOCOLS

Chapter 4

Analytical strategies

As discussed in **Chapter 3**, the obsidian sourcing tradition is relatively long and prosperous, and the number of papers published in this field is still increasing (see Carter, 2014: Fig.1). Its success is mostly due to the particular ‘qualities’ of this material which, when considered together, introduce new information on past populations (*cf.* **Chapter 1**). Numerous methods are available to archaeometrists for the analysis of obsidians, and many have been previously applied - however not always in a sensible way (*cf.* **Chapter 3**). The obsidian sourcing discipline has hence been somehow ‘victim of its success’ in two different ways:

- Its success and apparent ease of application have at times encouraged inexperienced users to apply some of the sourcing techniques themselves; this has been mostly demonstrated with studies involving portable technologies such as pXRF. The use of this technique has spread quite hastily in the world of Archaeology, and is applied in a wide range of studies - some of them disregarding the main challenges inherent to such a method (*e.g.* standardisation, calibration protocols, data treatment, appropriate and exhaustive sampling). The issue was raised a few years ago by Speakman and Shackley (2013), who strongly recommended that pXRF users be consistent in their analytical procedure, and urging them to ensure the accuracy and reproducibility of their data as well as to avoid ‘internally consistent’ results through the measurement of international standards (Speakman and Shackley, 2013:1435).
- The development of a large number of methods applicable to obsidian has consequently multiplied the number of analyses. Although this is a positive

evolution for the field, it also led to the production of heterogeneous results when ideally, it should be possible to compare the data obtained with the same method – even if acquired in different laboratories. Mostly focused on the methodological development, sourcing studies were also at times conducted without real regard to the archaeological question behind the assemblage under study.

Our multi-disciplinary research group makes a priority to address these concerns by (i) relying on the use of certified materials (NIST, BCR, RGM *inter alia*) to assess the accuracy, reproducibility, and sensitivity of our analyses, and (ii) adopting an analytical strategy tailored to the artefacts, and designed to maximise the information from every studied assemblage. The archaeological question is at the centre of every study we undertake, where the sourcing results are coupled with the information brought by the archaeologist on the technological and typological characteristics of the archaeological objects. The concept of ‘analytical strategy’ is developed in the following paper.

This work was invited for publication in a special edition of the Journal of Archaeological Science: Reports, dedicated to the conference proceedings of the GeoMedislands (Géoarchéologie des îles méditerranéennes / Geoarchaeology of the Mediterranean islands) symposium held in Cargèse (Corsica) in June 2015.

This publication ‘distils’ the work conducted by our research group since the 1990s and initiated by the late Dr. Gérard Poupeau. We acknowledge that none of this work could have been accomplished without his input or the close collaboration maintained between the various specialists involved in our research team (see **Chapter 2**).

On sourcing obsidian assemblages from the Mediterranean area: analytical strategies for their exhaustive geochemical characterisation

Marie Orange^a, François-Xavier Le Bourdonnec^b, Ludovic Bellot-Gurlet^c, Carlo Lugliè^d, Stéphan Dubernet^b, Céline Bressy-Leandri^c, Anja Scheffers^a, Renaud Joannes-Boyau^a

^a *Southern Cross GeoScience, Southern Cross University, Military Road, PO Box 157, Lismore, NSW 2480, Australia*

^b *IRAMAT-CRP2A, UMR 5060 CNRS-Université Bordeaux Montaigne, Maison de l'Archéologie, Esplanade des Antilles, 33607 Pessac, France*

^c *Sorbonne Universités, UPMC Université Paris 6, MONARIS 'de la Molécule aux Nano-objets : Réactivité, Interactions et Spectroscopies', UMR 8233, UPMC-CNRS, 75005 Paris, France*

^d *LASP, Dipartimento di Storia, Beni Culturali e Territorio, Università di Cagliari, 09124 Cagliari, Italy*

^e *LAMPEA, UMR 7269, Aix-Marseille Université-CNRS-MCC, Ministère de la Culture et de la Communication, DRAC de Corse*

This article is dedicated to the memory of Dr. Gérard Poupeau.

Highlights

- Non-destructive and exhaustive analyses of lithic assemblages are recommended
- The concept of analytical strategy for obsidian sourcing studies is introduced.
- Integration of sourcing results with typo-technological data is imperative.
- The importance of international multidisciplinary collaborations is highlighted.

Abstract

This paper presents an overview of the work conducted by our research group in the Mediterranean area. Initiated in the 1990s by the late Gérard Poupeau, our research relies on international and multidisciplinary collaborations to endeavour archaeological and anthropological issues linked to the diffusion and consumption of the obsidian raw material during the Neolithic period. Our line of action is to develop flexibly unique analytical strategies, tailored to each obsidian assemblage considered for a sourcing study. Drawing its strength from the complementarity of the methods available within our group, *i.e.* visual characterisation, SEM-EDS, ED-XRF, pXRF, PIXE, and LA-ICP-MS, this approach allows for the exhaustive and non-destructive analysis of those assemblages, thus optimising the potential of sourcing studies. Working hand in hand with archaeologists, the results are closely integrated to the information brought by the typological and technological characteristics of the artefacts, in the aim to reconstruct an overview of the obsidian economy at site level, but also to replace it in a broader – regional and supra-regional – context.

Keywords

Obsidian sourcing; analytical strategy; archaeology; Western Mediterranean; Aegean

4.1. Introduction

The geochemical sourcing of obsidian artefacts has long been a successful way to improve our understanding of the socioeconomic context of past populations (Renfrew, 1969; Clark, 1981; Elam, 1993; Glascock *et al.*, 1998). Emerging in the 1960s with the work of Cann and Renfrew (1964), and Renfrew *et alii* (1966, 1968, *i.a.*), obsidian sourcing studies in archaeology have constantly been expanding over the last decades (Williams-Thorpe, 1995; Tykot, 1996; Freund, 2013: Fig. 1; Carter, 2014: Fig. 1). Such a thriving and popular field however requires constant monitoring to assess where the discipline as a whole is heading. Victim of its success, obsidian sourcing was indeed sometimes used without real consideration for the underlying archaeological issue. This type of study, generally focusing on the development of a particular analytical method or protocol, likely resulted from the constant search for an ‘ideal’ and ‘universal’ sourcing technique (Francaviglia, 1984) that would supersede all the others.

While the development of efficient and reliable methods and protocols is certainly essential, this trend not only led to the multiplication of the techniques applied to the obsidian material but, consequently, to the proliferation of heterogeneous – and thus hardly comparable – sourcing data. This ‘idealistic’ methodological quest was later given less importance, to focus on the instrumentation that was readily available to the researchers working in the field, and to find new – preferably non-destructive – ways to apply them to obsidian geochemical characterisation (Gratuze *et al.*, 1993; Davis, 1994; Acquafredda *et al.*, 1999; De Francesco *et al.*, 2008, 2011; Poupeau *et al.*, 2010a; Forster and Grave, 2012; Frahm, 2012c; Le Bourdonnec *et al.*, 2005, 2006, 2014, *inter alia*). This ‘switch’ eventually brought the attention back to the essence of obsidian geochemical sourcing itself: providing information to resolve the archaeological problem(s) associated with each specific assemblage. Following this reasoning, the analysis is once again regarded as a means to an end (Carter, 2014:23), *i.e.* bringing

information to the archaeological context, and not as the end itself (see *e.g.* discussion in Freund, 2013:786). Finally, it implies that the assemblage, depending on its characteristics, dictates the choice of the analytical method(s), and not the opposite. This is the principle of analytical strategy, formerly introduced by Poupeau *et alii* (2007:82) and developed here.

4.2. Geographical and Archaeological framework

The research presented here focuses on obsidian sourcing in the Mediterranean area, and more particularly on the Western Mediterranean (see *e.g.* Francaviglia, 1988; Tykot, 1997) and the Aegean (Carter and Contreras, 2012; Frahm *et al.*, 2014c *inter alia*). Obsidian sources involved in this study are displayed on the map in **Figure 4.1**: the Monte Arci in Sardinia (SA, SB1, SB2, SC), Pantelleria (Balata dei Turchi and Lago di Venere), Lipari, Palmarola, Melos, and Yali. The Near Eastern obsidian sources have been intentionally excluded, because their number and geochemical complexity put them outside the scope of this study.

Following former studies on Sardinian sites that used a source-based perspective (Le Bourdonnec *et al.*, 2006; Lugliè *et al.*, 2007, 2008a, 2008b, 2009, 2011; Lugliè, 2012), our research recently focused on collections from Neolithic sites in Corsica, Tunisia, Southern France, and Northern Italy (Bressy *et al.*, 2008; Le Bourdonnec *et al.*, 2010, 2011, 2014, 2015a; Lugliè *et al.*, 2014). Through the Neolithic period, the island of Corsica and the North-western Mediterranean offer an interesting framework, since obsidian has a variable significance in the different lithic assemblages. This varies according to several characteristics: the chronological context, the number of artefacts and their typo-technological status, the relative distance between the sites and the

obsidian sources, as well as the proportion of sources distribution in the raw matter supply.

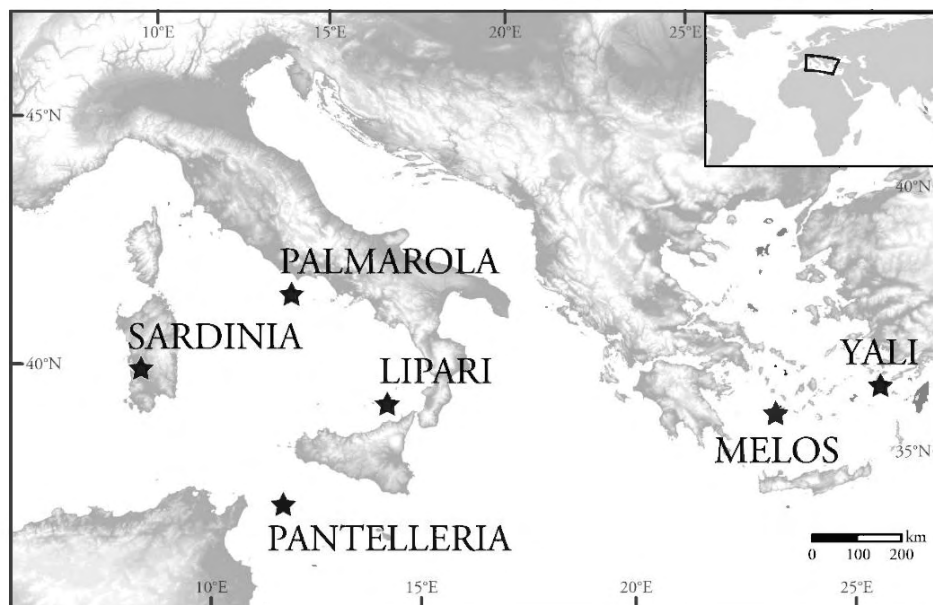


Figure 4.1. Map of the main obsidian sources of the Western Mediterranean and Aegean areas: Sardinia (Monte Arci: SA, SB1, SB2, SC), Pantelleria (Balata dei Turchi, Lago di Venere), Lipari, Palmarola, Melos, and Yali.

In solving archaeological problems of this complexity, a ‘fluid’ and adaptable approach to the studies of obsidian provenance is required, as quite specific archaeological questions can originate from either a handful or several hundred – if not thousands – of artefacts. Therefore, as a result of our flexible strategy comprising the possibility to use visual characterisation as well as a combination of analytical techniques, the sourcing of the whole collections can be achieved. This ultimately allows us to provide a sound interpretation to each underlying cultural and socio-economic issue.

For instance, over twenty years of provenance studies revealed that obsidian circulation in Neolithic Corsica (6th- 4th millennium B.C.) was mainly dependent on procurement from the close island of Sardinia. More recently, even though for a long time the Monte

Arci source has been considered exclusive, our analytical strategy detected the presence of a few obsidians from Palmarola in Corsica (Le Bourdonnec *et al.*, 2014, 2015b). This suggests that an internal interaction took place inside the Northern Tyrrhenian basin, mainly during the first pioneer phase of the Western Mediterranean neolithisation, during the Early and Middle Neolithic. In addition, by the full Middle Neolithic (late 5th millennium BC) the decrease in use of the dominant SB2 type from the Monte Arci source (Sardinia) in favour of a preferential and almost exclusive supply of SC and SA types (Tykot, 1996) has been explained in terms of an intervened large scale obsidian exploitation and production, in substitution of the older 'village-based' reduction system. This shift seems to be linked to the setup of specific spheres of influence in obsidian distribution from the sources of Lipari and Sardinia, so that Corsica was involved in the consistent and massive spread of the Monte Arci SA type obsidians and, in lesser amount, SC type obsidians towards the Northern Tyrrhenian and the Western Mediterranean (Lugliè, 2012).

The significance and relevance of these obsidian exploitation patterns can only be assessed in the frame of a combined provenance and typo-technological study. Therefore, in order to obtain provenance results that could be discerningly discussed, this research selected collections fulfilling the following characteristics: (a) collections issued from documented archaeological contexts with fine stratigraphic/chronological resolution (often from quite recent and extensive excavations), (b) collections that will be typologically and technologically studied in order to discuss the chaîne opératoire, and (c) collections that could document a specific problem (*e.g.* diachronic trends of source exploitation, focus on a specific cultural phase, relation with other materials exchange networks in the frame of the increase of cultural interactions, *etc.*).

4.3. Methods available within our research group

A multitude of methods is now available for obsidian sourcing (see Poupeau *et al.*, 2007, 2014; Shackley, 2011; Orange *et al.*, 2016). Our research group has access to quite a large panel of non-destructive and partially destructive methods, including: visual characterisation, Scanning-Electron Microscopy coupled to Energy Dispersive Spectroscopy [SEM-EDS], portable X-Ray Fluorescence Spectroscopy [pXRF], Energy Dispersive X-Ray Fluorescence Spectroscopy [ED-XRF], Ion Beam Analysis [IBA], and Laser Ablation Inductively Coupled Plasma Mass Spectrometry [LA-ICP-MS]. The advantages and limits of each method are considered here, along with their discrimination potential for the sources of the Mediterranean and Aegean areas.

4.3.1. Visual characterisation

The most readily accessible tool for obsidian characterisation is indubitably the human eye. Several macroscopic features can indeed help to distinguish different obsidian sources: transmittance (translucency, opacity), surface (texture, lustre), inclusions, flow banding (*e.g.* “difference in crystallinity or vesicularity”; Gonnermann and Manga, 2005:136, *inter alia*). Considered together, these characteristics can allow the visual sourcing of up to 70–97 % of an assemblage (Lugliè *et al.*, 2007, 2008a; Milić *et al.*, 2013), depending on the observer's experience to visually recognize the different obsidian sources of a given geographical area. The success of this approach also depends on the assemblage itself: artefacts that are too thick or too small to show their true coloration, presenting a cortex and/or substantial surface alterations are more difficult – if not impossible – to attribute. Yet the cortex itself, combined with other characteristics, can be a good (or even decisive) indicator of provenance, being the result of different degrees of alteration of various original surfaces. Low-cost and time-efficient (a trained

eye can source an artefact in seconds), this method can nevertheless provide an efficient preliminary sorting/screening of an assemblage (Tykot and Ammerman, 1997). A combined visual and typo-technological analysis may also reduce the number of artefacts to be analysed, identifying elements coming out from the same parental unit. Furthermore, this can easily be conducted in-situ, thus permitting the sourcing of artefacts that cannot be transported to the laboratory (see *e.g.* Pierce, 2015).

4.3.2. SEM-EDS

Scanning Electron Microscopy coupled to Energy Dispersive Spectroscopy detector, or SEM-EDS, has been used in the field of obsidian sourcing for over 20 years (Acquafredda *et al.*, 1996, 1999; Le Bourdonnec *et al.*, 2006). Available in a large number of research facilities, it however requires the most invasive sample preparation in our panel of sourcing methods, *i.e.* the application of a carbon coating or the sampling of a small portion of the artefact (a fresh surface of only 1 to 2 mm² is necessary for the analysis). Yet, this partially destructive protocol enables to produce results quickly with a very limited cost and allows – when conducted non-destructively with a carbon coating – to analyse artefacts ranging from a few micrometres to *ca.* 15 cm (Acquafredda *et al.*, 1999:321).

At the IRAMAT-CRP2A, our research group has access to a JEOL JMS 6460 LV scanning electron microscope equipped with an energy dispersive spectrometer (Oxford Industries INCA x-sight). The user interface displays a live image of the sample, permitting to choose the flattest area for analysis, and to avoid surface alterations and inclusions where possible, which is also facilitated by the micrometre-sized electron beam. In addition, it allows for an instant monitoring of the results.

The Western Mediterranean and Aegean sources are easily discriminated with this method, even when we only take into account the CaO, Al₂O₃, and SiO₂ contents (see **Figure 4.2**). A discriminant analysis involving the Na₂O, Al₂O₃, SiO₂, K₂O, and CaO contents after additive log-ratio (alr) transformation (see Aitchison, 1982; Fe₂O₃ contents as common divider) also clearly distinguishes the subtypes of the Monte Arci source (**Figure 4.3**; see also Le Bourdonnec *et al.*, 2006), despite what had been indicated in previous studies (Tykot, 1995). However, this method does not allow the measurement of trace elements, which is a limiting factor for more complex obsidian sourcing, *e.g.* in the Near East (see Poupeau *et al.*, 2010b). When applied to the archaeological samples (here, 223 artefacts from different Neolithic Corsican sites are taken into account), the attribution to each source is manifest (**Figure 4.4**).

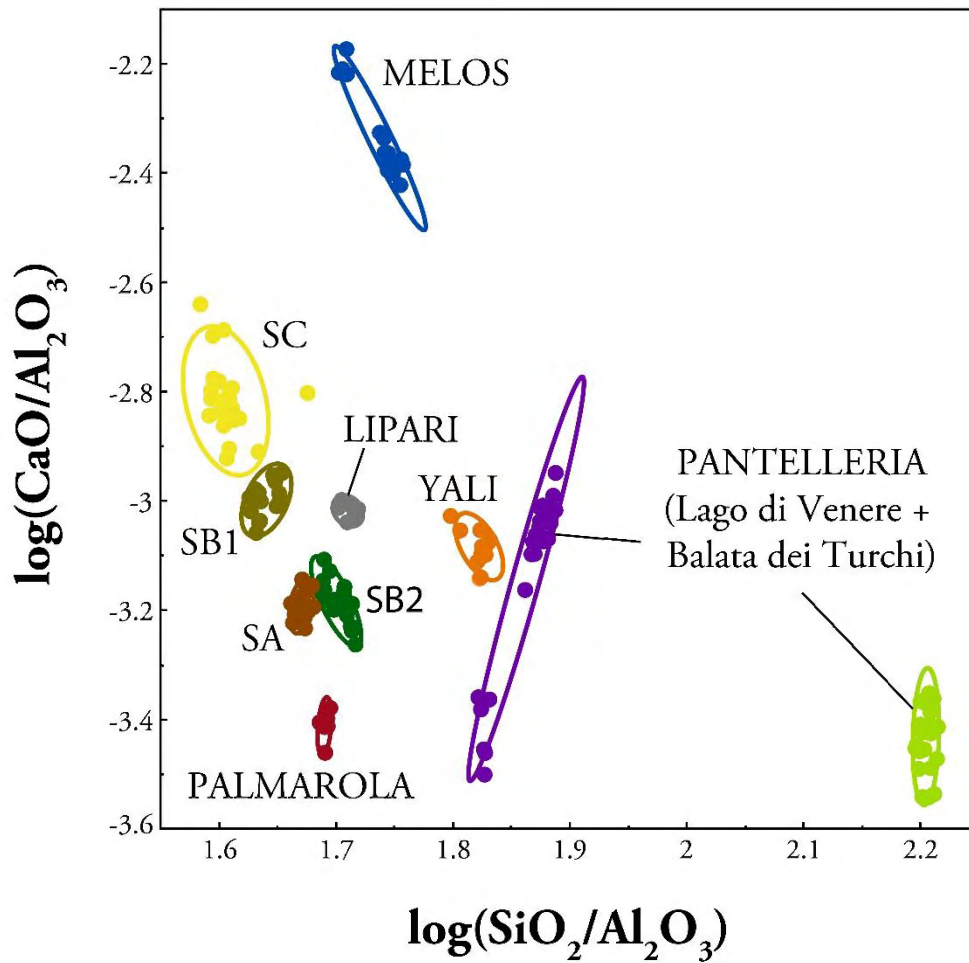


Figure 4.2. Comparison of the $\log(\text{SiO}_2/\text{Al}_2\text{O}_3)$ and $\log(\text{CaO}/\text{Al}_2\text{O}_3)$ ratios obtained by SEM-EDS (IRAMAT-CRP2A) for 175 geological samples from the Mediterranean area (90 % density ellipses). Analyses conducted at the IRAMAT-CRP2A (France); see Le Bourdonnec *et al.*, 2010.

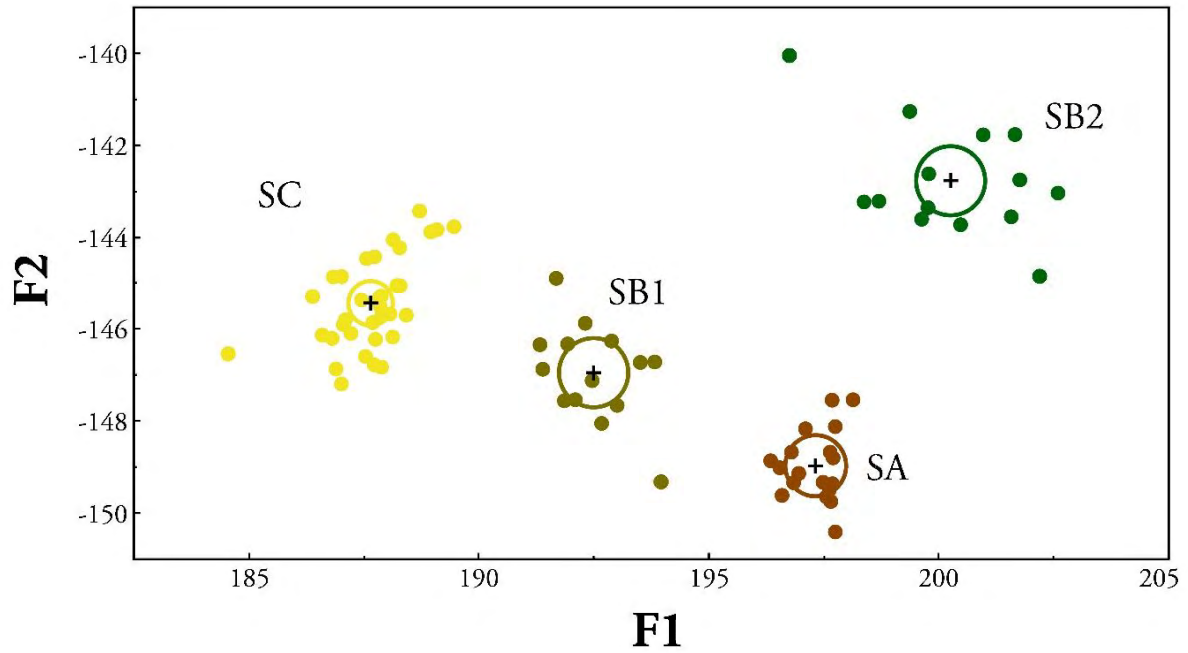


Figure 4.3. Discriminant analysis achieved with the JMP software (SAS Inc. 2012) after additive log-ratio (alr) transformation of the Na_2O , Al_2O_3 , SiO_2 , K_2O , and CaO contents (common denominator for alr: Fe_2O_3) obtained by SEM-EDS on 80 geological samples from the Monte Arci (SA, SB1, SB2 and SC subtypes). The ellipses represent the 95 % confidence region to contain the true mean of each geological sample group. $F1 = - 2.035 \text{ Na}_2\text{O} - 80.102 \text{ Al}_2\text{O}_3 + 93.578 \text{ SiO}_2 - 3.356 \text{ K}_2\text{O} - 5.864 \text{ CaO}$; $F2 = 46.597 \text{ Na}_2\text{O} - 118.527 \text{ Al}_2\text{O}_3 - 3.385 \text{ SiO}_2 + 72.787 \text{ K}_2\text{O} + 10.778 \text{ CaO}$. Analyses conducted at the IRAMAT-CRP2A (France); see Le Bourdonnec *et al.*, 2010.

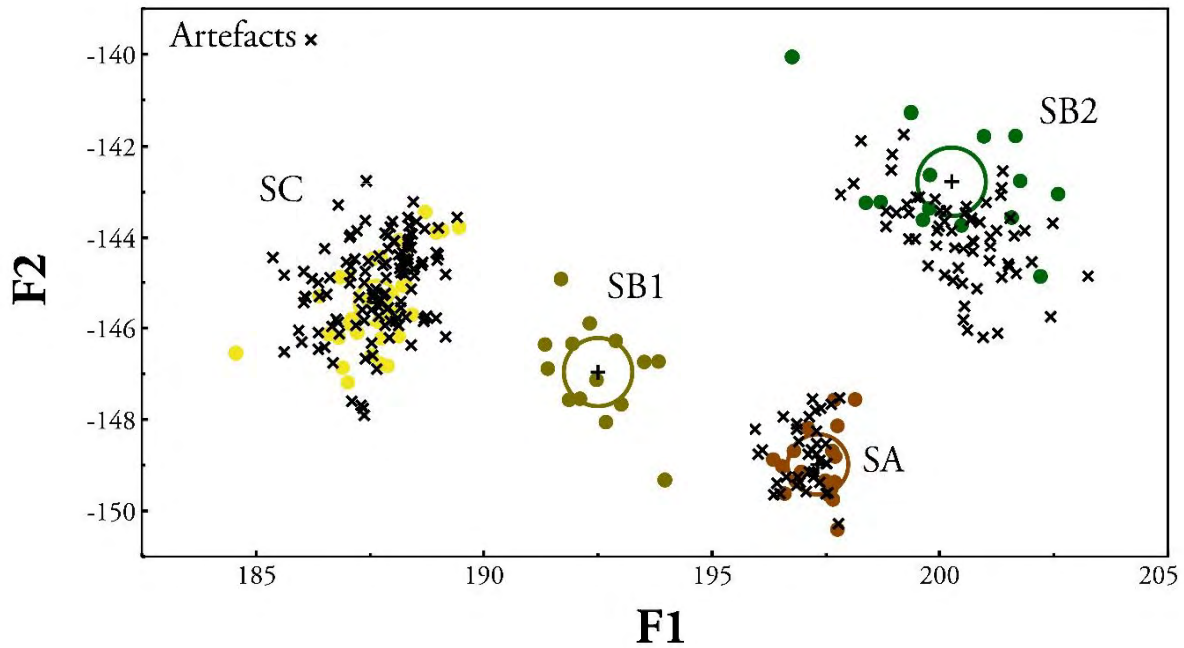


Figure 4.4. Discriminant analysis achieved with the JMP software (SAS Inc., 2012) after alr transformation of the Na_2O , Al_2O_3 , SiO_2 , K_2O , and CaO contents (common denominator for alr: Fe_2O_3) obtained by SEM-EDS on 80 geological samples from the Monte Arci [SA, SB1, SB2 and SC subtypes] (Le Bourdonnec *et al.*, 2010) and 223 archaeological samples from Neolithic sites situated in Corsica (Le Bourdonnec *et al.*, 2006, 2010, 2014, 2015b, and unpublished data). The ellipses represent the 95 % confidence region to contain the true mean of each geological sample group. $F1 = -2.035 \text{ Na}_2\text{O} - 80.102 \text{ Al}_2\text{O}_3 + 93.578 \text{ SiO}_2 - 3.356 \text{ K}_2\text{O} - 5.864 \text{ CaO}$; $F2 = 46.597 \text{ Na}_2\text{O} - 118.527 \text{ Al}_2\text{O}_3 - 3.385 \text{ SiO}_2 + 72.787 \text{ K}_2\text{O} + 10.778 \text{ CaO}$. Analyses conducted at the IRAMAT-CRP2A (France).

4.3.3. Bench top ED-XRF

With the SEM-EDS, Energy Dispersive X-Ray Fluorescence Spectroscopy is probably one of the most available analytical methods for obsidian sourcing. Its capacity to measure elements within the mid-Z X-ray region (mainly between Ti and Nb; see Shackley, 2011; Glascock, 2011) allows to discriminate between the obsidian sources of many geographical areas, *i.e.* Near East (Carter and Shackley, 2007; Nadooshan *et al.*, 2013; Orange *et al.*, 2013), Northeast Asia (Hall and Kimura, 2002; Ikeya, 2014), North and South America (Smith *et al.*, 2007; Glascock, 2011), Western Mediterranean (Francaviglia, 1988; Lugliè *et al.*, 2014) *inter alia*. As a surface analysis, when used in non-destructive mode, this method is sensitive to eventual surface irregularities and weathering, and to the geometry and size/thickness of the samples (see Davis *et al.*, 2011), all of which can often be a limiting factor when analysing excavated artefacts (Shackley, 2011). Conducted on appropriate samples, it however offers a fast analysis (5 to 15 min per sample), with quite a low cost associated compared to other methods (*e.g.* LA-ICP- MS, PIXE).

At the CRP2A, the ED-XRF analyses are conducted with a Seiko SEA 6000vx analyser equipped with a Rh source (50 kV/1 mA) and a SDD Vortex detector, and allowing an automated analysis (stage travel: 330(X) × 250(Y) × 150(Z) mm). The 3 × 3 mm beam collimator allows avoiding eventual heterogeneities in the material, while the sample chamber dimensions (580(W) × 450(D) × 150(H) mm) permits the analysis of large samples.

The ED-XRF easily distinguishes between the main obsidian sources of the Aegean (see *e.g.* Carter and Contreras, 2012) and the Western Mediterranean area. In **Figure 4.5** is presented a Principal Component Analysis (PCA) made on clr (centered log-ratio; see Aitchison, 1982) transformed data (MnO, Fe₂O₃, Zn, Ga, Rb, Sr, Y, and Zr contents)

from 24 geological samples from the Western Mediterranean (see Lugliè *et al.*, 2014), displaying the potential of the ED-XRF for this area. When applied to the artefacts of the archaeological sites considered (**Figure 4.6**; 703 samples analysed from Corsica, Sardinia, Southern France, and Northern Italy), the same PCA shows clear attributions to the different sources.

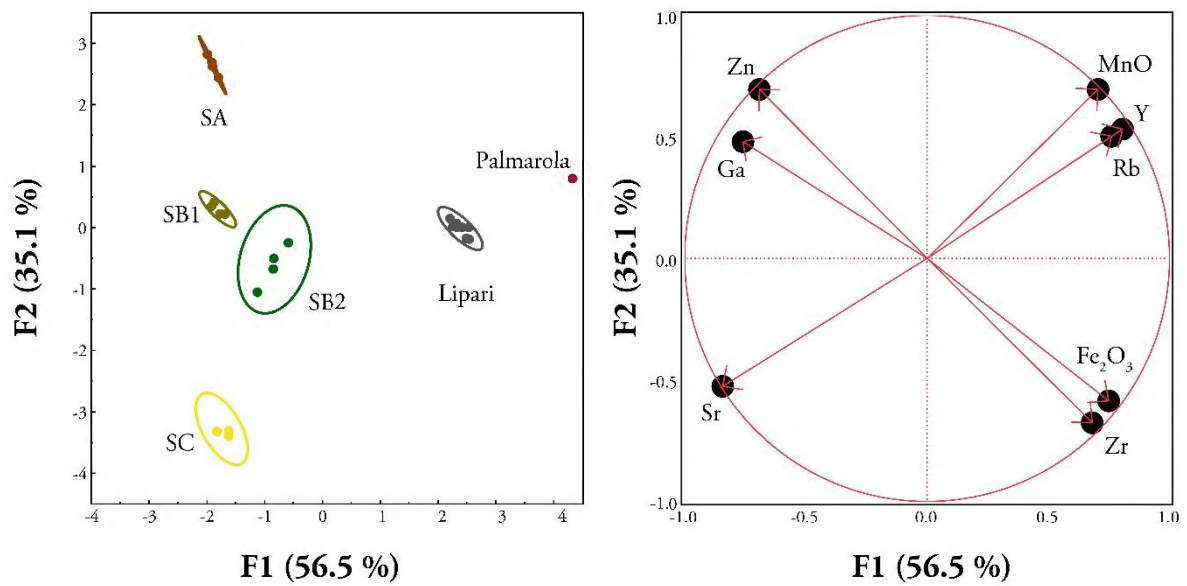


Figure 4.5. Principal Component Analysis conducted with the JMP software (SAS Inc., 2012) after clr transformation of the MnO, Fe₂O₃, Zn, Ga, Rb, Sr, Y, and Zr contents obtained by ED-XRF (IRAMAT-CRP2A) on 24 geological samples from the Western Mediterranean area. 99 % density ellipses. Data published in Lugliè *et al.*, 2014, and unpublished data.

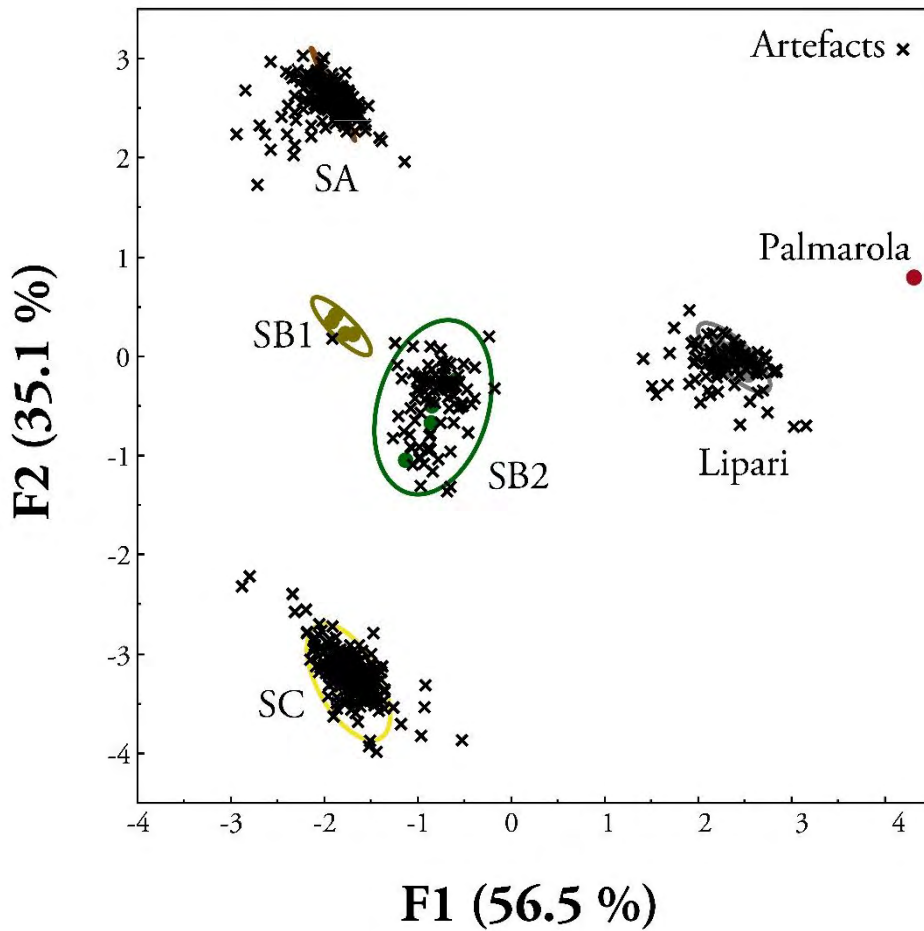


Figure 4.6. Principal Component Analysis conducted with the JMP software (SAS Inc., 2012) after clr transformation of the MnO, Fe₂O₃, Zn, Ga, Rb, Sr, Y, and Zr contents obtained by ED-XRF (IRAMAT-CRP2A) on 24 geological samples (Western Mediterranean) and 703 archaeological samples (from Corsica, Sardinia, Southern France, and Northern Italy; Neolithic period). 99 % density ellipses. Data published in Lugliè *et al.*, 2014, and unpublished data.

4.3.4. Portable XRF

Portable X-ray Fluorescence Spectroscopy [pXRF], is an ideal method for a non-destructive, fast and low-cost analysis of obsidian samples (Freund and Tykot, 2011; Le Bourdonnec *et al.*, 2015b), offering the additional possibility to analyse samples directly on the site. Like ED-XRF, pXRF is sometimes considered as a ‘surface’ analysis, although the X-rays penetrate more in the sample than particles (electrons or protons), resulting in a probed volume of about a few mm³. Albeit sensitive to surface alterations (weathering), the limitations of the pXRF chiefly lies in the size and shape of the samples that can be analysed: the diameter of the beam (3 mm minimum for the instrument used here) restricts this method to samples with a flat surface, while their thickness should be of at least 3 mm in order to simplify the calculation of quantification by considering an ‘infinite’ target (although see Ferguson, 2012 for smaller dimension limits). Strictly non-destructive, its availability and rapidity makes it a method of choice for the analysis of large assemblages, whether it is located on the archaeological site itself, in a museum, or in the laboratory.

The main elements necessary for the discrimination of the major obsidian sources in the Mediterranean (see *e.g.* Milić, 2014:Fig. 3 for the distinction between the Aegean sources) can be measured with pXRF, *e.g.* K, Ti, Mn, Fe, Zn, Rb, Sr, Zr, and Nb. A first series of analyses have been conducted by some members of our research group with a Niton XL3 Series analyser pXRF (RX tube: 50 kV; detector: Si-PIN) as part of a test program developed in collaboration with Philippe Dillmann from the LAPA laboratory (CEA/CNRS-IRAMAT UMR 5060 CNRS). A total of 41 geological samples from the Western Mediterranean have hence been geochemically characterised, as well as 343 artefacts from Corsica. Using the $\log(\text{Rb}/\text{Sr})$ and $\log(\text{Zn}/\text{Sr})$ ratios, the discrimination of the sources (**Figure 4.7**) and the attribution of the archaeological samples (from Neolithic Corsica) is visibly made (**Figure 4.8**).

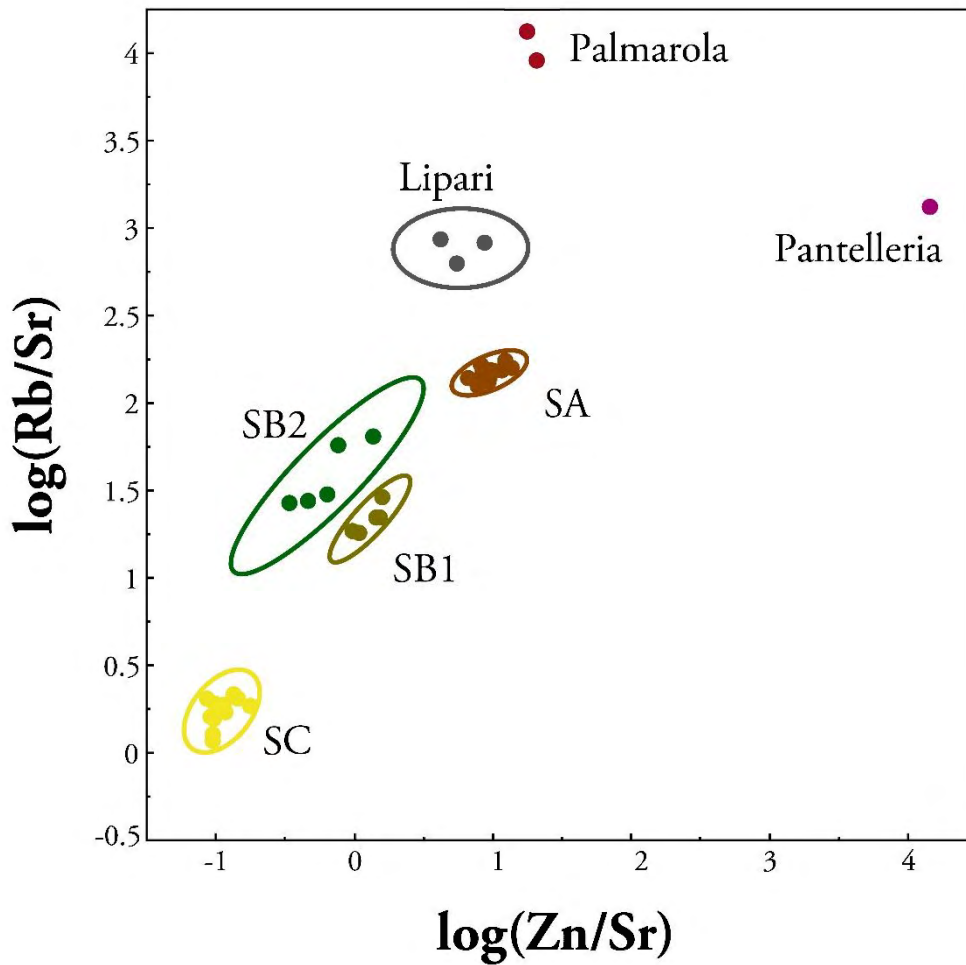


Figure 4.7. Comparison of the $\log(\text{Zn}/\text{Sr})$ and $\log(\text{Rb}/\text{Sr})$ ratios obtained by pXRF for 41 geological samples from the Western Mediterranean area. 99 % density ellipses. Non-destructive analysis conducted with a Niton XL3 Series analyser pXRF (RX tube: 50 kV; detector: Si-PIN), as part of the program-test LAPA (CEA/CNRS-IRAMAT UMR 5060 CNRS). Data published in Le Bourdonnec *et al.*, 2015b.

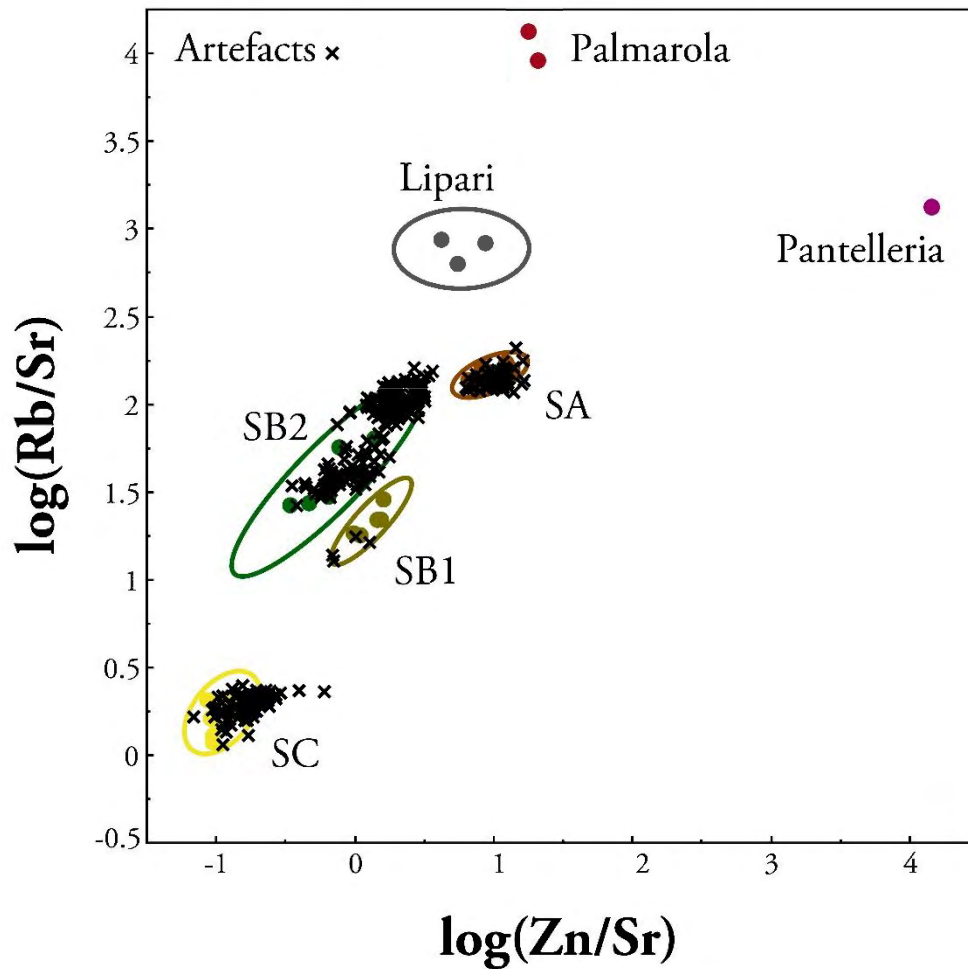


Figure 4.8. Comparison of the $\log(\text{Zn}/\text{Sr})$ and $\log(\text{Rb}/\text{Sr})$ ratios obtained by pXRF for 41 geological samples from the Western Mediterranean area (Le Bourdonnec *et al.*, 2015b) and 343 archaeological samples from Corsica (unpublished data). 99 % density ellipses. Non-destructive analysis conducted with a Niton XL3 Series analyser pXRF (RX tube: 50 kV; detector: Si-PIN), as part of the program-test LAPA (CEA/CNRS-IRAMAT UMR 5060 CNRS).

4.3.5. IBA - PIXE

Among all the methods available within our research group, Particle Induced X-ray Emission spectroscopy [PIXE] is probably the less accessible and one of the most expensive. It indeed requires access to a particle accelerator, not uncommon but often quite inaccessible. Nevertheless, collaborations with the C2RMF (*Centre de recherche et de Restauration des Musées de France*) in Paris and the CENBG (*Centre Etudes Nucléaires de Bordeaux Gradignan*) in Gradignan gave our research team the privilege of accessing this high-precision instrumentation.

A total of 25 geological samples and 541 artefacts have been analysed thus far at the C2RMF in the AGLAE facility (*Accélérateur Grand Louvre d'Analyses Élémentaires*; Calligaro *et al.*, 2002), which external micro-beam set-up allows for the analysis of larger samples (Le Bourdonnec *et al.*, 2005, 2011). At the CENBG, the AIFIRA platform (*Applications Interdisciplinaires de Faisceaux d'Ions en Région Aquitaine*) presents a nuclear microprobe capable to analyse very small samples, due to its 5- μm beam diameter (Llabador *et al.*, 1990). A total of 30 obsidian geological samples and 134 artefacts were thus analysed at this facility.

The PIXE has the capability to clearly distinguish the Aegean sources (see *e.g.* Bellot-Gurlet *et al.*, 2008) as well as the Western Mediterranean sources by its ability to measure non-destructively major, minor and trace elements (here we measure Na_2O , Al_2O_3 , SiO_2 , K_2O , CaO , TiO_2 , MnO , Fe_2O_3 , Zn , Ga , Rb , Sr , Y , Zr , and Nb). For the latter, this can clearly be shown by a binary diagram involving the $\log(\text{MnO}/\text{Zr})$, $\log(\text{Rb}/\text{Zn})$, $\log(\text{Zn}/\text{Zr})$, and $\log(\text{Rb}/\text{Zr})$ ratios (**Figures 4.9 and 4.10**). Once applied to the artefacts (Sardinia, Southern France, Corsica, and Tunisia), the same diagrams (**Figures 4.11 and 4.12**) confirm its potential to attribute archaeological samples of unknown origin to one

of those sources. Presenting no volumetric constraint, one should note that this method is however sensitive to surface alterations.

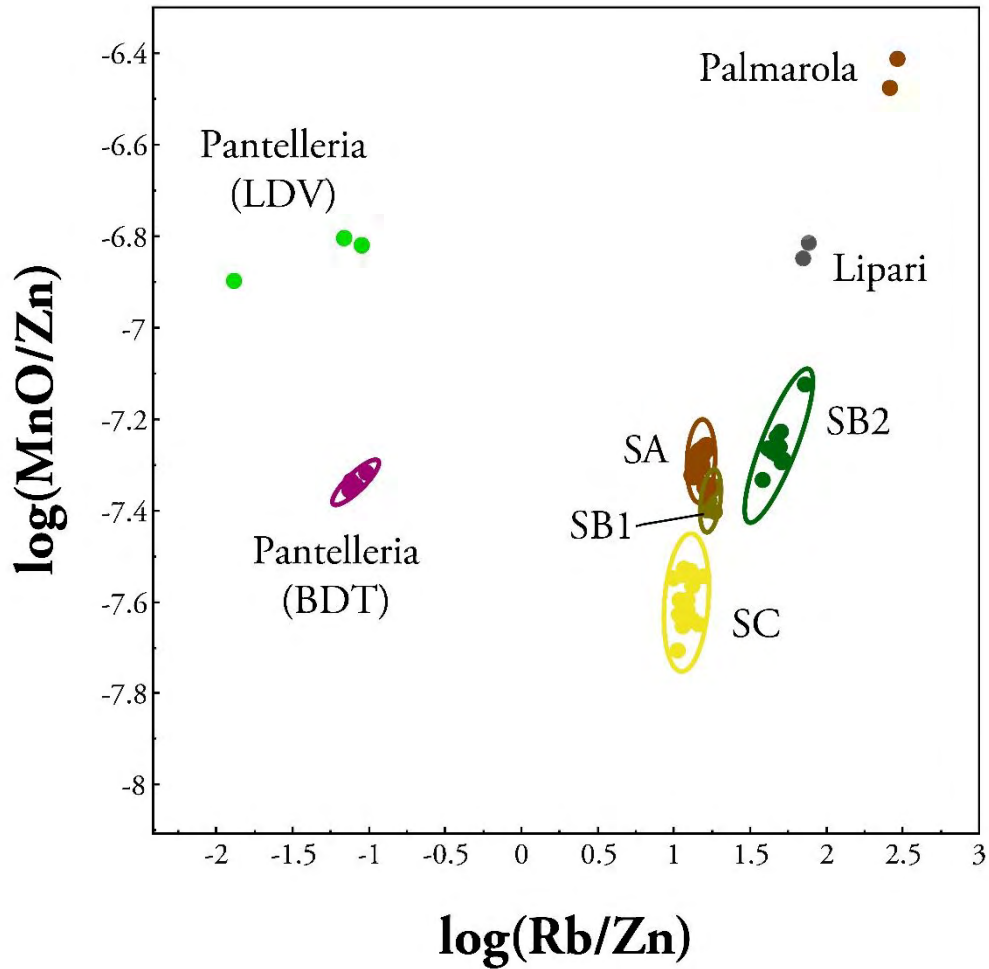


Figure 4.9. Comparison of the $\log(\text{Rb}/\text{Zn})$ and $\log(\text{MnO}/\text{Zn})$ ratios obtained by PIXE (CENBG, AIFIRA) for 55 geological samples from the Western Mediterranean area (see Lugliè *et al.*, 2007, 2008a, 2009; Mulazzani *et al.*, 2010; Poupeau *et al.*, 2000). 99 % density ellipses. Data published in Lugliè *et al.*, 2007, 2008a, 2009; Mulazzani *et al.*, 2010; Poupeau *et al.*, 2000.

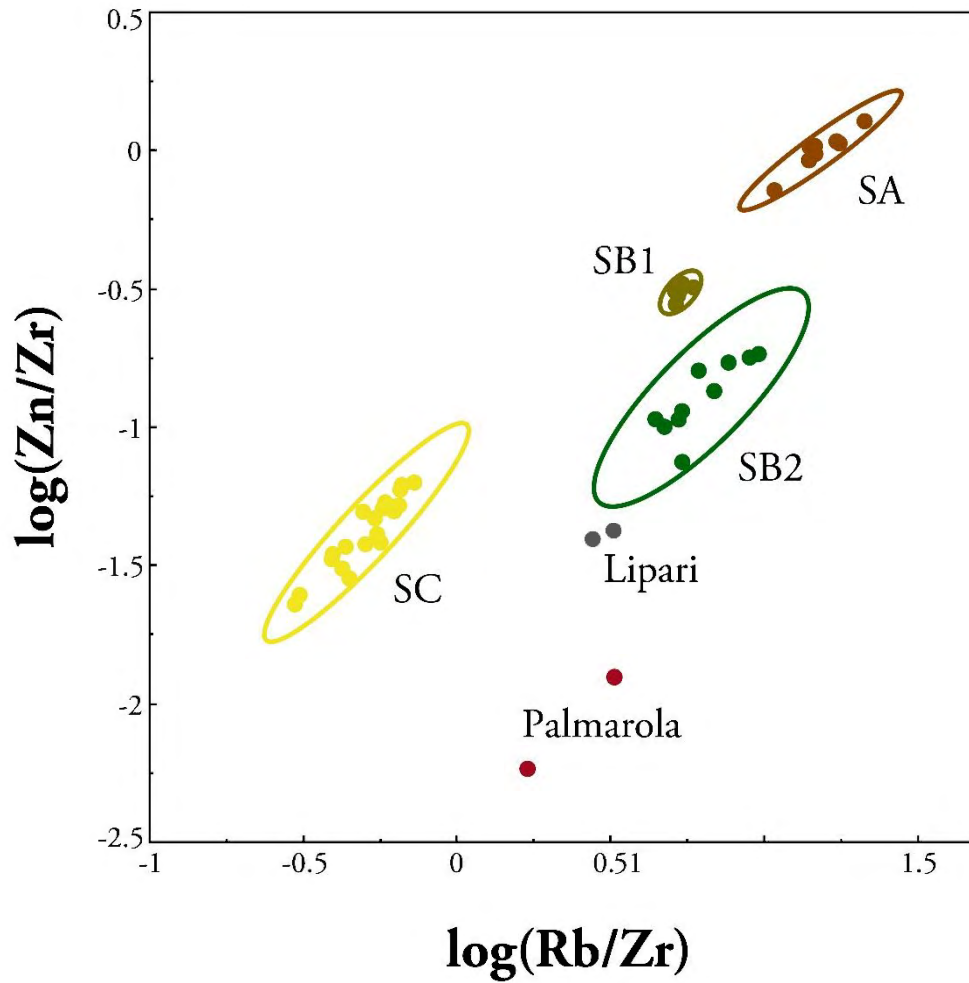


Figure 4.10. Comparison of the $\log(\text{Rb}/\text{Zr})$ and $\log(\text{Zn}/\text{Zr})$ ratios obtained by PIXE (CENBG, AIFIRA) for 44 geological samples from the Western Mediterranean area; focus on the sources of Sardinia (Monte Arci: SA, SB1, SB2, SC), Lipari, and Palmarola. 99 % density ellipses. Data published in Lugliè *et al.*, 2007, 2008a, 2009; Mulazzani *et al.*, 2010; Poupeau *et al.*, 2000.

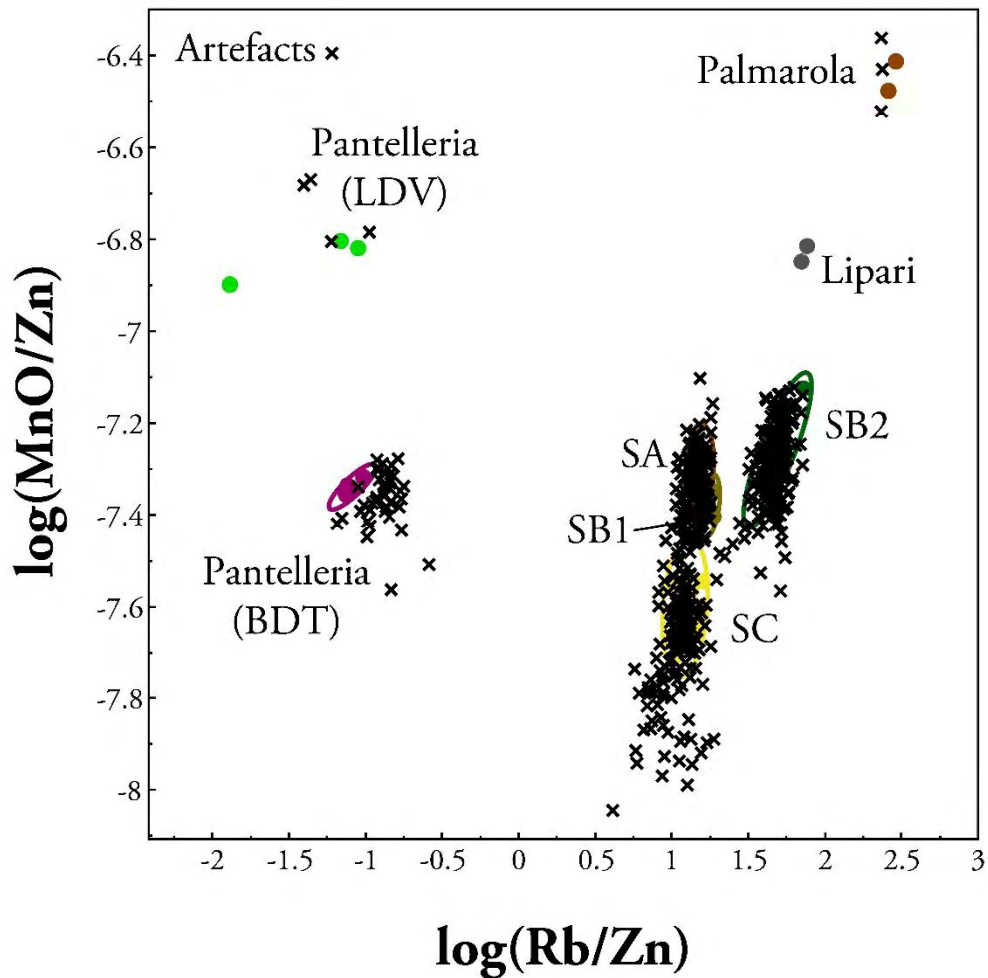


Figure 4.11. Comparison of the $\log(\text{Rb}/\text{Zn})$ and $\log(\text{MnO}/\text{Zn})$ ratios obtained by PIXE (CENBG, AIFIRA) for 55 geological samples from the Western Mediterranean area (see Lugliè *et al.*, 2007, 2008a, 2009; Mulazzani *et al.*, 2010; Poupeau *et al.*, 2000) and 675 archaeological samples from Sardinia, Southern France, Corsica, and Tunisia. 99 % density ellipses. Bressy *et al.*, 2008; Le Bourdonnec, 2007; Le Bourdonnec *et al.*, 2010, 2015a, 2015b; Lugliè *et al.*, 2007, 2008b, 2008a, 2009; Poupeau *et al.*, 2000; and unpublished data.

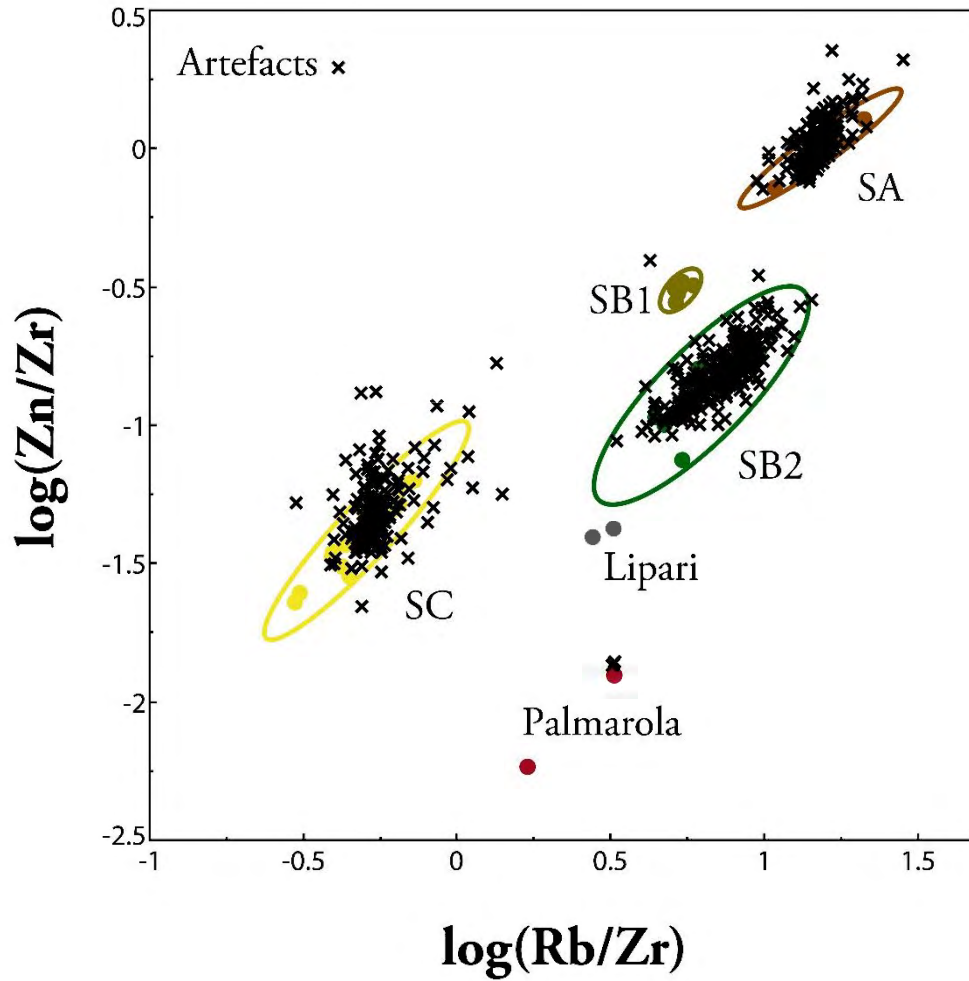


Figure 4.12. Comparison of the $\log(\text{Rb}/\text{Zr})$ and $\log(\text{Zn}/\text{Zr})$ ratios obtained by PIXE (CENBG, AIFIRA) for 44 geological samples (99 % density ellipses) (Lugliè *et al.*, 2007, 2008a, 2009 ; Poupeau *et al.*, 2000) and 626 archaeological samples (Bressy *et al.*, 2008; Le Bourdonnec 2007; Le Bourdonnec *et al.*, 2010, 2015b; Lugliè *et al.*, 2007, 2008b, 2008a, 2009; Poupeau *et al.*, 2000 and unpublished data).

4.3.6. LA-ICP-MS

Much like the PIXE, LA-ICP-MS is a less available, more expensive geochemical characterisation technique. However, it has several advantages that make it an ideal complement to other, more easily accessible methods. LA-ICP-MS is considered a ‘virtually’ non-destructive technique, *i.e.* the ablation performed is invisible to the naked eye (between 20 and 200 μm width). This sampling procedure preserves the integrity of the sample, allowing for further characterisation analyses with other methods, but also use-wear and typo-technological studies, or even a potential exhibition in a museum. Albeit subject to controversy, the ablation process presents the advantage to overcome eventual surface alterations present on the sample. Furthermore, the area required is so small that it increases our chances to analyse samples with a relatively irregular surface; this is also greatly facilitated by the live image of the sample provided by the camera located in the ablation chamber, which allows choosing the most suitable – *i.e.* flat and unaltered – zone for the ablation.

The LA-ICP-MS also delivers a fast analysis (only a few minutes per sample) with limited sample manipulations, since up to 100 samples can be placed at the same time in our chamber cell (15 × 15 cm), depending on their size. It produces highly precise and accurate results (Gratuze *et al.*, 2001) and offers the ability to measure up to 30 elements with very low detection limits (Russo *et al.*, 2002).

The protocol developed during the last two years by our research team at the SOLARIS laboratory at Southern Cross University, using an ESI (Electro Scientific Industries, Inc.) NWR213 Laser Ablation System (solid state Nd-YAG deep UV laser [213 nm]) coupled to an Agilent 7700× ICP-MS, is tailored to the analysis of Western Mediterranean and Aegean obsidians (Orange *et al.*, 2016, **Chapter 5**). Taking into account the major issues reported to occur with LA-ICPMS analysis such as elemental fractionation (see *e.g.*

Jackson, 2001; Russo *et al.*, 2002; Speakman and Neff, 2005), our protocol uses ablation lines and measures 14 isotopes (^{28}Si , ^{45}Sc , ^{66}Zn , ^{85}Rb , ^{88}Sr , ^{89}Y , ^{90}Zr , ^{93}Nb , ^{133}Cs , ^{137}Ba , ^{146}Nd , ^{147}Sm , ^{208}Pb , ^{232}Th , and ^{238}U) to distinctly discriminate between the sources, and to attribute artefacts to those sources.

In less than 2 years, 175 geological samples from the Western Mediterranean and Aegean areas, as well as 538 artefacts from Corsican Neolithic sites were successfully characterised with this new optimised protocol, as shown here by a simple binary diagram opposing the logarithmic transformation of the ($^{88}\text{Sr}/^{93}\text{Nb}$) and ($^{133}\text{Cs}/^{93}\text{Nb}$) ratios (Figures 4.13 and 4.14).

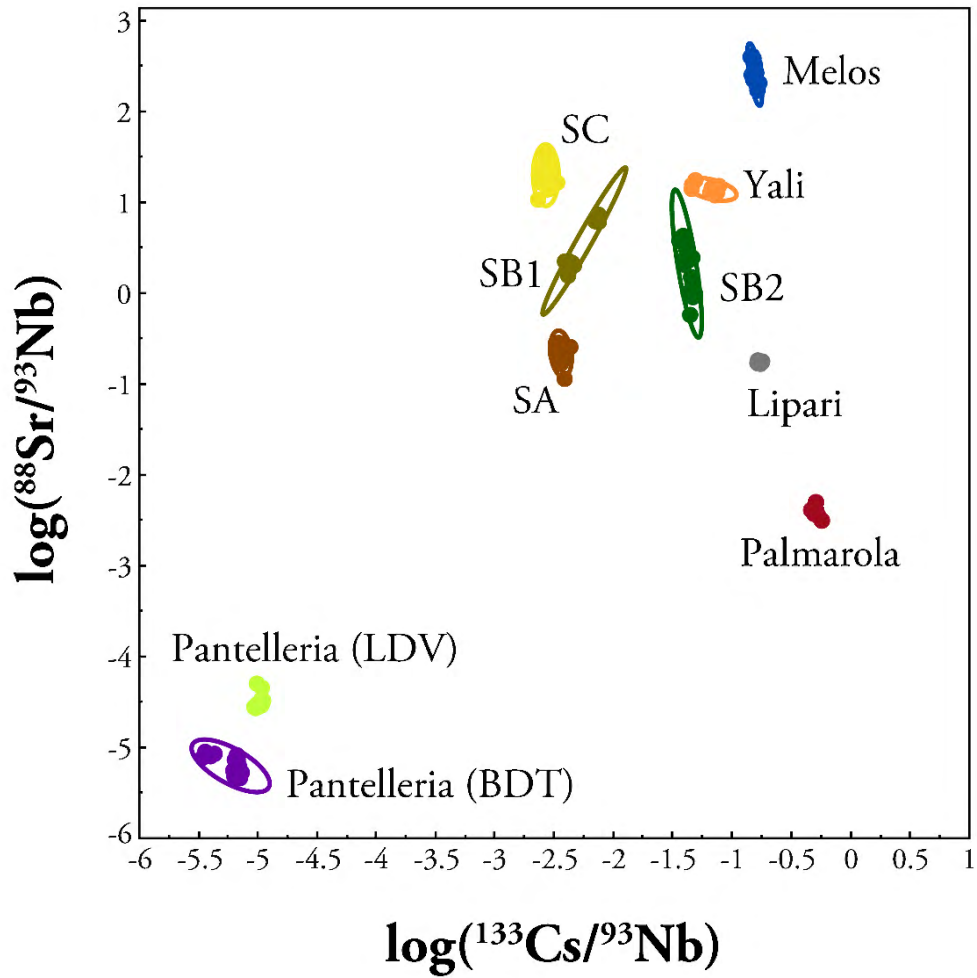


Figure 4.13. Comparison of the $\log(^{133}\text{Cs}/^{93}\text{Nb})$ and $\log(^{88}\text{Sr}/^{93}\text{Nb})$ ratios obtained by LA-ICP-MS (SOLARIS, SCU) for 175 geological samples from the Western Mediterranean and the Aegean area. 99 % density ellipses. Orange *et al.*, 2016 (Chapter 5).

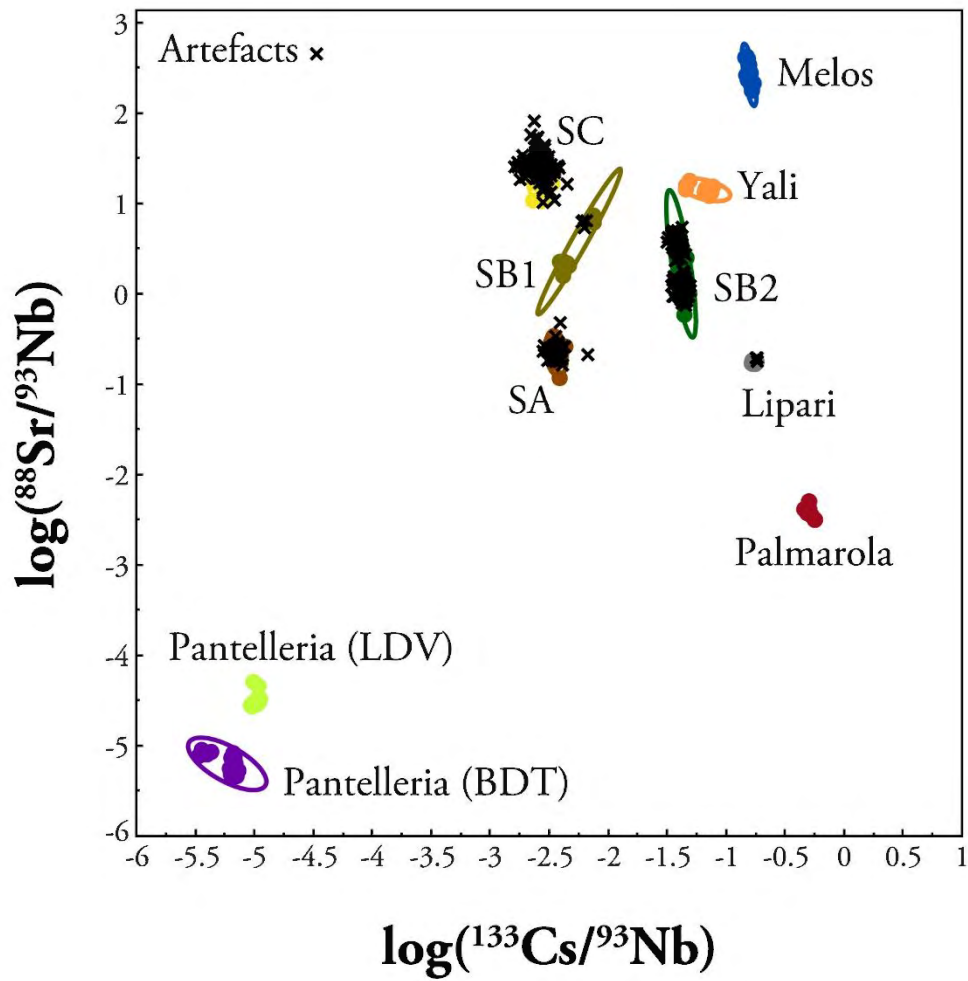


Figure 4.14. Comparison of the $\log(^{133}\text{Cs}/^{93}\text{Nb})$ and $\log(^{88}\text{Sr}/^{93}\text{Nb})$ ratios obtained by LA-ICP-MS (SOLARIS, SCU) for 175 geological samples from the Western Mediterranean and the Aegean area (Orange *et al.*, 2016 [Chapter 5]) and 538 archaeological samples (Neolithic levels, Corsica). 99 % density ellipses.

4.4. Discussion

When designing an obsidian sourcing study, several objectives have to be fulfilled:

- A diachronic and synchronic selection of well-documented assemblages
- An exhaustive characterisation of those assemblages
- A non-destructive or partially/virtually non-destructive analysis.

These objectives ensure that (a) the produced results are included in the general archaeological debate, (b) conclusions can be made on the overall obsidian economy of the site, and (c) the integrity of the archaeological samples is preserved and further analyses (use-wear, typo-technology, *etc.*) can still be performed on the artefacts when returned to the archaeologist.

To this end, a number of interdependent challenges and decisions that arise from either the assemblage's characteristics or the project's specifics, and constituting the limiting factors of the study, must be considered:

- Availability of the assemblage – determines if the samples can be analysed in the laboratory or if an in-situ analysis is required
- Budget and deadline
- Number of samples within the assemblage
- Samples' size, geometry, and surface state (possible alterations, weathering)
- Type of analysis requested by the Archaeologist/Heritage authorities– destructive or non-destructive
- Geographical area – chosen method (or synergies between methods) will depend on the 'geochemical complexity' of the potential sources considered
- Availability of the instrument(s)

Some of those considerations will deeply influence the choice of the characterisation method, since each has its own limitations and advantages. Designing an analytical strategy implies to take into consideration each technique's capacities to achieve the characterisation of every artefact regardless of its size, shape or surface state. This is the concept summarised in **Figure 4.15**.

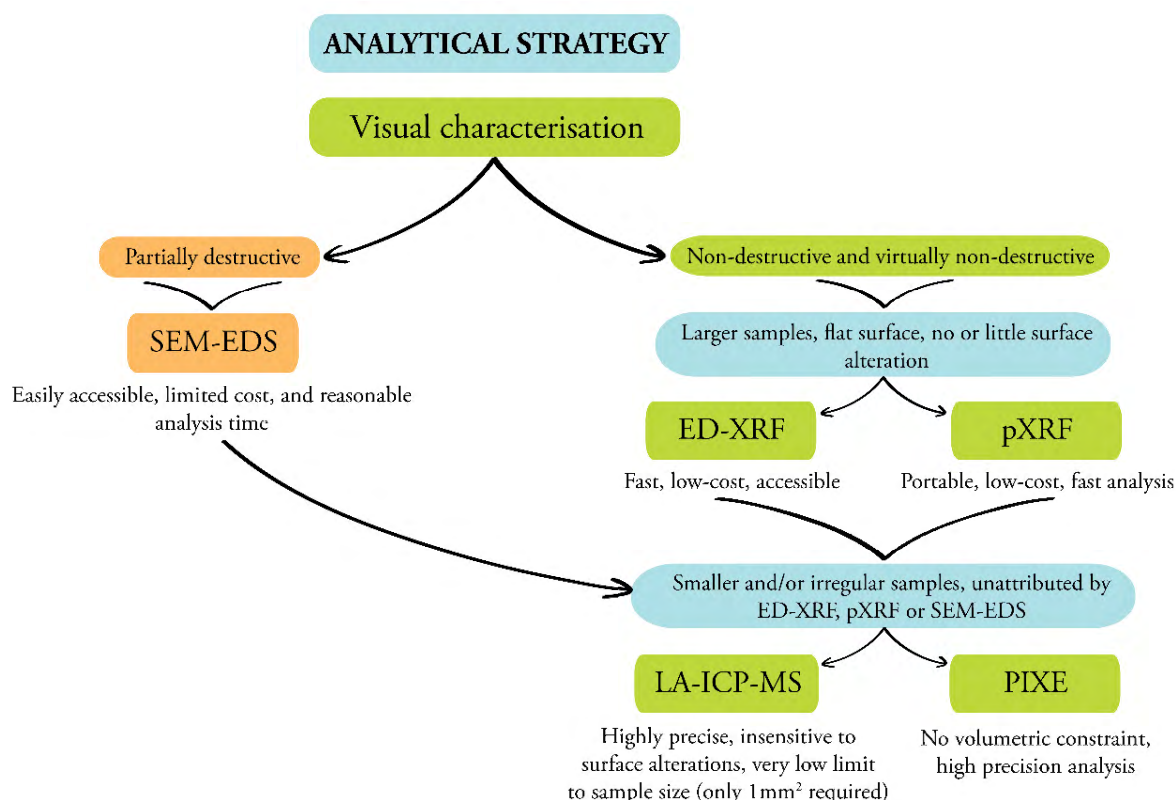


Figure 4.15. Concept and unfolding of the analytical strategy for obsidian sourcing studies.

The first step of our analytical strategy is to consider visual sourcing, easily available within our research group (CL). As described previously, this method can allow an initial screening and sorting of an assemblage, without any further instrumentation other than the naked eye of an experimented observer. The synergy with typo-technological studies

is advantageous because the study of the assemblage will drive an eventual sampling, or reveal the refitting of some artefacts, thus reducing the required analyses. It also helps to obtain an idea on all the samples' size, shape and surface state for further analysis. Any sample that can be attributed to a potential source can then be set aside, while smallest samples or those presenting a high thickness and/or surface alterations, preventing an easy visual characterisation can be redirected to analytical techniques.

If the archaeologist allows a partially destructive analysis, the relatively flat samples exempt from major surface alterations and of sufficient dimensions can be analysed by SEM-EDS. If a non-destructive approach is recommended, ED-XRF or pXRF methods are primarily considered, due to their availability and relatively limited cost. Nevertheless, most assemblages also present small, thin, irregular and/ or altered artefacts that cannot be characterised by the aforementioned methods. For those, analyses by LA-ICP-MS or PIXE have to be conducted. Mainly, the PIXE presents the advantage of having no volumetric constraint, while the only real limitation with the LA-ICP-MS is the size of the chamber in the laser ablation system.

The flexibility acquired by this multi-method strategy gives researchers the possibility to privilege the most important practical 'parameter' in each study, be it the cost of the analyses (fixed by the budget) or the timeframe (when a deadline has to be met). More importantly, relying on a flexible analytical strategy allows for an exhaustive characterisation of the studied assemblages. In our case, it enabled the successful sourcing of close to 10,000 archaeological objects in the last decade (see **Table 4.1**). One can argue why exhaustiveness is important or not, but we firmly believe that each artefact has 'a story to tell'. Several studies indeed indicated that isolated obsidian artefacts could originate from a different source than the rest of the assemblage (Orange *et al.*, 2013; Carter *et al.*, 2013, *inter alia*). Once coupled with the typo-technological data, such epiphenomenon can provide substantial information on the population under study, in

addition to what has been learnt from more common consumption and procurement patterns, *e.g.* a connection with a different population or contemporary site.

Table 4.1. Summary table relating the number of archaeological samples (artefacts) analysed with each sourcing method available within our research group, *i.e.* visual characterisation, SEM-EDS, ED-XRF, pXRF, PIXE, and LA-ICP-MS.

Sourcing method	Number of artefacts analysed
Visual characterisation	7459
SEM-EDS	223
ED-XRF	703
pXRF	343
PIXE	675
LA-ICP-MS	538
TOTAL	9941

The potential of analytical strategies also depends on (and calls for) collaborative projects. Each researcher within the research group might be part of a different university and/or a different department (Geology, Archaeology, Anthropology, GeoScience, Chemistry, *etc.*), thus giving access to various laboratories and instrumentations. Most importantly, such diversity in the researchers' specialties and affiliations allows for multidisciplinary projects, where complementary fields of expertise are brought together to answer a more general archaeological question. Much like the complementarity of the methods themselves, the complementarity of the different skills certainly make a substantial difference to the way we consider and 'make' research, allowing to take it a few steps further (see *e.g.* Binder *et al.*, 2011). In all cases, sourcing results should not be used and interpreted by themselves: a thorough typological and technological study

should always accompany those results (Poupeau *et al.*, 2007; Le Bourdonnec, 2007). Finally, the adoption of such analytical strategy naturally raises and forces the issue of inter-comparability of the results. A thorough control of the method's reliability (accuracy, precision, reproducibility; see Hughes, 1998; Frahm, 2012d) through the use of international standards and regular checks is indeed required if one wants to be able to compare the obtained compositions and provenance assignments (see Speakman and Shackley, 2013), but also if we want to provide results that can be fully used in future studies. Our methods' validity and reliability has been demonstrated numerous times in our work (Le Bourdonnec *et al.*, 2010; Poupeau *et al.*, 2010b; Orange *et al.*, 2016 [Chapter 5], *inter alia*).

4.5. Conclusions

As early as 1984, Francaviglia drew attention to the fact that there is no ideal method that would solve every issue encountered in the field of obsidian sourcing. Again in Shackley, (1998), Shackley raised the case, admitting that “[...] *the problem design and the level of precision needed to address that design will determine which instrument is the best for a given project.*” (p. 7). The concept of analytical strategy introduced by our research group is thus not new, but it remains to be systematically applied. Nonetheless, there is nowadays a general awareness that the archaeological question should be at the centre of our preoccupations.

Contrary to what happened in the past, the pursuit for more efficient and more precise sourcing techniques (see *e.g.* Frahm and Feinberg, 2013; Kudriavtsev *et al.*, 2015; Yi and Jwa, 2016), the reassessment of ‘older’ methods (Frahm, 2012c), or even the multiplication of pXRF applications across the world (Craig *et al.*, 2007; Jia *et al.*, 2010; Burley *et al.*, 2011; Sheppard *et al.*, 2011; Milić, 2014, Neri *et al.*, 2015, *i.a.*) are not

conducted self-sufficiently anymore, *e.g.* for the only purpose of method development. This is an essential turn in the history of our field, one which can only help increase our understanding of the techno- economic behaviour of past populations.

In conclusion, when focusing on an archaeological question the emphasis should be put on the design of a flexible analytical strategy customised for each specific and particular lithic assemblage. This type of approach has been adopted by our research group since 2003, and is reflected in the various studies published since (see *e.g.* Bressy *et al.*, 2008; Carter *et al.*, 2008; Lugliè *et al.*, 2008a; Orange *et al.*, 2013; Le Bourdonnec *et al.*, 2014). As explained above, this facilitates the exhaustive characterisation of lithic assemblages, while optimizing both the time and cost of the analyses. It also allows for a cross-validation of the results when the same samples can be analysed by two or more methods, and most importantly initiate and maintain national and international collaborations between laboratories. Last but not least, we must insist again on the fact that the use of an analytical strategy is quite useless if not applied to well-documented assemblages, and fully integrated with typological and technological study of those assemblages (Poupeau *et al.*, 2009; Le Bourdonnec, 2007), as it has already been the case in several studies (see *e.g.* Lugliè *et al.*, 2007, 2009; Carter *et al.*, 2006; Gibaja *et al.*, 2013; Le Bourdonnec *et al.*, 2014).

While the general picture of obsidian diffusion and consumption in the Western Mediterranean is slowly being reconstituted (see Lugliè, 2012), further studies are constantly required to refresh and supplement our view of this particular phenomenon. This paper has shown how the adoption of analytical strategies can undeniably help optimise obsidian sourcing studies conducted in this aim.

Acknowledgements

The authors would like to thank all participants to the projects mentioned in this paper. At the IRAMAT-CRP2A, this concerns in particular Yannick Lefrais for his management of the SEM-EDS, Brigitte Spiteri for the sample preparation, and Pierre Machut. At the IRAMAT-LMC, we wish to thank Philippe Dillmann for his contribution to pXRF experiments. The authors are also grateful to present and former members of the CENBG for their precious help during the PIXE analyses: Philippe Alfaut, Matthieu Compin, Laurent Daudin, Philippe Moretto, Laurent Serani, and Stéphanie Sorieul. At Arcane (Gradignan, France), the authors thank Hervé Guegan, Quy Le Minh, and Benoît Ridard. Finally, the authors wish to express their gratitude to Thomas Calligaro, Jean- Claude Dran, Thiéry Guillou, Quentin Lemasson, Brice Moignard, Claire Pacheco, Laurent Pichon, and Joseph Salomon† from the C2RMF.

Marie Orange's Ph.D. is funded by a Postgraduate scholarship from Southern Cross University and by part of an Australian Research Council discovery grant [DP140100919]. This project has been financially supported by the Conseil Régional d'Aquitaine, the ANR (French National Research Agency; no. ANR-10-LABX-52), and the Université Bordeaux Montaigne PSE (Politique Scientifique d'Établissement). Part of the PIXE measures at AGLAE were funded by the Eu-Artech (ref. 06–05) and Charisma (ref 10–21) European programs.

Chapter 5

Improving LA-ICP-MS protocol for obsidian sourcing studies

Among the methods available to our research group presented in **Chapter 4**, the LA-ICP-MS has been at the centre of this research project. Based on previous studies employing this technique and drawing from the recent reviews of its application in the field (Speakman and Shackley, 2005), our objective was to design an analysis protocol specific to obsidian sourcing studies in the Western Mediterranean area.

Mainly, this approach aimed to ensure the reliability (accuracy and precision) of the data produced while optimising the time required for the analysis – time being a critical factor in most research projects. This was mostly achieved by reducing the list of elements measured, which was condensed to 15 when most studies measure up to 30 (see *e.g.* Barca *et al.*, 2007). Within this research project we reviewed the literature relevant to the Western Mediterranean area and noted that only a handful of elements were actually involved in the sources discrimination and the sourcing of archaeological samples (mainly Zn, Rb, Sr, Y, Zr, Cs, Ba, and Nd). Our protocol also enhances the sensitivity of our measures through the use of ablation lines instead of punctual ablations (widespread in obsidian sourcing studies, see *e.g.* Gratuze *et al.*, 2001). The use of ablation lines also addresses several analytical issues commonly encountered with LA-ICP-MS analyses, such as element fractionation or signal stability (Speakman and Shackley, 2005).

To illustrate the reliability of our analyses, our optimised protocol (named 'V2') was compared to:

- A protocol using ablation lines but measuring 30 isotopes (referred to as 'V1') – enabling the evaluation of the differences in sensitivity and accuracy between two protocols assaying a different number of isotopes;
- Previous studies delivering data on the BCR2-G (glass) standard – this allowed a check for any matrix-induced effects;
- Previous studies using different methods and presenting data on the SA, SB1, SB2, and SC obsidian types (Monte Arci source) – such data ensured the validity of our protocol for obsidian sourcing studies.

The contents of this chapter have been published in the STAR journal (doi:10.1080/20548923.2016.1236516).

Sourcing obsidian: a new optimised LA-ICP-MS protocol

Marie Orange¹, François-Xavier Le Bourdonnec², Anja Scheffers¹, Renaud Joannes-Boyau¹

¹ *Southern Cross GeoScience, Southern Cross University, Military Road, PO Box 157, Lismore, NSW, 2480, Australia*

² *IRAMAT-CRP2A, UMR 5060 CNRS-Université Bordeaux Montaigne, Maison de l'Archéologie, Esplanade des Antilles, 33607 Pessac, France*

Abstract

Laser Ablation-Inductively Coupled Plasma-Mass Spectrometry [LA-ICP-MS] is one of the most successful analytical techniques used in archaeological sciences. Applied to the sourcing of lithic raw materials, it allows for fast and reliable analysis of large assemblages. However, the majority of published studies omit important analytical issues commonly encountered with laser ablation. This research presents a new advanced LA-ICP-MS protocol developed at Southern Cross GeoScience (SOLARIS laboratory, Southern Cross University, Australia), which optimizes the potential of this cutting-edge geochemical characterization technique for obsidian sourcing. This new protocol uses ablation lines with a reduced number of assayed elements (specific isotopes) to achieve higher sensitivity as well as increased precision and accuracy, in contrast to previous studies working with ablation points and an exhaustive list of measured isotopes. Applied to obsidian sources from the Western Mediterranean region, the Carpathian basin, and the Aegean, the results clearly differentiate between the main outcrops, thus

demonstrating the efficiency of the new advanced LA-ICP-MS protocol in answering fundamental archaeological questions.

Statement of significance

Our new LA-ICP-MS protocol, specifically tailored for the geochemical sourcing of obsidian artefacts in the Western Mediterranean area, was developed at SOLARIS (Southern Cross GeoScience, Southern Cross University, Australia) with a top-of-the-range Agilent 7700x ICP-MS coupled to a an ESI NWR213 Laser Ablation System. Taking into account the common analytical issues encountered with the LA-ICP-MS technique, we focused on two parameters: the use of ablation lines instead of ablation points, and the development of a reduced list of measured isotopes. The use of ablation lines aims to compensate for any sample heterogeneity, achieve a higher count rate as well as a better signal stability, and also reduce laser-induced elemental fractionation. The measured isotopes have been carefully selected amongst the most efficient to discriminate between the different obsidian sources. This shortened list of isotopes achieves precise and accurate measurements with a higher sensitivity, and with the use of ablation lines, contributes to enhancing the potential of this geochemical characterization technique for obsidian sourcing.

Data availability

The LA-ICP-MS results for the obsidian geological samples from the Mediterranean area are available as supplementary data.

Keywords

LA-ICP-MS; Geochemistry; Lithic sourcing; Obsidian; Archaeology; Western Mediterranean

5.1. Introduction

Geochemical characterization methods currently used for obsidian sourcing studies in archaeology include: X-Ray Fluorescence spectroscopy [XRF] (Carter and Shackley, 2007; Freund, 2014 *i.a.*), Particle Induced X-ray Emission spectroscopy [PIXE] (Constantinescu *et al.*, 2013; Le Bourdonnec *et al.*, 2015c), Laser Ablation-Inductively Coupled Plasma-Mass Spectrometry [LA-ICP-MS] (Binder *et al.*, 2011; Reepmeyer *et al.*, 2011), Scanning Electron Microscopy coupled to energy dispersive X-ray spectroscopy [SEM-EDS] (Acquafredda and Muntoni, 2008; Le Bourdonnec *et al.*, 2010), and Instrumental Neutron Activation Analysis [INAA] (Santi *et al.*, 2010; Kuzmin and Glascock, 2014). Alternative characterization methods also exist that are based on the structural or magnetic properties of obsidian (McDougall *et al.*, 1983; Stewart *et al.*, 2003; Bellot-Gurlet *et al.*, 2004; Carter *et al.*, 2009; Frahm and Feinberg, 2013).

However, even non-destructive techniques have various limitations when applied to the analysis of archaeological samples (artefacts). Specifically, limitations may arise in relation to the size and shape (flatness) of the artefact (Davis *et al.*, 2011), the eventual surface, and by extent geochemical alterations (see Poupeau *et al.*, 2010b), and even the ability to discriminate between sources of a given geographical area (depending on the elements the chosen method can measure; see *e.g.* Orange *et al.*, 2013). Of the available methods, LA-ICP-MS is one of the more recent and most efficient tools, allowing a

virtually non-destructive multi-element analysis with high accuracy and precision in a short time period (Gratuze *et al.*, 2001; Barca *et al.*, 2007; Barca *et al.*, 2012).

Despite improved understanding of common analytical problems encountered with laser ablation (see Speakman and Neff, 2005) and the adoption of adequate protocols by several specialists in the field (see *e.g.* Speakman *et al.*, 2002, 2007; Glascock *et al.*, 2005; Tabares *et al.*, 2005), numerous LA-ICP-MS protocols for obsidian sourcing studies (*cf. e.g.* Gratuze, 1999; Barca *et al.*, 2007; Eerkens *et al.*, 2008) were developed disregarding some of these issues. Most studies still use discrete ablation points, despite the fact that use of ablation lines and rasters is a well-established means of overcoming elemental fractionation (Jackson, 2001), which is one of the main issues of LA-ICP-MS analysis. Lines and rasters also allow for a higher count rate, achieve better signal stability and help compensate for sample heterogeneity (Speakman and Neff, 2005). Most obsidian sourcing studies were also assaying up to 30 isotopes, when only a handful of these isotopes are typically used to discriminate between the obsidian sources and attribute the artefacts to those sources (see *e.g.* Carter *et al.*, 2006; Bellot-Gurlet *et al.*, 2008; Binder *et al.*, 2011).

Here we present, validate, and explain the rationale underlying a protocol designed to optimize the LA-ICP-MS technique for obsidian sourcing. Geological and archaeological obsidian samples were analysed as a means of testing this new protocol, which improves analytical sensitivity, accuracy, reliability, and efficiency (*i.e.* swiftness in regard to the aforementioned factors) by focusing on two main changes: (a) the use of a reduced list of assayed isotopes, and (b) the use of ablation lines instead of ablation points, as advised in earlier methodological studies.

5.2. Instrumentation and protocols

5.2.1. Instrumentation

SOLARIS consists of an ESI (Electro Scientific Industries, Inc.) NWR213 Laser Ablation System (solid state Nd-YAG deep UV laser [213 nm]) with a 150 mm x 150 mm high performance large format cell coupled to an Agilent 7700x ICP-MS. Data were acquired and treated using MassHunter Workstation software and calibration was performed with the NIST SRM 611 international standard [National Institute of Standards and Technology; Standard Reference Material]. An internal standardization was achieved using the NIST 613 international standard, which has a similar SiO₂ content to obsidian (generally > 70 wt %; see Heide and Heide, 2011), analyzed at the beginning and end of each run. Results obtained by ICP-MS on the ²⁸Si isotope are calibrated against the SiO₂ content of NIST 613 (72.1 %; see Jochum *et al.*, 2011).

5.2.2. V1 and V2 protocols

The hypothesis explored here is that a reduced number of assayed isotopes can achieve a better sensitivity. This led to the development and comparison of two different protocols: one commonly found in the literature (named V1) employs an exhaustive list of measured isotopes, the second – optimised (V2) – employs a reduced list of isotopes. The instrumental settings used for both protocols are summarized in the **Table 5.1**.

From this exhaustive list, 15 selected isotopes were measured in the V2 protocol: ²⁸Si, ⁴⁵Sc, ⁶⁶Zn, ⁸⁵Rb, ⁸⁸Sr, ⁸⁹Y, ⁹⁰Zr, ⁹³Nb, ¹³³Cs, ¹³⁷Ba, ¹⁴⁶Nd, ¹⁴⁷Sm, ²⁰⁸Pb, ²³²Th, and ²³⁸U. These isotopes were selected on the basis of: (a) the level of accuracy obtained, (b) their occurrence in previous obsidian sourcing studies, and (c) their potential to discriminate between obsidian sources as per these previous studies. Selecting isotopes measured by

other research groups helped us to compare the results of this study (isotopic content, accuracy, or precision) to the results from other instrumentations and protocols (see 5.3.2 and 5.3.3). The V1 protocol included 30 specific isotopes to analyze: ^7Li , ^{27}Al , ^{28}Si , ^{31}P , ^{39}K , ^{43}Ca , ^{47}Ti , ^{55}Mn , ^{66}Zn , ^{69}Ga , ^{78}Se , ^{85}Rb , ^{88}Sr , ^{89}Y , ^{90}Zr , ^{93}Nb , ^{133}Cs , ^{137}Ba , ^{139}La , ^{140}Ce , ^{146}Nd , ^{147}Sm , ^{157}Gd , ^{165}Ho , ^{166}Er , ^{178}Hf , ^{181}Ta , ^{208}Pb , ^{232}Th , and ^{238}U .

Table 5.1. LA-ICP-MS instrumental parameters for the V1 and V2 protocols.

	Instrumental settings	
	<i>Geological samples</i>	<i>Archaeological samples</i>
Plasma gas	Argon	Argon
Carrier gas	0.81 L/min	0.81 L/min
Laser output wavelength	213 nm	213 nm
Laser output energy	40 % (≈ 0.044 mJ/pulse)	80 % (≈ 0.389 mJ/pulse)
Fluence	< 3 J/cm ²	< 40 J/cm ²
Sampling depth	6.6 mm	6.6 mm
Ablation mode	Line	Line
Line length	1.2 mm	0.6 mm
Spot size	60 μm	40 μm
Scan speed	10 $\mu\text{m}/\text{sec}$	5 $\mu\text{m}/\text{sec}$
Pre-ablation	No	No
Sampling time	2:15 min	2:15 min
Ablation depth	5 μm	10 μm
Frequency	10 Hz	10 Hz
RF power	1380 W	1380 W
RF matching	1.36 V	1.36 V
Extraction lens 1 voltage	0.0 V	0.0 V
Extraction lens 2 voltage	-190 V	-190 V
Omega bias -cs	-90 V	-90 V
Omega lens -cs	9.2 V	9.2 V

5.2.3. Laser ablation parameters

As previously mentioned, the use of ablation lines in LA-ICP-MS analyses has been proven to reduce element fractionation, correct for sample heterogeneity and achieve higher count rates (Speakman and Neff, 2005). To our knowledge, such an ablation protocol has rarely been applied to obsidian sourcing (although see *e.g.* Speakman *et al.*, 2002; Tabares *et al.*, 2005). Usually, the sample ablation consists of several ablation points of a diameter ranging between 40 to 100 μm , with a depth reaching up to 250 μm , and an acquisition time of about 60 s per point (see *e.g.* Gratuze *et al.*, 2001; Barca *et al.*, 2007; Khalidi *et al.*, 2010). In this study, we opted to use ablation lines in order to optimize the LA-ICP-MS technique. With our protocol designed for both geological and archaeological obsidian samples, the ablation settings have been tailored specifically for each sample type. The same instrumental parameters were utilized in both cases (see **Table 5.1**).

Geological samples

The geological samples were cut and embedded in an epoxy resin (Epofix, Struers), then polished down to $\frac{1}{4}$ μm using a polycrystalline diamond solution (see polishing protocol and scans of the resins in **Appendix C**). Before analysis, the geological samples were rinsed in distilled water in an ultrasonic bath for five minutes, then rinsed consecutively with running tap water, distilled water, and alcohol. On these polished sections, an ablation line of 1.2 mm with a scan speed of 10 $\mu\text{m}/\text{sec}$ achieved a 2:15 min signal, and a spot size of 60 μm width and 5 μm depth was used to attain the best results possible. A laser output of 40 % [energy per pulse \approx 0.044 mJ] was selected.

Archaeological samples

For the archaeological samples, the protocol was adapted to minimize the impact of ablation and thus maximize the preservation of the artefact. Accordingly, the ablation line was reduced to 40 μm wide (thinner than human hair) and 0.6 mm long, making it barely visible to the naked eye and considered as virtually non-destructive. The depth of the line was increased to 10 μm in order to minimize the effects of any geochemical surface alteration (often present on artefacts; see Poupeau *et al.*, 2010b). To compensate for a loss of signal due to the shorter and narrower ablation line, the scan speed was lowered to 5 $\mu\text{m}/\text{sec}$ and the output amplified to 80 % [energy per pulse \approx 0.389 mJ] instead of 40 % as with the geological samples. Preparation of the archaeological samples before analysis involved cleaning in distilled water in an ultrasonic bath for five minutes, followed by successive thorough rinses of distilled water, alcohol, and acetone.

5.3. Results and discussion

5.3.1. Sensitivity: V1 vs. V2 protocol

In order to compare the sensitivity of our V1 and V2 protocols, a series of measurements were obtained on the same day, under similar plasma conditions on the NIST 613 SRM. For all of the isotopes common to both protocols (^{66}Zn , ^{85}Rb , ^{88}Sr , ^{89}Y , ^{90}Zr , ^{93}Nb , ^{133}Cs , ^{137}Ba , ^{146}Nd , ^{147}Sm , ^{208}Pb , ^{232}Th , and ^{238}U), a simple comparison of the raw counts shows that higher count rates were achieved with the second protocol (**Table 5.2**), and so a higher sensitivity (raw count rate/expected concentration in ppm) was established. Indeed, since fewer isotopes were selected in the V2 protocol but the total acquisition time per line stays the same (2:15 min), each isotope signal will be acquired for a longer

period (2:15 min divided by 15 instead of 30). Therefore, higher count rates were achieved, resulting in higher sensitivity.

5.3.2. Reliability of the V2 protocol

A total of 200 geological samples and 538 archaeological samples from four sites (Orange *et al.*, submitted for publication; Orange *et al.*, in prep.; Mazet *et al.*, in prep.) was analyzed with the V2 protocol during a total of 25 runs. In order to assess the accuracy, precision, and reproducibility of our analyses, the NIST 613 Standard Reference Material [SRM], with a nominal composition of 72.1 % SiO₂, 13.7 % Na₂O, 11.9 % CaO and 2.03 % Al₂O₃ (mass fraction, mg/kg), was measured at the beginning and end of each run. The BCR-2G glass standard was also analyzed to check for any matrix-induced effect in our V2 protocol.

Table 5.2. Comparison of the raw counts and sensitivity results for ⁶⁶Zn, ⁸⁵Rb, ⁸⁸Sr, ⁸⁹Y, ⁹⁰Zr, ⁹³Nb, ¹³³Cs, ¹³⁷Ba, ¹⁴⁶Nd, ¹⁴⁷Sm, ²⁰⁸Pb, ²³²Th, and ²³⁸U between the V1 and V2 protocols. Certified concentrations: GeoRem. The number of rows [Nb rows] indicates the number of measurements obtained within a single ablation line, after statistical treatment with removal of the outliers with JMP statistical software (SAS).

	V1 - NIST 613 (cps)	V2 - NIST 613 (cps)	Certified concentration (ppm)	Sensitivity V1 protocol	Sensitivity V2 protocol
<i>Nb rows</i>	35	77			
⁶⁶ Zn	351	458	39.1	9	12
⁸⁵ Rb	3509	3844	31.4	112	122
⁸⁸ Sr	15212	16460	78.4	194	210
⁹³ Nb	5935	6490	38.9	153	167
¹³³ Cs	9046	10023	42.7	212	235

¹³⁷ Ba	1124	1247	39.3	29	32
¹⁴⁶ Nd	1893	2043	35.5	53	58
¹⁴⁷ Sm	1677	1805	37.7	44	48
²⁰⁸ Pb	4873	5314	38.57	126	138
²³² Th	7304	8230	37.79	193	218
²³⁸ U	9731	10839	37.4	260	290

Accuracy

A total of 50 measurements of the NIST 613 SRM were obtained at the start and end of each of the 25 analysis runs (see complete data in **Appendix F**), and used to determine the accuracy of the V2 protocol. The accuracy was calculated as the relative error between the contents acquired with this research protocol and reference values from the GeoRem database (Max Planck Institute's Geochemical Database for Reference Materials and Isotopic Standards), and reported in **Table 5.3**.

For ²³²Th, the relative error does not exceed 6 %, and for the majority of isotopes the relative error is below 5 %, and less than 3 % for five of them (⁸⁵Rb, ⁸⁸Sr, ¹³⁷Ba, ²⁰⁸Pb and ²³⁸U). To further our assessment of the V2 protocol accuracy, we also compared the relative error obtained on the same number of measurements (n=8) on the NIST 613 standard between the V1 and V2 protocol. For the majority of isotopes assessed, the relative error here again calculated against the reference values of the GeoRem database is lower with the V2 protocol results than the V1 protocol results (see **Table 5.3**). This new protocol is therefore producing accurate results while achieving higher sensitivity for isotope discrimination.

Table 5.3. Comparison of the ^{45}Sc , ^{66}Zn , ^{85}Rb , ^{88}Sr , ^{89}Y , ^{90}Zr , ^{93}Nb , ^{133}Cs , ^{137}Ba , ^{146}Nd , ^{147}Sm , ^{208}Pb , ^{232}Th and ^{238}U contents with uncertainty (± 1 standard deviation) obtained on the NIST SRM 613 standard between the V2 protocol (total number of measurements = 50) and the reference values recommended by the NIST and the GeoRem database. The concentrations obtained for each isotope (with the exception of ^{45}Sc , which was unassessed with the V1 protocol) and corresponding relative error are also compared between the V1 and V2 protocol for the same number of measurements (n=8). Relative error (Rel. err.) calculated in comparison with the GeoRem reference values. Concentrations (Conc.) are in ppm.

	NIST	GeoRem	V2 (50 measures)		V1 (8 measures)		V2 (8 measures)	
	Conc.	Conc.	Conc. (1sd)	Rel. err.	Conc.	Rel. err.	Conc.	Rel. err.
^{45}Sc		39.9(2.5)	38.0(1.3)	4.8 %				
^{66}Zn		39.1(1.7)	41.3(3.4)	5.7 %	37.2	4.9 %	38.1	2.6 %
^{85}Rb	31.4(0.4)	31.4(0.4)	31.0(0.9)	1.3 %	32.2	2.5 %	31.2	0.6 %
^{88}Sr	78.4(0.2)	78.4(0.2)	78.0(3.5)	0.5 %	81.1	3.4 %	77.9	0.6 %
^{89}Y		38.3(1.4)	36.3(1.6)	5.1 %	36.4	5.0 %	35.6	7.0 %
^{90}Zr		37.9(1.2)	36.2(1.6)	4.4 %	34	10.3 %	35.2	7.1 %
^{93}Nb		38.9(2.1)	37.2(0.8)	4.3 %	38.2	1.8 %	36.7	5.7 %
^{133}Cs		42.7(1.8)	40.7(1.1)	4.7 %	43.3	1.4 %	40.6	4.9 %
^{137}Ba	38.6(2.6)	39.3(0.9)	39.3(1.3)	0.05 %	40	1.8 %	39.3	0 %
^{146}Nd	36	35.5(0.7)	33.6(0.8)	5.4 %	33.1	6.8 %	33.6	5.4 %
^{147}Sm	39	37.7(0.8)	35.9(1.1)	4.8 %	34.8	7.7 %	35.8	5.0 %
^{208}Pb	38.57(0.2)	38.57(0.2)	39.67(1.76)	2.9 %	39.3	1.9 %	38	1.5 %
^{232}Th	37.79(0.08)	37.79(0.08)	35.54(1.30)	6.0 %	35.9	5.0 %	34.9	7.6 %
^{238}U	37.38(0.08)	37.38(0.08)	36.41(0.59)	2.7 %	38.8	3.7 %	36.6	2.1 %

Precision

To compare the precision of the analysis between the exhaustive (V1) and optimised (V2) protocols, the standard error of the mean was calculated for each of the 13 isotopes assayed in both protocols (8 measurements). The results are presented in **Table 5.4** and show, for each isotope, a considerably lower standard error of the mean for the V2 protocol as well as a lower standard deviation – *i.e.* a higher precision of the measurements. This clearly reflects that a smaller number of isotopes assayed multiplies the measurement points, consequently increasing the precision. The same conclusion would be made if it was possible to compare our data to previous studies using several ablation points (data unavailable/unpublished), since an ablation line is in fact constituted of a series of points, *i.e.* about 70 to 80 in our V2 protocol, a quantity that would be difficult to reach in a reasonable time with punctual ablation ICP-MS analysis protocols.

As demonstrated in **Table 5.4**, only the ^{66}Zn isotope, which may have interferences with polyatomic structures (*e.g.* $^{50}\text{Ti}^{16}\text{O}$; see Evans and Giglio, 1993), presents a higher standard error of the mean than for the V1 protocol.

Table 5.4. Comparison of the standard error of the mean (Std. err. mean) of the concentrations obtained on the NIST SRM 613 international standard for the 13 isotopes common to the V1 and V2 protocols (^{66}Zn , ^{85}Rb , ^{88}Sr , ^{89}Y , ^{90}Zr , ^{93}Nb , ^{133}Cs , ^{137}Ba , ^{146}Nd , ^{147}Sm , ^{208}Pb , ^{232}Th , and ^{238}U). Average contents (Ave.) and standard deviations (Std. dev.) obtained on 8 measurements. Contents are in ppm.

	V1			V2		
	Ave. (n=8)	Std. dev.	Std. err. mean	Ave. (n=8)	Std. dev.	Std. err. mean
^{66}Zn	37.2	1.73	0.66	37.4	2.38	1.26
^{85}Rb	32.2	1.69	0.64	31.1	1.18	0.45
^{88}Sr	81.1	5.13	1.94	77.5	2.05	0.85
^{89}Y	36.4	2.57	0.97	35.7	1.72	0.64
^{90}Zr	34	2.42	0.91	35.3	1.61	0.58
^{93}Nb	38.2	2.31	0.87	36.6	0.72	0.31
^{133}Cs	43.3	3.58	1.35	40.5	1.13	0.46
^{137}Ba	40	2.02	0.76	39.3	0.99	0.38
^{146}Nd	33.1	1.83	0.69	33.5	0.55	0.23
^{147}Sm	34.8	1.83	0.69	35.9	1.15	0.43
^{208}Pb	39.3	1.57	0.59	38.3	1.53	0.51
^{232}Th	35.9	2.6	0.98	35	1.12	0.38
^{238}U	38.8	3.47	1.31	36.5	0.72	0.28

Reproducibility

The reproducibility of the analyses through time was also assessed and represents a crucial factor in archaeological studies, particularly to sourcing studies. Using the same international standard (NIST SRM 613) the evolution of the ^{66}Zn , ^{88}Sr , ^{133}Cs , ^{137}Ba , and ^{146}Nd concentrations was observed over a 6 month period, as illustrated in **Figure**

5.1 (23 measurements represented). The variations frequently remain within a 2σ range, thus attesting to the repeatability of these measurements.

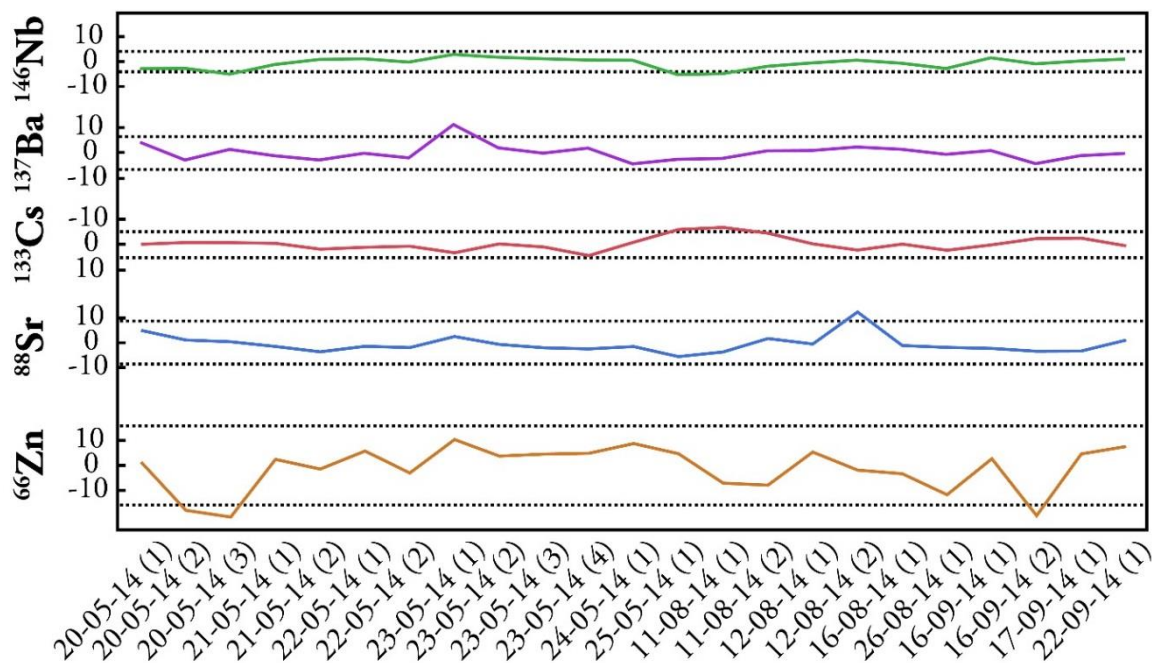


Figure 5.1. Evolution of the measured ^{66}Zn , ^{88}Sr , ^{133}Cs , ^{137}Ba , and ^{146}Nd contents on the NIST SRM 613 international standard over 5 months (23 measures represented). Data obtained by LA-ICP-MS with V2 protocol. The dotted lines represent the $\pm 2\sigma$ dispersion.

Matrix-induced effect and comparison to a common protocol

The BCR-2G standard (glass, basaltic composition; USGS, 2014) from the U.S. Geological Survey (USGS) was analyzed several times to control for matrix-induced effects (see complete data in **Appendix G**). The obtained average composition was compared against the USGS and GeoRem reference values, as well as against the values obtained by Barca *et alii* (2007) with LA-ICP-MS (see **Table 5.5**).

Table 5.5. Comparison of the measured ^{45}Sc , ^{66}Zn , ^{85}Rb , ^{88}Sr , ^{89}Y , ^{90}Zr , ^{93}Nb , ^{133}Cs , ^{137}Ba , ^{146}Nd , ^{147}Sm , ^{208}Pb , ^{232}Th , and ^{238}U concentrations and uncertainties (± 1 standard deviation) obtained on basalt USGS standard BCR-2G (glass) in a previous LA-ICP-MS study (Barca *et al.*, 2007), this study, and the reference values recommended by the USGS and the GeoRem database. The relative error (Rel. error) is calculated in comparison with reference values of the GeoRem database. In bold: isotopes for which this study achieves a higher accuracy compared to a previous LA-ICP-MS study (Barca *et al.*, 2007). Contents are in ppm.

Isotope	USGS	GeoRem	Barca <i>et al.</i> , 2007 (n=18)	Rel. error	This study (n=4)	Rel. error
^{45}Sc	33(2)	33(2)	35(1)	6.1 %	35(1)	6.1 %
^{66}Zn	127(9)	125(5)	152(12)	21.6 %	168(5)	34.4 %
^{85}Rb	48(2)	47(0.5)	48(1)	2.1 %	46(1)	2.1 %
^{88}Sr	346(14)	342(4)	325(7)	5.0 %	325(3)	5.0 %
^{89}Y	37(2)	35(3)	33(1)	5.7 %	34(1)	2.9 %
^{90}Zr	188(16)	184(15)	168(3)	8.7 %	186(7)	1.1 %
^{93}Nb		12.5(1)	11.5(0.4)	8.0 %	11.3(0.3)	9.6 %
^{133}Cs	1.1(0.1)	1.16(0.07)	1.13(0.09)	2.6 %	1.10(0.03)	5.2 %
^{137}Ba	683(28)	683(7)	642(27)	6.0 %	674(13)	1.3 %
^{146}Nd	28(2)	28.9(0.3)	28(1)	3.1 %	28.6(0.8)	1.0 %
^{147}Sm	6.7(0.3)	6.59(0.07)	6(0.3)	9.0 %	6.6(0.2)	0.2 %
^{208}Pb	11(2)	11(1)	10.6(0.9)	3.6 %	10.2(0.3)	7.3 %
^{232}Th	6.2(0.7)	5.9(0.3)	5.8(0.5)	1.7 %	6.0(0.2)	1.7 %
^{238}U	1.69(0.19)	1.69(0.12)	1.67(0.12)	1.2 %	1.68(0.06)	0.6 %

The accuracy was assessed as the relative error between the measured values and the reference values from the GeoRem database. Accurate results were obtained and the relative error remains systematically below 10 %, except for zinc concentration which appears problematic. Comparing this study with the ablation point protocol and an exhaustive isotope list protocol (Barca *et al.*, 2007), four isotopes were identified (^{66}Zn ,

^{93}Nb , ^{133}Cs and ^{208}Pb) with relatively higher accuracy; however, the optimal protocol (V2) achieved considerably better results on ^{89}Y , ^{90}Zr , ^{137}Ba , ^{146}Nd , ^{147}Sm and ^{238}U . The accuracy is comparable for the remaining isotopes (^{45}Sc , ^{85}Rb , ^{88}Sr and ^{232}Th).

5.3.3. Application to obsidian sourcing studies in the Western Mediterranean

Source discrimination and provenance attribution of artefacts

The viability of a specific method for obsidian sourcing does not only lie in its reliability (in which we entail sensitivity, precision, accuracy, and reproducibility; see *e.g.* Hughes, 1998; Frahm, 2012d for discussion), but also on its validity, *i.e.* its ability to distinguish between the relevant obsidian sources and to attribute obsidian artefacts from an assemblage to a specific source.

The concept of source is defined in this context as a specific geochemical signature and not as a geographical location (see Hughes and Smith, 1993). The primary known obsidian sources of the Western Mediterranean area, Carpathian basin, and Aegean area (**Figure 5.2**) were considered in this study to assess the validity of the V2 protocol for obsidian sourcing: Sardinia (sub-types SA, SB1, SB2 and SC; Lugliè *et al.*, 2006), Lipari (Chavez-Rivas *et al.*, 1991), Palmarola (Tykot *et al.*, 2005), Pantelleria (Balata dei Turchi and Lago di Venere; Francaviglia, 1988), Yali (Milić, 2014), Melos (Shelford *et al.*, 1982), Antiparos (Carter and Contreras, 2012) and the Carpathian sources (Bigazzi *et al.*, 1990). The complete dataset is presented in **Appendix D**.



Figure 5.2. Map of the main obsidian sources in the Mediterranean area: Monte Arci (Sardinia), Lipari, Palmarola, Pantelleria, Yali, Melos, Antiparos, and the Carpathians.

Using a log-ratio analysis of the compositional data (Aitchison, 1982), **Figure 5.3** displays a comparison between the $\log(^{133}\text{Cs}/^{93}\text{Nb})$ and the $\log(^{88}\text{Sr}/^{93}\text{Nb})$ ratios obtained with the V2 protocol on 200 geological samples. The choice of the ^{88}Sr , ^{93}Nb , and ^{133}Cs isotopes was motivated by two reasons: (a) they are often used in the discrimination of obsidian sources in the Western Mediterranean (*cf. e.g.* Barca *et al.*, 2007), and (b) their variation coefficient on the totality of the Western Mediterranean sources was among the highest, therefore allowing for a clearer graphical separation of the sources. As shown by the log-ratio analysis, the sources are clearly distinguished from one another, thus confirming the validity of the V2 protocol in the geographical area considered.

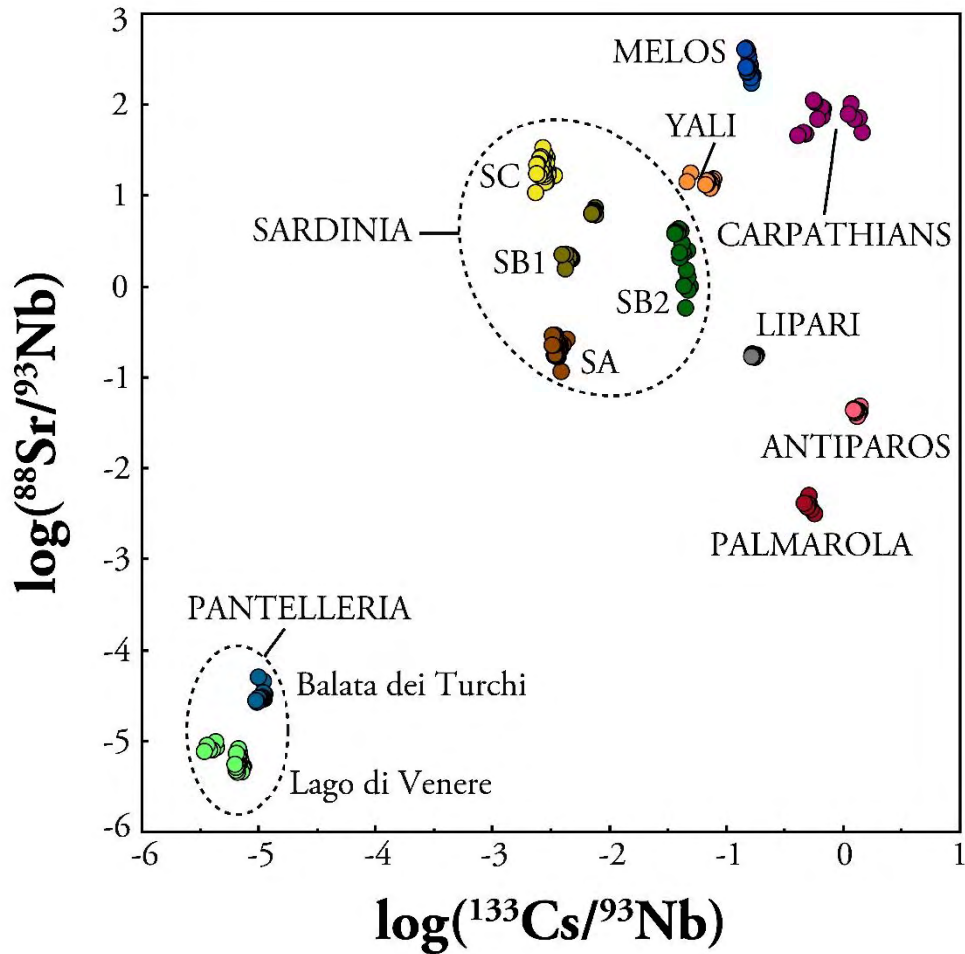


Figure 5.3. Comparison of $\log(^{133}\text{Cs}/^{93}\text{Nb})$ and the $\log(^{88}\text{Sr}/^{93}\text{Nb})$ ratios obtained by LA-ICP-MS (V2 protocol) on 200 geological samples from the Mediterranean region.

The validity of our protocol on the archaeological level, *i.e.* its capacity to attribute each artefact of an assemblage to a specific source, was assessed through the analysis of 538 archaeological samples from the Tyrrhenian area (Neolithic period). **Figure 5.4**, using here again a comparison between the $\log(^{133}\text{Cs}/^{93}\text{Nb})$ and the $\log(^{88}\text{Sr}/^{93}\text{Nb})$ ratios, shows the clear attribution of these artefacts to the sources of the Western Mediterranean (Sardinian sources of the Monte Arci, and Lipari).

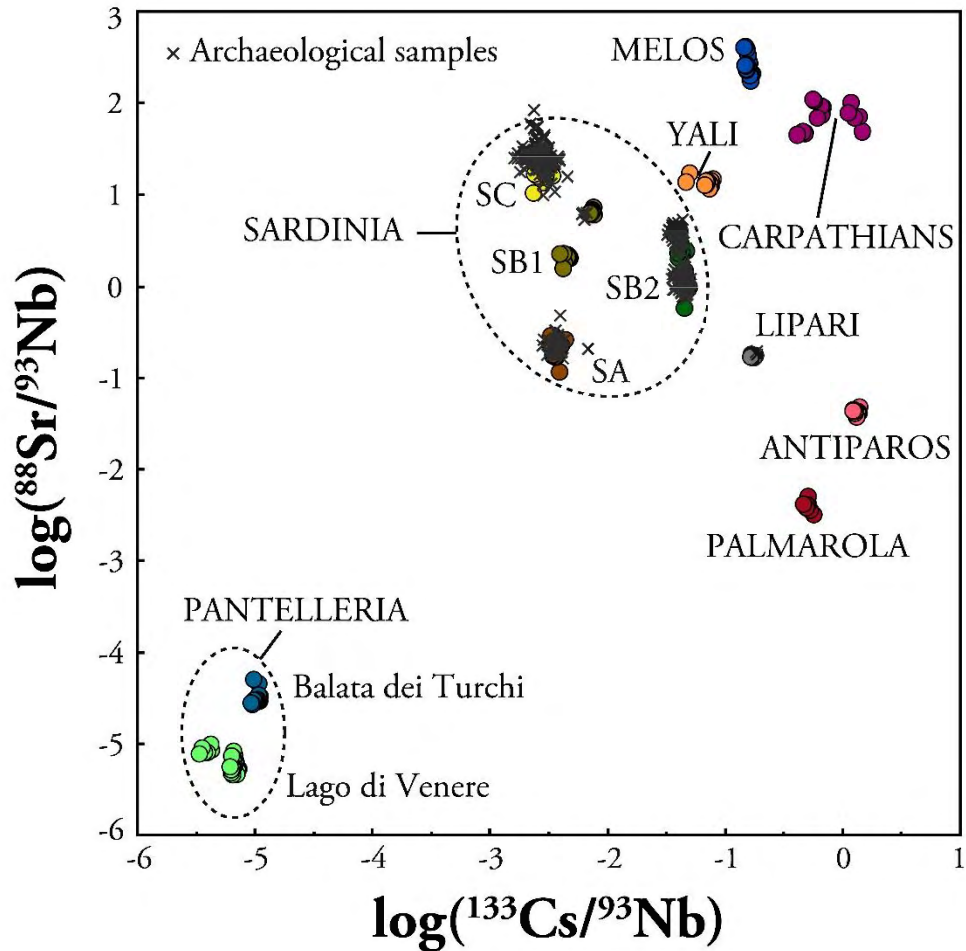


Figure 5.4. Comparison of $\log(^{133}\text{Cs}/^{93}\text{Nb})$ and the $\log(^{88}\text{Sr}/^{93}\text{Nb})$ ratios obtained by LA-ICP-MS (V2 protocol) on 200 geological samples from the Mediterranean region and 538 neolithic archaeological samples from the Tyrrhenian area.

Furthermore, the optimised protocol (V2) reduces the dispersion of the measurements, compared to the exhaustive protocol (V1) as is illustrated in **Figure 5.5**, where as an example the dispersion of the ^{88}Sr and ^{93}Nb contents for the same SA (n=21), SB1 (n=17), SB2 (n=18), and SC (n=26) Sardinian source samples is compared between both protocols.

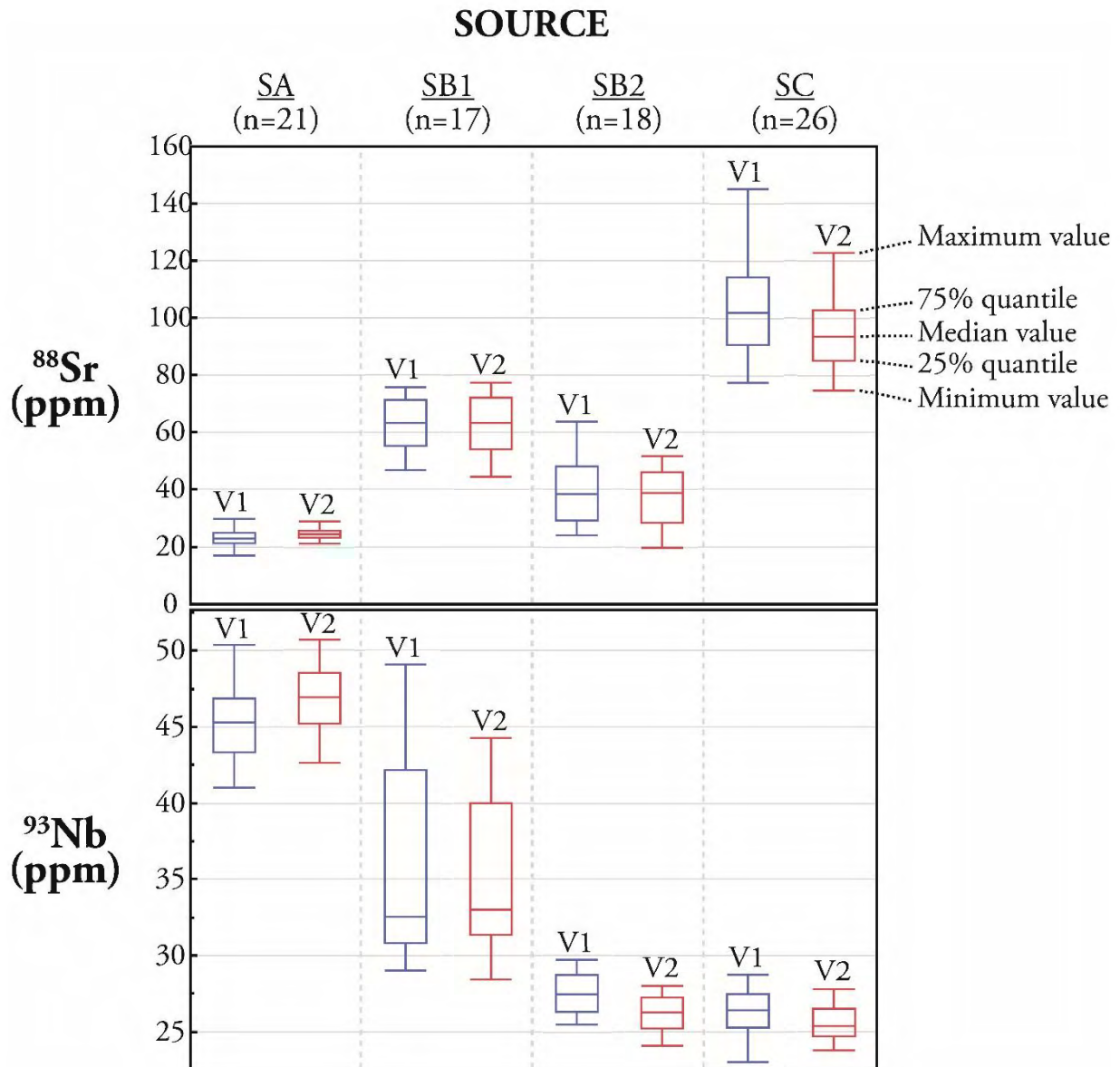


Figure 5.5. Dispersion of measurements for the ^{88}Sr and ^{93}Nb isotopes for the SA (n=21), SB1 (n=17), SB2 (n=18), and SC (n=26) obsidian source samples (Sardinia): comparison between exhaustive (V1) and optimised (V2) protocols. For each protocol and each source, the boxplot summarizes the minimum and maximum values (whiskers), the 25 and 75 % quantiles (lower and upper limits of the boxplot) and the median value (central line within the boxplot).

Comparison to previous studies

Obsidian source results on Sardinian sub-types SA, SB1, SB2 and SC were also compared to published data: the obsidian samples have been analyzed by PIXE (Le Bourdonnec *et al.*, 2011), ED-XRF (Energy Dispersive X-ray Fluorescence; Tykot, 1995), WD-XRF (Wavelength Dispersive X-ray Fluorescence; De Francesco *et al.*, 2008) and LA-ICP-MS (Barca *et al.*, 2007).

The ^{85}Rb , ^{88}Sr , ^{89}Y , ^{90}Zr , ^{93}Nb and ^{137}Ba contents for each study are described in **Table 5.6** and are in fairly good agreement. Only the measured ^{88}Sr concentration for the SC group is slightly lower than in the other studies, *i.e.* 82-106 ppm (taking into consideration 1 standard deviation) while other laboratories report values ranging from 95 to 167 ppm. This difference could eventually be explained by a difference in source sampling.

Table 5.6. (see next page) Comparison of the average ^{85}Rb , ^{88}Sr , ^{89}Y , ^{90}Zr , ^{93}Nb , and ^{137}Ba contents and uncertainties (± 1 standard deviation) for the SA, SB1, SB2, and SC sub-types obtained in this study and previous studies (Tykot, 1995, Barca *et al.*, 2007, De Francesco *et al.*, 2008, Le Bourdonnec *et al.*, 2011). Contents are in ppm.

Source	Method/Ref.	⁸⁵ Rb	⁸⁸ Sr	⁸⁹ Y	⁹⁰ Zr	⁹³ Nb	¹³⁷ Ba
SA	LA-ICP-MS [Our study] (n=21)	251(11)	24(2)	30(2)	73(5)	47(2)	121(11)
	PIXE [43] (n=8)	253(14)	28(4)	37	78(8)	57	
	ED-XRF [44] (n=8)	249(13)	26(4)	37(5)	91(5)	60(4)	
	WD-XRF [45] (n=15)	257(2)	31(1)	37(1)	96(1)	56(1)	127(4)
	LA-ICP-MS [19] (n=10)	270(28)	24(4)	33(4)	76(8)	49(4)	126(29)
SB1	LA-ICP-MS [Our study] (n=17)	237(10)	63(10)	23(5)	123(17)	35(5)	363(97)
	PIXE [43] (n=6)	250(10)	65(4)		121(6)		
	ED-XRF [44] (n=9)	231(13)	96(11)	27	177(26)	44(5)	
	WD-XRF [45] (n=6)	245(2)	68(13)	30(5)	132(17)	45(7)	255(39)
	LA-ICP-MS [19] (n=8)	264(55)	34(7)	20(2)	100(5)	27(3)	203(50)
SB2	LA-ICP-MS [Our study] (n=18)	243(18)	38(10)	19(2)	102(14)	26(1)	207(68)
	PIXE [43] (n=10)	239(14)	42(9)	22(4)	108(12)	31	
	ED-XRF [44] (n=7)	247(9)	42(10)	20(4)	124(16)	42(1)	
	WD-XRF [45] (n=3)	246(1)	40(4)	21(1)	120(9)	30(1)	164(38)
	LA-ICP-MS [19] (n=4)	249(11)	76(3)	23(2)	147(9)	33(1)	472(19)
SC	LA-ICP-MS [Our study] (n=26)	169(6)	94(12)	19(2)	199(17)	26(1)	824(76)
	PIXE [43] (n=20)	179(10)	148(19)	24(2)	241(23)	33(5)	
	ED-XRF [44] (n=6)	161(8)	145(5)	26(4)	261(12)	36(4)	
	WD-XRF [45] (n=11)	175(2)	134(3)	24(1)	213(3)	30(1)	899(19)
	LA-ICP-MS [19] (n=8)	188(13)	115(20)	24(2)	237(13)	28(3)	992(151)

5.4. Conclusions

This study demonstrates the new LA-ICP-MS protocol developed at Southern Cross University improves analytical reliability, validity and efficiency when applied to identifying obsidian provenance in the Western Mediterranean.

Analysis of the NIST SRM 613 international standard using the enhanced protocol (V2) demonstrated improved ability to obtain accurate and precise measurements with a higher sensitivity and within a very limited time frame (3 to 5 punctual measurement of about 60 s are usually used in previous studies, where our protocol produces a series of 70 to 80 measurement points in 2:15 min). Comparing the data obtained on the BCR-2G basalt standard (USGS) by a standard protocol using ablation points and an exhaustive list of isotopes (Barca *et al.*, 2007), our optimised protocol using lines and fewer isotopes obtained better or comparable results, when considering the accuracy of the measurements – V1 analysis was more accurate than V2 for only 4 of 14 isotopes. Furthermore, when the V2 protocol is applied to the Mediterranean obsidian sources, differentiation between sources is particularly distinct, thus confirming the validity of the optimised protocol (V2) as a sourcing tool in obsidian provenance research. Further study is required to investigate the rather low precision and accuracy results of the ^{66}Zn isotope, as well as the application of the V2 protocol rationale to further obsidian sources in the Mediterranean area (*e.g.* Near East).

In conclusion, the use of a refined LA-ICP-MS protocol tailored specifically to the target material is a demonstrably effective means of optimizing this cutting-edge geochemical characterization technique. In obsidian sourcing, it is particularly important for a meticulous selection of isotopes to be measured in order to discriminate between the sources of a particular geographical area: the more judiciously selected the list of isotopes, the better results.

Conflict of interest statement

The authors confirm there are no conflicts of interest.

Author biographies

Marie Orange is a Ph.D. student within Southern Cross GeoScience, Southern Cross University, Australia. Her research focuses on obsidian trade in the Western Mediterranean during the Neolithic period.

Dr. François-Xavier Le Bourdonnec is an Associate Professor of Archaeological Sciences at Bordeaux Montaigne University. His work deals with circulation and economy of prehistoric lithic raw materials.

Dr. Renaud Joannes-Boyau is a Senior Research Fellow at Southern Cross University, Lismore, NSW, Australia, in charge of the ESR dating and Laser-Ablation ICP-MS laboratories. His research involves the application of physical techniques to archaeological problematics, in particular the direct dating of fauna and hominid fossil remains as well as the investigation of isotopic signature in fossil teeth and bones to reconstruct dietary changes and diagenetic processes.

Dr. Anja Scheffers is a professor at Southern Cross University, Australia. Her research focuses on how coastal environments have changed in the past. She is particularly interested in processes that shape and modify coastal landscapes over a variety of length and time scales and the coupling and feedback between such processes, their rates, and their relative roles, especially in the contexts of variation in climatic and tectonic influences and in light of changes due to human impact.

Acknowledgements

The authors wish to thank Matthew Tonge for his management of the LA-ICP-MS and his help during the analyses, as well as Mark Rosicky and Diane Fyfe for their precious help. We also thank Valerie Schoepfer, Stan Kinis, Trent McIntyre, and Dr. Scott Johnston for proofreading this paper. Marie Orange's Ph.D is funded by a Postgraduate scholarship from SCU (Southern Cross University) and part of an Australian Research Council discovery grant [DP140100919]. This research program has been financially supported by the ANR (French National Research Agency; n°ANR-10-LABX-52) and the Université Bordeaux Montaigne PSE (Politique Scientifique d'Établissement).

PART III

-

ARCHAEOLOGICAL CHALLENGES IN THE
WESTERN MEDITERRANEAN: APPLICATION OF
THE ANALYTICAL STRATEGIES IN NEOLITHIC
CORSICA

Chapter 6

The Cauria plateau

The following study was conducted on two sites of the Cauria plateau (South Corsica, Sartene), Renaghju and I Stantari, both presenting occupation levels dated from the Middle Neolithic. As described in **Chapter 2**, the excavation of these sites is part of a larger project led by André D'Anna and Pascal Tramoni on the plateau, the PCR '*Statues-menhirs, Menhirs et Mégalithisme de la Corse*' (Statues-menhirs, Menhirs, and Megalithism in Corsica).

The obsidian assemblage (Middle Neolithic) from both sites are here analysed following our analytical strategy developed in **Chapter 4**, and using the LA-ICP-MS protocol designed during the Ph.D. project and presented in **Chapter 5**.

These analyses enabled the introduction of new information on the diffusion and consumption patterns of the obsidian material in the Cauria plateau, and in the larger regional context.

The contents of this chapter have been submitted for publication in the journal Geoarchaeology.

Obsidian economy on the Cauria plateau (South Corsica, Middle Neolithic): new evidence from Renaghju and I Stantari

Marie Orange¹, François-Xavier Le Bourdonnec², André D'Anna³, Pascal Tramoni⁴,
Carlo Lugliè⁵, Ludovic-Bellot-Gurlet⁶, Anja Scheffers¹, Henri Marchesi⁷, Jean-Louis
Guendon³, Renaud Joannes-Boyau¹

¹ *Southern Cross GeoScience, Southern Cross University, Australia*

² *IRAMAT-CRP2A, UMR 5060 CNRS – Université Bordeaux Montaigne, France*

³ *LAMPEA, UMR 7269, CNRS, MCC, MMSH, Aix-Marseille Université, Aix-en-Provence, France*

⁴ *INRAP Méditerranée, UMR 5140, Archéologie Des Sociétés Méditerranéennes, 390 Avenue de Pérols, 34970 Lattes, France*

⁵ *Dipartimento di Scienze Archeologiche e Storico-Artistiche, Università di Cagliari, Cagliari, Italy*

⁶ *Sorbonne Universités, UPMC Université Paris 6, MONARIS 'de la Molécule aux Nano-objets : Réactivité, Interactions et Spectroscopies', UMR 8233, UPMC-CNRS Paris, France*

⁷ *DRAC/SRA de Languedoc-Roussillon, Montpellier, France*

Abstract

This paper aims to study and compare the obsidian economies of Renaghju and I Stantari, two neighbouring Neolithic sites located on the Cauria plateau (south-western Corsica). The occupation phase 3 of Renaghju and phase 1 of I Stantari, both dated from the Middle Neolithic period (5th millennium B.C.), have provided respectively 112 and 99 obsidian artefacts. The entire assemblages have been geochemically characterized virtually non-destructively using LA-ICP-MS at SOLARIS (Southern Cross University [SCU]). Our analyses, coupled to the typo-technological data, revealed rather different consumption patterns for the two sites despite their comparable nature (megalithic sites) and geographical proximity (400 meters distance).

Introduction

Obsidian sourcing has long been a successful tool for the study of past population movement, by retracing cultural contacts and revealing procurement, trade and exchange patterns (see *e.g.* Cann and Renfrew, 1964; Williams-Thorpe, 1995; Poupeau *et al.*, 2010a). Often treated as an end itself instead of as a ‘means to an end’, the discipline has deeply evolved in the recent decades to embrace a more integrated and contextualised approach. Lately, the following trends can be observed:

- the development of analytical strategies (Carter *et al.*, 2006; Le Bourdonnec, 2007; see also **Chapter 4**), relying on the combination of different techniques (virtually or strictly non-destructive) to achieve the exhaustive characterization of the assemblages. As already illustrated in various studies (Lugliè *et al.*, 2009; Orange *et al.*, 2013; Freund, 2014 *i.a.*), such an approach allows the extraction of the maximum amount of information from the lithic assemblages and is crucial

to better understand the economy of the obsidian material at site level and in a larger regional context;

- the integration of the sourcing results with the typo-technological information (see *e.g.* Carter *et al.*, 2006; Eerkens *et al.*, 2008) in order to better apprehend the use of the raw material and discuss in details the *chaîne opératoire*. This sometimes reveals complex consumption patterns - where ‘diffusion’ not always equals ‘interaction’ between two groups (Perlès, 2012). Among the areas where those research perspectives are being followed, the Western Mediterranean is undoubtedly one of the most prosperous. By the means of collaborative and multidisciplinary research projects, more than 11 000 artefacts (all periods combined) have hitherto been sourced in this region (Poupeau *et al.*, 2014). It is also where, through a close collaboration between archaeologists and archaeometrists, the typo-technological aspects have regularly been integrated to the chemical analyses in the study of complete collections (Lugliè *et al.*, 2007, 2008, 2009; Bressy *et al.*, 2010; Poupeau *et al.*, 2010a; Le Bourdonnec *et al.*, 2010, 2011, 2012, 2015; Freund and Tykot, 2011 *inter alia*).

Following these trends, the present paper opens the discussion on the obsidian economy of the Middle Neolithic occupation levels of the Renaghju (phase 3) and I Stantari (phase 1) settlements. Situated on the Cauria plateau, one of the most informative areas for the study of the Neolithic period in Corsica (D’Anna *et al.*, 2007a, 2007b; D’Anna, 2013), they are chiefly renowned for their stone alignments (**Figure 6.1**), spotted by Prosper Mérimée as early as 1839 (Mérimée, 1840).

Both sites present relatively long, substantial, and complex settlement sequences (D’Anna *et al.*, 2001, 2007a, 2007b; D’Anna, 2014), and therefore are rich in information about the social, cultural, and economic patterns in place at the time. Yet

only the Cardial Early Neolithic level of Renaghju (phase 1) has so far been thoroughly studied and published (Bressy *et al.*, 2003, 2007; Le Bourdonnec *et al.*, 2015a).



Figure 6.1. Stone alignments of the Renaghju (left) and I Stantari (right) sites.

The latest publication, involving a total of 622 obsidian artefacts sourced either by visual characterisation, PIXE, or SEM-EDS, has shown that the majority of the assemblage was made using the Sardinian obsidian source, mainly SA (45.3 %), then SB2 (35.4 %), and SC (19.1 %). One artefact was found to match the distant source of Palmarola (eastern Tyrrhenian Sea; **Figure 6.2**), thus indicating rather early (6th millennium B.C.) direct or indirect contact(s) between the two islands. This illustrates the multiple links between the islands of the Western Mediterranean, through the complex Neolithisation processes and evolutions. The obsidian economy of both sites for the Middle Neolithic are here compared to each other (synchronic perspective) and then put in contrast with the results obtained on the Early Neolithic occupation level of Renaghju (diachronic perspective; see Le Bourdonnec *et al.*, 2015a for the study of the EN obsidian assemblage of Renaghju).

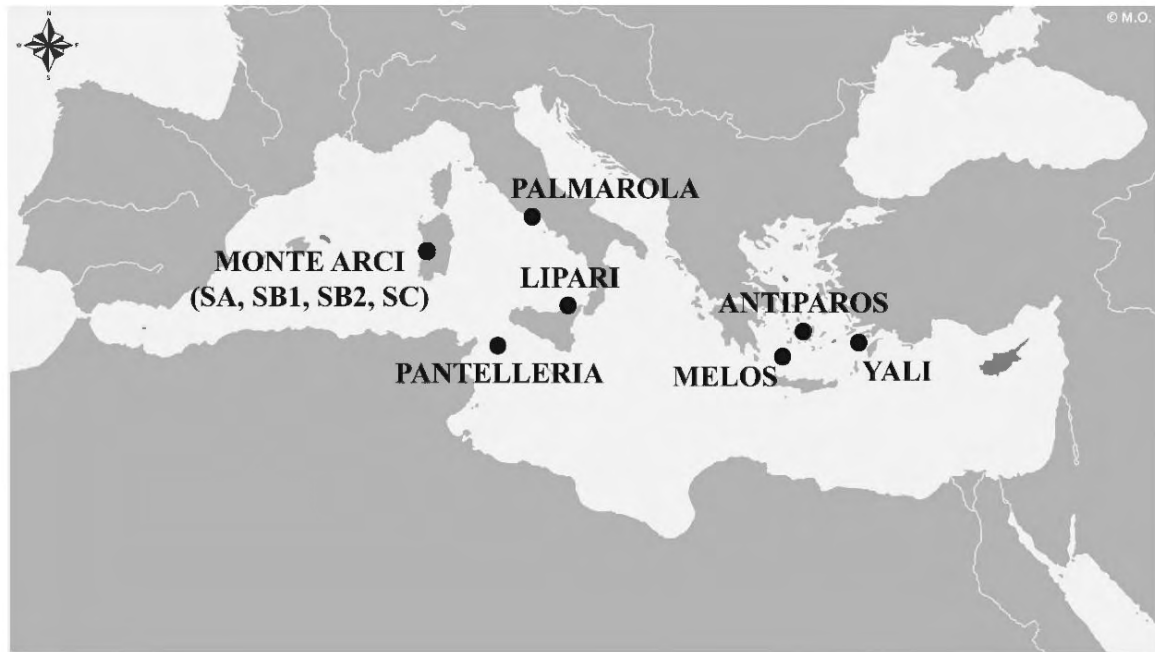


Figure 6.2. General map of the Mediterranean area displaying the main obsidian sources of the Western Mediterranean (Monte Arci [SA, SB1, SB2, SC], Lipari, Palmarola, Pantelleria) and the Aegean (Melos, Yali, Antiparos).

6.1. Archaeological background and lithic industries

6.1.1 *The Cauria plateau*

General topography

The Cauria plateau, located in the South-West of Sartène (**Figure 6.3**), is an area of about 15 km by 5 km and is part of a system of old staged surfaces dropping down to the sea: the Pastini (altitude of *ca.* 300 m), Migliari (*ca.* 200 m), and Cauria (*ca.* 120 m) plateaus. Towards the south-east, the rock massifs of di U Grecu (267 m) and di a Villa (225 m) isolate Cauria from the sea. This morphological unit divides and dominates two deep costal river valleys, the Navara (north-west) and the Ortolo (south-east) (D’Anna *et al.*, 2006, 2007b).

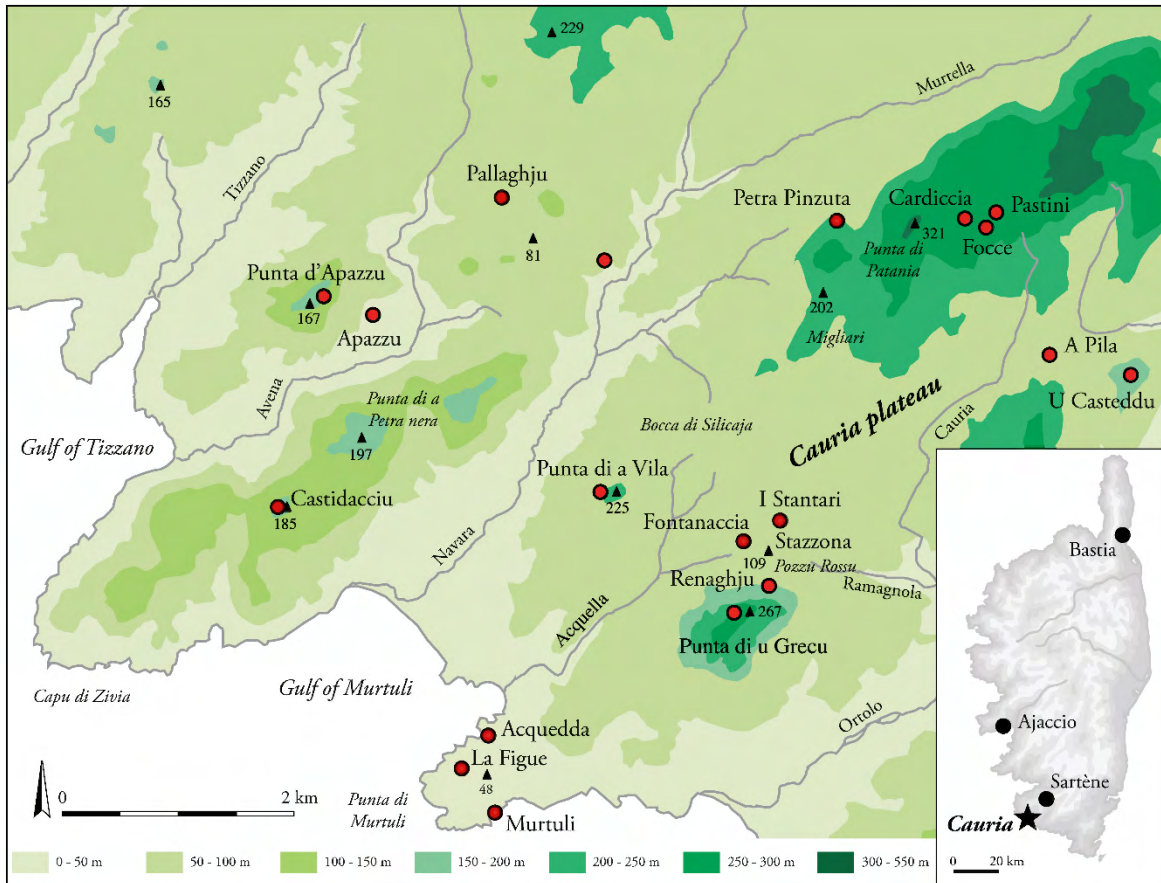


Figure 6.3. Location of the Cauria plateau and the main archaeological sites cited in the text.

Located in the ‘crystalline’ (or ‘hercynian’) Corsica, this entire complex is mostly constituted of a large batholith, in which three major magmatic associations have been identified. Around Cauria, only the calc-alkalic granitoids can be found: they are mostly acidic materials with a monzo-granodioritic composition (porphyroïd monzogranites from the Tizzano unit), closely associated with scarcer basic gabbro-dioritic rocks. This complex presents itself as a region-wide plutonic megastructure with a north-west/south-east orientation, dipping with a north-south trend.

The Cauria plateau itself displays a gentle slope down to the south/south-west, with maximum altitudes of 140 m at Furcanese (at the edge of the Bocca di Silicaja), and

120 m at the Fontanaccia dolmen. To the south-west, this flat area rises to the high valley of the Cauria stream, towards the di a Pila pass. To the east flows the Ramagnola stream, upswinging towards the Ortolo. To the south-west, it opens to the sea through the Acquella valley, between the Punta di a Villa and the Punta di u Grecu. The latest – and the largest – relief directly dominates the plateau and hosts numerous chaotic assemblies of massive blocks often composed of hollowed out caverns named *taffoni*.

On the southern part of the Cauria plateau, at the foot of the u Grecu massif and in between the Ortolo to the east and the sea to the west, the Pozzu Rossu ‘alveolus’ culminates at 110 meters above sea level. Open towards the Acquella and the Ramagnola streams, it presents an ovoid shape of 300 to 400 meters from north to south, and less than a kilometre from east to west. Its centre presents a topographic depression, marshy and poorly drained, orientated towards the Ramagnola: the Pozzu Rossu. The alveolus is congested with granitic arena (origin of the toponym ‘Renaghju’) from which a series of small residual reliefs emerges (*e.g.* tor, chaos). The geomorphologic map established at the beginning of the survey was crucial to allowing a better understanding and management of the sites’ implantations (D’Anna *et al.*, 2006:458: Fig. 2; D’Anna *et al.*, 2007b: 336: Fig. 2).

Cauria and the megalithic phenomenon

Described as early as 1839 by Prosper Mérimée during his first journey to Corsica, the main megalithic sites of the area have been long known. They include several monuments: the Fontanaccia dolmen, and the megalithic standing stones of Renaghju and I Stantari. They were later studied by Adrien de Mortillet, who published a first synthesis towards the end of the 19th century following a mission conducted in 1883 for the *Ministère de l’Instruction Publique* (French Department of Education; Mortillet,

1892). It was only during the second part of the 20th century (1955-1975), with the work of Roger Grosjean and his team – mainly Jean Liégeois and Georges Perreti, that the Cauria plateau finally became the centre of attention. Several excavations were organised on the following structures: the I Stantari stones (1964, 1968), the Renaghju site (1975), and the u Grecu massif (exploratory survey; Grosjean, 1964, 1968; Liégeois and Perreti, 1976). Some of the monoliths were straightened at Renaghju, but at I Stantari the operations involved the reconstitution of a complete row of stones, including two of the most famous *statue-menhirs* in Corsica. Following these excavations, the Cauria plateau was considered as one of the prime locations for the Corsican Prehistory (Grosjean, 1965, 1966, 1967). Between 1994 and 2013, planned excavations have been conducted on the main sites and allowed a precise examination of their chronology, implantation, and organisation. It also helped to reveal that the megalithic sites were not the sole prehistoric and protohistoric remains on and around the plateau, where several Neolithic, Bronze Age, or Iron Age open-air sites (u Grecu, Crucanesi), shelters (Cauria X, Cauria XIII), and burials (Renaghju 2, Cauria IV, XX, and XXI) have since then been identified.

Renaghju and I Stantari have both delivered an important amount of material (D'Anna *et al.*, 2006, 2007a, 2007b; D'Anna, 2013, 2014), especially regarding the lithic industries. Until now, our work had solely focused on the origin of chert and obsidian artefacts present on the Early Neolithic Cardial level of Renaghju (Bressy *et al.*, 2003, 2007; Le Bourdonnec *et al.*, 2015a). The I Stantari site, just like the Neolithic and Bronze Age levels of Renaghju, had only been the focus of limited investigations within the official excavation report.

The strength of the present study is to have been conducted on complete assemblages issued from thoroughly dated and contextualised stratigraphic levels, clearly integrated to the general cultural evolution of the Neolithic in Corsica and attributed to well-

defined cultural groups. It thus significantly contributes to a better perception and definition of the Middle Neolithic in Corsica, and of the groups that are a part of it.

6.1.2. Renaghju

More than twenty years after the last surveys on the Renaghju site (1975), a new series of programmed excavations were finally conducted, taking place between 1994 and 2000. They allowed the excavation of a large area (*ca.* 500 m²), and resulted in the constitution of thoroughly complete documentation.

Situated at the south end of the Pozzu Rossu alveolus and at the foot of the northern-eastern slope of the u Grecu massif (*cf.* **Figure 6.3**), Renaghju is on the western border of a detrital cone, part of which has been integrated into the settlement during its evolution. Implanted near a freshwater spring, its occupation sequence is relatively long, *i.e.* from the Early Neolithic to modern times. The stratigraphy presents different sedimentary units, each comprising several occupation phases (**Figure 6.4**; D'Anna *et al.*, 2001, 2003, 2007a).

At the base of the stratigraphy, a sandy silty sedimentary context with small gravels houses the first occupation phases (1 and 2). These remains originate from a structured settlement dated from the Early Neolithic (6th millennium B.C.) and are characterised by a geometric Cardial facies, also called Filiestru-Basi-Pienza style (D'Anna *et al.*, 2001). This settlement consisted of a mud house with internal (small fireplaces, brazier) and external (large combustion and heating structures) fireplaces. Most of the analyses had previously focused on the lithic materials – chert and obsidian – found in phase 1 (Bressy *et al.*, 2003, 2007; Le Bourdonnec *et al.*, 2014).

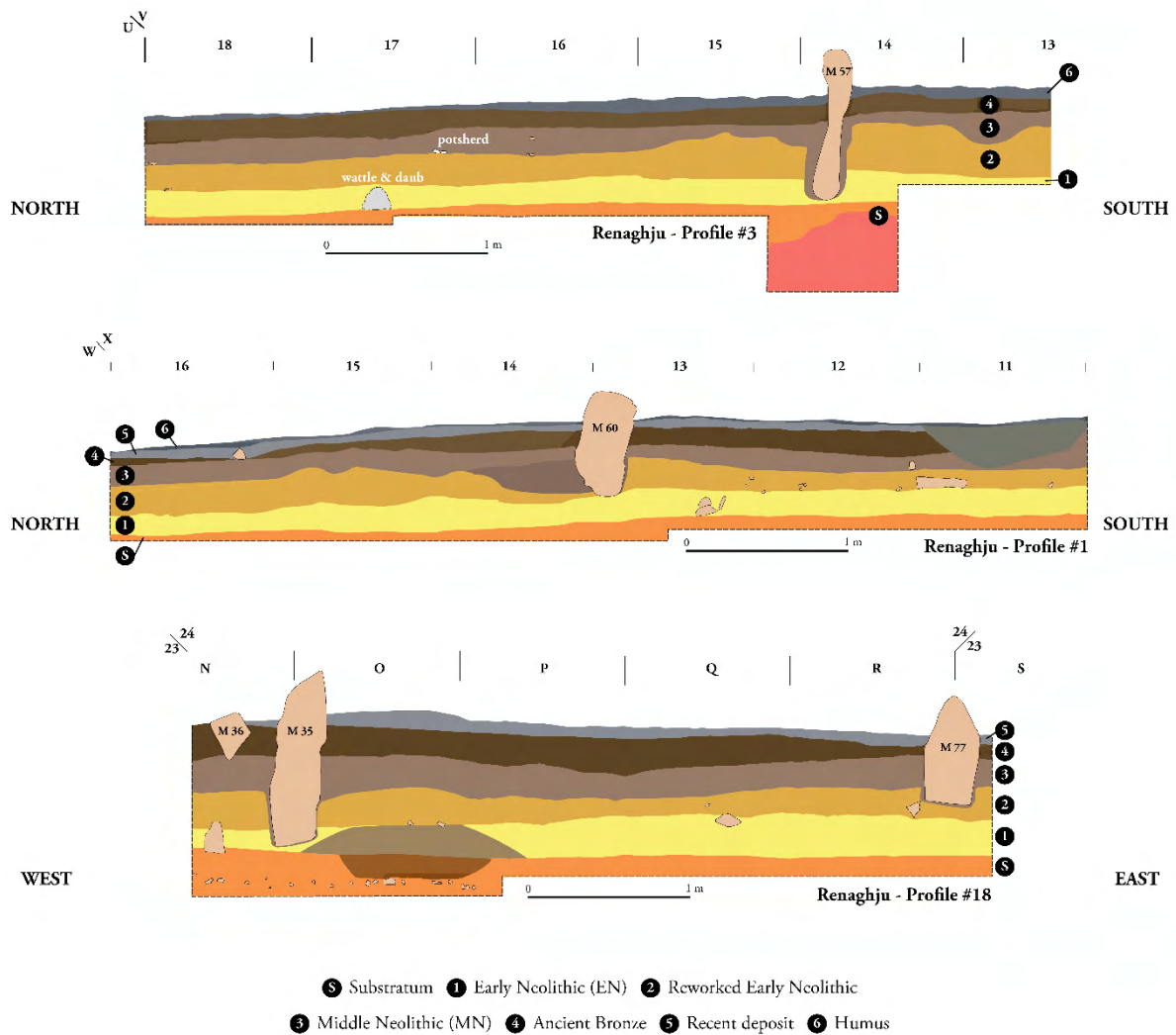


Figure 6.4. Stratigraphic profiles #3, #1, and #18 of the Renaghju archaeological site.

Two small structures, made of heated rocks and situated on the same level as the standing stones, have been the object of radiometric dating, placing them between 4685 and 4365 cal. B.C., with higher probabilities around 4515-4370 cal. B.C. (D'Anna *et al.*, 2003; D'Anna, 2014). The phase 3 megalithic monument is thus inscribed in the Middle Neolithic period, which we consider to take place *ca.* 4600-4400 cal. B.C. Remarkably, this is a thousand years older than the dates previously determined for the Corsican megalithism phenomenon (Grosjean, 1966, 1967, 1971; D'Anna *et al.*, 1997, 1998).

On the upper section the standing stones are inscribed in two different sedimentary units, clearly revealing two distinct megalithic monuments. The most recent was built at the beginning of the Bronze Age or at the end of the Neolithic period (*ca.* 2000 B.C., phase 4). The most ancient was constructed during the Middle Neolithic (phase 3). In the stratigraphy (*cf.* **Figure 6.4**), this monument is situated above the Early Neolithic levels, after a phase of abandonment highlighted by a sedimentary accretion. The monument comprises 64 monoliths (42 menhirs and steles) predominantly arranged in two main rows oriented north-west/south-east, and associated with another curved row featuring in its centre a 2.65 m high menhir-stele of an irregular shape (**Figure 6.5**).

The artefacts associated are relatively scarce, and only consists of a small ceramics assemblage involving short neck dishes and bowls (S profile) with simple or double line decorations made of small round imprints (**Figure 6.6**). They can be compared to the Sardinian Bonuighinu productions (Loria and Trump, 1978; Atzeni, 1981; Usai, 2009; Tramoni and D'Anna, *in press*).

The present paper includes the study of the small obsidian lithic assemblage associated with this megalithic structure, and thus hopes to provide a first insight into the Middle Neolithic period on the Cauria plateau. Apart from the 112 obsidian artefacts excavated in the phase 3 level (see examples in **Figure 6.7**), we also note the presence of artefacts made of quartz, hyaline quartz, rhyolite, chert, and other hard rocks. If we exclude the quartz, of local origin and for which the actual use for the fabrication of tools and weapons can be questioned, the main raw lithic material is obsidian (41 % of the assemblage, against 31 % for the chert and 26 % for the rhyolite). These proportions differ greatly from what has been observed for the same materials in the phase 1 occupation level (65 % chert, 21 % obsidian, 13 % rhyolite).

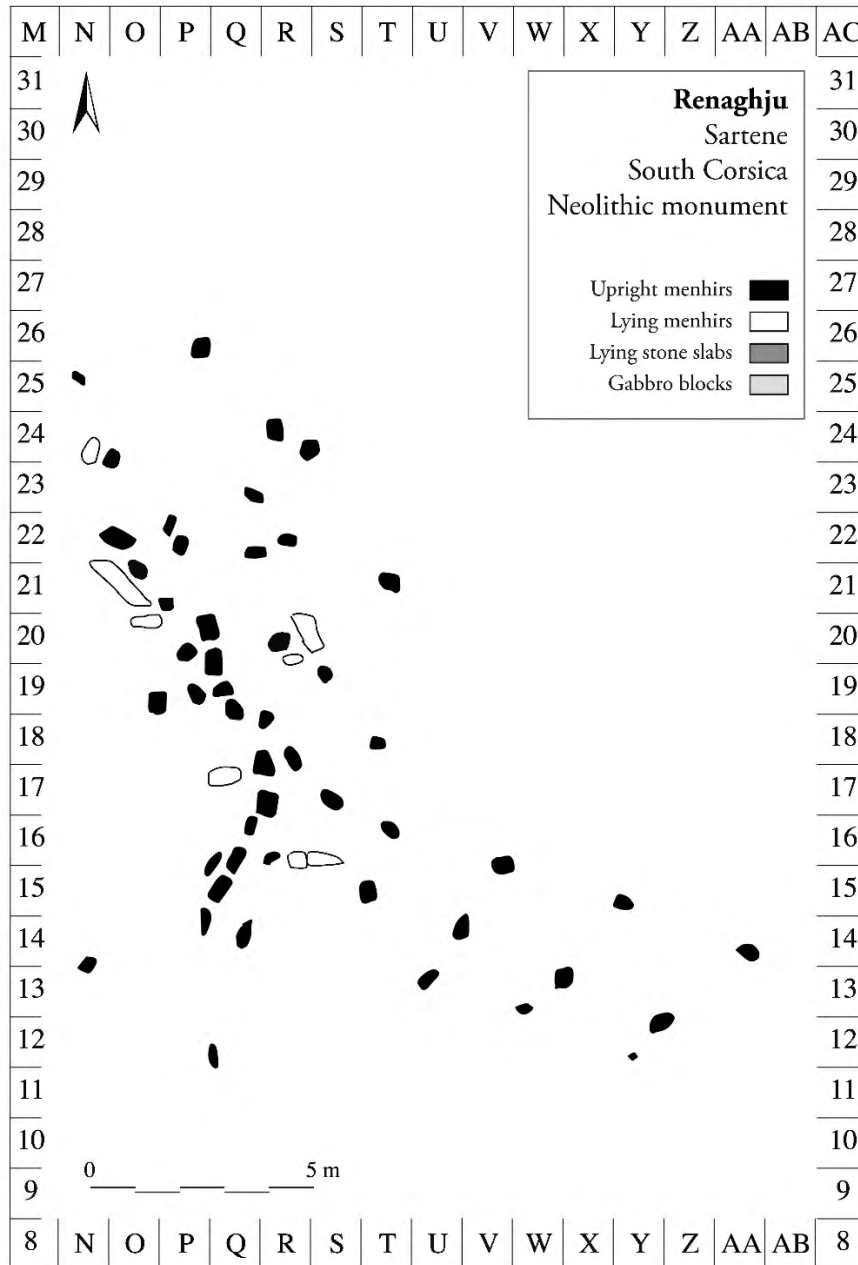


Figure 6.5. Renaghju, Neolithic monument: spatial distribution of the menhirs (upright and lying), stone slabs, and gabbro blocks.

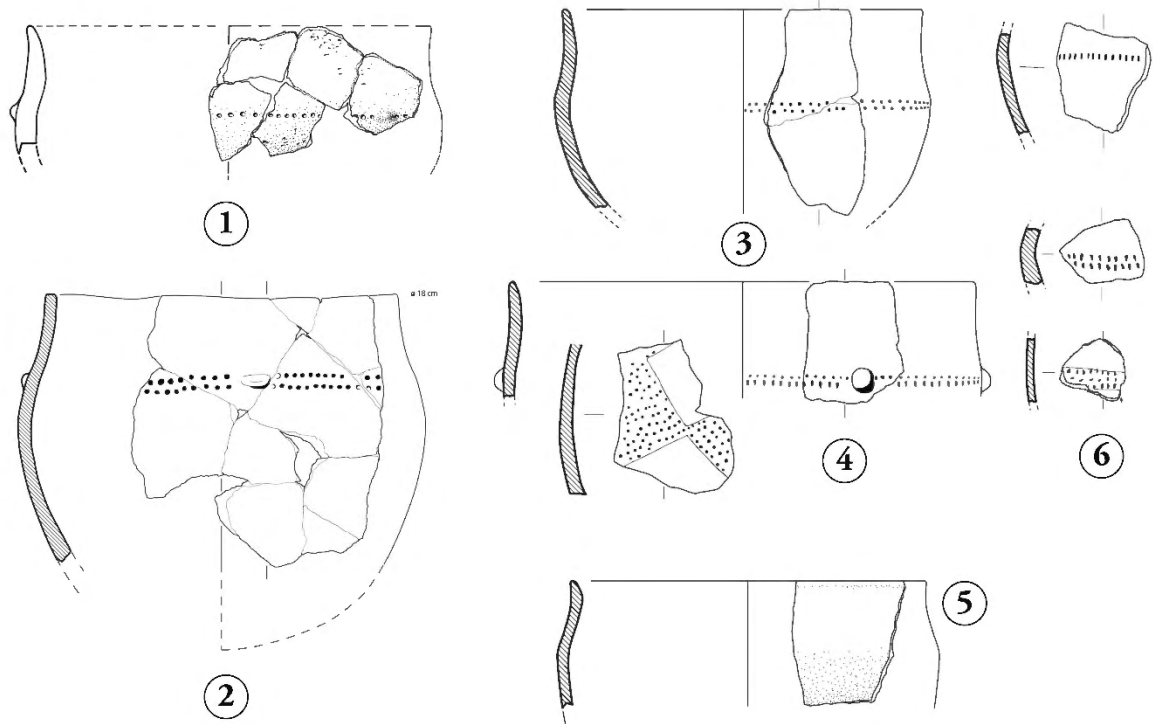


Figure 6.6. Ceramics fragments from Corsica – Middle Neolithic I (Curasian, punched, Bonuighinu). 1: Renaghju, Sartene, Cauria plateau. 2: Lecci, San Ciprianu. 3-6: Murtuli, Sartene. Drawings by Pascal Tramoni.

6.1.3. *I Stantari*

At the northern boundary of the Pozzu Rossu and approximately 400 meters north from the Renaghju settlement, *I Stantari* is located at the upper end of the Cauria plateau (*cf.* **Figure 6.3**). Located near a freshwater spring, the site is implanted above a marshy dale containing hydromorphic arena, in which sedimentation – fed by colluvial deposits – seems partly contemporary to the megalithic monuments from the Neolithic and Bronze Age periods. The stratigraphy of the site allows the recognition of different occupation and construction phases associated with three main sedimentary units (**Figure 6.8**).

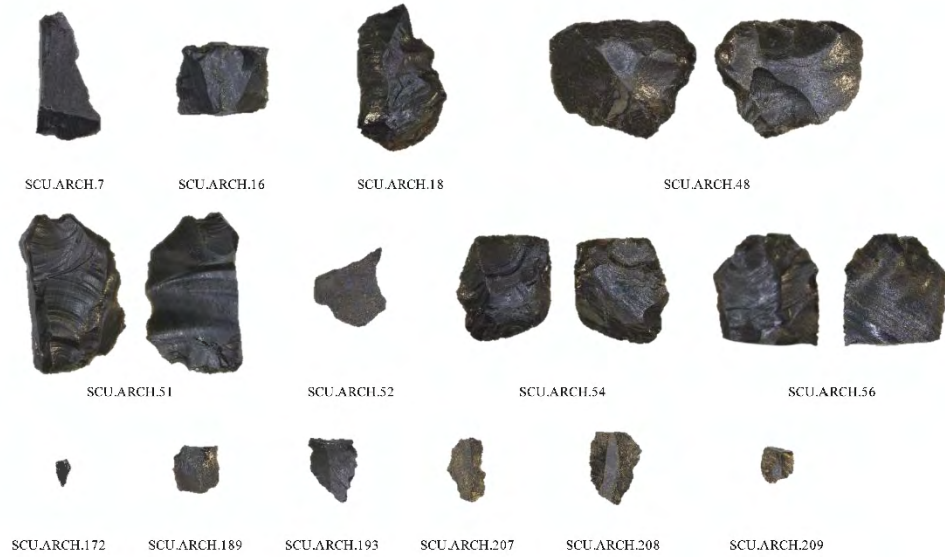
SA



SB2



SC



Ind.



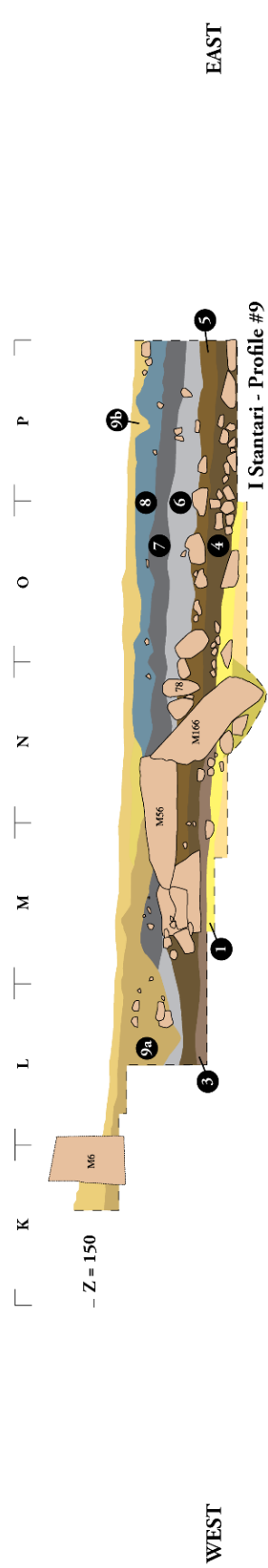
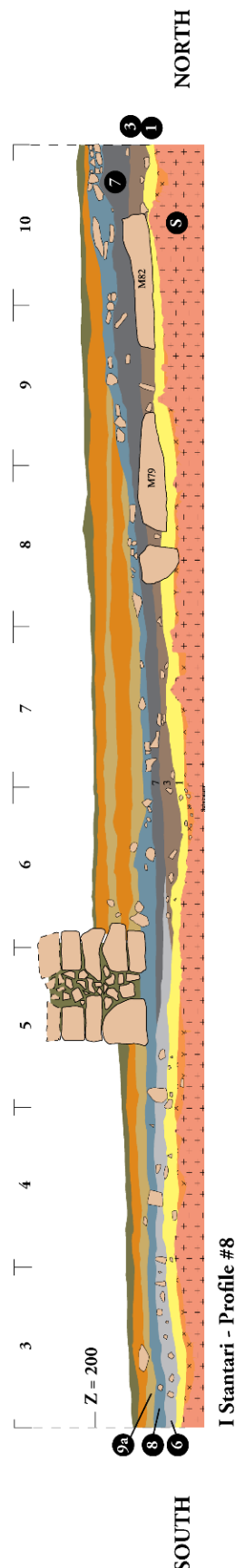
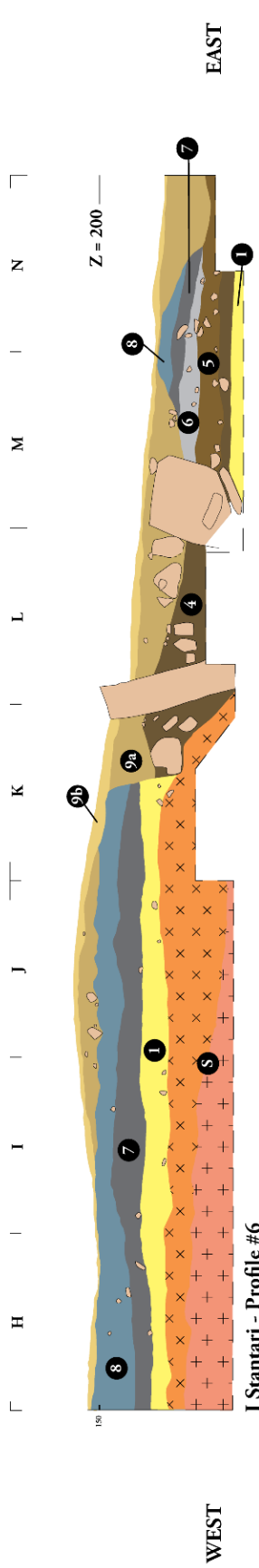
Figure 6.7. (previous page) Examples of obsidian artefacts from the Renaghju phase 3 and I Stantari assemblages.

The upper section of the stratigraphy, directly below the excavations of Roger Grosjean and largely disturbed by those, shows layers of loamy sediments of a grey to black colour, reflecting various modern and medieval agrarian structures (respectively phases 8 and 7), or attesting alternating periods of activity, abandonment, and destruction (phase 6).

In the middle section of the stratigraphy, some brown sandy-clay sediments – slightly loamy and more or less gravelly – integrate monumental remains. They attest of a complex site involving three rows of standing stones, steles, armed steles and statues-menhirs. The western row (phases 4 and 5) comprises the famous steles and the armed statues (**Figure 6.9**) with explicit anatomic representations on their eastern face: faces and arms, diverse clothing attire and a warrior panoply, helmets, swords, and harnesses. They are just as explicit on the western face, with the representation of an erected phallus. This monument is implanted on a slight eastern slope, and built on a terrace/podium that contributes to making the display ostentatious.

All of these characteristics and features (stratigraphy, artefacts, stone monuments), along with the radiometric dating conducted on the site, point to a final Bronze occupation of this monument. It was preceded by an earlier edifice involving large standing stones – without any kind of figuration on their surface, and erected during the Late Neolithic - Early Bronze age (phases 2 and 3), *i.e.* contemporary of the Renaghju phase 4. This level is very disturbed and its organisation/structure thus remains relatively unclear.

Figure 6.8. (next page) Stratigraphic profiles of the I Stantari site. A: Profile #6 (2002), West-East, H to N, 15 to 16. B: Profile #8 (2005), South-North, M to N, 3 to 10. C: Profile #9 (2003, 2007), K to P, 19 to 20.



- S Substratum
- 1 Middle Neolithic (ca. 4000 BC)
- 2 Final Bronze a (1400-1200 BC)
- 3 Final Bronze b (1200-1000 BC)
- 4 Final Bronze c (1000-800 BC)
- 5 Antiquity (300 BC - 200 AD)
- 6 Middle Age (11th-14th c.)
- 7 Modern (18th-19th c.)
- 8 Contemporary (20th c.)
- 9a Contemporary (20th c.)
- 9b Contemporary (20th c.)

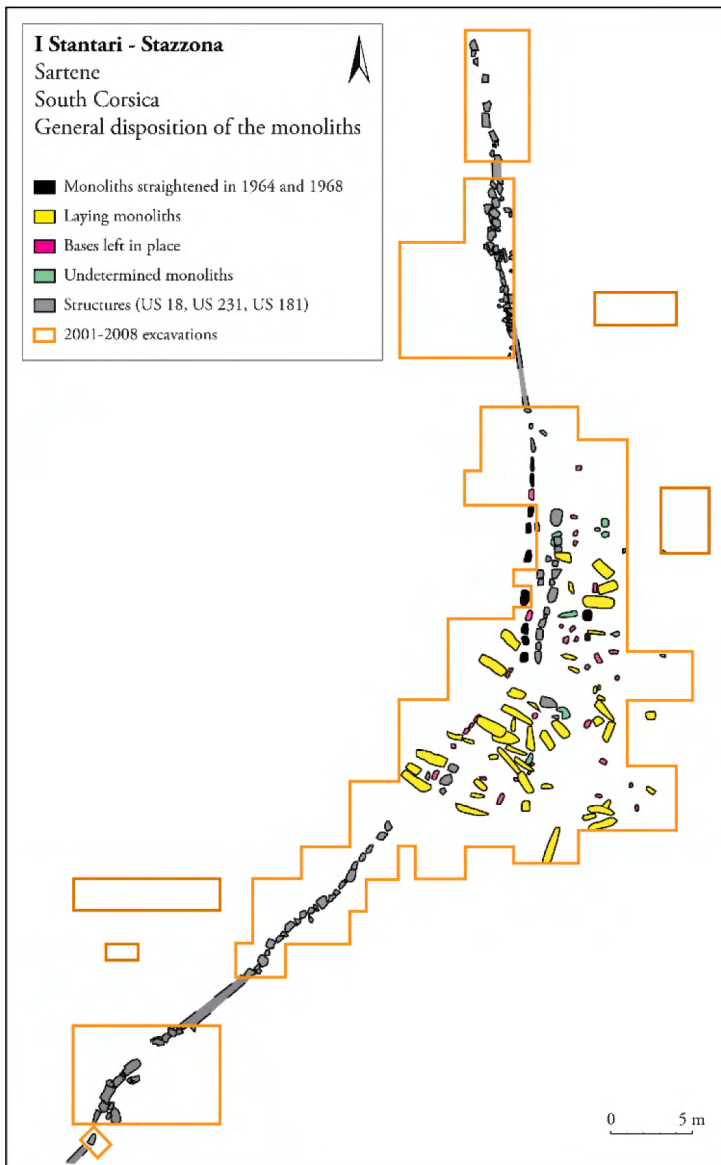


Figure 6.9. (previous page) I Stantari-Stazzona structure: general disposition of the monoliths (left). I Stantari, Neolithic monument: spatial distribution of the monoliths (right).

The base of the stratigraphy is constituted of a layer of a brown-yellow sand – slightly clayey and incorporating grit and small pebbles, and is located directly above the rocky substrate. It integrates the first architecture made of small steles implanted near a large habitat. This constitutes the phase 1 of the I Stantari settlement. The monument's organisation is difficult to determine, comprising a minimum of 30 sub-trapezoidal and rectangular steles without any particular orientation. The artefacts excavated (ceramics, lithic industry) and the comparisons made with the Renaghju site allow the placement of the use of this monument to the Middle Neolithic period (thus contemporary of Renaghju phase 3).

The lithic industry of this Middle Neolithic level has only been the object of unpublished preliminary studies. It comprises a total of 200 artefacts made of obsidian, chert, rhyolite, and quartz which have not all been necessarily knapped. Obsidian is slightly dominant, representing 50 % of the total assemblage – 56 % if quartz is excluded. Chert represents 28 % (32 % if quartz is excluded), and rhyolite 10 % (11 % quartz excluded). The artefacts are of small dimensions (between 3 and 20 mm), with numerous broken fragments. The obsidian is mainly represented by small flakes, then by bladelets. The tools, made from flakes or bladelets, exhibit either irregular lateral removals or continuous abrupt retouching for the realization of geometric tools. The *pièces esquillées* dominate the assemblage.

Two major observations can therefore be made about this assemblage: (a) obsidian is predominantly used, and (b) the totality of the assemblage (*ca.* 80 %) is made of raw

materials originating from Sardinia, while raw materials available either in Corsica or more locally on the Cauria plateau (*e.g.* rhyolite) are largely secondary. Furthermore, primary flakes, secondary flakes, and nucleus fragments suggest that knapping was performed *in-situ*.

6.2. Obsidian sourcing

6.2.1. Analytical protocols and sampling

Analytical protocols

The LA-ICP-MS analytical method has proved its efficiency for obsidian provenance analysis (see *i.a.* Gratuze, 1999; Carter *et al.*, 2006; Barca *et al.*, 2007). Virtually non-destructive, this technique is fast enough (a few minutes per sample) to allow the geochemical characterization of large collections within a reasonable time frame. Furthermore, the set of analysed trace elements allows the discrimination of obsidian sources from various geographic contexts.

In this study the samples were analysed at the SOLARIS laboratory (Southern Cross GeoScience, Southern Cross University) following a LA-ICP-MS protocol recently optimised for obsidian sourcing (*cf.* **Chapter 5**). Because the analyses were conducted by micro-sampling – laser ablation – on the surface of the artefacts, the sample preparation only involved the cleaning of the objects: after being placed 5 minutes in an ultrasonic bath to remove potential contamination from soil, they were rinsed successively with tap water, distilled water, ethanol, and acetone, then dried in the open air. The analytical instrument itself consists of an Agilent 7700 Series ICP-MS, coupled to a NWR213 laser ablation system (Nd:YAG deep UV laser at 213 nm). The MassHunter Workstation software is used to control the instrument, acquire and analyse

the data. The ablation parameters applied to the artefacts are reported in **Table 6.1**; this protocol was developed to reduce the ablation of the archaeological objects to a minimum - *i.e.* approximately the width of a human hair (40 μm).

A total of 13 isotopes, which allow the discrimination of Mediterranean obsidian sources (see **Chapters 4 and 5**), were measured: ^{45}Sc , ^{66}Zn , ^{85}Rb , ^{88}Sr , ^{89}Y , ^{90}Zr , ^{93}Nb , ^{133}Cs , ^{137}Ba , ^{146}Nd , ^{147}Sm , ^{208}Pb , ^{232}Th , and ^{238}U . At the beginning and end of each run, the international standard NIST SRM 613 was analysed to ensure the accuracy (always better than 6.5 %, see **Table 6.2**), precision and reproducibility of our measures (see **Chapter 5**).

Table 6.1. Ablation parameters adopted for the LA-ICP-MS analyses conducted on the archaeological samples at SOLARIS (SCU, Australia). The ablation parameters used for the geological samples can be found in Orange *et al.*, 2016, along with the analytical protocol developed (**Chapter 5**).

Ablation parameters	Archaeological samples
<i>Spot size</i>	40 μm
<i>Laser pulse frequency</i>	10 Hz
<i>Laser power (output)</i>	80 %
<i>Scan speed</i>	5 $\mu\text{m}/\text{sec}$
<i>Depth</i>	10 μm
<i>Passes</i>	1
<i>Line length</i>	0.6 mm
<i>Total time acquisition per line</i>	2:15 min

Table 6.2. Comparison of the ^{45}Sc , ^{66}Zn , ^{85}Rb , ^{88}Sr , ^{89}Y , ^{90}Zr , ^{93}Nb , ^{133}Cs , ^{137}Ba , ^{146}Nd , ^{147}Sm , ^{208}Pb , ^{232}Th , and ^{238}U contents with uncertainty (± 1 standard deviation) obtained on the NIST SRM 613 standard during this study (16 measurements over 8 runs) and the reference values recommended by the NIST and the GeoRem database. Relative error calculated in comparison with the GeoRem reference values. Concentrations are in ppm.

	NIST	GeoRem	This study (16 measures)	
	Concentration	Concentration	Concentration (1sd)	Relative error
^{45}Sc		39.9(2.5)	38.5(0.8)	3.6%
^{66}Zn		39.1(1.7)	41.0(4.2)	4.9%
^{85}Rb	31.4(0.4)	31.4(0.4)	30.5(0.5)	2.9%
^{88}Sr	78.4(0.2)	78.4(0.2)	76.2(1.1)	2.8%
^{89}Y		38.3(1.4)	37.0(0.5)	3.5%
^{90}Zr		37.9(1.2)	36.9(0.4)	2.7%
^{93}Nb		38.9(2.1)	37.3(0.4)	4.2%
^{133}Cs		42.7(1.8)	40.0(0.6)	6.4%
^{137}Ba	38.6(2.6)	39.3(0.9)	38.7(0.8)	1.6%
^{146}Nd	36	35.5(0.7)	33.6(0.6)	5.3%
^{147}Sm	39	37.7(0.8)	36.2(0.6)	4.1%
^{208}Pb	38.57(0.2)	38.57(0.2)	38.89(1.95)	0.82%
^{232}Th	37.79(0.08)	37.79(0.08)	35.69(0.58)	5.55%
^{238}U	37.38(0.08)	37.38(0.08)	35.98(0.54)	3.79%

Sampling

Thanks to the swiftness of the analytical protocol, the geochemical compositions of the entire obsidian assemblages from the Middle Neolithic levels of each site (211 artefacts) were determined. No selection of the artefacts was performed beyond a first sorting by raw material type. However, if quartz and chert are easy to visually distinguish from

obsidian, small artefacts made of rhyolite can sometimes be trickier to differentiate from the less glassy types of Sardinian obsidians. In such cases the artefact was selected for geochemical analysis to try to determine its classification.

Performed analyses involved 112 artefacts for Renaghju phase 3 and 99 for I Stantari phase 1, whose chemical signatures were compared to those of the main obsidian sources in the Mediterranean region (**Figure 6.2**). This reference database is made of 200 geological samples from our collection (see **Chapter 5**), originating from Sardinia (Monte Arci complex: SA, SB1, SB2, and SC subtypes), Lipari, Palmarola, Pantelleria (Balata dei Turchi and Lago di Venere), the Carpathian basin, as well as the Aegean Sea (Melos, Yali, and Antiparos sources).

6.2.2. Sourcing results

Renaghju

The complete obsidian assemblage of Renaghju phase 3, including 112 artefacts, has been geochemically characterised by LA-ICP-MS. The results are reported in **Appendix H1**. The fact that the compositions “*provide information on relative rather than absolute values of the components of compositions, that relative values are characterised by ratios and that logarithms of ratios are simpler to handle mathematically and interpret statistically than ratios*” (Aitchison, 2002:3) motivated our choice to use a logratio⁶ analysis (see Aitchison, 1986) instead of a standard multivariate analysis for the statistical treatment of the obtained data. The Zr, Nb, and Cs elements being amongst the most significant for the characterization of obsidians, they are frequently used for sources discrimination as well as artefact attribution in the Western Mediterranean area (Tykot *et al.*, 2011; Terradas *et al.*, 2013; Freund, 2014 *i.a.*) and elsewhere (Orange *et al.*, 2013; Kellett *et al.*, 2013

⁶ Logarithms of the ratios of the concentrations.

i.a.). Therefore we chose to compare the $\log(^{133}\text{Cs}/^{93}\text{Nb})$ and $\log(^{90}\text{Zr}/^{93}\text{Nb})$ ratios (**Figure 6.10**), which discriminate all Mediterranean sources and clearly show that a total of 58 artefacts can be attributed to the SB2 sub-source, 37 to SC, and 16 to SA (see **Table 6.3**).

Table 6.3. Number of artefacts – and proportions within the complete assemblage – attributed to each source for the Renaghju and I Stantari Middle Neolithic assemblages.

SITE	Nb. artefacts	SA	SB2	SC	Other facies
<i>Renaghju Phase 3</i>	112	16	58	37	1 unknown
<i>% of the assemblage</i>		14 %	52 %	33 %	> 1 %
<i>I Stantari Phase 1</i>	99	6	38	51	4 unknowns
<i>% of the assemblage</i>		6 %	38 %	52 %	4 %

Besides Zr, Nb, and Cs, Sr was also revealed to be a diagnostic element, and clearly confirms the attributions made with the log-ratio analysis: for the artefacts assigned to the SC group, it varies from 87 to 143 ppm, while for SA and SB2 its concentrations are much lower, respectively ranging between 20-25 ppm and 22-45 ppm. The ^{89}Y , ^{137}Ba , and ^{232}Th values also participate to match the artefacts to the sources. Only one artefact (SCU.ARCH.86; see **Figure 6.7** and **Appendix H1**), run several times to ensure the results, could not be matched with any of the sources of our geological database. A further macroscopic examination, showing a fine grained matrix, suggests that this object could be made of rhyolite rather than obsidian.

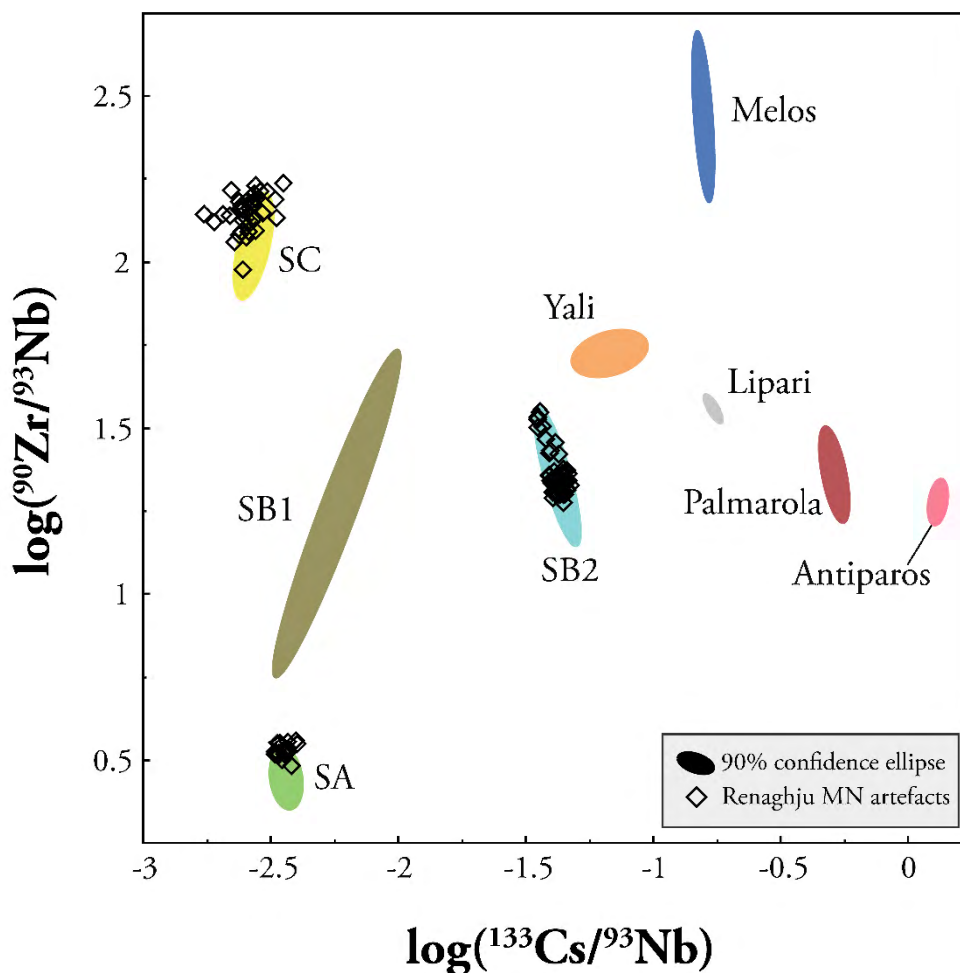


Figure 6.10. Comparison of the $\log(^{133}\text{Cs}/^{93}\text{Nb})$ and $\log(^{90}\text{Zr}/^{93}\text{Nb})$ ratios obtained by LA-ICP-MS on 111 artefacts from the Renaghju phase 3 (MN) assemblage and 200 geological samples from the Mediterranean area (Monte Arci [SA, SB1, SB2, SC], Lipari, Palmarola, Melos, Yali, and Antiparos). 90 % normal density ellipses. For reasons of clarity, the sources of Pantelleria (Balata dei Turchi and Lago di Venere) and the Carpathians are not represented in the graph.

I Stantari

A total of 99 obsidian objects excavated from the phase 1 occupation level (Middle Neolithic) of I Stantari were analysed by LA-ICP-MS. The results are presented in **Appendix H2**. The same log-ratio analysis as for the Renaghju assemblage, comparing the $\log(^{133}\text{Cs}/^{93}\text{Nb})$ and $\log(^{90}\text{Zr}/^{93}\text{Nb})$ ratios, allowed us to identify the presence of the

same sources (SA, SB2, and SC) although in different proportions (**Figure 6.11**); four artefacts remain unassigned and could possibly represent a different source or material type (see below). The majority has been revealed to be made of SC obsidian (51 artefacts, *i.e.* about half of the assemblage), 38 artefacts were attributed to the SB2 source, and 6 to SA. The ^{90}Zr values, very close to those obtained for Renaghju (66-76 ppm for the artefacts made of SA obsidian, 82-112 ppm for SB2 and 185-233 ppm for SC) clearly show the three clusters corresponding to each source.

Nonetheless, a total of 4 artefacts remain of an unknown origin (SCU.ARCH.130, SCU.ARCH.158, SCU.ARCH.182, and SCU.ARCH.196; see **Figure 6.7** and **Appendix H2**), as their chemical composition could not clearly match one of our sources. The SCU.ARCH.182 sample, comparably to SCU.ARCH.86 in the Renaghju assemblage, has revealed a fine grained matrix suggesting a rhyolite. The remaining unknowns are presenting similar visual characteristics: dark grey, sometimes slightly blue semi-opaque to opaque glass with a greasy lustre. While several elements (Rb, Cs, Nd, Th) could suggest a SB2 origin, strontium contents (74, 83, and 92 ppm) are however closer to those of the SC source (75-123 ppm, see **Chapter 5**), and too high to match the SB2 group (20-52 ppm).

Likewise, zirconium contents (150, 170, and 188 ppm) appear to be too high to correspond to the SB2 group (ranging from 82 to 124 ppm), whereas it seems to better match the SC group (174-233 ppm). The presence of these distinctive materials, maybe corresponding to rhyolites or to some intermediary facies between rhyolite and obsidian, already observed on other sites in Corsica and Sardinia (unpublished results), will be investigated in further studies to allow their interpretation as well as the thorough and exhaustive study of the lithic assemblages considered.

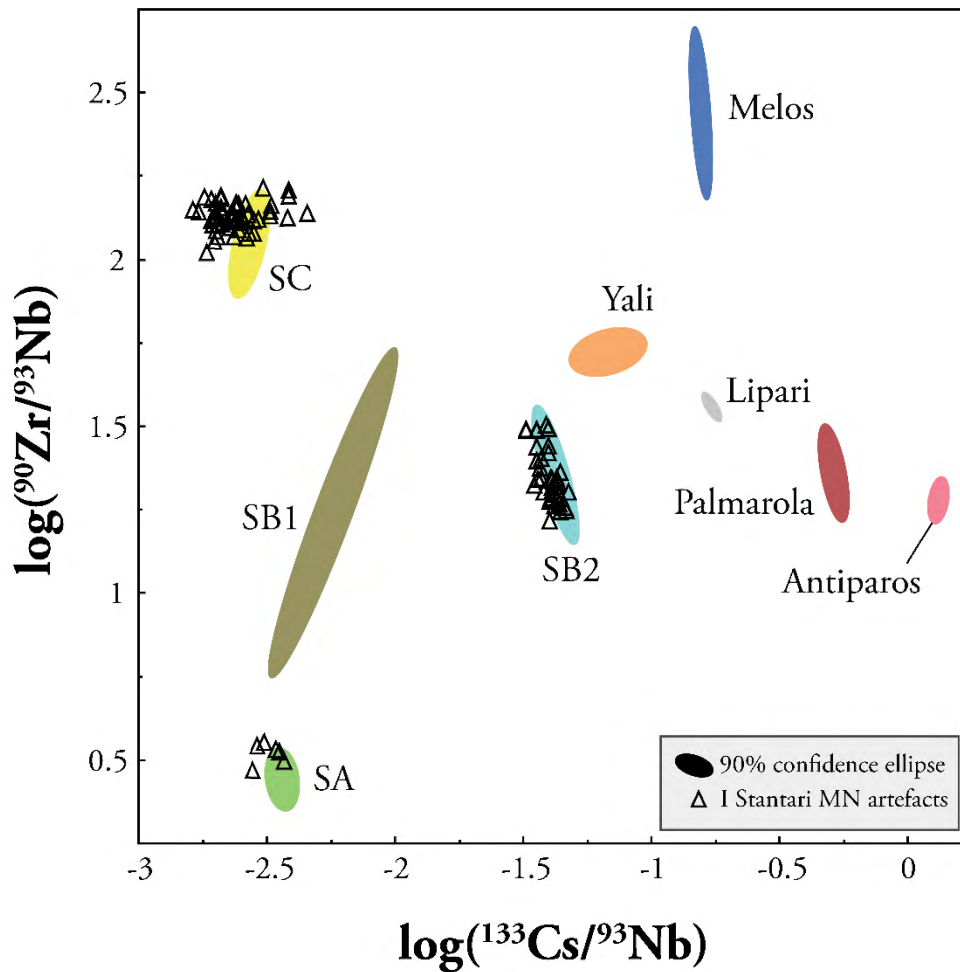


Figure 6.11. Comparison of the $\log(^{133}\text{Cs}/^{93}\text{Nb})$ and $\log(^{90}\text{Zr}/^{93}\text{Nb})$ ratios obtained by LA-ICP-MS on 95 artefacts from the I Stantari phase 1 (MN) assemblage and 200 geological samples from the Mediterranean area (Monte Arci [SA, SB1, SB2, SC], Lipari, Palmarola, Melos, Yali, and Antiparos). 90 % normal density ellipses. For reasons of clarity, the sources of Pantelleria (Balata dei Turchi and Lago di Venere) and the Carpathians are not represented in the graph.

6.3. Outcomes, Discussion, and Conclusions

Within Corsica, it has always been apparent that the obsidian raw materials mostly came from Sardinia (Courtin, 1972; Lanfranchi, 1976, 1980, 1987; Vaquer, 2007), as

confirmed by the most recent studies (e.g. Bressy *et al.*, 2007, 2008; Le Bourdonnec *et al.*, 2010, 2014, 2015). With the exception of Basi (south-western Corsica, see Tykot, 1996, 2002) and Renaghju phase 1 (Le Bourdonnec *et al.*, 2015a), previous studies have however generally been conducted on a limited number of samples, sometimes collected from poorly dated occupation levels, and whose real significance can be quite unclear. Such uncertainties obviously constitute a serious obstacle to the formulation of detailed interpretations on the obsidian circulation patterns (Costa and Cesari, 2003; Costa, 2006). The present study was on the contrary conducted on the complete assemblage from Renaghju phase 3 and I Stantari phase 1, whose levels of occupation have been clearly defined and dated.

The importance of obsidian in lithic material supply in Corsica clearly increased from the Early Neolithic (EN) to the Middle Neolithic (MN): marginal during the EN phases, it becomes more frequent in the MN levels where it sometimes dominates over other raw materials, such as in Vasculacciu or Tivulaghju. It is only in the Late Neolithic Basian sites that obsidian becomes dominant (75 % in Basi and Monte Grosso, 88 % in Costa di u Monte, *inter alia*). In both Renaghju and I Stantari Middle Neolithic (MN) levels, obsidian is the main raw material used for the lithic industries, and is largely dominant over chert (and quartz). However, subsequent studies will be needed to confirm that trend in the larger context of the Cauria plateau and the Sartene region.

The results obtained by LA-ICP-MS analysis clearly show, for both sites, an exclusive use of the Sardinian sources of the Monte Arci - SA, SB2, and SC (*cf.* **Table 6.3**). The SB1 subtype is completely absent from both assemblages, which matches the general tendency for the whole Neolithic period in Corsica and Sardinia (Lugliè *et al.*, 2008), and is probably explained by the lower knapping qualities of its obsidian.

In Renaghju phase 3, the predominance of the SB2 obsidian subtype – which constitutes about 52 % of the entire assemblage – is uncommon, but not surprising: its preferential use is a common behaviour in the contact zone and outside the island during both the EN and the first stages of MN (see *e.g.* Lugliè *et al.*, 2007, 2008). However, the relatively high frequency of SC type obsidians (33 %) is more surprising, in particular when compared to the amount of SA type obsidians (14 %). Such ‘deficiency’ in SA type obsidians in regards to the SC type is a relatively new feature, even amongst the innovations of the second half of the 5th millennium B.C., although a similar case seems to appear (only 50 artefacts were analysed by XRF) at Costa di U Monte (Poggio-Mezzana) where only 24 % of the characterised artefacts are matched with SA while 76 % matched SC (Bressy *et al.*, 2008). When a significant number of artefacts is analysed, SA and SC type obsidians are however usually consumed in relatively equal proportions. This is for example the case for the obsidian assemblage of the MN level of Basi (Sicurani, 2008) where of over 125 objects characterised by EMP-WDS, 45 % matched the SA subtype and 50 % matched the SC subtype. However, at Basi and Costa di U Monte the SB2 type is mostly absent (completely absent in the latter, only 3 % of the assemblage in the former).

Similarly, the obsidian distribution of I Stantari phase 1 does not correlate with the general picture of obsidian diffusion outside of Sardinia for the MN period, with a relatively high use of the SB2 type obsidians (38 % of the assemblage). Here the SC subtype is however predominant (52 %), followed by a sporadic use of the SA type (6 %). In the few sites available for comparison, SA and SC usually prevail (slightly more SC than SA), as observed in Basi (MN, Sicurani, 2008), I Calanchi (LN, Sicurani, 2008; Le Bourdonnec *et al.*, 2010), and Costa di U Monte (Poggio-Mezzana, MN/LN, Bressy *et al.*, 2008).

Unfortunately, few obsidian-bearing Middle Neolithic sites are available for comparison, and even fewer have had their obsidian assemblage exhaustively characterised. In the current state of knowledge we can however observe that, during the overall Middle Neolithic period, the SC type is generally dominant. It is the case in the G sector at Vasculacciu, whereas in the B sector the SB2 and SC obsidian types are equally prevalent. The preponderance of SC has also been observed at Costa di U Monte, A Fuata, and Monte Revincu, as well as for the Late Neolithic sites of Basi and Monte Grosso.

If we compare the obsidian consumption in Renaghju between the EN and the MN periods (**Figure 6.12**), a clear shift in the proportions of each obsidian Sardinian types can be observed: the use of the SA type, slightly prevailing over the SB2 type during the EN with 45 % of the assemblage, is considerably reduced during the MN (14 %). The SB2 type obsidians are then used in the majority (52 %), followed by the SC type obsidians (33 %). This change could potentially be explained by the relatively limited number of artefacts present in the phase 3 assemblage. The ‘anomalous’ ratio might hence have been emphasized by the presence of just a few raw matter units/blanks introduced and differently reduced in the site. A thoroughly combined visual/technological analysis is here needed to be able to offer further insights.

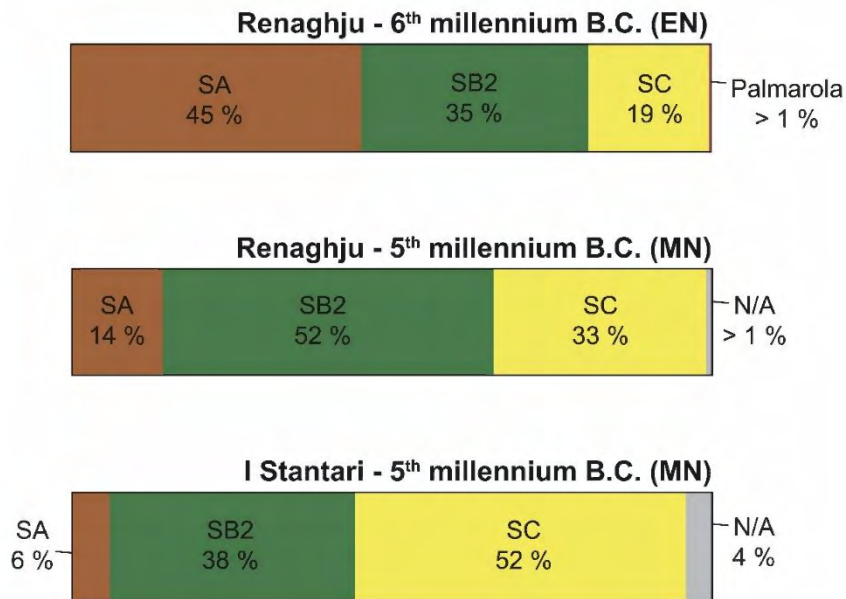


Figure 6.12. Bar charts (100 % stacked columns) comparing the obsidian consumption revealed at Renaghju phase 1 (EN), Renaghju phase 3 (MN), and I Stantari phase 1 (MN). N/A: artefacts non-attributed to a specific obsidian source.

The situation is again different at I Stantari, where the proportions are inverted – SC is dominant (52 %), followed by SB2 (38 %), and SA (6 %). The difference between the MN levels of Renaghju and I Stantari will have to be confirmed. If substantiated, it could however potentially be explained by two different reasons. A first hypothesis relies on the function of the sites: while Renaghju is solely a ceremonial site, I Stantari however associates both a ceremonial *locus* and a large habitat structure. A second hypothesis involves their actual chronology: the available data suggest that the two sites are not exactly contemporary. The material and radiometric dating show that Renaghju is inscribed in the early phase of the Middle Neolithic (Corsican facies Bonu Ighinu; 4800-4400 B.C.), while I Stantari, like Monte Revincu (Leandri *et al.*, 2007; Bressy *et al.*, 2008), could however belong to the end of the 5th millennium B.C. (Presian style, 4440-4000 B.C.), a period during which the large SC obsidian workshops became fully

operational and increased the amount of obsidians of this type that circulated within the long-distance exchange networks.

These two hypotheses are not necessarily contradictory. The phase 3 of Renaghju is inscribed in the transition period between an early Middle Neolithic (*cf.* Bonu Ighinu) and a recent Middle Neolithic (*cf.* San Ciriaco). It is during that transition phase that the megalithism appears in Corsica, which confirms that these displays are embedded in a period of strong chrono-cultural evolution. The rise of the megalithic phenomenon bears witness of the management of external relationships (D'Anna, 2013, 2015).

The present work confirms that obsidian sourcing studies conducted on complete and well dated assemblages can significantly contribute to our knowledge of the chrono-cultural evolution of these communities.

Chrono-cultural comparisons with assemblages from other sites are however unachievable, chiefly because of the low number and the nature of previous studies (analysis of a limited amount of artefacts, sourcing results not studied in connection with typo-technological data or larger archaeological context). It is therefore evident that only the multiplication of sourcing campaigns on well-documented and well-contextualised assemblages will allow the verification of our hypotheses.

Acknowledgments

Within Southern Cross GeoScience, we would like to thank Matthew Tonge for his management of the LA-ICP-MS and his help during the analyses, as well as Mark Rosicky and Diane Fyfe for their precious help. At the CRP2A, we wish to thank Yannick Lefrais and Brigitte Spiteri for their technical assistance, as well as Pierre Guibert for his support. The missions on the field were funded by grants from the *Collectivité*

Territoriale de Corse and the PCR '*Matières premières lithiques en Corse : territoires et interactions culturelles au Néolithique*' (INRAP). Marie Orange's PhD is funded by a Postgraduate scholarship from SCU and partly from the Australian Research Council discovery grant [DP140100919]; her time at the CRP2A facility in France was financed by a PSE project (Université Bordeaux Montaigne), '*Études de provenance de l'obsidienne préhistorique : de l'importance d'une comparaison inter-laboratoire et inter-méthodes*'.

Chapter 7

The Abri des Castelli site

7.1. The Abri des Castelli site: context and lithic industries

7.1.1. General context

Discovered in 2003, the Abri des Castelli is the first high-altitude Neolithic site excavated in Corsica, whereas most sites from this period are usually located in the lowlands. Situated in northern Corsica on the Corte municipality (**Figure 1.3**) it culminates at about 2140 meters asl⁷ where a granitic boulder, detached from the adjacent granitic inselberg, offers a shelter of approximately 7 m² (**Figure 7.1**). This rock shelter is associated with three other areas on the plateau (**Figure 7.2**): a main settlement situated at 2000 meters asl - ‘I Pozzi’, a rhyolite outcrop (250 meters from the rock shelter, and between 2080 and 2130 meters of altitude), and a restricted area located on the ridge which could have allowed the occupants of the Castelli plateau to control the northern slope of the mountain.



Figure 7.1. The Abri des Castelli – view from the north-east. ©N. Marini. Mazet, Dir. 2011.

⁷ asl: above sea level.

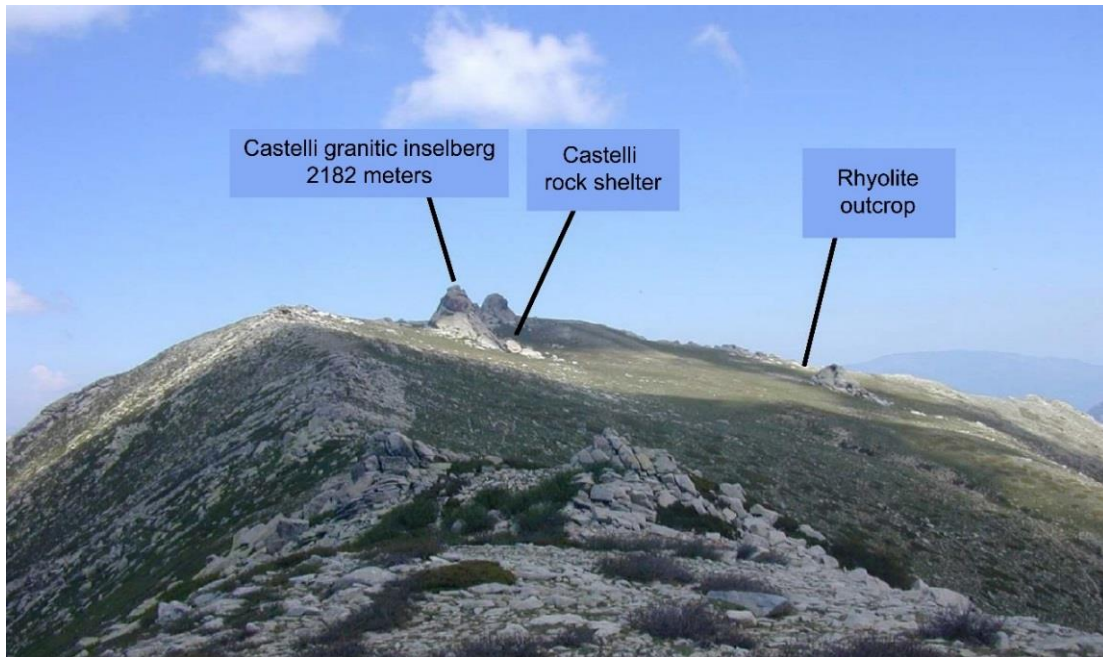


Figure 7.2. The Castelli plateau – view from the south-west. ©S. Mazet. Mazet, Dir. 2011.

A succession of 5 excavation campaigns conducted between 2008 and 2014 on the Castelli rock shelter revealed a long occupation sequence, starting from the Early Neolithic. In total, three main occupation periods were revealed during the Neolithic (**Figure 7.3**), two of which were clearly dated by ^{14}C (Mazet, Dir., 2011):

- Middle Neolithic:
 - Layer 1: 4958 ± 55 B.P. (LT 4436A: 3939-3642 cal. B.C. [2σ])
- Early Neolithic:
 - Level G: 6325 ± 55 B.P. (LT 4435A: 5469-5212 cal. B.C. [2σ])

Below the surface level is a disturbed layer in which the majority of the piercing projectile points ‘à crans obtus’ was found. This could indicate that the site might also have been occupied during the Late Neolithic, although more punctually (Mazet, Dir.,

2010:64). Such a hypothesis will have to be confirmed by further excavation campaigns, which are currently under way.

Archaeological structures of the site include paved hearts, retaining walls, and a storage pit, supplemented by a debitage workshop. The large amount of lithic remains excavated from such a restricted area suggests that it was mainly dedicated to the production of stone tools, while the I Pozzi open air site probably constituted the main seasonal settlement (Mazet, Dir., 2011:60).

7.1.2. Lithic industries

The lithic industry of the site was thus abundant, with a total of 7786 artefacts collected thus far in the rock shelter itself, all occupation levels considered. Several raw materials are represented (**Table 7.1**), and are both local and exogenous. Local materials involve a grey rhyolite likely obtained from the nearby outcrop, a reddish rhyolite (facies present at the Monte Cinto, situated north of the Abri des Castelli, see **Figure 1.3**), and quartz, omnipresent on the plateau. A small proportion of the assemblage is made of obsidian (n=620, > 8 %) and flint (n=15, > 0.2 %), which cannot be found on the Corsican island. Microscopic studies (see Mazet *et al.*, 2014) revealed a Sardinian origin for the flint artefacts (Perfugas basin; *cf.* **Figure 2.2**).

It is important to note that the lithic artefacts recovered from the rock shelter include a large number of projectile points, *i.e.* 98 cutting projectile points, 40 piercing projectile points, and 55 lunate projectile points. This substantial proportion of projectile points might indicate that the Castelli plateau may have been used as a hunting territory.

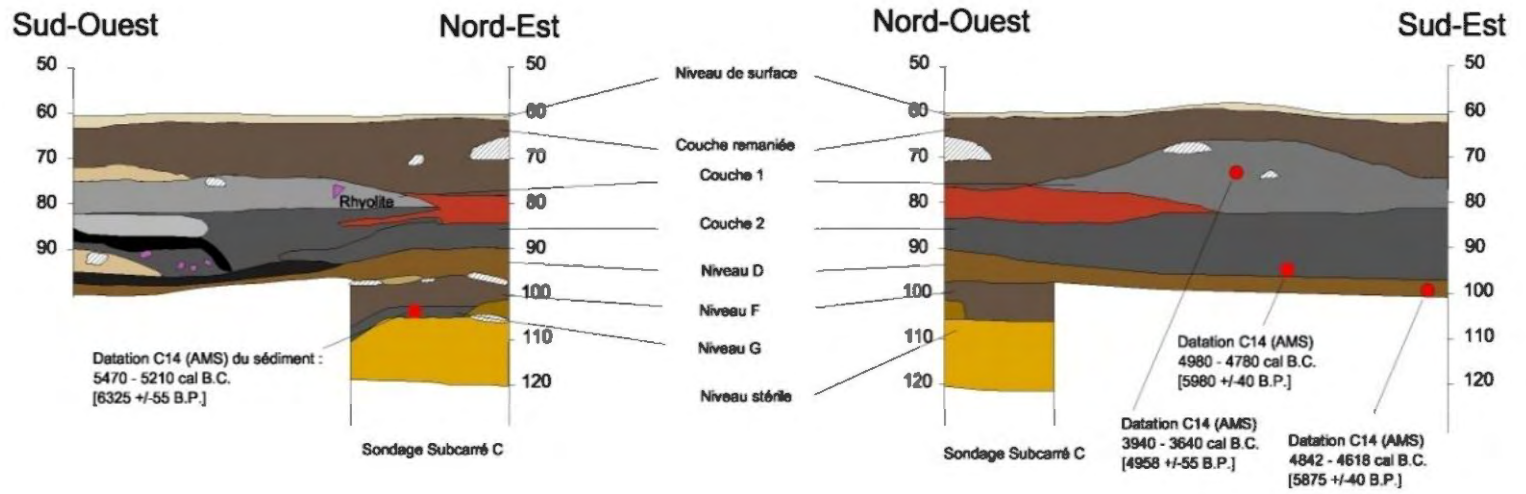


Figure 7.3. (previous page) Stratigraphy of the Abri des Castelli site. Southwest-Northeast cross-section (left) and Northwest-Southeast cross-section (right). Source: Mazet, Dir., 2011.

Table 7.1. Summary table of the different raw materials present at the Abri des Castelli site.

Raw Material	Total number of artefacts excavated		
	All occupation levels	5 th millennium B.C.	4 th millennium B.C.
Rhyolite	6563	2464	2633
Obsidian	620	205	288
Flint	15	6	3
Quartz	588	396	145

Regarding the obsidian industry, a typological and technological study of the assemblage is currently underway (Lauriane Martinet, under the direction of Didier Binder, CEPAM), but first observations show the presence of several characteristic elements such as lunate projectile points (n=21), cutting projectile points (n=8), piercing projectile points (n=2), blades (n=4), and bladelets (n=14). The debitage of obsidian on the site is attested by the presence of different by-products such as flakes, chips, and retouch chips. Obsidian cores are however absent from the assemblage while, in contrast, numerous rhyolite *nuclei* (n=67) were found on the site and at the associated outcrop.

7.2. Sourcing obsidian from the Castelli shelter: previous analyses and analytical strategy

7.2.1 Previous sourcing campaigns

The first characterisation campaign of the Castelli shelter obsidian assemblage was conducted by SEM-EDS at the IRAMAT-CRP2A on the artefacts excavated in 2008 that could be sampled for a partially destructive analysis. These measurements, performed by Dr. Le Bourdonnec (Mazet, Dir., 2011:52-54), revealed an exclusive use of Sardinian obsidians, and more particularly of the SC (n=39), SA (n=11), and SB2 (n=5) subtypes. Only one artefact revealed an unexpected geochemical composition, matching the SC Sardinian subtype with its Ca and Fe contents but presenting incoherent Na and Al contents. After a second analysis confirming the inconsistencies observed in its geochemical composition, this artefact was excluded from the SEM-EDS results (obsidian 515).

Further analyses were achieved by PIXE on the 18 artefacts remaining artefacts (including obsidian 515), and which necessitated a strictly non-destructive analysis. These measures were conducted at the CENBG (France) and confirmed the exclusive Sardinian origin, with 7 artefacts attributed to the SA type, the same amount to the SC type, and 4 to the SB2 type (see Mazet *et al.*, 2011).

7.2.2. Analytical strategy

In keeping with our recent objective to exhaustively and non-destructively analyse archaeological assemblages within a reasonable amount of time and budget, the newly available Abri des Castelli obsidians – *i.e.* issued from the 2009 and 2010 excavations – were recently considered for geochemical characterisation. This involved a total of 539

obsidian artefacts coming from the 4th millennium B.C. (n=267), 5th millennium B.C. (n=123), as well as from the surface and disturbed layers (n=149).

To achieve the sourcing of these particular artefacts, we chose to use two characterisation methods readily available to us, *i.e.* ED-XRF and LA-ICP-MS. The former was used on the artefacts presenting a sufficient size as well as satisfactory geometrical and surface characteristics (*cf.* **Chapter 4**, see also Davis *et al.*, 2011), while the latter was reserved for the smallest, thinnest and/or most irregular artefacts, as well as those unattributed with the first method.

7.3. ED-XRF analyses

7.3.1. Protocol

The ED-XRF analyses were conducted at the IRAMAT-CRP2A by Dr. Le Bourdonnec and Ms Perruchini (Masters' student). Using a benchtop SEA6000VX High Sensitivity X-Ray Analyzer from Seiko Instruments (see http://www.seiko-instruments.de/files/technical_data_sea6000vx.pdf) equipped with a 3 x 3 mm collimator, the contents of 11 minor and trace elements were measured for 122 artefacts: TiO₂, MnO, Fe₂O₃, Zn, Ga, Rb, Sr, Y, Zr, Nb, and Th. The results are reported in **Appendix I1**.

7.3.2. Results

The geochemical compositions obtained by ED-XRF on the 122 artefacts from the Abri des Castelli (**Appendix I1**) were compared to those of the 24 geological samples from the Western Mediterranean area including the sources of Sardinia (SA, SB1, SB2, and SC), Lipari, and Palmarola. A comparison of the log(Sr/Rb) and log(Zn/Rb) ratios (**Figure 7.4**) allowed us to attribute the majority of the artefacts to the Sardinian sources,

and to further distinguish 3 different origins within the Monte Arci massif: SC (n=67), SB2 (n=32), and SA (n=15). The remaining 8 artefacts (1700, 2271, 2582, 2654, 4175, 4991, 5626, and 100147) have unfortunately presented incoherent geochemical compositions, which did not match any of the sources taken into consideration in the geographical area. Their geochemical composition was aimed to be determined by LA-ICP-MS during the second step of our analytical strategy (see below).

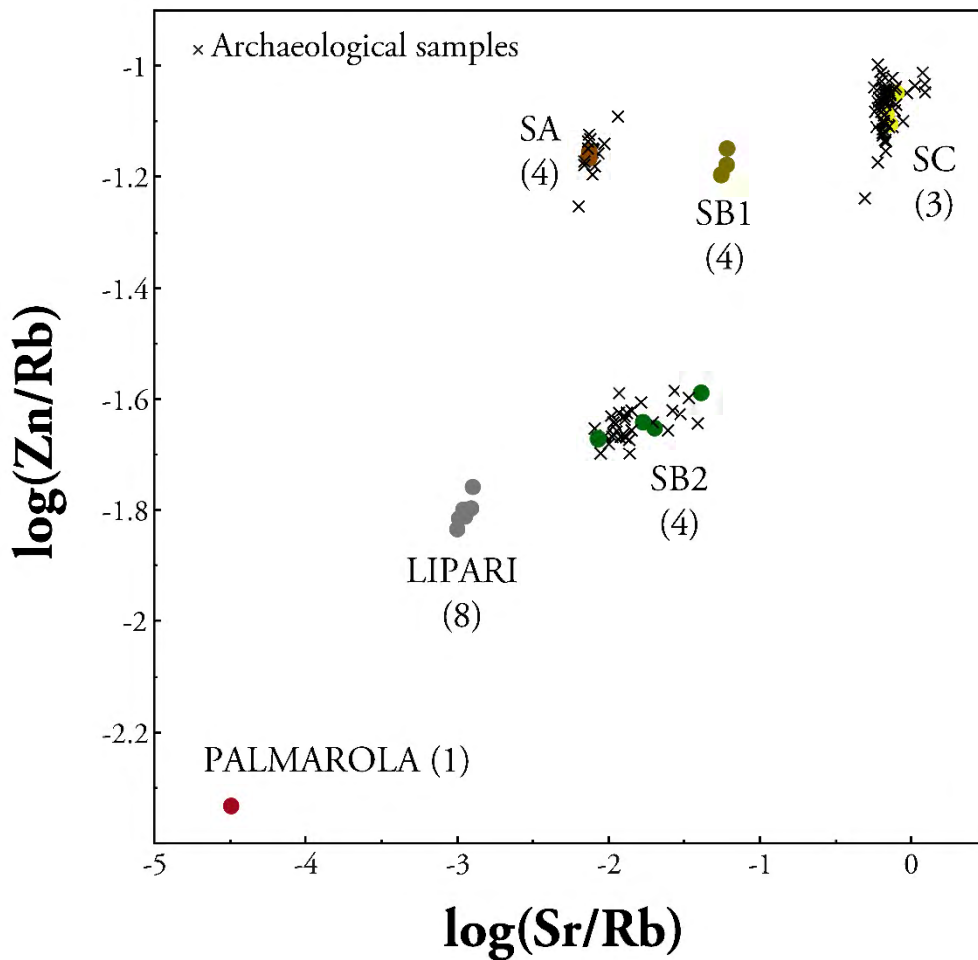


Figure 7.4. Comparison of the $\log(\text{Sr/Rb})$ and $\log(\text{Zn/Rb})$ ratios obtained by ED-XRF on 114 artefacts from the Abri des Castelli site and 24 geological samples from the Western Mediterranean area (Sardinia [SA, SB1, SB2, SC], Lipari, and Palmarola).

7.4. LA-ICP-MS analyses

7.4.1. Protocol

The rest of the artefacts - 344 involving 8 unattributed by ED-XRF - were characterised by LA-ICP-MS at the SOLARIS laboratory (Southern Cross University, Australia) with an Agilent 7700 Series ICP-MS coupled to a NWR213 (Nd:YAG deep UV laser [213 nm]) laser ablation system. Following our recently developed protocol (see **Chapter 5**), a line of 0.6 mm length, 40 μm width, and 10 μm depth was ablated on each archaeological sample. The NIST 613 international standard was analysed at the beginning and end of each run to ensure the accuracy and reproducibility of our analyses (data reported in **Chapter 5** and **Appendix F**). A total of 14 isotopes was measured (^{45}Sc , ^{66}Zn , ^{85}Rb , ^{88}Sr , ^{89}Y , ^{90}Zr , ^{93}Nb , ^{133}Cs , ^{137}Ba , ^{146}Nd , ^{147}Sm , ^{208}Pb , ^{232}Th , and ^{238}U), and the results compared to those of our geological database, including the main sources of the Western Mediterranean area (Monte Arci, Lipari, Palmarola, Pantelleria) and reference points on the Carpathian and Aegean (Yali, Antiparos, Melos) sources.

7.4.2. Results

Following the LA-ICP-MS results obtained on the 344 artefacts of the Abri des Castelli (complete data reported in **Appendix I2**), we were able to match the majority of this assemblage (95 %) with the Sardinian obsidian source of the Monte Arci. This is clearly illustrated in a comparison of the $\log(^{133}\text{Cs}/^{93}\text{Nb})$ and $\log(^{88}\text{Sr}/^{93}\text{Nb})$ ratios in **Figure 7.5**. More precisely, the SB2 and SC obsidian types largely prevail, respectively representing 39.8 % and 39.5 % of the assemblage (n=137, n=136). Less than 15 % was attributed to the SA type, and even less to the SB1 type (≈ 1 %).

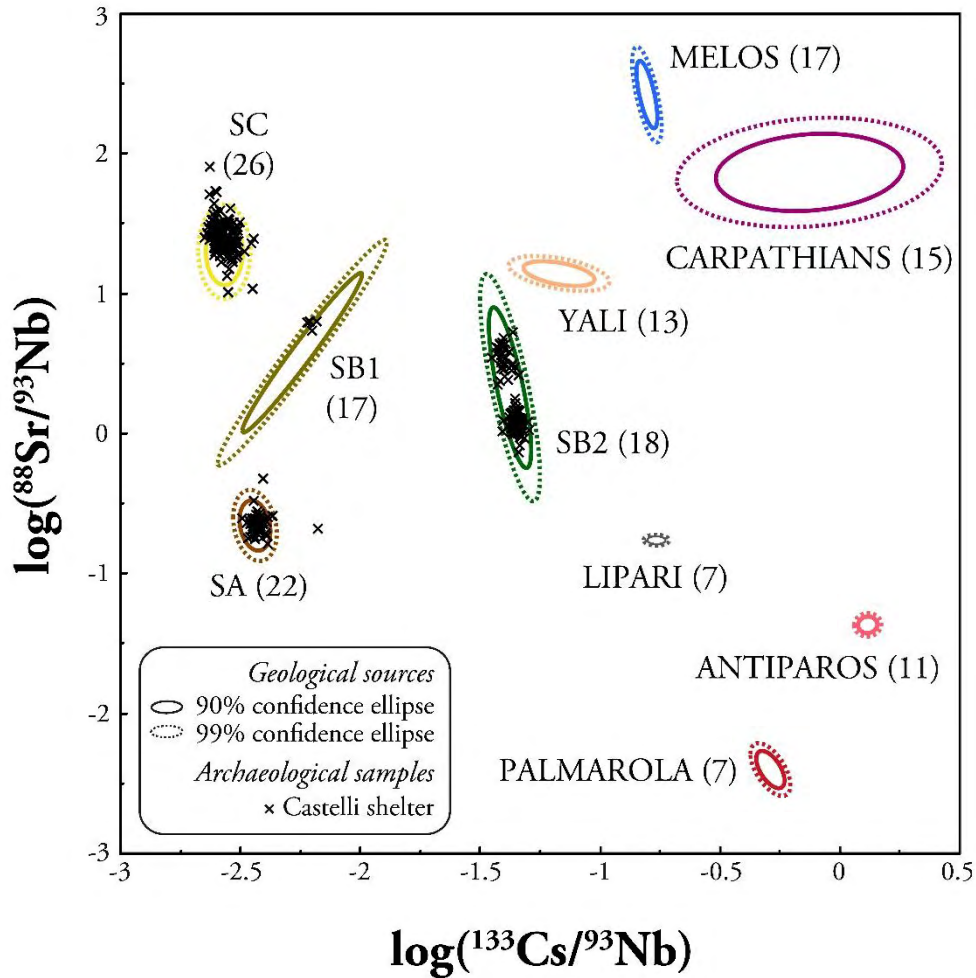


Figure 7.5. Comparison of the $\log(^{133}\text{Cs}/^{93}\text{Nb})$ and $\log(^{88}\text{Sr}/^{93}\text{Nb})$ ratios obtained by LA-ICP-MS on 328 artefacts from the Abri des Castelli site and 153 geological samples from the Mediterranean area (Sardinia [SA, SB1, SB2, SC], Lipari, Palmarola, Melos, Yali, Antiparos, and the Carpathian sources). For reasons of clarity, the sources of Pantelleria (Balata dei Turchi and Lago di Venere) are not represented.

However, we were unable to match the remaining 16 artefacts (see data in **Appendix I2**) to any of the sources taken into consideration in our study. Among these 16 unattributed artefacts, three (1700, 5626, and 2654) were already presenting unexpected geochemical compositions when analysed by ED-XRF at the IRAMAT-CRP2A (see above). Their geochemical composition is indeed unexpected: some isotopes (^{133}Cs ,

^{238}U) show concentrations resembling what we could find for the SB2 source, while others (^{88}Sr , ^{137}Ba) rather indicate a SC origin. Interestingly, their composition resembles one of the artefacts from I Stantari (see **Chapter 6; Appendix H2**) that could not be attributed to any of the geological sources. As mentioned during this previous study, these artefacts might correspond to rhyolites or to some intermediary facies between obsidian and rhyolite. In any case, their provenance will have to be investigated further.

The remaining five artefacts unattributed by ED-XRF were able to be matched with a specific source with the LA-ICP-MS analyses: 2271, 2582, and 100147 matched the SB1 source, while 14175 and 4991 matched SB2 (*cf.* **Appendix I2**).

7.5. Discussion and conclusions

7.5.1. *General obsidian economy of the site*

A total of 515 artefacts from the Abri des Castelli were thus successfully characterised across the different sourcing campaigns (**Table 7.2**) and as part of a more recent analytical strategy, allowing a first distribution to be drawn of the obsidian types within the general obsidian consumption of the site.

Solely originating from the Monte Arci source in Sardinia, the Abri des Castelli assemblage shows overall a clear predilection for the SC type which constitutes 47 % of the total assemblage characterised. Following are the SB2 type obsidians (34 % of the total assemblage), some SA type obsidians (n=84, 16 %), and even fewer SB1 obsidians (n=4, > 1 %).

Table 7.2. Summary table of the different obsidian sources used on the Abri des Castelli settlement, their proportions, and the number of artefacts characterised by each analytical method. N/A indicates the number of artefacts that we were not able to attribute with the characterisation methods applied.

ORIGIN	ED-XRF	PIXE	SEM-EDS	LA-ICP-MS	Total	%
SA	15	7	11	51	84	16 %
SB1	-	-	-	4	4	0.8 %
SB2	32	4	5	137	178	34 %
SC	67	7	39	136	249	47 %
N/A	8	-	-	16	16	3 %
Total	122	18	55	344	539	-

7.5.2. Comparison between the 5th and 4th millennia B.C.

If we consider the obsidian consumption of the site per occupation period (leaving aside the obsidians originating from the reworked layer and those obtained during surface prospections [n=81]), the analyses reveal a change of proportions between the 5th and the 4th millennia B.C. (see **Table 7.3.** and **Figure 7.6**). During the 5th millennium B.C., it appears that the obsidians from the SB2 source are predominant (n=77, 38 % of the assemblage), while SC obsidians are less used, representing only 18 % (n=37) of the assemblage for this occupation period. The SA and SB1 obsidian subtypes are even scarcer, constituting only less than 4 % (< 0.5 % for SB1) of the assemblage. These ratios visibly change during the 4th millennium where the majority of the assemblage (n=152, 53 %) then originated from the SC source. The rest are almost equally distributed between the SA and SB2 types, with respectively 19 % and 16 % of the total assemblage (n=55, n=47), as well as a sporadic use of the SB1 obsidians (n=3, 1 %).

However, the significant fraction of obsidians unattributed, 11 % for the 4th millennium and up to 40 % for the 5th millennium B.C., suggests that the source proportions (especially in the 5th millennium) could change with further characterisations.

Table 7.3. Obsidian sourcing results for the Abri des Castelli assemblage: source proportions and unattributed artefacts by occupation period (4th and 5th millennium B.C.). N/A indicates the number of artefacts that we were not able to attribute with the characterisation methods applied, and Unav. the artefacts that were unavailable for analysis and are yet to be characterised.

ATTRIBUTION	5 th millennium B.C.	4 th millennium B.C.
SA	8	55
SB1	1	3
SB2	77	47
SC	37	152
N/A	0	10
Unav.	82	21
<i>Total</i>	<i>205</i>	<i>288</i>

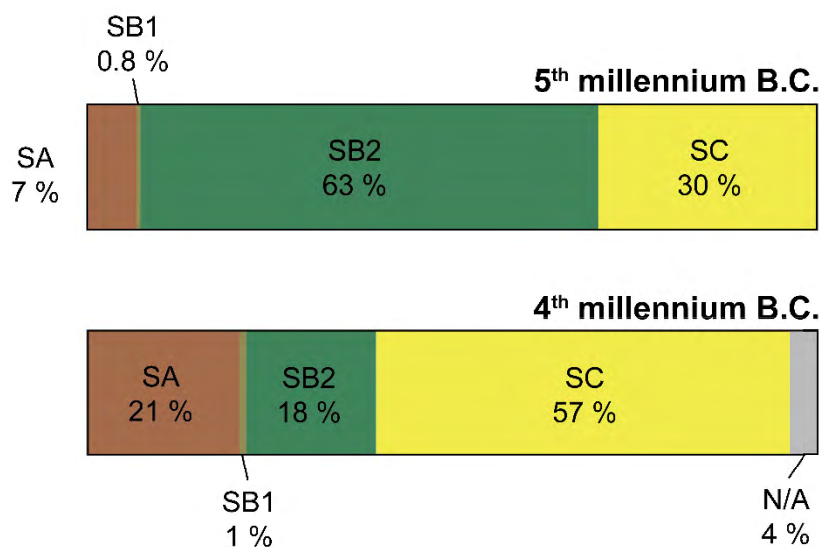


Figure 7.6. Obsidian source proportions per occupation period at the Abri des Castelli site. N/A indicates the percentage of artefacts that we were not able to attribute with the characterisation methods applied.

7.5.3. Comparison with the obsidian economy of other archaeological sites

The exclusive presence of obsidians originating from the Monte Arci in Sardinia during the Neolithic at the Castelli shelter is consistent with the observations made on other sites in Corsica (see **Chapter 2**).

The results obtained for the Abri des Castelli however have to be considered with precaution, as the amount of unattributed/un-analysed artefacts is relatively high (40 % for the 5th millennium B.C. level, and 11 % for the 4th millennium B.C. level), and further analyses could very well change the proportions of each subtype found on the site, or even reveal the use of another source – especially for the 5th millennium B.C.

Hence, no real comparison or definite conclusion can so far arise for our analyses, and only further studies will give us the possibility to draw diffusion and consumption patterns of the obsidian raw material in the Castelli shelter.

7.6. Further studies

The advancement of this interdisciplinary research project will require the completion of several steps:

- the integration of the typological and technological characteristics of the assemblage to the sourcing results,
- the contextualisation of the artefacts within the archaeological context of the site,
- the elaboration of hypotheses regarding the obsidian economy of the site for the Neolithic period,
- a synchronic and diachronic analysis of the data obtained, and
- the contextualisation of all of the data above to a wider regional context.

To achieve these aims, further analyses are programmed to characterise the remaining artefacts, investigate further the unexpected results obtained for the 16 unattributed obsidians, and determine the provenance of the most recently excavated material. So far, only part of the material excavated during the 2008, 2009, and 2010 campaigns has been studied. For the 5th millennium B.C., the high portion of unattributed or not yet analysed artefacts (40 %) is preventing us from making accurate conclusions on the obsidian consumption patterns in place during this particular period, or to reconstruct an evolution of these patterns for the overall occupation of the site.

Complementary studies will therefore focus on pursuing the exhaustive analysis of the assemblage, and the integration of these results with the information brought by their typo-technological study, to help complete our knowledge of this exceptional high altitude site.

Chapter 8

A Guaita

8.1. The A Guaita archaeological site

8.1.1. General context

The A Guaita site is located in northern Corsica (Cap Corse; see **Figure 1.3**), in the Morsiglia municipality (Lorenzi, 2011a). This open-air settlement, situated on a low coastal hill - 107 meters above sea level (**Figure 8.1**), has been excavated since 2004 under the supervision of Françoise Lorenzi (Université de Corse). The last excavation campaign was conducted in 2013, after which the site was restored to its original state following the last prefectorial authorisation decree (23rd May 2012). The complete study of this archaeological site and of the materials excavated is still underway, and a synthesis of the work so far achieved by the different specialists involved is programmed for the near future.



Figure 8.1. View of the A Guaita site from Centuri (Cap Corse). The arrow indicates the location of the upper terrace of the site. ©F. Lorenzi. Adapted from Lorenzi, 2011a.

The excavations revealed two occupation phases (Lorenzi, 2011a): an Early Neolithic level (layer 3; late 6th millennium B.C. – first half of the 5th millennium B.C.) and a Middle-Late Neolithic occupation level (layer 2a and 2b; second half of the 5th millennium B.C.). The Early Neolithic phase has already been attested at the neighbouring site of Lumaca (Lorenzi, 2000), the inhabitants of which were likely to have been in contact with the A Guaita population (Lorenzi, 2011a:24).

The general stratigraphy of A Guaita is however relatively disturbed by a dense vegetal cover (roots, *etc.*; bioturbations), which disadvantaged any radiocarbon dating. Therefore, the proposed chrono-cultural attributions were inferred from the abundant archaeological material excavated (Lorenzi, 2011a:18).

The originality of the site lies in two important features. First, the Early Neolithic level contains ceramics representing two different cultural trends from the Tyrrhenian area: the *ceramica cardiale* and the *ceramica a line incise* facies (see **Figure 8.2**; *cf.* Lorenzi, 2011a; Gabriele and Lorenzi, 2014). The presence of ceramics *a line incise* in Corsica is unprecedented, and bears witness of cultural contacts between the island and extra-insular groups from Tuscany or the northern Latium, where this type of ceramic is well attested. The combination of the two trends has also been revealed in Tuscany on the Cala Giovanna Piano site (Lorenzi, 2011b:231), where other lithic elements corroborate contacts between the two regions. Second, the presence of a large quadrangular settlement structure attributed to the 4th millennium B.C. (level 2a; see Le Bourdonnec *et al.*, 2014: Fig.3), somewhat comparable to those found at A Fuata (Neuville, 2007) or Monte Revincu (Léandri, 2007), is however a unique find in this part of the island (Cap Corse).

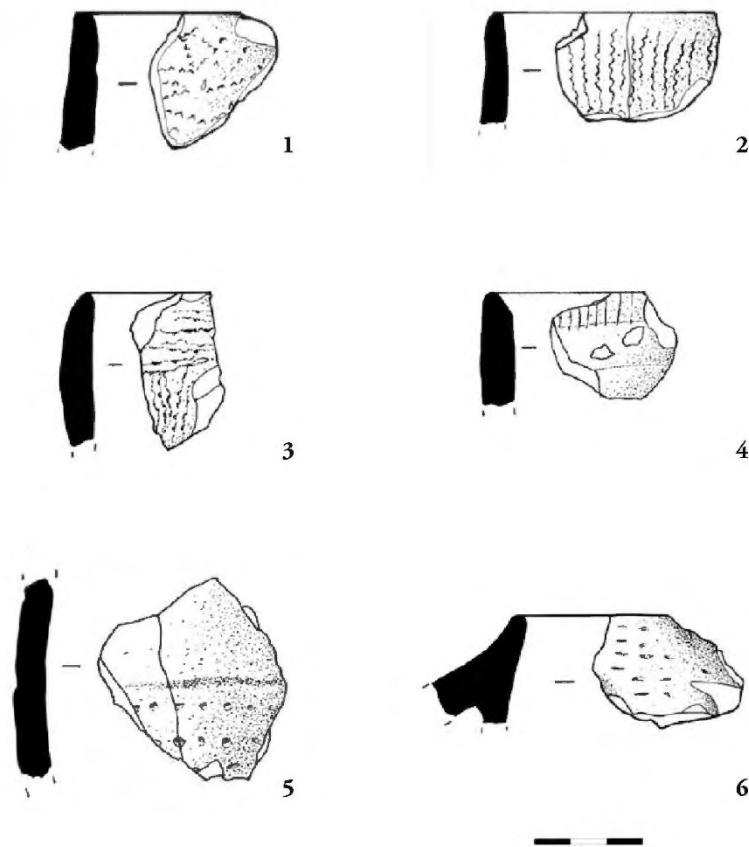


Figure 8.2. *Ceramica cardiale* (1-4) and *ceramica a line incise* (5, 6) elements from the A Guaita site. Technical drawing by F. Lorenzi. Adapted from Lorenzi, 2011b.

8.1.2. *Lithic industries*

The lithic industry of A Guaita is relatively dense and diversified. The raw materials mostly consist of exogenous materials, with the exception of the rhyolite and quartz probably obtained locally (Balagne, Lorenzi, 2011b:230). Exogenous materials are jasper and flint, which might have been found in Sardinia or Tuscany, as well as obsidian. The latter represents almost half of the total lithic assemblage in the levels 3 and 2b - 44 % in each, a ratio that decreases to 28 % in the level 2a; these proportions however seem to match what is usually observed in the area (see Le Bourdonnec 2014:327).

Characteristic obsidian elements consist of some blades and bladelets, borers (**Figure 8.3**), and scrapers.

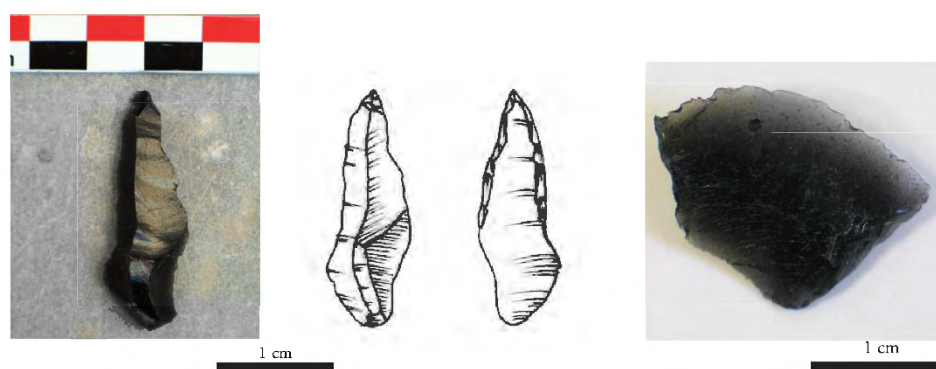


Figure 8.3. Obsidian borer from the A Guaita site: photography (left) and technical drawing (centre). Obsidian armature *à tranchant transversal* (right). Photography: ©N. Mattei – from Lorenzi, 2011a. Drawing by F. Lorenzi, from Lorenzi, 2011b.

8.2. Sourcing obsidian from A Guaita: previous analyses and analytical strategy

8.2.1. Previous sourcing campaigns

A first sourcing campaign was conducted on part of the A Guaita obsidians (140 artefacts), issued from every occupation level of the site. This study, published recently (Le Bourdonnec *et al.*, 2014), used SEM-EDS and PIXE to characterise these artefacts. The SEM-EDS analyses were conducted in destructive mode at the IRAMAT-CRP2A and allowed the attribution of 122 artefacts to the Sardinian source of the Monte Arci and the island-source of Palmarola (see details in **Table 8.1**; *cf.* Le Bourdonnec *et al.*, 2014: Table 3). The 18 remaining artefacts, which could not be sampled, were analysed non-destructively by PIXE at the C2RMF (AGLAE platform), along with the two artefacts previously attributed to the Palmarola source with SEM-EDS.

If we only consider the 69 obsidian artefacts issued from the Middle Neolithic occupation level (second half of the 5th millennium B.C.), the majority originated from the SC (n=33) and SB2 (n=24) Sardinian subtypes, followed by the SA subtype (n=12). If obsidians from Palmarola are present in the Early and Late Neolithic levels, they are apparently absent in between these periods (see **Table 8.1**).

Table 8.1. Summary of the A Guaita obsidian artefacts attributions (n=140) after SEM-EDS and PIXE analyses. Adapted from Le Bourdonnec *et al.*, 2014.

PERIOD	LEVEL	SA	SB2	SC	PALMAROLA
Early Neolithic	3	-	4	7	1
Middle Neolithic	2b	12	24	33	-
Late Neolithic	2a	10	14	20	1
Superficial layer (modified)	1	1	8	5	-
<i>Total</i>		23	50	65	2

8.2.2. Analytical strategy

The majority of the A Guaita obsidian assemblage left to analyse was found to be suitable for ED-XRF measurements, *i.e.* they displayed satisfactory size, shape, and surface state (see **Chapter 4**). This represents a further 161 artefacts, excavated between 2006 and 2013 in the levels 1 (disturbed surface layer), 2a, 2b, and 3. As a complement to the ED-XRF analyses, conducted at the IRAMAT-CRP2A laboratory in France, the LA-ICP-MS technique was also brought into this project to analyse any artefact presenting problematic results or not matching the geochemical composition of the sources taken into consideration in the previous set of analyses.

8.3. ED-XRF analyses

8.3.1. Protocol

The ED-XRF analyses were conducted at the IRAMAT-CRP2A laboratory, with a benchtop SEA6000VX High Sensitivity X-Ray Analyzer from Seiko Instruments equipped with a 3 x 3 mm collimator (to overcome any heterogeneity such as mineral inclusions). The Rh source (50 kV / 1 mA) and the SDD Vortex detector allow the measurement of the contents of at least a dozen of minor and trace elements. Here we chose to assay the following: TiO₂, MnO, Fe₂O₃, Zn, Ga, Rb, Sr, Y, Zr, Nb, and Th. The complete set of results is presented in **Appendix J1**.

8.3.2. Results

Once compared to the geochemical signature of the geological samples from the main Western Mediterranean sources (n=24) – obtained under the same analytical conditions, we observe that the fingerprint of 155 of the studied artefacts match the specific source of the Monte Arci in Sardinia (see **Chapter 2**). This is clearly illustrated in a comparison of the log(Zn/Rb) and log(Sr/Rb) ratios (**Figure 8.4**), where 36 artefacts were assimilated to the SA subtype, 50 to the SB2, and 69 to SC (see also **Table 8.2**).

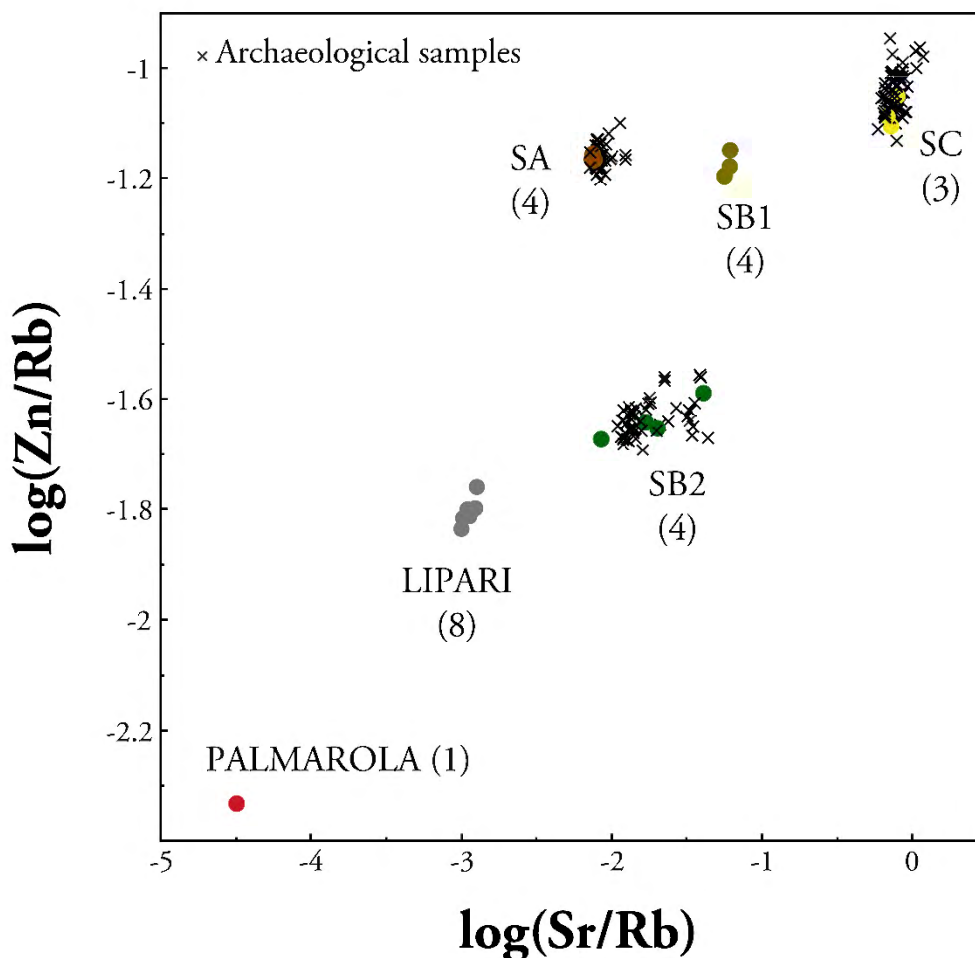


Figure 8.4. Comparison of the $\log(\text{Sr/Rb})$ and $\log(\text{Zn/Rb})$ ratios obtained by ED-XRF on 161 artefacts from A Guaita and 24 geological samples from the Western Mediterranean area (Sardinia [SA, SB1, SB2, SC], Lipari, and Palmarola).

The origin of 6 artefacts could however not be determined (AG09-2b-22, AG10-2b-131, AG12-2a-63, AG12-2b-14, AG13-2b-tamis Z4b, and AG13-3-150). To ensure that the unexpected geochemical compositions obtained – *i.e.* not matching any of the sources taken into consideration in the ED-XRF sourcing campaign – were not caused by the samples themselves (geometry, size/thickness) or by any analytic dysfunction, LA-ICP-MS analyses were programmed on these 6 artefacts.

8.4. LA-ICP-MS analyses

8.4.1. Protocol

In 2015 and as part as this research project focusing on the obsidian diffusion and economies in Corsica during the Middle Neolithic period, the 6 artefacts from A Guaita of an unknown origin were analysed virtually non-destructively at the SOLARIS laboratory (Southern Cross University) by LA-ICP-MS. The instrumentation available at the SOLARIS laboratory consists of an Agilent 7700 Series ICP-MS coupled to a NWR213 (Nd:YAG deep UV laser [213nm]) ablation system. The NIST 613 international standard was analysed at the beginning and end of each run to ensure the accuracy and reproducibility of our analyses (data reported in **Chapter 5** and **Appendix F**). A total of 14 minor and trace isotopes were assayed, following the protocol developed as part of the present research project (see **Chapter 5**): ^{45}Sc , ^{66}Zn , ^{85}Rb , ^{88}Sr , ^{89}Y , ^{90}Zr , ^{93}Nb , ^{133}Cs , ^{137}Ba , ^{146}Nd , ^{147}Sm , ^{208}Pb , ^{232}Th , and ^{238}U .

8.4.2. Results

Using a comparison of the $\log(^{133}\text{Cs}/^{93}\text{Nb})$ and $\log(^{88}\text{Sr}/^{93}\text{Nb})$ ratios (see Aitchison, 1982) we were able to conclude on the origin of 4 of the 6 artefacts. Their geochemical fingerprint indeed matches the Lipari source (n=3) and the SA subtype (n=1), as illustrated in **Figure 8.5**. The two artefacts presenting an unexpected composition could not be matched with any of the sources of our database (including geological samples from the Western Mediterranean and Aegean Area, and a reference point from the Carpathian sources, see **Chapter 5**), as shown by the results summarised in **Appendix J2**. Their geochemical signature is however very similar to those of the I Stantari and Abri des Castelli artefacts that we were unable to attribute with LA-ICP-MS (*cf.* **Chapters 6 and 7**; **Appendices H2 and I2**), only with slightly lower Zr contents (163

in average instead of 182 for the Abri des Castelli artefacts), and slightly lower Ba contents (534 instead of 584). As already discussed for the two aforementioned sites, these artefacts might not be obsidians, but rather rhyolites or a slightly different facies, between obsidian and rhyolite. Once again, these results will have to be explored further to identify the origin of these particular samples.

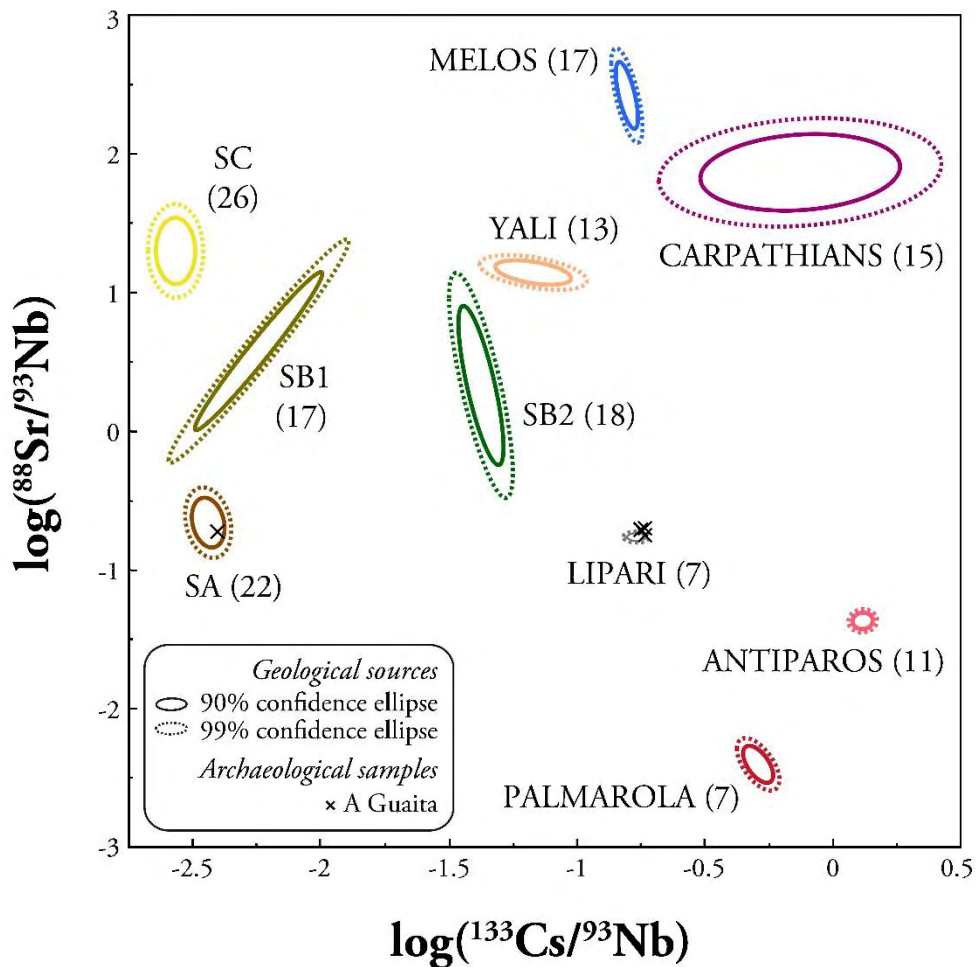


Figure 8.5. Comparison of the $\log(^{133}\text{Cs}/^{93}\text{Nb})$ and $\log(^{88}\text{Sr}/^{93}\text{Nb})$ ratios obtained by LA-ICP-MS on 4 artefacts from A Guaita and 153 geological samples from the Mediterranean area (Sardinia [SA, SB1, SB2, SC], Lipari, Palmarola, Melos, Yali, Antiparos, and the Carpathian sources). For reasons of clarity, the sources of Pantelleria (Balata dei Turchi and Lago di Venere) are not represented.

8.5. Discussion and conclusions

The adoption of a tailored analytical strategy adapted to the A Guaita assemblage has permitted the analysis of 302 artefacts in total, within which only 2 were not attributed to a specific source. The number of artefacts assigned to each geological source by each method is summarised in **Table 8.2**, as well as the percentage that each source represents within the overall obsidian assemblage.

Table 8.2. Summary table of the different obsidian sources used at A Guaita, their proportions, and the number of artefacts characterised by each analytical method.

ORIGIN	SEM-EDS	PIXE	ED-XRF	LA-ICP-MS	Total	%
SA	18	5	36	1	59	20 %
SB1	-	-	-	-	-	-
SB2	48	2	50	-	100	33 %
SC	54	11	69	-	134	44 %
Palmarola	(2)	2	-	-	2	1.3 %
Lipari	-	-	-	3	3	1 %
Unknown	-	-	6	2	2	>1 %
Total attributed	120(122)	20	155	4	302	-

As shown in **Figure 8.6**, the majority of the A Guaita artefacts came from Sardinia, and more specifically from the SA, SB2, and SC sources – with respectively 20 %, 33 %, and 44 % of the assemblage. As seen in the previous case studies and in **Chapter 2**, such a general pattern is certainly common in Corsica. More unusual however is the presence of not one, but two different raw materials originating from other sources than the Monte Arci: Palmarola (n=4) and Lipari (n=3). Their presence is not rare, as Palmarola obsidians are attested in a few sites (Castiglione, Salotti *et al.*, 2000; A Guaita, Le Bourdonnec *et al.*, 2014; Renaghju, Le Bourdonnec *et al.*, 2015a), and the obsidians of

Lipari were found in A Fuata (Le Bourdonnec *et al.*, 2010; *cf.* **Figure 1.3**). To our knowledge, it is however the first time that both raw materials are present on the same Corsican Neolithic site.

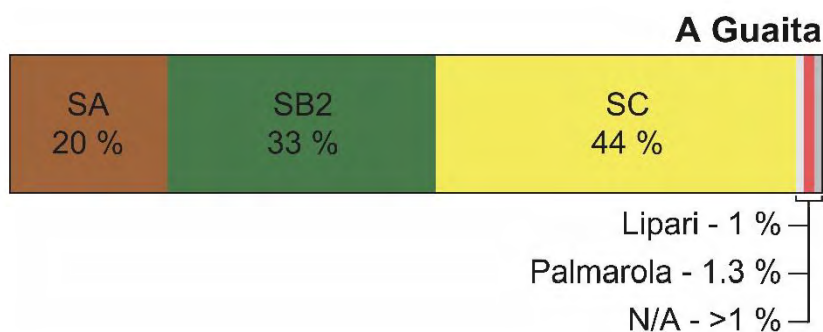


Figure 8.6. Obsidian source proportions at A Guaita. N/A indicates the percentage of artefacts that we were not able to attribute with the characterisation methods applied.

A discussion on the proportions of obsidian raw materials on the A Guaita site is somewhat delicate. Indeed, as mentioned before no absolute dating was obtained on the site, due to the intense vegetal cover and the numerous bioturbations observed. Further conclusions will need the integration of the typological and technological data of the artefacts to the sourcing results, as well as a thorough contextualisation of these results with the general archaeological information of the site itself.

Regarding the latter, a complete synthesis of the studies conducted on the site is in preparation, and will be published in the coming year within a monographic publication. This manuscript, directed by F. Lorenzi, will include reports from several experts on the different aspects of the site and its material, *e.g.* ceramics (M. Gabriele), stratigraphy (D. Battesti, M. Parisi), lithic industries (J. Sicurani, J. Conforti, B. Zamagni), and lithic raw material provenance (F.-X. Le Bourdonnec, M. Orange, C. Bressy-Leandri).

General Conclusions

Synthesis

The aims of this Ph.D. research project were threefold.

The first objective was to review and assess the way obsidian provenance studies have been conducted in the past and how they are conducted today, and to propose a different approach to enable the exhaustive analysis of the assemblages available for study. The ‘analytical strategy’ prescribed to attain this objective, as demonstrated in **Chapter 4**, is achieved through the complementarity of the methods available through collaborations, and allows the consideration of the numerous challenges inherent to the analysis of archaeological materials. This analytical strategy was followed in the archaeological applications undertaken in the present study (see **Chapters 6, 7, and 8**).

Secondly, an investigation of the LA-ICP-MS protocols generally used in the field of obsidian sourcing was performed (see **Chapter 5**). Following the review of past studies, we proposed here an optimised analysis protocol for the geochemical characterisation of obsidian artefacts from the Western Mediterranean. This protocol (i) builds on previous studies which investigated the use of ablation lines instead of ablation points, which helps to compensate for any sample heterogeneity, to achieve a higher count rate as well as a better signal stability, and to reduce laser-induced elemental fractionation, and (ii) improves the precision of our measurements by the means of a limited list of assayed isotopes, mainly selected by their potential to discriminate the geological sources considered.

The final and overall purpose of this research project was to use and apply the two ‘tools’ primarily developed – analytical strategy and optimised LA-ICP-MS protocol – to

obsidian archaeological assemblages from the Western Mediterranean, issued from sites bearing Middle Neolithic occupation phases, to ultimately bring new information on the social and economic features of these communities. Three settlements from Corsica, an island South of France, were chosen for this project: Renaghju and I Stantari (**Chapter 6**), the Castelli shelter (**Chapter 7**), and A Guaita (**Chapter 8**). The obsidian assemblage associated with their Middle Neolithic layer was geochemically characterised and matched with the possible sources. Thanks to the analytical strategy adopted, which allowed the analysis of each and every artefact of the assemblages considered, our study revealed, for example, a sporadic use of obsidian material from the source-island of Lipari at the A Guaita site. As mentioned in **Chapter 2**, if the majority of a Corsican obsidian assemblage usually originated from the Monte Arci source in Sardinia (*cf.* **Chapter 1**), it is however not uncommon to find one artefact or a handful coming from an obsidian source external to the Corso-Sardinian complex (see **Chapter 2**). Artefacts from other such ‘external’ sources hence provide a crucial information when reconstructing the obsidian diffusion and consumption patterns of a site, by highlighting (i) a contact with other obsidian procurement networks, or (ii) an eventual access to the outcrop in question.

Conclusions

This overall Ph.D. project finalises and ‘embodies’ some concepts previously mentioned by our research group, such as the analytical strategy, and continues the work already initiated in the intention to further our knowledge of the past populations under study.

The sourcing results obtained here bring new and substantial information on the obsidian economies (diffusion and consumption patterns) in place at the aforementioned archaeological sites for the Middle Neolithic period. Once completely integrated with

the typo-technological data, they will help to complete our knowledge of this important period of our evolution, so far relatively limited due to the low number of Corsican middle Neolithic sites studied to this day.

In this work we have thus deepened our knowledge of the Corsican Neolithic culture through the obsidian phenomenon. Producing new data, this thesis was however limited in time, and thus only represents a first assessment/overview of these long-term projects, of which the course and duration are often troubled by the work in collaboration with a large number of specialists.

Further studies

Our endeavour to further our understanding of the Middle Neolithic communities of Corsica will continue through the completion of the studies started within this Ph.D. project, with the integration of the typo-technological data to the sourcing results, but also the comparison of the conclusions made on the obsidian economies with the information gathered on other materials (*i.e.* lithic or ceramic). Finally, these research projects will bring together the totality of the data collected on the sites, and synchronic and diachronic comparisons will be made to complete a general ‘picture’ of the evolution of the Middle Neolithic phase in this region.

The results obtained on the Abri des Castelli and on the A Guaita sites will also be submitted for publication in peer-reviewed journals shortly.

Furthermore, this endeavour will also be carried on beyond this Ph.D. project, with the initiation of new research projects on several Corsican sites: the Listrella e Stabielle (North-Western Corsica) and the Basi (Southern Corsica) settlements. These projects will be conducted in collaboration with the Archaeologists in charge of the sites (Pascal

Tramoni for Listrella e Stabielle; Thomas Perrin for Basi) and the specialists in charge of their study. The first results obtained on the former were already presented at the International Symposium on Archaeometry [ISA] 2016 in Kalamata, Greece (15th-21st May 2016), while the data collected so far on the Basi assemblage will be introduced at the 12th RMPR meeting (Rencontres Méridionales de Préhistoire Récente) held in Bayonne, France, later this year (29th September – 1st October 2016).

Finally, the research project '*PAST-OBS: De la transhumance à la mine : le rôle des pasteurs nomades dans les exploitations protohistoriques de l'obsidienne en Iran et au Caucase*' ('PAST-OBS: From transhumance to mine: the role of the nomadic pastoralists in the protohistorical exploitation of the obsidian material in Iran and in the Caucasus'), led by Dr. Le Bourdonnec from the Université Bordeaux Montaigne (IRAMAT-CRP2A, Pessac, France), was initiated in collaboration with the laboratories Archéorient (UMR 5133, Lyon France), Archéozoologie et Archéobotanique (UMR 7209, MNHN, Paris, France), DAI – Eurasien Abteilung – 'Aussenstele Teheran' (Berlin, Germany), the CENBG (UMR 5797, Gradignan, France), the IRAMAT-CEB (UMR 5060, Orléans, France), the IRAMAT-LMC (UMR 5060, Saclay, France), and SOLARIS – Southern Cross University (Lismore, Australia). Funded by the LaScArBx (LabEx) – a research programme supported by the ANR (ANR-10-LABX-52), this project will entail a one-year post-doctoral position, which will allow me to investigate the obsidian economies on archaeological sites of the Sirab region in Nakhchivan (Azerbaijan), employing the analytical strategy and the LA-ICP-MS optimised protocol developed during the course of this Ph.D study. This project will complement the larger research program led in the area since 2013, looking at the emergence of the first mining industries in the Caucasus (Program ANR/DFG 'Mines', Dir. Dr. Catherine Marro, Dr. Thomas Stöllner).

REFERENCES

ACQUAFREDDA, P. & PAGLIONICO, A. 2004. SEM-EDS microanalysis of microphenocrysts of Mediterranean obsidians: a preliminary approach to source discrimination. *European Journal of Mineralogy*, 16: 419-429.

ACQUAFREDDA, P. & MUNTONI, I. M. 2008. Obsidian from Pulo di Molfetta (Bari, Southern Italy): provenance from Lipari and first recognition of a Neolithic sample from Monte Arci (Sardinia). *Journal of Archaeological Science*, 35, 947-955.

ACQUAFREDDA, P., LORENZONI, S. & ZANETTIN, E. 1996. Discrimination of Melos, Lipari, Palmarola obsidian using SEM-EDS. In: DEMIRCI, S., ÖZER, A. M. & SUMMERS, G. D. (eds.). *The proceedings of the 29th International Symposium on Archaeometry, Ankara 1994*. Tübitak, Ankara, 87-97.

ACQUAFREDDA, P., ANDRIANI, T., LORENZONI, S. & ZANETTIN, E. 1999. Chemical characterization of obsidians from different Mediterranean sources by non-destructive SEM-EDS analytical method. *Journal of Archaeological Science*, 26, 315-325.

AITCHISON, J. 1982. The statistical analysis of compositional data. *Journal of the Royal Statistical Society, Series B (Methodological)*, 139-177.

AMBROSE, W., ALLEN, C., O'CONNOR, S., SPRIGGS, M., OLIVEIRA, N. V. & REEPMEYER, C. 2009. Possible obsidian sources for artifacts from Timor: narrowing the options using chemical data. *Journal of Archaeological Science*, 36, 607-615.

AMBROZ, J. A., GLASCOCK, M. D. & SKINNER, C. E. 2001. Chemical Differentiation of Obsidian within the Glass Buttes Complex, Oregon. *Journal of Archaeological Science*, 28, 741-746.

AMMERMAN, A. J. 1979. A Study of Obsidian Exchange Networks in Calabria. *World Archaeology*, 11, 95-110.

AMMERMAN, A. J. & ANDREFSKY, W. 1982. Reduction Sequences and the Exchange of Obsidian in Neolithic Calabria. In: ERICSON, J. E. & EARLE, T. K. (eds.) *Contexts for Prehistoric Exchange*. New York, New York: Academic Press.

AMMERMAN, A. J., CESANA, A. & TERRANI, M. 1990. Neutron Activation Analysis of Obsidian from Two Neolithic Sites in Italy. *Journal of Archaeological Science*, 17(2): 209-220.

ASTRUC, L., GRATUZE, B., PELEGRIN, J. & AKKERMANS, P. 2007. From production to use: a parcel of obsidian bladelets at Sabi Abyad II. *Technical Systems and Near Eastern PPN Communities*, 327-341.

BARCA, D., DE FRANCESCO, A. M. & CRISCI, G. M. 2007. Application of Laser Ablation ICP-MS for characterization of obsidian fragments from peri-Tyrrhenian area. *Journal of Cultural Heritage*, 8, 141-150.

BARCA, D., LUCARINI, G. & FEDELE, F. G. 2012. The Provenance of Obsidian Artefacts from the Wādī Ath-Thayyilah 3 Neolithic Site (Eastern Yemen Plateau) by LA-ICP-MS. *Archaeometry*, 54, 603-622.

BARGE, O. & CHATAIGNER, C. 2003. The procurement of obsidian: factors influencing the choice of deposits. *Journal of Non-Crystalline Solids*, 323, 172-179.

BAR-YOSEF, O., VANDERMEERSCH, B., ARENSBURG, B., BELFER-COHEN, A., GOLDBERG, P., LAVILLE, H., MEIGNEN, L., RAK, Y., SPETH, J. D. & TCHERNOV, E. 1992. The excavations in Kebara Cave, Mt. Carmel [and comments and replies]. *Current anthropology*, 497-550.

BECK, L. 2014. Recent trends in IBA for cultural heritage studies. *Nuclear Instruments and Methods in Physics Research Section B: Beam Interactions with Materials and Atoms*, 332, 439-444.

BELLOT-GURLET, L. & BRESSY-LEANDRI, C. 2014. Milieux, matériaux et ressources. Les matériaux colorants. In: PERRIN, T., MANEN, C. & SÉJALON, P. (eds.) *Le Néolithique ancien de la plaine de Nîmes (Gard, France)*. Toulouse.

BELLOT-GURLET, L., CALLIGARO, T., DORIGHEL, O., DRAN, J. C., POUPEAU, G. & SALOMON, J., 1999. PIXE analysis and fission track dating of obsidian from South American prehispanic cultures (Colombia, Ecuador). *Nuclear Instruments and Methods in Physics Research Section B: Beam Interactions with Materials and Atoms*, 150, 616-621.

BELLOT-GURLET, L., LE BOURDONNEC, F.-X., POUPEAU, G. & DUBERNET, S. 2004. Raman micro-spectroscopy of western Mediterranean obsidian glass: one step towards provenance studies? *Journal of Raman Spectroscopy*, 35, 671-677.

BELLOT-GURLET, L., POUPEAU, G., SALOMON, J., CALLIGARO, T., MOIGNARD, B., DRAN, J.-C., BARRAT, J.-A. & PICHON, L. 2005. Obsidian

provenance studies in archaeology: A comparison between PIXE, ICP-AES and ICP-MS. *Nuclear Instruments and Methods in Physics Research Section B: Beam Interactions with Materials and Atoms*, 240: 583-588.

BELLOT-GURLET, L., PELON, O. & SÉFÉRIADÈS, M. L. 2008. Détermination de provenance d'une sélection d'obsidiennes du palais minoen de Malia (Crète). *Comptes Rendus Palevol*, 7, 419-427.

BIGAZZI, G., BONADONNA, F., BELLUOMINI, G. & MALPIERI, L. 1971. Italian Obsidians. IV. Dating by Fission Track Methods. *Bulletin of the Geological Society of Italy*, 90(4): 469-480.

BIGAZZI, G., MÁRTON, P., NORELLI, P. & ROZLOŽNIK, L. 1990. Fission Track Dating of Carpathian Obsidians and Provenance Identification. *Nuclear Tracks and Radiation Measurements*, 17(3), 391-396.

BIGAZZI, G., ODDONE, M. & RADÌ, G. 2005. The Italian Obsidian Sources. *Archeometriai Műhely*, 1, 1-13.

BINDER, D. & COURTIN, J. 1994. Un point sur la circulation de l'obsidienne dans le domaine provençal. *Gallia préhistoire*, 36, 310-322.

BINDER, D., GRATUZE, B., MOURALIS, D. & BALKAN-ATLI, N. 2011. New investigations of the Göllüdağ obsidian lava flows system: a multi-disciplinary approach. *Journal of Archaeological Science*, 38, 3174-3184.

BINDER, D., GRATUZE, B. & VAQUER, J. 2012. La circulation de l'obsidienne dans le sud de la France au Néolithique. *Congrès Internacional Xarxes al Neolític – Neolithic Networks - Rubricatum: revista del Museu de Gavà*.

BOWEN, N. L. 1928. *The evolution of igneous rocks*, Princeton, New Jersey, Princeton University Press.

BOWMAN, H. R., ASARO, F. & PERLMAN, I. 1973. On the Uniformity of Composition in Obsidians and Evidence for Magmatic Mixing. *The Journal of Geology*, 81, 312-327.

BRESSY, C. 2002. *Caractérisation et gestion du silex des sites mésolithiques et néolithiques du nord-ouest de l'arc alpin. Une approche pétrographique et géochimique*, Thèse de doctorat de l'Université Aix-Marseille I.

BRESSY, C., BELLOT-GURLET, L., D'ANNA, A., PELLETIER, D. & TRAMONI, P. 2003. Provenance et gestion des matières premières lithiques du site néolithique ancien cardial de Renaghju (Sartène, Corse-du-Sud). In: SURMELY, F., ed. Les matières premières lithiques en Préhistoire, Table Ronde internationale, Aurillac, 20-22 juin 2002. *Préhistoire du Sud-Ouest*, 71-79.

BRESSY, C. S., D'ANNA, A., POUPEAU, G., LE BOURDONNEC, F.-X., BELLOT-GURLET, L., LEANDRI, F., TRAMONI, P. & DEMOUCHE, F. 2008. Chert and obsidian procurement of three Corsican sites during the 6th and 5th millenniums BC. *Comptes Rendus Palevol*, 7, 237-248.

BRESSY, C., LE BOURDONNEC, F. X., BELLOT-GURLET, L., COLONNA, A., D'ANNA, A., ERRERA, M. G. L., FEDERZONI, N., LEANDRI, F., LUGLIÈ, C., POUPEAU, G. & TRAMONI, P. 2010. Matières premières lithiques en Corse néolithique : étude de cas. In: DELESTRE, X. & MARCHESI, H., eds. *Archéologie des rivages méditerranéens : 50 ans de recherche : [actes du colloque d'Arles, 28-29-30 octobre 2009]*. Errance, Paris, 193-197.

BUCHNER, G. 1949. Ricerche sui giacimenti e sulle industrie ossidiane in Italia. *Rivista di Scienze Preistoriche*, 4, 162-186.

BURGER, R. & GLASCOCK, M. 2002. Tracking the Source of Quispisisa Type Obsidian from Huancavelica to Ayacucho. In: *Andean Archaeology I* (William Isbell & Helaine Silverman, eds.): 341-368; Springer, United States.

BURLEY, D. V., SHEPPARD, P. J. & SIMONIN, M. 2011. Tongan and Samoan volcanic glass: pXRF analysis and implications for constructs of ancestral Polynesian society. *Journal of Archaeological Science*, 38, 2625-2632.

CADOUX, A., PINTI, D. L., AZNAR, C., CHIESA, S. & GILLOT, P.-Y. 2005. New chronological and geochemical constraints on the genesis and geological evolution of Ponza and Palmarola Volcanic Islands (Tyrrhenian Sea, Italy). *Lithos*, 81, 121-151.

CALEY, E. R. 1951. Early history and literature of archaeological chemistry. *Journal of Chemical Education*, 28, 64-66.

CALEY, E. R. 1967. The early history of chemistry in the service of archaeology. *Journal of Chemical Education*, 44, 120-123.

CALLIGARO, T., DRAN, J.-C., MOIGNARD, B., PICHON, L., SALOMON, J. & WALTER, P. 2002. Ion beam analysis with external beams: recent set-up improvements. *Nuclear Instruments and Methods in Physics Research B*, 188, 135-140.

CAMPS, G. 1988. *Préhistoire d'une île. Les origines de la Corse*, Paris, Errance.

CANN, J. R. & RENFREW, C. 1964. The Characterization of Obsidian and Its Application to the Mediterranean Region. *Proceedings of the Prehistoric Society*, 30, 11-131.

CARTER, E. A., HARGREAVES, M. D., KONONENKO, N., GRAHAM, I., EDWARDS, H. G. M., SWARBRICK, B. & TORRENCE, R. 2009. Raman spectroscopy applied to understanding Prehistoric Obsidian Trade in the Pacific Region. *Vibrational Spectroscopy*, 50, 116-124.

CARTER, T. 2014. The contribution of obsidian characterization studies to early prehistoric archaeology. In: YAMADA, M. & ONO, A., eds. *Lithic Raw Material Exploitation and Circulation in Prehistory: A Comparative Perspective in Diverse Palaeoenvironments*, Liège, Belgique. ERAUL 138, 23-33.

CARTER, T. & SHACKLEY, M. S. 2007. Sourcing Obsidian from Neolithic CatalHoyuk (Turkey) Using Energy Dispersive X-Ray Fluorescence. *Archaeometry*, 49, 437-454.

CARTER, T. & CONTRERAS, D. A. 2012. The character and use of the Soros Hill Obsidian source, Antiparos (Greece). *Comptes Rendus Palevol*, 11, 595-602.

CARTER, T., POUPEAU, G., BRESSY, C. & PEARCE, N. J. G. 2006. A new programme of obsidian characterization at Çatalhöyük, Turkey. *Journal of Archaeological Science*, 33, 893-909.

CARTER, T., DUBERNET, S., KING, R., LE BOURDONNEC, F. X., MILIĆ, M., POUPEAU, G. & SHACKLEY, M. S. 2008. Eastern Anatolian obsidians at Catalhoyuk, and the reconfiguration of regional interaction in the Early Ceramic Neolithic. *Antiquity*, 82, 900-909.

CARTER, T., LE BOURDONNEC, F. X., KARTAL, M., POUPEAU, G., CALLIGARO, T. & MORETTO, P. 2011. Marginal perspectives: Sourcing obsidian from the Öküzini Cave (SW Turkey). *Paléorient*, 37(2): 123-149.

CARTER, T., GRANT, S., KARTAL, M., COŞKUN, A. & ÖZKAYA, V. 2013. Networks and Neolithisation: sourcing obsidian from Körtik Tepe (SE Anatolia). *Journal of Archaeological Science*, 40, 556-569.

CAUVIN, J. 1998. La signification symbolique de l'obsidienne. In: CAUVIN, M., GOURGAUD, A., GRATUZE, B., ARNAUD, N., POUPEAU, G., POIDEVIN, J. & CHATAIGNER, C. (eds.) *L'obsidienne au Proche et Moyen Orient. Du volcan à l'outil*. British Archaeological Reports International Series.

CESSFORD, C. & CARTER, T. 2005. Quantifying the Consumption of Obsidian at Neolithic Çatalhöyük, Turkey. *Journal of Field Archaeology*, 30, 305-315.

CHATAIGNER, C. 1994. Les propriétés géochimiques des obsidiennes et la distinction des sources de Bingöl et du Nemrut Dag. *Paléorient*, 20: 9-17.

CHATAIGNER, C., POIDEVIN, J. L. & ARNAUD, N. O. 1998. Turkish occurrences of obsidian and use by prehistoric peoples in the Near East from 14,000 to 6,000 BP. *Journal of Volcanology and Geothermal Research*, 85: 517-537.

CHATAIGNER, C., IŞIKLI, M., GRATUZE, B. & ÇIL, V. 2013. Obsidian Sources in the Regions of Erzurum and Kars (North-East Turkey): New Data. *Archaeometry*, 56: 351-374.

CHAVEZ-RIVAS, F., ZAMORANO-ULLOA, R., GALLAND, D., REGNARD, J. & CHAPPERT, J. 1991. Magnetic resonance and magnetization studies of natural volcanic glasses: Lipari obsidians. *Journal of Applied Physics*, 69, 5468.

CHERRY, J. F., FARRO, E. Z. & MINC, L. 2008. Field Exploration and Instrumental Neutron Activation Analysis of the Obsidian Sources in Southern Armenia. *International Association for Obsidian Studies Bulletin*, 39.

CHILDE, V. G. 1925. *The dawn of European civilization*, London.

CIVETTA, L., CORNETTE, Y., CRISCI, G., GILLOT, P. Y., ORSI, G. & REQUEJO, C. S. 1984. Geology, Geochronology and Chemical Evolution of the Island of Pantelleria. *Geological Magazine*, 121, 541-562.

CIVETTA, L., CORNETTE, Y., GILLOT, P. & ORSI, G. 1988. The eruptive history of Pantelleria (Sicily Channel) in the last 50 ka. *Bulletin of Volcanology*, 50, 47-57.

CLARK, J.-E. 1981. Multi-faceted approach to the study of Mesoamerican obsidian trade: an example from early Chiapas. Paper presented at the 46th annual meeting of the Society for American Archaeology in San Diego, California.

CONSTANTINESCU, B., CRISTEA-STAN, D., KOVÁCS, I. & SZÓKEFALVINAGY, Z. 2013. Provenance studies of Central European Neolithic obsidians using external beam milli-PIXE spectroscopy. Nuclear Instruments and Methods in Physics Research Section B: Beam Interactions with Materials and Atoms.

COOTE, G., WHITEHEAD, N. & MCCALLUM, G. 1972. A rapid method of obsidian characterisation by inelastic scattering of protons. *Journal of Radioanalytical and Nuclear Chemistry*, 12: 491-496.

CORTESE, M., FRAZZETTA, G. & LA VOLPE, L. 1986. Volcanic History of Lipari (Aeolian Islands, Italy) During the Last 10,000 Years. *Journal of Volcanology and Geothermal Research* 27, 113-133.

CRAIG, N., SPEAKMAN, R. J., POPELKA-FILCOFF, R. S., GLASCOCK, M. D., ROBERTSON, J. D., SHACKLEY, M. S. & ALDENDERFER, M. S. 2007. Comparison of XRF and PXRF for analysis of archaeological obsidian from southern Perú. *Journal of Archaeological Science*, 34, 2012-2024.

D'ANNA, A. 2013. Les statues-menhirs de Corse : chronologie et contextes, l'exemple de Cauria. In: GRUAT, P. & GARCIA, D. (eds.) *Stèles et statues du début de l'âge du Fer dans le Midi de la France (VIII^e-IV^e s. av. J.-C.) : chronologies, fonctions et comparaisons : Actes de la table ronde de Rodez*. Lattes / Paris: Association pour la Diffusion de l'Archéologie méridionale / Epona.

D'ANNA, A. 2014. Le plateau de Cauria (Sartène, Corse-du-Sud), quinze années de recherches archéologiques, un bilan d'étape. In: SÉNÉPART, I., LÉANDRI, F., CAULIEZ, J., PERRIN, T. & THIRAULT, É. (eds.) *Chronologie de la Préhistoire récente. Actualité de la recherche. Actes des 10^e Rencontres Méridionales de Préhistoire Récente*, Porticcio, 18-20 octobre 2012. Toulouse Archives d'Écologie Préhistorique.

D'ANNA, A., MARCHESI, H., TRAMONI, P., GILABERT, C. & DEMOUCHE, F. 2001. Renaghju (Sartène, Corse-du-Sud), un habitat de plein-air néolithique ancien en Corse. *Bulletin de la Société préhistorique française*, 98, 431-444.

D'ANNA, A., GUENDON, J.-L., ORSINI, J.-B., PINET, L. & TRAMONI, P. 2006. Nouvelles recherches sur les alignements mégalithiques d'I Stantari (Sartène, Corse du

Sud). Paysages et peuplements : aspects culturels et chronologiques en France méridionale: actualité de la recherche, 11, 455-472.

D'ANNA, A., GUENDON, J.-L., ORSINI, J.-B., PINET, L. & TRAMONI, P. 2007. Les alignements mégalithiques du plateau de Cauria (Sartène, Corse-du-Sud). Corse et Sardaigne préhistoriques: relations et échanges dans le contexte méditerranéen: Actes du 128e Congrès national des Sociétés savantes, Bastia 2003, 211-223.

D'ANNA, A. (DIR.), ANDRÉ, G., DUMAS, V., GUENDON, J.-L., ORSINI, J.-B., PÊCHE-QUILICHINI, K. & SOULA, F. 2009. Cauria. Site mégalithique de Stazonna – I Stantari. Sartène, Corse-du-Sud. Rapport 2009, Collectivité Territoriale de Corse, Musée départemental de Préhistoire Corse, UMR 6636 Laboratoire méditerranéen de Préhistoire Europe – Afrique, Université de Provence - C.N.R.S. - Ministère de la Culture et de la Communication – I.R.D, Maison Méditerranéenne des Sciences de l'Homme, Décembre 2009.

DAVIS, M. K. 1994. Bremsstrahlung ratio technique applied to the non-destructive energy dispersive X-ray fluorescence analysis of obsidian. International Association for Obsidian Studies Bulletin, 11, 9-10.

DAVIS, M. K., JACKSON, T., SHACKLEY, M. S., TEAGUE, T. & HAMPEL, J. 2011. Factors Affecting the Energy-Dispersive X-Ray Fluorescence (EDXRF) Analysis of Archaeological Obsidian. In: SHACKLEY, M. S. (ed.) X-Ray Fluorescence Spectrometry (XRF) in Geoarchaeology. Springer New York.

DE FRANCESCO, A. M., CRISCI, G. M. & BOCCI, M. 2008. Non-destructive analytic method using XRF for determination of provenance of archaeological obsidians from the Mediterranean area: a comparison with traditional XRF methods. Archaeometry, 50, 337-350.

DE FRANCESCO, A., BOCCI, M. & CRISCI, G. M. 2011. Non-destructive Applications of Wavelength XRF in Obsidian Studies. In: SHACKLEY, M. S. (ed.) X-Ray Fluorescence Spectrometry (XRF) in Geoarchaeology. Springer New York.

DE MORTILLET, A. 1893. Rapport sur les monuments mégalithiques de la Corse, Paris.

DELERUE, S. 2007. L'obsidienne dans le processus de Néolithisation du Proche-Orient (12 000-6500 av. J.-C.). Unpublished PhD Thesis, Université Michel de Montaigne Bordeaux III, France.

- DI PAOLA, G. M., PUXEDDU, M. & SANTACROCE, R. 1975. K-Ar ages of Monte Arci volcanic complex (central-western Sardinia). *Rendiconti della Societa Italiana di Mineralogia e Petrologia* 31.
- DIXON, J. E., CANN, J. R. & RENFREW, C. 1968. Obsidian and the Origins of Trade. *Scientific American*, 218, 38-46.
- DUERDEN, P., BIRD, J. R., SCOTT, M. D., CLAYTON, E., RUSSELL, L. H. & COHEN, D. D. 1980. PIXE-PIGME studies of artefacts. *Nuclear Instruments and Methods*, 168(1-3): 447-452.
- DÜRING, B. S. & GRATUZE, B. 2013. Obsidian exchange networks in Prehistoric Anatolia: New data from the Black Sea region. *Paleorient*, 39, 173-182.
- DUTTINE, M., VILLENEUVE, G., POUPEAU, G., ROSSI, A. M. & SCORZELLI, R. B. 2003. Electron spin resonance of Fe³⁺ ion in obsidians from Mediterranean islands. Application to provenance studies. *Journal of Non-Crystalline Solids*, 323: 193-199.
- DUTTINE, M., SCORZELLI, R. B., POUPEAU, G., BUSTAMANTE, A., BELLIDO, A. V., LATTINI, R. M. & GUILLAUME-GENTIL, N. 2009. Provenance study of obsidians from the archaeological site of La Maná (Ecuador) by electron spin resonance (ESR), SQUID magnetometry and ⁵⁷Fe Mössbauer spectroscopy. In: *Proceedings of the 10th Latin American Conference on the Applications of the Mössbauer Effect (LACAME 2006)*, Rio de Janeiro, Brazil, 5–9 November 2006 (C. Larica, R. C. Mercader, C. Partiti & J.R. Gancedo, eds.): 85-90; Berlin, Heidelberg, Springer.
- EBERT, C. E., DENNISON, M., HIRTH, K. G., MCCLURE, S. B. & KENNETT, D. J. 2015. Formative Period Obsidian Exchange along the Pacific Coast of Mesoamerica. *Archaeometry*, 57, 54-73
- EERKENS, J. W., FERGUSON, J. R., GLASCOCK, M. D., SKINNER, C. E. & SHARON, A. W. 2007. Reduction Strategies and Geochemical Characterization of Lithic Assemblages: A Comparison of Three Case Studies from Western North America. *American Antiquity*, 72(3), 585-597.
- EERKENS, J. W., SPURLING, A. M. & GRAS, M. A. 2008. Measuring prehistoric mobility strategies based on obsidian geochemical and technological signatures in the Owens Valley, California. *Journal of Archaeological Science*, 35, 668-680.

- ELAM, J. M. 1993. Post-Formative Obsidian Exchange in Oaxaca, Mexico. University of Missouri: Columbia.
- EVANS, H. & GIGLIO, J. 1993. Interferences in inductively coupled plasma mass spectrometry – A Review. *Journal of Analytical Atomic Spectrometry*, 8, 1-18.
- FARR, H. 2006. Seafaring as social action. *Journal of Maritime Archaeology*, 1, 85-99.
- FERGUSON, J. R. 2012. X-Ray fluorescence of obsidian: approaches to calibration and the analysis of small samples. In: SHUGAR, A. N. & MASS, J. L. (eds.) *Handheld XRF for Art and Archaeology*. Leuven: Leuven University Press.
- FOERSTNER, H. 1881. Nota preliminare sulla geologia dell'isola di Pantelleria secondo gli studi fatti negli anni 1874-1881. *Bollettino del R. Comitato Geologico d'Italia*, 12, 532-556.
- FORSTER, N. & GRAVE, P. 2012. Non-destructive PXRF analysis of museum-curated obsidian from the Near East. *Journal of Archaeological Science*, 39, 728-736.
- FRAHM, E. 2012a. What Constitues an Obsidian "Source"?: Landscape and Geochemical Considerations and Their Archaeological Implications. *International Association for Obsidian Studies Bulletin*, 46, 16-28.
- FRAHM, E. 2012b. Distinguishing Nemrut Dağ and Bingöl A obsidians: geochemical and landscape differences and the archaeological implications. *Journal of Archaeological Science*, 39, 1436-1444.
- FRAHM, E. 2012c. Non-Destructive Sourcing of Bronze Age Near Eastern Obsidian Artefacts: Redeveloping and Reassessing Electron Microprobe Analysis for Obsidian Sourcing. *Archaeometry*, 54, 623-642.
- FRAHM, E. 2012d. Non-destructive sourcing of bronze age near eastern obsidian artefacts: redeveloping and reassessing electron microprobe analysis for obsidian sourcing. *Archaeometry*, 54, 623-642.
- FRAHM, E. 2013. Is obsidian sourcing about geochemistry or archaeology? A reply to Speakman and Shackley. *Journal of Archaeological Science*, 40, 1444-1448.
- FRAHM, E. & DOONAN, R. C. P. 2013. The technological versus methodological revolution of portable XRF in archaeology. *Journal of Archaeological Science*, 40, 1425-1434.

- FRAHM, E. & FEINBERG, J. M. 2013. From flow to quarry: magnetic properties of obsidian and changing the scale of archaeological sourcing. *Journal of Archaeological Science*, 40, 3706-3721.
- FRAHM, E., FEINBERG, J. M., SCHMIDT-MAGEE, B. A., WILKINSON, K., GASPARYAN, B., YERITSYAN, B., KARAPETIAN, S., MELIKSETIAN, K., MUTH, M. J. & ADLER, D. S. 2014a. Sourcing geochemically identical obsidian: multiscalar magnetic variations in the Gutansar volcanic complex and implications for Palaeolithic research in Armenia. *Journal of Archaeological Science*, 47, 164-178.
- FRAHM, E., SCHMIDT, B. A., GASPARYAN, B., YERITSYAN, B., KARAPETIAN, S., MELIKSETIAN, K. & ADLER, D. S. 2014b. Ten Seconds in the Field: Rapid Armenian Obsidian Sourcing with Portable XRF to Inform Excavations and Surveys. *Journal of Archaeological Science*, 41, 333-348.
- FRAHM, E., DOONAN, R., KILIKOGLU, V. 2014c. Handheld portable X-ray fluorescence of aegean obsidians. *Archaeometry* 56 (2), 228–260.
- FRANCAVIGLIA, V. 1984. Characterization of Mediterranean obsidian sources by classical petrochemical methods. *Preistoria Alpina*, 20, 311-332.
- FRANCAVIGLIA, V. 1988. Ancient Obsidian Sources on Pantelleria (Italy). *Journal of Archaeological Science*, 15, 109-122.
- FREUND, K. P. 2013. An assessment of the current applications and future directions of obsidian sourcing studies in archaeological research. *Archaeometry*, 55, 779-793.
- FREUND, K. P. 2014. Obsidian Consumption in Chalcolithic Sardinia: A View from Bingia 'e Monti. *Journal of Archaeological Science*, 41, 242-250.
- FREUND, K. P. & TYKOT, R. H. 2011. Lithic Technology and Obsidian Exchange Networks in Bronze Age Nuragic Sardinia (Italy). *Archaeological and Anthropological Sciences*, 3, 151-164.
- FREUND, K. P. & BATIST, Z. 2014. Sardinian Obsidian Circulation and Early Maritime Navigation in the Neolithic as Shown Through Social Network Analysis. *The Journal of Island and Coastal Archaeology*, 9, 364-380.
- FREUND, K. P., TYKOT, R. H. & VIANELLO, A. 2015. Blade production and the consumption of obsidian in Stentinello period Neolithic Sicily. *Comptes Rendus Palevol*, 14, 207-217.

GABRIELE, M. & LORENZI, F. 2014. La céramique du Néolithique ancien d'A Guaita dans le contexte tyrrhénien : typo-morphologie et étude de provenance. In: SÉNÉPART, I., LÉANDRI, F., CAULIEZ, J., PERRIN, T. & THIRAULT, É. (eds.) *Chronologie de la Préhistoire récente dans le Sud de la France. Acquis 1992-2012. Actualité de la recherche. Actes des 10e Rencontres Méridionales de Préhistoire Récente*, Porticcio, 18–20 octobre 2012. Toulouse: Archives d'Écologie Préhistorique.

GIBAJA, J. F., LEA, V., LUGLIÈ, C., BOSCH, J., GASSIN, B. & TERRADAS-BATLLE, X. 2013. Between Sardinia and Catalonia: contacts and relationships during the Neolithic.

GILABERT, C., LEANDRI, F., JORDA, C., ASSOUS-PLUNIAN, M., DEMOUCHE, F., BELLOT-GURLET, L., BRESSY, C., CHABAL, L., ERRERA, M. G. & LE BOURDONNEC, F.-X. 2011. Le site du Monte Revincu: nouvelles données sur un village néolithique moyen du nord de la Corse. *Marges, frontières et transgressions: Actualité de la recherche: Actes des 8e Rencontres Méridionales de Préhistoire Récente*, Marseille (13), 7-8 novembre 2008, 283-297.

GLASCOCK, M. D. 2011. Comparison and Contrast between XRF and NAA: Used for Characterization of Obsidian Sources in Central Mexico. In: SHACKLEY, M. S. (ed.) *X-Ray Fluorescence Spectrometry (XRF) in Geoarchaeology*. Springer New York.

GLASCOCK, M. D., BRASWELL, G. E. & COBEAN, R. H. 1998. A systematic approach to obsidian source characterization. In: SHACKLEY, M. S. (ed.) *Archaeological Obsidian Studies, Method and Theory*. New York and London: Plenum Press.

GLASCOCK, M. D., SPEAKMAN, R. J. & POLLARD, H. P. 2005. LA-ICP-MS as a Supplement to Abbreviated-INAA for Obsidian Artifacts from the Aztec-Tarascan Frontier. In: SPEAKMAN, R. J. & NEFF, H. (eds.) *Laser Ablation-ICP-MS in Archaeological Research*. Albuquerque: University of New Mexico Press.

GLASCOCK, M. D., KUZMIN, Y. V., GREBENNIKOV, A. V., POPOV, V. K., MEDVEDEV, V. E., SHEWKOMUD, I. Y. & ZAITSEV, N. N. 2011. Obsidian provenance for prehistoric complexes in the Amur River basin (Russian Far East). *Journal of Archaeological Science*, 38: 1832-1841.

GONNERMANN, H. M. & MANGA, M. 2005. Flow banding in obsidian: A record of evolving textural heterogeneity during magma deformation. *Earth and Planetary Science Letters*, 236, 135-147.

- GOODALE, N., BAILEY, D. G., JONES, G. T., PRESCOTT, C., SCHOLZ, E., STAGLIANO, N. & LEWIS, C. 2012. pXRF: a study of inter-instrument performance. *Journal of Archaeological Science*, 39: 875-883.
- GORDUS, A. A., WRIGHT, G. A. & GRIFFIN, J. B. 1968. Obsidian sources characterized by neutron-activation analysis. *Science*, 161: 382-384.
- GOURGAUD, A. 1998. Géologie de l'obsidienne. In: CAUVIN, M.-C., GOURGAUD, A., GRATUZE, B., ARNAUD, N., POUPEAU, G. & POIDEVIN, J. L. (eds.) *L'obsidienne au Proche-Orient et au Moyen-Orient : du volcan à l'outil*. Oxford: Archaeopress.
- GRATUZE, B. 1999. Obsidian Characterization by Laser Ablation ICP-MS and its Application to Prehistoric Trade in the Mediterranean and the Near East: Sources and Distribution of Obsidian With the Aegean and Anatolia. *Journal of Archaeological Science* 26(10), 869-881.
- GRATUZE, B., BARRANDON, J. N., AL ISA, K. & CAUVIN, C. 1993. Non-Destructive Analysis of Obsidian Artefacts Using Nuclear Techniques: Investigations of Provenance of Near Eastern Artefacts. *Archaeometry*, 35(1), 11-21.
- GRATUZE, B., BLET-LEMARQUAND, M. & BARRANDON, J. N. 2001. Mass spectrometry with laser sampling: A new tool to characterize archaeological materials. *Journal of Radioanalytical and Nuclear Chemistry*, 247, 645-656.
- GREEN, R. C. 1998. A 1990's Perspective on Method and Theory in Archaeological Volcanic Glass Studies. In: SHACKLEY, M. S. (ed.) *Archaeological Obsidian Studies: Method and Theory*. New York: Plenum Press.
- GRIFONI CREMONESI, R. 2012. Éléments d'homogénéité ou d'hétérogénéité au cours du Néolithique de l'Italie. In: BORRELL, M., BORRELL, F., BOSCH, J., CLOP, X. & MOLIST, M. (eds.) *Congrés Internacional Xarxes al Neolític – Neolithic Networks - Rubricatum: revista del Museu de Gavà*.
- GROSJEAN, R. 1955. *Les Statues-menhirs de la Corse. Etudes Corses*. Ajaccio: Archives Départementales de la Corse.
- GROSJEAN, R. 1964. Découverte d'un alignement de statuesmenhirs à Cauria (Sartène). *Comptes-rendus des Séances de l'Académie des Inscriptions et Belles-Lettres*, 327-342.

- GROSJEAN, R. 1968. Nouvelles statues-stèles découvertes en Corse. *BSPF*, 65-8, 195-198.
- GUILAINE, J. 2005. *La mer partagée. La Méditerranée avant l'écriture, 7000-2000 avant Jésus-Christ*, Paris, Hachette Littérature.
- GUILAINE, J. & VAQUER, J. 1994. Les obsidiennes à l'ouest du Rhône. *Gallia préhistoire*, 36, 323-327.
- HALL, M. & KIMURA, H. 2002. Quantitative EDXRF Studies of Obsidian Sources in Northern Hokkaido. *Journal of Archaeological Science*, 29, 259-266.
- HALLAM, B. R., WARREN, S. E. & RENFREW, C. 1976. Obsidian in the Western Mediterranean: Characterisation by Neutron Activation Analysis and Optical Emission Spectroscopy. *Proceedings of the Prehistoric Society*, 42, 85-110.
- HAMILTON, W. J. 1842. *Researches on Antiquities and Geology in Asia Minor, Pontus and Armenia: with some account of their antiquities and geology*. London, J. Murray.
- HANCOCK, R. G. V. & CARTER, T. 2010. How reliable are our published archaeometric analyses? Effects of analytical techniques through time on the elemental analysis of obsidians. *Journal of Archaeological Science*, 37, 243-250.
- HARBOTTLE, G. 1982. Chemical characterization in archaeology. In: ERICSON, J. E. & EARLE, T. K. (eds.) *Contexts for Prehistoric Exchange*. New York: Academic Press.
- HEIDE, K. & HEIDE, G. 2011. Vitreous state in nature – Origin and properties. *Chemie der Erde - Geochemistry*, 71, 305-335.
- HUGHES, R. E. 1998. On Reliability, Validity, and Scale in Obsidian Sourcing Research. In: RAMENOFSKY, A. F. & STEFFEN, A. (eds.) *Unit Issues in Archaeology: Measuring Time, Space, and Material*. Salt Lake City: University of Utah Press.
- HUGHES, R. E. & LEES, W. B. 1991. Provenance Analysis of Obsidian from Two Late Prehistoric Archaeological Sites in Kansas. *Transactions of the Kansas Academy of Science (1903-)*, 94, 38-45.
- HUGHES, R. E. & SMITH, R. L. 1993. Archaeology, geology, and geochemistry in obsidian provenance studies. In: STEIN, J. & LINSE, A. (eds.) *Effects of Scale on*

Archaeological and Geoscientific Perspectives. Boulder, Colorado: Geological Society of America.

IKEYA, N. 2014. Identification of Archaeological Obsidian Sources in Kanto and Chubu Regions (Central Japan) by Energy Dispersive X-ray Fluorescence Analysis. In: ONO, A., GLASCOCK, M. D., KUZMIN, Y. V. & SUDA, Y. (eds.) *Methodological Issues for Characterisation and Provenance Studies of Obsidian in Northeast Asia*. Oxford, England: BAR International Series 2620, Archaeopress.

INIZAN, M.-L., REDURON, M., ROCHE, H. & TIXIER, J. 1995. *Technologie de la pierre taillée*, Paris, Cercle de Recherches et d'Etudes Préhistoriques, C.N.R.S.

IZUHO, M., FERGUSON, J. R., GLASCOCK, M. D., ODA, N., AKAI, F., NAKAZAWA, Y. & SATO, H. 2014. Integration of obsidian compositional studies and lithic reduction sequence analysis at the Upper Palaeolithic site of Ogachi-Kato 2, Hokkaido, Japan. In: *Methodological Issues for Characterisation and Provenance Studies of Obsidian in Northeast Asia* (Akira Ono, Michael D. Glascock, Yaroslav V. Kuzmin & Yoshimitsu Suda, eds.): 125-142; Oxford, England, BAR International Series 2620, Archaeopress.

JACKSON, S. 2001. The application of Nd:YAG lasers in LA-ICP-MS. In: SYLVESTER, P. (ed.) *Laser-Ablation-ICPMS in the Earth sciences: principles and applications*. St Johns, Newfoundland: Mineralogical Association of Canada.

JEHASSE, J. 1976. Informations archéologiques. Circonscription de Corse. *Gallia Préhistoire*, Tome 19, 607-615.

JIA, P. W., DOELMAN, T., CHEN, C., ZHAO, H., LIN, S., TORRENCE, R. & GLASCOCK, M. D. 2010. Moving sources: A preliminary study of volcanic glass artifact distributions in northeast China using PXRF. *Journal of Archaeological Science*, 37, 1670-1677.

JOCHUM, K. P., WEIS, U., STOLL, B., KUZMIN, D., YANG, Q., RACZEK, I., JACOB, D. E., STRACKE, A., BIRBAUM, K., FRICK, D. A., GÜNTHER, D. & ENZWEILER, J. 2011. Determination of Reference Values for NIST SRM 610–617 Glasses Following ISO Guidelines. *Geostandards and Geoanalytical Research*, 35, 397-429.

KELLER, J. & SEIFRIED, C. 1990. The present status of obsidian source identification in Anatolia and the Near East. *PACT* 25, 57-85.

KHALIDI, L., OPPENHEIMER, C., GRATUZE, B., BOUCETTA, S., SANABANI, A. & AL-MOSABI, A. 2010. Obsidian sources in highland Yemen and their relevance to archaeological research in the Red Sea region. *Journal of Archaeological Science*, 37, 2332-2345.

KOKONENKO, N., TORRENCE, R. & WHITE, P. 2015. Unexpected uses for obsidian: experimental replication and use-wear/residue analyses of chopping tools. *Journal of Archaeological Science*, 54, 254-269.

KUDRIAVTSEV, Y., GALLARDO, S., AVENDAÑO, M., RAMÍREZ, G., ASOMOZA, R., MANZANILLA, L. & BERAMENDI, L. 2015. Chemical analysis of obsidian by a SIMS/EDX combined system. *Nuclear Instruments and Methods in Physics Research Section B: Beam Interactions with Materials and Atoms*, 343, 153-157.

KUZMIN, Y. V. & GLASCOCK, M. D. 2014. The neutron activation analysis of volcanic glasses in the Russian Far East and neighbouring Northeast Asia: a summary of the first 20 years of research. In: ONO, A., GLASCOCK, M. D., KUZMIN, Y. V. & SUDA, Y. (eds.) *Methodological Issues for Characterisation and Provenance Studies of Obsidian in Northeast Asia*. Oxford, England: British Archaeological Reports 2620, Archaeopress.

KUZMIN, Y. V., GLASCOCK, M. D. & IZUHO, M. 2013. The Geochemistry of the Major Sources of Archaeological Obsidian on Hokkaido Island (Japan): Shirataki and Oketo. *Archaeometry*, 55, 355-369.

LE BOURDONNEC, F. X. 2007. *Aspects archéométriques de la circulation de l'obsidienne Préhistorique. Développements analytiques et applications en Corse, Sardaigne et Éthiopie*, Université Michel de Montaigne Bordeaux 3, France, Unpublished PhD Thesis.

LE BOURDONNEC, F. X., DELERUE, S., DUBERNET, S., MORETTO, P., CALLIGARO, T., DRAN, J. C. & POUPEAU, G. 2005. PIXE characterization of Western Mediterranean and Anatolian obsidians and Neolithic provenance studies. *Nuclear Instruments and Methods in Physics Research Section B: Beam Interactions with Materials and Atoms*, 240, 595-599.

LE BOURDONNEC, F.-X., POUPEAU, G. & LUGLIÈ, C. 2006. SEM-EDS analysis of western Mediterranean obsidians: a new tool for Neolithic provenance studies. *Comptes Rendus Geoscience*, 338, 1150-1157.

LE BOURDONNEC, F.-X., BONTEMPI, J.-M., MARINI, N., MAZET, S., NEUVILLE, P. F., POUPEAU, G. & SICURANI, J. 2010. SEM-EDS characterization of western Mediterranean obsidians and the Neolithic site of A Fuata (Corsica). *Journal of Archaeological Science*, 37, 92-106.

LE BOURDONNEC, F.-X., POUPEAU, G., LUGLIÈ, C., D'ANNA, A., BELLOT-GURLET, L., BRESSY-LEANDRI, C. S., PASQUET, A. & TRAMONI, P. 2011. New data and provenance of obsidian blocks from Middle Neolithic contexts on Corsica (western Mediterranean). *Comptes Rendus Palevol*, 10, 259-269.

LE BOURDONNEC, F.-X., NOMADE, S., POUPEAU, G., GUILLOU, H., TUSHABRAMISHVILI, N., MONCEL, M.-H., PLEURDEAU, D., AGAPISHVILI, T., VOINCHET, P., MGELADZE, A. & LORDKIPANIDZE, D. 2012. Multiple origins of Bondi Cave and Ortvale Klde (NW Georgia) obsidians and human mobility in Transcaucasia during the Middle and Upper Palaeolithic. *Journal of Archaeological Science*, 39, 1317-1330.

LE BOURDONNEC, F.-X., POUPEAU, G., LORENZI, F., MACHUT, P. & SICURANI, J. 2014. Typologie et provenance de l'obsidienne du site néolithique d'A Guaita (NW Cap Corse, Corse, France). *Comptes Rendus Palevol*, 317-331.

LE BOURDONNEC, F. X., D'ANNA, A., POUPEAU, G., LUGLIÈ, C., BELLOT-GURLET, L., TRAMONI, P. & MARCHESI, H. 2015a. Obsidians artefacts from Renaghju (Corsica Island) and the Early Neolithic circulation of obsidian in the Western Mediterranean. *Archaeological and Anthropological Sciences*, 441-462.

LE BOURDONNEC, F.-X., BELLOT-GURLET, L., LUGLIÈ, C., BRESSY-LEANDRI, C. 2015b. Archéométrie de l'obsidienne: déchiffrer la circulation d'une matière première. *Nouvelles de l'Archéologie*, 138, 23-27.

LE BOURDONNEC, F.-X., POUPEAU, G., BOUSSOFARA, R., DUBERNET, S., MORETTO, P., COMPIN, M. & MULAZZANI, S. 2015c. Obsidians from the Kerkennah Islands (eastern Tunisia) and the PIXE elemental compositions of the Mediterranean peralkaline obsidians. *Nuclear Instruments and Methods in Physics Research Section B: Beam Interactions with Materials and Atoms*.

LÉA, V., PELLISSIER, M., GRATUZE, B., BOUCETTA, S. & LEPÈRE, C. 2010. Renouvellement des données sur la diffusion de l'obsidienne sarde en contexte chasséen (Midi de la France): la découverte du site des Terres Longues (Trets, Bouches-du-Rhône). In: LUGLIÈ, C. (ed.) *L'ossidiana del Monte Arci nel Mediterraneo*. Nuovi

apporti sulla diffusione, sui sistemi di produzione e sulla loro cronologia, Atti del 5° Convegno internazionale (Pau, Italia, 27-29 Giugno 2008). Ales.

LÉANDRI, F., DEMOUCHE, F., COSTA, L. J., TRAMONI, P., GILABERT, C., BÉRAUD, A. & JORDA, C. 2007. Le site du Monte-Revincu (Santo-Pietro-di-Tenda, Haute-Corse) : Contribution à la connaissance du Néolithique moyen de la Corse. In: D'ANNA, A., CÉSARI, J., OGEL, L. & VAQUER, J. (eds.) Corse et Sardaigne préhistoriques, relations et échanges dans le contexte méditerranéen, Actes des congrès nationaux des sociétés historiques et scientifiques, 128^e, Bastia, Corsica, France, Avril 2003. Document Préhistorique 22.

LEROI-GOURHAN, A. 1943. L'Homme et la Matière, Paris, Éditions Albin Michel.

LEROI-GOURHAN, A. 1971. Évolution et techniques. L'homme et la matière. Paris, Albin Michel (1^{ère} édition 1943).

LIÉGEOIS, J. 1975. Compte rendu de fouilles 1975, lieu dit Rinaiu-Scaglio. 3.

LLABADOR, Y., BERTAULT, D., GOUILLAUD, J. C. & MORETTO, P. 1990. Advantages of High-Speed Scanning for Microprobe Analysis of Biological Samples. Nuclear Instruments & Methods in Physics Research Section B-Beam: Interactions with Materials and Atoms, 49, 435-440.

LORENZI, F. 2011a. Le site néolithique d'A Guaita (Commune de Morsiglia) dans le Cap Corse. In: WEISS, M. C. (ed.) Tribune des chercheurs : archéologie préhistorique, Corse d'hier et de demain (nouvelle série), 3. Bastia: Société des sciences historiques et naturelles de la Corse.

LORENZI, F. 2011b. Le site d'A Guaita (Morsiglia, Haute-Corse) : une étape majeure de la néolithisation du Cap Corse. In: SÉNÉPART, I., PERRIN, T., THIRAUT, É. & BONNARDIN, S. (eds.) Marges, frontières et transgressions. Actualité de la recherche. Actes des huitièmes Rencontres Méridionales de Préhistoire Récente, Marseille. Toulouse: Archives d'écologie préhistorique.

LUGLIÈ, C. 2006. Risorse litiche e tecnologia nel Neolitico antico della Sardegna, Rome, Università degli studi di Roma «La Sapienza».

LUGLIÈ, C. 2009. L'obsidienne néolithique en Méditerranée occidentale. In: MONCEL, M.-H. & FRÖHLICH, F. (eds.) L'Homme et le précieux. Matières

minérales précieuses de la Préhistoire à aujourd'hui. Oxford, England: B.A.R. International Series 1934, Archaeopress.

LUGLIÈ, C. 2012. From the perspective of the source. Neolithic production and exchange of Monte Arci Obsidians (Central-Western Sardinia). In: BORRELL, M., BORRELL, F., BOSCH, J., CLOP, X. & MOLIST, M. (eds.) *Congrés Internacional Xarxes al Neolític – Neolithic Networks - Rubricatum: revista del Museu de Gavà*.

LUGLIÈ, C., LE BOURDONNEC, F.-X., POUPEAU, G., BOHN, M., MELONI, S., ODDONE, M. & TANDA, G. 2006. A map of the Monte Arci (Sardinia Island, Western Mediterranean) obsidian primary to secondary sources. Implications for Neolithic provenance studies. *Comptes Rendus Palevol*, 5, 995-1003.

LUGLIÈ, C., LE BOURDONNEC, F.-X., POUPEAU, G., ATZENI, E., DUBERNET, S., MORETTO, P. & SERANI, L. 2007. Early Neolithic obsidians in Sardinia (Western Mediterranean): the Su Carroppu case. *Journal of Archaeological Science*, 34, 428-439.

LUGLIÈ, C., LE BOURDONNEC, F. X., POUPEAU, G. & SANNA, I. 2008. Monte Arci obsidians Provenance in the Direct Procurement Zone: the Case-Study of Sa Punta - Marceddì (Central-Western Sardinia). In: GUELI, A. (ed.) *Scienza e Beni Culturali, Atti del V Congresso Nazionale di Archeometria (Siracusa, 26–29 Febbraio 2008)*. Siracusa: Morrone Editore.

LUGLIÈ, C., LE BOURDONNEC, F.-X., POUPEAU, G., CONGIA, C., MORETTO, P., CALLIGARO, T., SANNA, I. & DUBERNET, S. 2009. Obsidians in the Rio Saboccu (Sardinia, Italy) campsite: Provenance, reduction and relations with the wider Early Neolithic Tyrrhenian area. *Comptes Rendus Palevol*, 7, 249-258.

LUGLIÈ, C., LE BOURDONNEC, F. X. & POUPEAU, G. 2014. Caratterizzazione elementare e provenienza delle ossidiane mediante analisi non distruttiva PIXE e EDXRF. In: VENTURINO GAMBARI, M. (ed.) *La memoria del passato. Castello di Annone tra archeologia e storia*. Alessandria: LineLab.edizioni.

MACDONALD, R., SMITH, R. L. & THOMAS, J. E. 1992. *Chemistry of the Subalkalic Silicic Obsidians*. U. S. Geological Survey Professional Paper Washington, D.C., Government Printing Office.

MALMQVIST, K. G. 2004. Accelerator-based ion beam analysis - an overview and future prospects. *Radiation Physics and Chemistry*, 71, 817-827.

MAZET, S. (Dir.). 2010. Rapport d'opération archéologique. Fouille programmée annuelle de l'Abri des Castelli (2140 m), Università di Corsica Pasquale Paoli.

MAZET, S. (Dir.). 2011. Rapport d'opération archéologique. Fouille programmée annuelle de l'Abri des Castelli (2140 m), Università di Corsica Pasquale Paoli.

MAZET, S., BOMTEMPI, J. M., BRANCH, N., BOSCHIAN, G., DUBERNET, S., FORTI, A., GABRIELE, M., LE BOURDONNEC, F.-X., JOLY, C., MARINI, N., POUPEAU, G. & WILKINSON, K., 2011. Une occupation néolithique de haute-montagne : l'Abri des Castelli (Corte, Haute-Corse). Archéométrie 2011 - Colloque du G.M.P.C.A., Liège (Belgique), 11-15 avril 2011, abstract and poster.

MAZET, S., BONTEMPI, J.-M., MARINI, N., BOSCHIAN, G., BRESSY-LEANDRI, C., FORTI, A., GABRIELE, M., LE BOURDONNEC, F.-X., JOLY-DELANOË, C. & WILKINSON, K. 2014. L'abri des Castelli (2140 m, Corte): une occupation néolithique de haute-montagne. In: SÉNÉPART, I., LÉANDRI, F., CAULIEZ, J., PERRIN, T. & THIRAUT, É. (eds.) Chronologie de la Préhistoire récente dans le Sud de la France. Acquis 1992-2012. Actualité de la recherche. Actes des 10e Rencontres Méridionales de Préhistoire Récente, Porticcio, 18-20 Octobre 2012. Toulouse: Archives d'Écologie Préhistorique.

McCOY, M. D., LADEFOGED, T. N., CODLIN, M., SUTTON, D. G., 2014. Does Carneiro's circumscription theory help us understand Maori history? An analysis of the obsidian assemblage from Pouerua Pa, New Zealand (Aotearoa), *Journal of Archaeological Science*, 42: 467-475.

MCDUGALL, J. M., TARLING, D. H. & WARREN, S. E. 1983. The magnetic sourcing of obsidian samples from Mediterranean and near Eastern sources. *Journal of Archaeological Science*, 10, 441-452.

MELONI, S., LUGLIÈ, C., ODDONE, M. & GIORDANI, L. 2007. Diffusion of obsidian in the Mediterranean basin in the neolithic period: A trace element characterization of obsidian from Sardinia by instrumental neutron activation analysis. *Journal of Radioanalytical and Nuclear Chemistry*, 271, 533-539.

MÉRIMÉE, P. 1840. Notes d'un voyage en Corse, Paris, Adam Biro, 1989.

MILIĆ, M. 2014. PXRF characterisation of obsidian from central Anatolia, the Aegean and central Europe. *Journal of Archaeological Science*, 41, 285-296.

MILIĆ, M., BROWN, K. & CARTER, T. 2013. The Chipped stone. Appendix 21.1. A visual characterization of the Çatalhöyük obsidian. In: HODDER, I. (ed.) *Substantive Technologies at Çatalhöyük: Reports from the 2000-08 Seasons*. British Institute at Ankara, London; Cotsen Institute of Archaeology Press, Los Angeles: 1-7 [on CD]: Çatalhöyük Research Project Series Volume 9, BIAA Monograph 48, *Monumenta Archaeologica* 31.

MILLHAUSER, J. K., RODRÍGUEZ-ALEGRÍA, E. & GLASCOCK, M. D. 2011. Testing the accuracy of portable X-ray fluorescence to study Aztec and Colonial obsidian supply at Xaltocan, Mexico. *Journal of Archaeological Science*, 38, 3141-3152.

MILLHAUSER, J. K., FARGHER, L. F., HEREDIA ESPINOZA, V. Y., BLANTON, R. E. 2015. The geopolitics of obsidian supply in Postclassic Tlaxcallan: A portable X-ray fluorescence study, *Journal of Archaeological Science*, 58: 133-146.

MULAZZANI, S., LE BOURDONNEC, F.-X., BELHOUCHE, L., POUPEAU, G., ZOUGHLAMI, J., DUBERNET, S., TUFANO, E., LEFRAIS, Y. & KHEDHAIER, R. 2010. Obsidian from the Epipalaeolithic and Neolithic eastern Maghreb. A view from the Hergla context (Tunisia). *Journal of Archaeological Science*, 37, 2529-2537.

NADOOSHAN, F. K., AYVATWAND, M., DEGHANIFAR, H., GLASCOCK, M. D. & PHILLIPS, S. C. 2007. WDXRF Spectroscopy of Obsidian Tools in the Northwest of Iran. *International Association for Obsidian Studies Bulletin*, 37, 3-6.

NADOOSHAN, F. K., ABEDI, A., GLASCOCK, M. D., ESKANDARI, N. & KHAZAEI, M. 2013. Provenance of prehistoric obsidian artefacts from Kul Tepe, northwestern Iran using X-ray fluorescence (XRF) analysis. *Journal of Archaeological Science*, 40, 1956-1965.

NAZAROFF, A. J., PRUFER, K. M. & DRAKE, B. L. 2010. Assessing the applicability of portable X-ray fluorescence spectrometry for obsidian provenance research in the Maya lowlands. *Journal of Archaeological Science*, 37, 885-895.

NEFF, H. 1998. Units in Chemistry-Based Ceramic Provenance Investigations. In: RAMENOFKY, A. F. & STEFFEN, A. (eds.) *Unit Issues in Archaeology: Measuring Time, Space, and Material*. University of Utah Press.

NEFF, H. 2000. Neutron Activation Analysis for Provenance Determination in Archaeology. In: CILIBERTO, E. & SPOTO, G. (eds) *Modern Analytical Methods in Art and Archaeology*. Chemical Analysis Series, Volume 155. New York, John Wiley & Sons.

NERI, L. A. M., PAWLIK, A. F., REEPMAYER, C., MIJARES, A. S. B. & PAZ, V. J. 2015. Mobility of early islanders in the Philippines during the Terminal Pleistocene/Early Holocene boundary: pXRF-analysis of obsidian artefacts. *Journal of Archaeological Science*, 61, 149-157.

NEVE, S.R., BARKER, P.H., HOLROYD, S., SHEPPARD, P.J. 1994. Obsidian sourcing by PIXE analysis at Aura2. *New Zealand Journal of Archaeology*, 16, 93-121.

ODDONE, M., MARTON, P., BIGAZZI, G. & BIRO, K. T. 1999. Chemical characterisations of Carpathian obsidian sources by instrumental and epithermal neutron activation analysis. *Journal of Radioanalytical and Nuclear Chemistry*, 240, 147-153.

ORANGE, M., CARTER, T. & LE BOURDONNEC, F.-X. 2013. Sourcing obsidian from Tell Aswad and Qdeir 1 (Syria) by SEM-EDS and EDXRF: Methodological implications. *Comptes Rendus Palevol*, 12, 173-180.

ORANGE, M., LE BOURDONNEC, F.-X., SCHEFFERS, A., JOANNES-BOYAU, R. 2016. Sourcing obsidian in Archaeology: a new optimised LA-ICP-MS protocol. *Science and Technology of Archaeological Research*, 2(2), 192-202.

ORANGE, M., LE BOURDONNEC, F.-X. & BELLOT-GURLET, L. *in press 1*. Obsidian provenance analysis in Archaeology: 50 years of methodological developments. In: CHAPOULIE, R., SEPULVEDA, M. & WRIGHT, V. (eds.), *Manual de Arqueometria*. IFEA editions, Lima, Peru.

ORANGE, M., LE BOURDONNEC, F.-X., BELLOT-GURLET, L., LUGLIÈ, C., DUBERNET, S., BRESSY-LEANDRI, C., SCHEFFERS, A., JOANNES-BOYAU, R. *in press 2*. On sourcing obsidian assemblages from the Mediterranean area: analytical strategies for their exhaustive geochemical characterisation. *Journal of Archaeological Science: Reports*.

ORANGE, M., LE BOURDONNEC, F.-X., D'ANNA, A., TRAMONI, P., LUGLIÈ, C., BELLOT-GURLET, L., SCHEFFERS, A., MARCHESI, H., GUENDON, J.-L., JOANNES-BOYAU, R. *submitted for publication*. Obsidian economy on the Cauria plateau (South Corsica, Middle Neolithic): new evidence from Renaghju and I Stantari.

ORDONEZ, E. 1892. Algunas Obsidianas de Mexico. *Memorias de la Sociedad Científica Antonio Alzate*, 6, 33-45.

PARKS, G. A. & TIEH, T. T. 1966. Identifying the geographical source of artefact obsidian. *Nature*, 211, 289-290.

- PELEGRIN, J. 2015. Lithics and Archaeology A2 - Wright, James D. International Encyclopedia of the Social & Behavioral Sciences (Second Edition). Oxford: Elsevier.
- PERLÈS, C. 2001. The early Neolithic in Greece. The first farming communities in Europe, Cambridge, Cambridge University Press.
- PERLÈS, C. 2012. Le statut des échanges au Néolithique. In: BORRELL, M., BORRELL, F., BOSCH, J., CLOP, X. & MOLIST, M. (eds.) Congrès Internacional Xarxes al Neolític – Neolithic Networks - Rubricatum: revista del Museu de Gavà.
- PERREAULT, C., BOULANGER, M. T., HUDSON, A. M., RHODE, D., MADSEN, D. B., OLSEN, J. W., STEFFEN, M. L., QUADE, J., GLASCOCK, M. D. & BRANTINGHAM, P. J. 2016. Characterization of obsidian from the Tibetan Plateau by XRF and NAA. *Journal of Archaeological Science: Reports*, 5, 392-399.
- PESSINA, A. & RADI, G. 2006. La diffusione dell'ossidiana nell'Italia centro-settentrionale. *Atti della XXXIX Riunione Scientifica dell'Istituto Italiano di Preistoria e Protostoria (Firenze 2004)*, 435-460.
- PICHLER, H. 1980. The island of Lipari. *Rendiconti della Società Italiana di Mineralogia e Petrologia*, 36, 415-440.
- PIERCE, D. E. 2015. Visual and geochemical analyses of obsidian source use at San Felipe Aztatán, Mexico. *Journal of Anthropological Archaeology*, 40, 266-279.
- POIDEVIN, J.-L. 1998. Les gisements d'obsidienne de Turquie et de Transcaucasie : géologie, géochimie et chronométrie. In: CAUVIN, M.-C., GOURGAUD, A., GRATUZE, B., ARNAUD, N., POUPEAU, G. & POIDEVIN, J. L. (eds.) *L'obsidienne au Proche-Orient et au Moyen-Orient : du volcan à l'outil*. Oxford: Archaeopress.
- POLLARD, A. M. & HERON, C. 2008. *Archaeological Chemistry*, Cambridge, The Royal Society of Chemistry.
- POUPEAU, G., BELLOT-GURLET, L., BRISOTTO, V. & DORIGHEL, O. 2000. Nouvelles données sur la provenance de l'obsidienne des sites néolithiques du Sud-Est de la France. *Comptes Rendus de l'Académie des Sciences - Series IIA - Earth and Planetary Science*, 330, 297-303.
- POUPEAU, G., LE BOURDONNEC, F.-X., DUBERNET, S., SCORZELLI, R. B., DUTTINE, M. & CARTER, T. 2007. Tendances actuelles dans la caractérisation des

obsidiennes pour les études de provenance. *ArchéoSciences. Revue d'archéométrie*, 31, 79–86.

POUPEAU, G., PIBOULE, M., LE BOURDONNEC, F. X. & DORIGHEL, O. 2009. L'obsidienne, or noir de la Préhistoire. In: MONCEL, M. H. & FRÖHLICH, F. (eds.) *L'Homme et le précieux. Matières minérales précieuses*. Oxford: BAR International series 1934.

POUPEAU, G., LUGLIÈ, C., D'ANNA, A., LE BOURDONNEC, F.-X., BELLOT-GURLET, L., CARTER, T. & BRESSY-LEANDRI, C. S. 2010a. Circulation et origine de l'obsidienne préhistorique en Méditerranée : un bilan de cinquante années de recherches. In: DELESTRE, X. & MARCHESI, H. (eds.) *Archéologie des rivages méditerranéens : 50 ans de recherche : actes du colloque d'Arles (Bouches-du-Rhône), 28-29-30 octobre 2009*. Errance.

POUPEAU, G., LE BOURDONNEC, F.-X., CARTER, T., DELERUE, S., STEVEN SHACKLEY, M., BARRAT, J.-A., DUBERNET, S., MORETTO, P., CALLIGARO, T., MILIĆ, M. & KOBAYASHI, K. 2010b. The use of SEM-EDS, PIXE and EDXRF for obsidian provenance studies in the Near East: a case study from Neolithic Çatalhöyük (central Anatolia). *Journal of Archaeological Science*, 37, 2705-2720.

POUPEAU, G., LE BOURDONNEC, F. X. & BELLOT-GURLET, L. 2014. Caractérisation et circulation de l'obsidienne. In: DILLMANN, P. & BELLOT-GURLET, L. (eds.) *Circulation et provenance des matériaux dans les sociétés anciennes, La contribution des méthodes archéométriques*. Collection "Sciences Archéologiques". Paris, Éditions des Archives Contemporaines, 9-33.

QUARTA, G., MARUCCIO, L. & CALCAGNILE, L. 2011. Provenance studies of obsidians from Neolithic contexts in Southern Italy by IBA (Ion Beam Analysis) methods. *Nuclear Instruments and Methods in Physics Research Section B: Beam Interactions with Materials and Atoms*, 269, 3102-3105.

RADI, G. & BOVENZI, G. 2007. La circolazione dell'ossidiana nell'area alto tirrenica. In: TOZZI, C. & WEISS, M.-C. (eds.) *Préhistoire et protohistoire de l'aire tyrrhénienne*. Ghezzano: Felici Editore.

REEPMAYER, C., SPRIGGS, M., ANGGRAENI, LAPE, P., NERI, L., RONQUILLO, W. P., SIMANJUNTAK, T., SUMMERHAYES, G., TANUDIRJO, D. & TIAUZON, A. 2011. Obsidian sources and distribution systems in Island

- Southeast Asia: new results and implications from geochemical research using LA-ICP-MS. *Journal of Archaeological Science*, 38, 2995-3005.
- RENFREW, C. 1969. Trade and culture process in European prehistory. *Current Anthropology*, 10(2/3), 151-169.
- RENFREW, C., DIXON, J. E. & CANN, J. R. 1966. Obsidian and Early Cultural Contact in the Near East. *Proceedings of the Prehistoric Society*, 32, 30-72.
- ROBIN, A.-K., MOURALIS, D., GRATUZE B. & AKKÖPRÜ, E. 2015. Apport de la pétrologie aux études de provenance de l'obsidienne (obsidian sourcing). Exemples d'Anatolie orientale. In: colloque du GMPCA, Archéométrie 2015, Besançon (France), 27-30/04/2015.
- RUSSO, R. E., MAO, X., LIU, H., GONZALEZ, J. & MAO, S. S. 2002. Laser ablation in analytical chemistry - a review. *Talanta*, 57, 425-451.
- SALOTTI, M., BELLOT-GURLET, L., JEAN-YVES, C., DUBOIS, J.-N., LOUCHART, A., MOURER-CHAUVIRE, C., OBERLIN, C., PEREIRA, E., POUPEAU, G. & TRAMONI, P. 2000. La fin du Pléistocène supérieur et le début de l'Holocène en Corse : Apports paléontologique et archéologique du site de Castiglione (Oletta, Haute-Corse). *Quaternaire*, 11, 219-230.
- SAND, C. & SHEPPARD, P. J. 2000. Long distance prehistoric obsidian imports in New Caledonia: characteristics and meaning. *Comptes Rendus de l'Académie des Sciences - Series IIA - Earth and Planetary Science*, 331, 235-243.
- SANTI, P., RENZULLI, A. & ODDONE, M. 2010. Increasing data (INAA) on Ecuadorian obsidian artifacts: preliminary provenance and a clue for pre-Columbian eastward trade. *Journal of Archaeological Science*, 37, 1753-1760.
- SAUNDERS, N. J. 2001. A Dark Light: Reflections on Obsidian in Mesoamerica. *World Archaeology*, 33, 220-236.
- SETZER, T. J. & TYKOT, R. H. 2010. Considering the Source: The Importance of Raw Material Characterization and Provenance in Obsidian Use-Wear Studies. In: LUGLIE, C. (ed.) *L'ossidiana del Monte Arci nel Mediterraneo. Nuovi apporti sulla diffusione, sui sistemi di produzione e sulla loro cronologia. Atti del 5 Convegno internazionale (Pau, Italia, 27-29 Giugno 2008)*.

SHACKLEY, M. S. 1994. Intersource and Intrasource Geochemical Variability in Two Newly Discovered Archaeological Obsidian Sources in the Southern Great Basin: Bristol Mountains, California and Devil Peak, Nevada. *Journal of California and Great Basin Anthropology*, 16, 118-129.

SHACKLEY, M. S. (ed.). 1998. *Archaeological obsidian studies. Method and theory*. New York and London, Plenum Press, 243 pp.

SHACKLEY, M. S. 1998. Intrasource Chemical Variability and Secondary Depositional Processes: Lessons from the American Southwest. In: SHACKLEY, M. S. (ed.) *Archaeological Obsidian Studies. Method and Theory*. New York and London, Plenum Press.

SHACKLEY, M. S. 2008. Archaeological Petrology and the Archaeometry of Lithic Materials. *Archaeometry*, 50, 194-215.

SHACKLEY, M. S. (ed.). 2011. *X-Ray Fluorescence Spectrometry (XRF) in Geoarchaeology*. New York, Springer: 231 pp.

SHACKLEY, M. S. 2011. An Introduction to X-Ray Fluorescence (XRF) Analysis in Archaeology. In: SHACKLEY, M. S. (ed.) *X-Ray Fluorescence Spectrometry (XRF) in Geoarchaeology*. Springer New York.

SHELFORD, P. 1982. The Geology of Melos, Kimolos and Poliagos: The Stratigraphy. In: RENFREW, C. & WAGSTAFF, M. (eds.) *An Island Polity: The Archaeology of Exploitation in Melos*. Cambridge, England: Cambridge University Press.

SHEPPARD, P. J., IRWIN, G. J., LIN, S. C. & MCCAFFREY, C. P. 2011. Characterization of New Zealand obsidian using PXRF. *Journal of Archaeological Science*, 38, 45-56.

SMITH, M. E., BURKE, A. L., HARE, T. S. & GLASCOCK, M. D. 2007. Sources of Imported Obsidian at Postclassic Sites in the Yautepec Valley, Morelos: A Characterization Study Using XRF and INAA. *Latin American Antiquity*, 18, 429-450.

SOULA, F. 2012. Les pierres dressées de l'aire corso-sarde. Etude systémique des territoires. Le pietre fitte dell'area corso-sarda. Studio sistemico dei territori, PhD Dissertation, Université d'Aix-Marseille et Université de Sassari-Italie.

SPEAKMAN, R. J. & NEFF, H. 2005. The application of laser ablation ICP-MS to the study of archaeological materials - an introduction. In: SPEAKMAN, R. J. & NEFF,

H. (eds.) Laser ablation–ICP–MS in archaeological research. Albuquerque: University of New Mexico Press.

SPEAKMAN, R. J. & SHACKLEY, M. S. 2013. Silo science and portable XRF in archaeology: a response to Frahm. *Journal of Archaeological Science*, 40, 1435-1443.

SPEAKMAN, R. J., NEFF, H., GLASCOCK, M. D. & HIGGINS, B. J. 2002. Characterization of Archaeological Materials by LA-ICP-MS. In: JAKES, K. (ed.) *Archaeological Chemistry: Materials, Methods, and Meaning*. Washington, DC: ACS Symposium Series 831. American Chemical Society.

SPEAKMAN, R. J., GLASCOCK, M. D., POPOV, V. K., KUZMIN, Y. V., PTASHINSKY, A. V. & GREBENNIKOV, A. V. 2005. Geochemistry of Volcanic Glasses and Sources of Archaeological Obsidian on the Kamchatka Peninsula (Russian Far East): First Results. *Current Research in the Pleistocene*, 22, 11-13.

SPEAKMAN, R. J., GLASCOCK, M. D., TYKOT, R. H., DESCANTES, C., THATCHER, J. J., SKINNER, C. E. & LIENHOP, K. M. 2007. Selected Applications of Laser Ablation ICP-MS to Archaeological Research. In: GLASCOCK, M. D., SPEAKMAN, R. J. & POPELKA-FILCOFF, R. S. (eds.) *Archaeological Chemistry: Analytical Methods and Archaeological Interpretation*. Washington, DC: ACS Publication Series 968, American Chemical Society.

STEWART, S. J., CERNICCHIARO, G., SCORZELLI, R. B., POUPEAU, G., ACQUAFREDDA, P. & DE FRANCESCO, A. 2003. Magnetic properties and ⁵⁷Fe Mössbauer spectroscopy of Mediterranean prehistoric obsidians for provenance studies. *Journal of Non-Crystalline Solids*, 323, 188-192.

SUMMERHAYES, G. R., BIRD, J. R., FULLAGAR, R., GOSDEN, C., SPECHT, J. & TORRENCE, R. 1998. Application of PIXE-PIGME to archaeological analysis of changing patterns of obsidian use in West New Britain, Papua New Guinea. In: SHACKLEY, M. S. (ed.) *Archaeological Obsidian Studies*. New York: Plenum.

SUMMERHAYES, G. R., KENNEDY, J., MATISOO-SMITH, E., MANDUI, H., AMBROSE, W., ALLEN, C., REEPMAYER, C., TORRENCE, R. & WADRA, F. 2014. Lepong: A New Obsidian Source in the Admiralty Islands, Papua New Guinea. *Geoarchaeology*, 29: 238-248.

TABARES, N. A., LOVE, M. W., SPEAKMAN, R. J., NEFF, H. & GLASCOCK, M. D. 2005. Straight from the Source: Obsidian Prismatic Blades at El Ujuxte. In:

SPEAKMAN, R. J. & NEFF, H. (eds.) *Laser Ablation ICP-MS in Archaeological Research*. Albuquerque: University of New Mexico Press.

TERRADAS, X., GRATUZE, B., BOSCH, J., ENRICH, R., ESTEVE, X., OMS, F. X. & RIBÉ, G. 2013. Neolithic diffusion of obsidian in the western Mediterranean: new data from Iberia. *Journal of Archaeological Science*.

THOMPSON, R. N. 1972. Evidence for a chemical discontinuity near the basalt-andesite transition in many anorogenic volcanic suites. *Nature*, 236, 106-110.

TOZZI, C. & WEISS, M.-C. 2001. Nouvelles données sur le Néolithique ancien de l'aire corso-toscane. *Bulletin de la Société Préhistorique Française*, 98, 445-458.

TUFANO, E. 2005. Studio tipologico e caratterizzazione chimica dell'industria litica su ossidina di Pantelleria, alla luce dei rinvenimenti di una fonte di approvvigionamento e di un sito archeologico dell'Età del Rame in località Bagno dell'Acqua. Napoli, Università degli Studi Suor Orsola Benincasa Napoli.

TYKOT, R. H. 1995. *Prehistoric Trade in the Western Mediterranean: The Sources and Distribution of Sardinian Obsidian*, Unpublished Ph.D. Dissertation. Harvard University, Cambridge, Massachusetts.

TYKOT, R. H. 1996. Obsidian Procurement and Distribution in the Central and Western Mediterranean. *Journal of Mediterranean Archaeology*, 9, 39-82.

TYKOT, R. H. 1997. Characterization of the Monte Arci (Sardinia) Obsidian Sources. *Journal of Archaeological Science*, 24, 467-479.

TYKOT, R. H. 2002a. New Approaches to the Characterization of Obsidian from the Mediterranean Island Sources: Interpreting Chronological Change in Neolithic Sardinia and Corsica. In: VANDIVER, P. B., GOODWAY, M., DRUZIK, J. R. & MASS, J. L. (eds.) *Materials Issues in Art and Archaeology VI*, Materials Research Society Proceedings 712.

TYKOT, R. H. 2002b. Geochemical Analysis of Obsidian and the Reconstruction of Trade Mechanisms in the Early Neolithic of the Western Mediterranean. In: JAKES, K. (ed.) *Archaeological Chemistry. Materials, Methods, and Meaning*. ACS Symposium Series 831. Washington, DC.

TYKOT, R. H. 2004. Scientific methods and applications to archaeological provenance studies. In: MARTINI, M., MILAZZO, M. & PIACENTINI, M. (eds.) *Physics*

Methods in Archaeometry. Proceedings of the International School of Physics “Enrico Fermi” Course CLIV. Bologna, Italy: Società Italiana di Fisica.

TYKOT, R. H. 2011. Obsidian Finds on the Fringes of the Central Mediterranean. In: VIANELLO, A. (ed.) *Exotica in the Western Mediterranean*. Oxbow Books.

TYKOT, R. H. & AMMERMAN, A. J. 1997. New directions in central Mediterranean obsidian studies. *Antiquity*, 71, 1000-1006.

TYKOT, R. H., SETZER, T. J., GLASCOCK, M. D. & SPEAKMAN, R. J. 2005. Identification and Characterization of the Obsidian Sources on the Island of Palmarola, Italy. *Geoarchaeological and Bioarchaeological Studies*, 3, 107-111.

USGS. http://crustal.usgs.gov/geochemical_reference_standards/ [Online]. [Accessed 12 Jan 2014].

VAQUER, J. 2006. La diffusion de l'obsidienne dans le Néolithique de Corse, du Midi de la France et de Catalogne. XXXIX Riunione Scientifica del I.I.P.P. « Materie prime e scambinella preistoria italiana nel cinquantenario della fondazione dell'Istituto Italiano di Preistoria e Protostoria ». Firenze, 25-27 novembre 2004, IIPP.

VAQUER, J. 2007. Le rôle de la zone nord-tyrrhénienne dans la diffusion de l'obsidienne en Méditerranée nord-occidentale au Néolithique. In: D'ANNA, A., CESARI, J., OGEL, L. & VAQUER, J. (eds.) *Corse et Sardaigne préhistoriques. Relations et échanges dans le contexte méditerranéen*. Paris, CTHS.

VOGEL, N., NOMADE, S., NEGASH, A. & RENNE, P. R. 2006. Forensic $^{40}\text{Ar}/^{39}\text{Ar}$ dating: a provenance study of Middle Stone Age obsidian artifacts from Ethiopia. *Journal of Archaeological Science*, 33, 1749-1765.

VOGT, J. R., GRAHAM, C. C., GLASCOCK, M. D. & COBEAN, R. H. 1982. A study of mesoamerican obsidian sources using activation analysis. *Journal of Radioanalytical Chemistry*, 69, 271-289.

WARD, G. K. 1974. A systematic approach to the definition of sources of raw material. *Archaeometry*, 16(1), 41-53.

WASHINGTON, H. S. 1913. The Volcanoes and Rocks of Pantelleria, Part II: Petrography. *Journal of Geology*, 21, 683-713.

WEIGAND, P. C., HARBOTTLE, G. & SAYRE, E. V. 1977. Turquoise sources and source analysis: Mesoamerica and the Southwestern U.S.A. In: EARLE, T. K. & ERICSON, J. E. (Eds.) *Exchange Systems in Prehistory*. New York, Academic Press.

WHITE, J. C., PARKER, D. F. & REN, M. 2009. The origin of trachyte and pantellerite from Pantelleria, Italy: insights from major element, trace element, and thermodynamic modelling. *Journal of Volcanology and Geothermal Research*, 179, 33-55.

WILLIAMS-THORPE, O. 1995. Obsidian in the Mediterranean and the Near East: a Provenancing Success Story. *Archaeometry*, 37, 217-248.

WILSON, L. 2007. Understanding prehistoric lithic raw material selection: Application of a gravity model. *Journal of Archaeological Method and Theory*, 14, 388-411.

YI, S. & JWA, Y.-J. 2015. On the provenance of prehistoric obsidian artifacts in South Korea. *Quaternary International*, 329, 37-43.

ZANELLA, E., FERRARA, E., BAGNASCO, L., OLLÀ, A., LANZA, R. & BEATRICE, C. 2012. Magnetite grain-size analysis and sourcing of Mediterranean obsidians. *Journal of Archaeological Science*, 39: 1493-1498.

ZHANG, Y. 1999. H₂O in rhyolitic glasses and melts: Measurement, speciation, solubility, and diffusion. *Reviews of Geophysics*, 37, 493-516.

ZIELINSKI, R. A., LIPMAN, P. W. & MILLARD JR, H. T. 1977. Minor-Element Abundances in Obsidian, Perlite, and Felsite of Calc-Alkalic Rhyolites. *American Mineralogist*, 62, 426-437.

APPENDICES

Appendix A

Co-authors' contribution statements (see following pages).

Statement of contribution to publications for Marie

Orange's thesis

Co-author: Ludovic Bellot-Gurlet

Chapter 3

Orange, M., Le Bourdonnec, F.-X., Bellot-Gurlet, L. in press. Obsidian provenance analysis in Archaeology: 50 years of methodological developments. In: Chapoulie, R., Sepulveda, M., Wright, V. (Eds.), Manual de Arqueometria. IFEA editions, Lima, Peru.

M. Orange participated during all stages of the development of this paper and provided an overall contribution greater than that of any co-author. MO undertook the review of the literature and wrote the manuscript, which was then revised with feedback from the co-authors.

Chapter 4

Orange, M., Le Bourdonnec, F.-X., Bellot-Gurlet, L., Lugliè, C., Dubernet, S., Bressy-Leandri, C., Scheffers, A., Joannes-Boyau, R., in press. On sourcing obsidian assemblages from the Mediterranean area: analytical strategies for their exhaustive geochemical characterisation, Journal of Archaeological Science: Reports.

M. Orange participated during all stages of the development of this paper and provided an overall contribution greater than that of any co-author. MO designed the research question discussed in this paper with FXLB and LBG. MO undertook the majority of the analyses, the data treatment, and interpreted the results with revisions and additional guidance from FXLB, RJB, LBG, SD, and AS. MO wrote the manuscript, which was then revised with feedback from the co-authors.

Chapter 6

Orange, M., Le Bourdonnec, F.-X., D'Anna, A., Tramoni, P., Lugliè, C., Bellot-Gurlet, L., Scheffers, A., Marchesi, H., Guendon, J.-L., Joannes-Boyau, R. submitted for publication. Obsidian economy on the Cauria plateau (South Corsica, Middle Neolithic): new evidence from Renaghju and I Stantari.

M. Orange participated during all stages of the development of this paper and provided an overall contribution greater than that of any co-author. MO designed the research project with the help of ADA, PT, and FXLB. MO conducted the analyses, the data treatment, and interpreted the results with revisions and additional guidance from FXLB, RJB, and AS. MO wrote the manuscript, which was then revised with feedback from the co-authors.

I, Ludovic Bellot-Gurlet, agree that the above descriptions of the contributions of authors to these publications are accurate and correct.

Signature:



Date:

12/07/2016

Statement of contribution to publications for Marie

Orange's thesis

Co-author: Carlo Lugliè

Chapter 4

Orange, M., Le Bourdonnec, F.-X., Bellot-Gurlet, L., Lugliè, C., Dubernet, S., Bressy-Leandri, C., Scheffers, A., Joannes-Boyau, R., in press. On sourcing obsidian assemblages from the Mediterranean area: analytical strategies for their exhaustive geochemical characterisation, *Journal of Archaeological Science: Reports*.

M. Orange participated during all stages of the development of this paper and provided an overall contribution greater than that of any co-author. MO designed the research question discussed in this paper with FXLB and LBG. MO undertook the majority of the analyses, the data treatment, and interpreted the results with revisions and additional guidance from FXLB, RJB, LBG, SD, and AS. MO wrote the manuscript, which was then revised with feedback from the co-authors.

Chapter 6

Orange, M., Le Bourdonnec, F.-X., D'Anna, A., Tramoni, P., Lugliè, C., Bellot-Gurlet, L., Scheffers, A., Marchesi, H., Guendon, J.-L., Joannes-Boyau, R. submitted for publication. Obsidian economy on the Cauria plateau (South Corsica, Middle Neolithic): new evidence from Renaghju and I Stantari.

M. Orange participated during all stages of the development of this paper and provided an overall contribution greater than that of any co-author. MO designed the research project with the help of ADA, PT, and FXLB. MO conducted the analyses, the data treatment, and interpreted the results with revisions and additional guidance from FXLB, RJB, and AS. MO wrote the manuscript, which was then revised with feedback from the co-authors.

I, Carlo Lugliè, agree that the above descriptions of the contributions of authors to these publications are accurate and correct.

Signature:

Date: July 12, 2016

Statement of contribution to publications for Marie

Orange's thesis

Co-author: Stéphan Dubernet

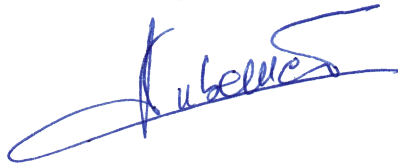
Chapter 4

Orange, M., Le Bourdonnec, F.-X., Bellot-Gurlet, L., Lugliè, C., Dubernet, S., Bressy-Leandri, C., Scheffers, A., Joannes-Boyou, R., in press. On sourcing obsidian assemblages from the Mediterranean area: analytical strategies for their exhaustive geochemical characterisation, *Journal of Archaeological Science: Reports*.

M. Orange participated during all stages of the development of this paper and provided an overall contribution greater than that of any co-author. MO designed the research question discussed in this paper with FXLB and LBG. MO undertook the majority of the analyses, the data treatment, and interpreted the results with revisions and additional guidance from FXLB, RJB, LBG, SD, and AS. MO wrote the manuscript, which was then revised with feedback from the co-authors.

I, Stéphan Dubernet, agree that the above description of the contribution of authors to this publication is accurate and correct.

Signature:



Date: 7th july 2016

Statement of contribution to publications for Marie

Orange's thesis

Co-author: André D'Anna

Chapter 6

Orange, M., Le Bourdonnec, F.-X., D'Anna, A., Tramoni, P., Lugliè, C., Bellot-Gurlet, L., Scheffers, A., Marchesi, H., Guendon, J.-L., Joannes-Boyau, R. submitted for publication. Obsidian economy on the Cauria plateau (South Corsica, Middle Neolithic): new evidence from Renaghju and I Stantari.

M. Orange participated during all stages of the development of this paper and provided an overall contribution greater than that of any co-author. MO designed the research project with the help of ADA, PT, and FXLB. MO conducted the analyses, the data treatment, and interpreted the results with revisions and additional guidance from FXLB, RJB, and AS. MO wrote the manuscript, which was then revised with feedback from the co-authors.

I, André D'Anna, agree that the above description of the contribution of authors to this publication is accurate and correct.

Signature:



Date:

12 juillet 2016

Statement of contribution to publications for Marie

Orange's thesis

Co-author: Pascal Tramoni

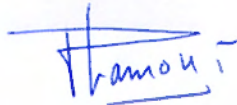
Chapter 6

Orange, M., Le Bourdonnec, F.-X., D'Anna, A., Tramoni, P., Lugliè, C., Bellot-Gurlet, L., Scheffers, A., Marchesi, H., Guendon, J.-L., Joannes-Boyau, R. submitted for publication. Obsidian economy on the Cauria plateau (South Corsica, Middle Neolithic): new evidence from Renaghju and I Stantari.

M. Orange participated during all stages of the development of this paper and provided an overall contribution greater than that of any co-author. MO designed the research project with the help of ADA, PT, and FXLB. MO conducted the analyses, the data treatment, and interpreted the results with revisions and additional guidance from FXLB, RJB, and AS. MO wrote the manuscript, which was then revised with feedback from the co-authors.

I, Pascal Tramoni, agree that the above description of the contribution of authors to this publication is accurate and correct.

Signature:



Date:

12 juillet 2016

Statement of contribution to publications for Marie

Orange's thesis

Co-author: Céline Bressy-Leandri

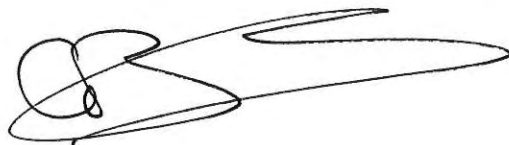
Chapter 4

Orange, M., Le Bourdonnec, F.-X., Bellot-Gurlet, L., Lugliè, C., Dubernet, S., Bressy-Leandri, C., Scheffers, A., Joannes-Boyau, R., in press. On sourcing obsidian assemblages from the Mediterranean area: analytical strategies for their exhaustive geochemical characterisation, *Journal of Archaeological Science: Reports*.

M. Orange participated during all stages of the development of this paper and provided an overall contribution greater than that of any co-author. MO designed the research question discussed in this paper with FXLB and LBG. MO undertook the majority of the analyses, the data treatment, and interpreted the results with revisions and additional guidance from FXLB, RJB, LBG, SD, and AS. MO wrote the manuscript, which was then revised with feedback from the co-authors.

I, Céline Bressy-Leandri, agree that the above description of the contribution of authors to this publication is accurate and correct.

Signature:



Date: 12/7/2016

Statement of contribution to publications for Marie

Orange's thesis

Co-author: Henri Marchesi

Chapter 6

Orange, M., Le Bourdonnec, F.-X., D'Anna, A., Tramoni, P., Lugliè, C., Bellot-Gurlet, L., Scheffers, A., Marchesi, H., Guendon, J.-L., Joannes-Boyau, R. submitted for publication. Obsidian economy on the Cauria plateau (South Corsica, Middle Neolithic): new evidence from Renaghju and I Stantari.

M. Orange participated during all stages of the development of this paper and provided an overall contribution greater than that of any co-author. MO designed the research project with the help of ADA, PT, and FXLB. MO conducted the analyses, the data treatment, and interpreted the results with revisions and additional guidance from FXLB, RJB, and AS. MO wrote the manuscript, which was then revised with feedback from the co-authors.

I, Henri Marchesi, agree that the above description of the contribution of authors to this publication is accurate and correct.

Signature:



Date:

12 juillet 2015

Statement of contribution to publications for Marie

Orange's thesis

Co-author: Jean-Louis Guendon


Chapter 6

Orange, M., Le Bourdonnec, F.-X., D'Anna, A., Tramonì, P., Lugliè, C., Bellot-Gurlet, L., Scheffers, A., Marchesi, H., Guendon, J.-L., Joannes-Boyau, R. submitted for publication. Obsidian economy on the Cauria plateau (South Corsica, Middle Neolithic): new evidence from Renaghju and I Stantari.

M. Orange participated during all stages of the development of this paper and provided an overall contribution greater than that of any co-author. MO designed the research project with the help of ADA, PT, and FXLB. MO conducted the analyses, the data treatment, and interpreted the results with revisions and additional guidance from FXLB, RJB, and AS. MO wrote the manuscript, which was then revised with feedback from the co-authors.

I, Jean-Louis Guendon, agree that the above description of the contribution of authors to this publication is accurate and correct.

Signature:

J.L. Guendon 

Date:

13 juillet 2016

Appendix B1

Identification of the geological samples from the Mediterranean area included in the geological database. With the exception of the Antiparos (Carter and Contreras, 2012) and Palmarola samples (PSE mission 2013), the geological samples have been transferred to Prof. Gérard Poupeau in the framework of the research led at the IRAMAT-CRP2A, and more particularly the Ph.D projects of Dr. Mathieu Duttine (2005) and Dr. François-Xavier Le Bourdonnec (2007).

GEOGRAPHICAL AREA	ORIGINAL ID	SCU ID	SCU RESIN ID	SOURCE (LA-ICP-MS)	ORIGIN / PUBLICATION
Western Mediterranean	102	SCU.GEOL.16	SAR#1	SB1	C. Lugliè
Western Mediterranean	103	SCU.GEOL.17	SAR#1	SB1	C. Lugliè
Western Mediterranean	105	SCU.GEOL.18	SAR#1	SB1	C. Lugliè
Western Mediterranean	109	SCU.GEOL.19	SAR#1	SB1	C. Lugliè
Western Mediterranean	111	SCU.GEOL.20	SAR#1	SB1	C. Lugliè
Western Mediterranean	113	SCU.GEOL.21	SAR#1	SB1	C. Lugliè
Western Mediterranean	115	SCU.GEOL.22	SAR#1	SB1	C. Lugliè
Western Mediterranean	117	SCU.GEOL.23	SAR#1	SB1	C. Lugliè
Western Mediterranean	120	SCU.GEOL.24	SAR#2	SB1	C. Lugliè
Western Mediterranean	119	SCU.GEOL.25	SAR#2	SB2	C. Lugliè
Western Mediterranean	124	SCU.GEOL.26	SAR#2	-	C. Lugliè
Western Mediterranean	126	SCU.GEOL.27	SAR#2	SB2	C. Lugliè
Western Mediterranean	128	SCU.GEOL.28	SAR#2	SB2	C. Lugliè
Western Mediterranean	131	SCU.GEOL.29	SAR#2	SB2	C. Lugliè

GEOGRAPHICAL AREA	ORIGINAL ID	SCU ID	SCU RESIN ID	SOURCE (LA-ICP-MS)	ORIGIN / PUBLICATION
Western Mediterranean	138	SCU.GEOL.30	SAR#3	SB2	C. Lugliè
Western Mediterranean	141	SCU.GEOL.31	SAR#3	SB2	C. Lugliè
Western Mediterranean	132	SCU.GEOL.32	SAR#2	SA	C. Lugliè
Western Mediterranean	134	SCU.GEOL.33	SAR#2	SA	C. Lugliè
Western Mediterranean	136	SCU.GEOL.34	SAR#3	SA	C. Lugliè
Western Mediterranean	143	SCU.GEOL.35	SAR#3	SA	C. Lugliè
Western Mediterranean	146	SCU.GEOL.36	SAR#3	SA	C. Lugliè
Western Mediterranean	147	SCU.GEOL.37	SAR#3	SA	C. Lugliè
Western Mediterranean	149	SCU.GEOL.38	SAR#3	SA	C. Lugliè
Western Mediterranean	151	SCU.GEOL.39	SAR#3	SA	C. Lugliè
Western Mediterranean	153	SCU.GEOL.40	SAR#4	SA	C. Lugliè
Western Mediterranean	155	SCU.GEOL.41	SAR#4	SA	C. Lugliè
Western Mediterranean	157	SCU.GEOL.42	SAR#4	SA	C. Lugliè
Western Mediterranean	159	SCU.GEOL.43	SAR#4	SC	C. Lugliè
Western Mediterranean	161	SCU.GEOL.44	SAR#4	SC	C. Lugliè
Western Mediterranean	168	SCU.GEOL.45	SAR#4	SC	C. Lugliè
Western Mediterranean	170	SCU.GEOL.46	SAR#4	SC	C. Lugliè
Western Mediterranean	171	SCU.GEOL.47	SAR#4	SC	C. Lugliè
Western Mediterranean	172	SCU.GEOL.48	SAR#5	SC	C. Lugliè
Western Mediterranean	173	SCU.GEOL.49	SAR#5	SC	C. Lugliè

GEOGRAPHICAL AREA	ORIGINAL ID	SCU ID	SCU RESIN ID	SOURCE (LA-ICP-MS)	ORIGIN / PUBLICATION
Western Mediterranean	175	SCU.GEOL.50	SAR#5	SC	C. Lugliè
Western Mediterranean	177	SCU.GEOL.51	SAR#5	SC	C. Lugliè
Western Mediterranean	179	SCU.GEOL.52	SAR#5	SC	C. Lugliè
Western Mediterranean	181	SCU.GEOL.53	SAR#5	SC	C. Lugliè
Western Mediterranean	183	SCU.GEOL.54	SAR#6	SC	C. Lugliè
Western Mediterranean	185	SCU.GEOL.55	SAR#6	SC	C. Lugliè
Western Mediterranean	187	SCU.GEOL.56	SAR#6	SC	C. Lugliè
Western Mediterranean	189	SCU.GEOL.57	SAR#6	SC	C. Lugliè
Western Mediterranean	191	SCU.GEOL.58	SAR#6	SC	C. Lugliè
Western Mediterranean	193	SCU.GEOL.59	SAR#6	SC	C. Lugliè
Western Mediterranean	SA-15	SCU.GEOL.60	SA#1	SA	A. M. De Francesco
Western Mediterranean	SA-40	SCU.GEOL.61	SA#1	SA	A. M. De Francesco
Western Mediterranean	SA-44	SCU.GEOL.62	SA#1	SA	A. M. De Francesco
Western Mediterranean	SA-46	SCU.GEOL.63	SA#1	SA	A. M. De Francesco
Western Mediterranean	SA-47	SCU.GEOL.64	SA#1	SA	A. M. De Francesco
Western Mediterranean	SA-49	SCU.GEOL.65	SA#2	SA	A. M. De Francesco
Western Mediterranean	SA-55	SCU.GEOL.66	SA#2	SA	A. M. De Francesco
Western Mediterranean	SA-60	SCU.GEOL.67	SA#2	SA	A. M. De Francesco
Western Mediterranean	SA-66	SCU.GEOL.68	SA#2	SA	A. M. De Francesco
Western Mediterranean	SA-67	SCU.GEOL.69	SA#2	SA	A. M. De Francesco

GEOGRAPHICAL AREA	ORIGINAL ID	SCU ID	SCU RESIN ID	SOURCE (LA-ICP-MS)	ORIGIN / PUBLICATION
Western Mediterranean	SB1-06	SCU.GEOL.70	SB1#1	SB2	A. M. De Francesco
Western Mediterranean	SB1-06b	SCU.GEOL.71	SB1#1	SB1	A. M. De Francesco
Western Mediterranean	SB1-08	SCU.GEOL.72	SB1#1	SB1	A. M. De Francesco
Western Mediterranean	SB1-13	SCU.GEOL.73	SB1#1	SB2	A. M. De Francesco
Western Mediterranean	SB1-14	SCU.GEOL.74	SB1#1	SB2	A. M. De Francesco
Western Mediterranean	SB1-15	SCU.GEOL.75	SB1#2	SB2	A. M. De Francesco
Western Mediterranean	SB1-16	SCU.GEOL.76	SB1#2	SB2	A. M. De Francesco
Western Mediterranean	SB1-17	SCU.GEOL.77	SB1#2	SB1	A. M. De Francesco
Western Mediterranean	SB1-52	SCU.GEOL.78	SB1#2	SB1	A. M. De Francesco
Western Mediterranean	SB1-64b	SCU.GEOL.79	SB1#2	SB1	A. M. De Francesco
Western Mediterranean	SB1-65	SCU.GEOL.80	SB1#2	SB1	A. M. De Francesco
Western Mediterranean	SB2-01	SCU.GEOL.81	SB2#1	SB1	A. M. De Francesco
Western Mediterranean	SB2-01b	SCU.GEOL.82	SB2#1	SB2	A. M. De Francesco
Western Mediterranean	SB2-13b	SCU.GEOL.83	SB2#1	SB1	A. M. De Francesco
Western Mediterranean	SB2-26b	SCU.GEOL.84	SB2#1	SB2	A. M. De Francesco
Western Mediterranean	SB2-48b	SCU.GEOL.85	SB2#1	SB2	A. M. De Francesco
Western Mediterranean	SB2-50b	SCU.GEOL.86	SB2#1	SB2	A. M. De Francesco
Western Mediterranean	SB2-74b	SCU.GEOL.87	SB2#1	SB2	A. M. De Francesco
Western Mediterranean	SB2-75b	SCU.GEOL.88	SB2#1	SB2	A. M. De Francesco
Western Mediterranean	SC-01	SCU.GEOL.89	SC#1	SC	A. M. De Francesco

GEOGRAPHICAL AREA	ORIGINAL ID	SCU ID	SCU RESIN ID	SOURCE (LA-ICP-MS)	ORIGIN / PUBLICATION
Western Mediterranean	SC-02	SCU.GEOL.90	SC#1	SC	A. M. De Francesco
Western Mediterranean	SC-04	SCU.GEOL.91	SC#1	SC	A. M. De Francesco
Western Mediterranean	SC-07a	SCU.GEOL.92	SC#1	SC	A. M. De Francesco
Western Mediterranean	SC-07b	SCU.GEOL.93	SC#1	SC	A. M. De Francesco
Western Mediterranean	SC-09	SCU.GEOL.94	SC#2	SC	A. M. De Francesco
Western Mediterranean	SC-11	SCU.GEOL.95	SC#2	SC	A. M. De Francesco
Western Mediterranean	SC-12	SCU.GEOL.96	SC#2	SC	A. M. De Francesco
Western Mediterranean	SC-15	SCU.GEOL.97	SC#2	SB2	A. M. De Francesco
Western Mediterranean	SC-21	SCU.GEOL.98	SC#2	SC	A. M. De Francesco
Western Mediterranean	Lipari Gabellotto	SCU.GEOL.99	LIP#1	Lipari	A. M. De Francesco
Western Mediterranean	Gab-1	SCU.GEOL.100	LIP#1	Lipari	-
Western Mediterranean	Gab-2	SCU.GEOL.101	LIP#1	Lipari	-
Western Mediterranean	eol-2	SCU.GEOL.102	LIP#1	Lipari	P. Acquafredda
Western Mediterranean	col-4	SCU.GEOL.103	LIP#1	Lipari	P. Acquafredda
Western Mediterranean	eol-8	SCU.GEOL.104	LIP#1	Lipari	P. Acquafredda
Western Mediterranean	col-10	SCU.GEOL.105	LIP#1	Lipari	P. Acquafredda
Western Mediterranean	Lago di Venere	SCU.GEOL.106	LDV#1	Lago di Venere	A. M. De Francesco
Western Mediterranean	Balate dei Turchi	SCU.GEOL.107	BDT#1	Balata dei Turchi	A. M. De Francesco
Western Mediterranean	Pant-2	SCU.GEOL.108	PANT#1	Lago di Venere	P. Acquafredda
Western Mediterranean	Pant-6	SCU.GEOL.109	PANT#1	Balata dei Turchi	P. Acquafredda

GEOGRAPHICAL AREA	ORIGINAL ID	SCU ID	SCU RESIN ID	SOURCE (LA-ICP-MS)	ORIGIN / PUBLICATION
Western Mediterranean	Pant-17	SCU.GEOL.110	PANT#1	Balata dei Turchi	P. Acquafredda
Western Mediterranean	Pant-20	SCU.GEOL.111	PANT#1	Balata dei Turchi	P. Acquafredda
Western Mediterranean	LdV-1	SCU.GEOL.112	LDV#1	Lago di Venere	-
Western Mediterranean	BALT-01	SCU.GEOL.113	BDT#1	Balata dei Turchi	E. Tufano
Western Mediterranean	BALT-02	SCU.GEOL.114	BDT#1	Balata dei Turchi	E. Tufano
Western Mediterranean	BALT-03	SCU.GEOL.115	BDT#1	Balata dei Turchi	E. Tufano
Western Mediterranean	BALT-04	SCU.GEOL.116	BDT#1	Balata dei Turchi	E. Tufano
Western Mediterranean	BALT-05	SCU.GEOL.117	BDT#1	Balata dei Turchi	E. Tufano
Western Mediterranean	BALT-06	SCU.GEOL.118	BDT#1	Balata dei Turchi	E. Tufano
Western Mediterranean	BALT-07	SCU.GEOL.119	BDT#1	Balata dei Turchi	E. Tufano
Western Mediterranean	BALT-08	SCU.GEOL.120	BDT#2	Balata dei Turchi	E. Tufano
Western Mediterranean	BALT-09	SCU.GEOL.121	BDT#2	Balata dei Turchi	E. Tufano
Western Mediterranean	BALT-10	SCU.GEOL.122	BDT#2	Balata dei Turchi	E. Tufano
Western Mediterranean	BALT-11	SCU.GEOL.123	BDT#2	Balata dei Turchi	E. Tufano
Western Mediterranean	BALT-12	SCU.GEOL.124	BDT#2	Balata dei Turchi	E. Tufano
Western Mediterranean	BALT-13	SCU.GEOL.125	BDT#2	Balata dei Turchi	E. Tufano
Western Mediterranean	BALT-14	SCU.GEOL.126	BDT#2	Balata dei Turchi	E. Tufano
Western Mediterranean	BALT-15	SCU.GEOL.127	BDT#2	Balata dei Turchi	E. Tufano
Western Mediterranean	BALT-16	SCU.GEOL.128	BDT#3	Balata dei Turchi	E. Tufano
Western Mediterranean	BALT-17	SCU.GEOL.129	BDT#3	Balata dei Turchi	E. Tufano

GEOGRAPHICAL AREA	ORIGINAL ID	SCU ID	SCU RESIN ID	SOURCE (LA-ICP-MS)	ORIGIN / PUBLICATION
Western Mediterranean	BALT-19	SCU.GEOL.131	BDT#3	Balata dei Turchi	E. Tufano
Western Mediterranean	BALT-20	SCU.GEOL.132	BDT#3	Balata dei Turchi	E. Tufano
Western Mediterranean	BALT-21	SCU.GEOL.133	BDT#3	Balata dei Turchi	E. Tufano
Western Mediterranean	LAGV-01	SCU.GEOL.134	LDV#1	Lago di Venere	E. Tufano
Western Mediterranean	LAGV-02	SCU.GEOL.135	LDV#1	Lago di Venere	E. Tufano
Western Mediterranean	LAGV-03	SCU.GEOL.136	LDV#1	Lago di Venere	E. Tufano
Western Mediterranean	LAGV-04	SCU.GEOL.137	LDV#1	Lago di Venere	E. Tufano
Western Mediterranean	LAGV-05	SCU.GEOL.138	LDV#1	Lago di Venere	E. Tufano
Western Mediterranean	LAGV-06	SCU.GEOL.139	LDV#1	Lago di Venere	E. Tufano
Western Mediterranean	LAGV-07	SCU.GEOL.140	LDV#2	Lago di Venere	E. Tufano
Western Mediterranean	LAGV-08	SCU.GEOL.141	LDV#2	Lago di Venere	E. Tufano
Western Mediterranean	LAGV-09	SCU.GEOL.142	LDV#2	Lago di Venere	E. Tufano
Western Mediterranean	LAGV-10	SCU.GEOL.143	LDV#2	Lago di Venere	E. Tufano
Western Mediterranean	LAGV-11	SCU.GEOL.144	LDV#2	Lago di Venere	E. Tufano
Western Mediterranean	LAGV-12	SCU.GEOL.145	LDV#2	Lago di Venere	E. Tufano
Western Mediterranean	LAGV-13	SCU.GEOL.146	LDV#2	Lago di Venere	E. Tufano
Western Mediterranean	LAGV-14	SCU.GEOL.147	LDV#2	Lago di Venere	E. Tufano
Western Mediterranean	LAGV-15	SCU.GEOL.148	LDV#3	Lago di Venere	E. Tufano
Western Mediterranean	LAGV-16	SCU.GEOL.149	LDV#3	Lago di Venere	E. Tufano
Western Mediterranean	LAGV-17	SCU.GEOL.150	LDV#3	Lago di Venere	E. Tufano

GEOGRAPHICAL AREA	ORIGINAL ID	SCU ID	SCU RESIN ID	SOURCE (LA-ICP-MS)	ORIGIN / PUBLICATION
Western Mediterranean	LAGV-18	SCU.GEOL.151	LDV#3	Lago di Venere	E. Tufano
Western Mediterranean	LAGV-19	SCU.GEOL.152	LDV#3	Lago di Venere	E. Tufano
Western Mediterranean	LAGV-20	SCU.GEOL.153	LDV#3	Lago di Venere	E. Tufano
Aegean	yali-01	SCU.GEOL.154	YALI#1	Yali	A. M. De Francesco
Aegean	yali-04	SCU.GEOL.155	YALI#1	Yali	A. M. De Francesco
Aegean	yali-06	SCU.GEOL.156	YALI#1	Yali	A. M. De Francesco
Aegean	yali-08	SCU.GEOL.157	YALI#1	Yali	A. M. De Francesco
Aegean	yali-09	SCU.GEOL.158	YALI#1	Yali	A. M. De Francesco
Aegean	yali-10	SCU.GEOL.159	YALI#1	Yali	A. M. De Francesco
Aegean	yali-11	SCU.GEOL.160	YALI#1	Yali	A. M. De Francesco
Aegean	yali-12	SCU.GEOL.161	YALI#2	Yali	A. M. De Francesco
Aegean	yali-13	SCU.GEOL.162	YALI#2	Yali	A. M. De Francesco
Aegean	yali-14	SCU.GEOL.163	YALI#2	Yali	A. M. De Francesco
Aegean	Gia-01	SCU.GEOL.164	YALI#2	Yali	-
Aegean	Gia-02	SCU.GEOL.165	YALI#2	Yali	-
Aegean	Gia-02b	SCU.GEOL.166	YALI#2	Yali	-
Aegean	dem-05	SCU.GEOL.167	DEM#1	Melos	A. M. De Francesco
Aegean	dem-06	SCU.GEOL.168	DEM#1	Melos	A. M. De Francesco
Aegean	dem-08	SCU.GEOL.169	DEM#1	Melos	A. M. De Francesco
Aegean	dem-14	SCU.GEOL.171	DEM#1	Melos	A. M. De Francesco

GEOGRAPHICAL AREA	ORIGINAL ID	SCU ID	SCU RESIN ID	SOURCE (LA-ICP-MS)	ORIGIN / PUBLICATION
Aegean	ml-01	SCU.GEOL.172	MIL#1	Melos	A. M. De Francesco
Aegean	ml-04	SCU.GEOL.174	MIL#1	Melos	A. M. De Francesco
Aegean	ml-07	SCU.GEOL.175	MIL#1	Melos	A. M. De Francesco
Aegean	ml-08	SCU.GEOL.176	MIL#1	Melos	A. M. De Francesco
Aegean	ml-13	SCU.GEOL.177	MIL#1	Melos	A. M. De Francesco
Aegean	ml-14	SCU.GEOL.178	MIL#1	Melos	A. M. De Francesco
Aegean	ml-15	SCU.GEOL.179	MIL#2	Melos	A. M. De Francesco
Aegean	ml-17	SCU.GEOL.180	MIL#2	Melos	A. M. De Francesco
Aegean	ml-19	SCU.GEOL.181	MIL#2	Melos	A. M. De Francesco
Aegean	ml-23	SCU.GEOL.182	MIL#2	Melos	A. M. De Francesco
Aegean	ml-24	SCU.GEOL.183	MIL#2	Melos	A. M. De Francesco
Aegean	ml-29	SCU.GEOL.184	MIL#2	Melos	A. M. De Francesco
Aegean	ml-12	SCU.GEOL.185	MIL#2	Melos	A. M. De Francesco
Western Mediterranean	PT1	SCU.GEOL.186	PALM#1	Palmarola	F.-X. Le Bourdonnec
Western Mediterranean	PT2	SCU.GEOL.187	PALM#1	Palmarola	F.-X. Le Bourdonnec
Western Mediterranean	PT3	SCU.GEOL.188	PALM#1	Palmarola	F.-X. Le Bourdonnec
Western Mediterranean	PT4	SCU.GEOL.189	PALM#2	Palmarola	F.-X. Le Bourdonnec
Western Mediterranean	PT5	SCU.GEOL.190	PALM#2	Palmarola	F.-X. Le Bourdonnec
Western Mediterranean	PT6	SCU.GEOL.191	PALM#2	Palmarola	F.-X. Le Bourdonnec
Western Mediterranean	PT7	SCU.GEOL.192	PALM#2	Palmarola	F.-X. Le Bourdonnec

GEOGRAPHICAL AREA	ORIGINAL ID	SCU ID	SCU RESIN ID	SOURCE (LA-ICP-MS)	ORIGIN / PUBLICATION
Aegean	Antiparos II.001	SCU.GEOL.192bis	ANTIP#1	Antiparos	T. Carter and D. Contreras
Aegean	Antiparos II.002	SCU.GEOL.193	ANTIP#1	Antiparos	T. Carter and D. Contreras
Aegean	Antiparos I.004	SCU.GEOL.194	ANTIP#1	Antiparos	T. Carter and D. Contreras
Aegean	Antiparos I.005	SCU.GEOL.195	ANTIP#1	Antiparos	T. Carter and D. Contreras
Aegean	Antiparos II.006	SCU.GEOL.196	ANTIP#1	Antiparos	T. Carter and D. Contreras
Aegean	Antiparos II.008	SCU.GEOL.197	ANTIP#1	Antiparos	T. Carter and D. Contreras
Aegean	Antiparos II.009	SCU.GEOL.198	ANTIP#1	Antiparos	T. Carter and D. Contreras
Aegean	Antiparos II.012	SCU.GEOL.199	ANTIP#1	Antiparos	T. Carter and D. Contreras
Aegean	Antiparos II.013	SCU.GEOL.200	ANTIP#1	Antiparos	T. Carter and D. Contreras
Aegean	Antiparos III.002	SCU.GEOL.201	ANTIP#2	Antiparos	T. Carter and D. Contreras
Aegean	Antiparos III.003	SCU.GEOL.202	ANTIP#2	Antiparos	T. Carter and D. Contreras
Aegean	Antiparos III.005	SCU.GEOL.203	ANTIP#2	Antiparos	T. Carter and D. Contreras
Aegean	Antiparos III.006	SCU.GEOL.204	ANTIP#2	Antiparos	T. Carter and D. Contreras
Aegean	Antiparos III.007	SCU.GEOL.205	ANTIP#2	Antiparos	T. Carter and D. Contreras
Aegean	Antiparos III.008	SCU.GEOL.206	ANTIP#2	Antiparos	T. Carter and D. Contreras
Aegean	Antiparos III.009	SCU.GEOL.207	ANTIP#2	Antiparos	T. Carter and D. Contreras
Aegean	Antiparos III.010	SCU.GEOL.208	ANTIP#2	Antiparos	T. Carter and D. Contreras
Aegean	Antiparos III.012	SCU.GEOL.209	ANTIP#2	Antiparos	T. Carter and D. Contreras
Aegean	Antiparos III.014	SCU.GEOL.210	ANTIP#2	Antiparos	T. Carter and D. Contreras
Aegean	Antiparos III.015	SCU.GEOL.211	ANTIP#2	Antiparos	T. Carter and D. Contreras

GEOGRAPHICAL AREA	ORIGINAL ID	SCU ID	SCU RESIN ID	SOURCE (LA-ICP-MS)	ORIGIN / PUBLICATION
Carpathians	PM 86/2 B	SCU.GEOL.212	CARPA#1	Carpathians	G. Bigazzi
Carpathians	PM 86/3 D	SCU.GEOL.213	CARPA#1	Carpathians	G. Bigazzi
Carpathians	PM 86/3 B	SCU.GEOL.214	CARPA#1	Carpathians	G. Bigazzi
Carpathians	PM 86/3 A	SCU.GEOL.215	CARPA#1	Carpathians	G. Bigazzi
Carpathians	PM 86/2 A	SCU.GEOL.216	CARPA#1	Carpathians	G. Bigazzi
Carpathians	PM 86/4 C	SCU.GEOL.217	CARPA#2	Carpathians	G. Bigazzi
Carpathians	PM 86/10 D	SCU.GEOL.218	CARPA#2	Carpathians	G. Bigazzi
Carpathians	PM 86/10 C	SCU.GEOL.219	CARPA#2	Carpathians	G. Bigazzi
Carpathians	PM 86/10 A	SCU.GEOL.220	CARPA#2	Carpathians	G. Bigazzi
Carpathians	PM 86/4 A	SCU.GEOL.221	CARPA#2	Carpathians	G. Bigazzi
Carpathians	PM 86/12 A	SCU.GEOL.222	CARPA#3	Carpathians	G. Bigazzi
Carpathians	PM 86/19 A	SCU.GEOL.223	CARPA#3	Carpathians	G. Bigazzi
Carpathians	PM 86/18	SCU.GEOL.224	CARPA#3	Carpathians	G. Bigazzi
Carpathians	PM 86/16 B	SCU.GEOL.225	CARPA#3	Carpathians	G. Bigazzi
Carpathians	PM 86/15 A	SCU.GEOL.226	CARPA#3	Carpathians	G. Bigazzi

Appendix B2

Identification and geo-referencing of the 44 geological samples from the Monte Arci massif (Sardinia) obtained in 2002. Table adapted from Lugliè, 2006. Source attributions obtained by LA-ICP-MS as part of this study.

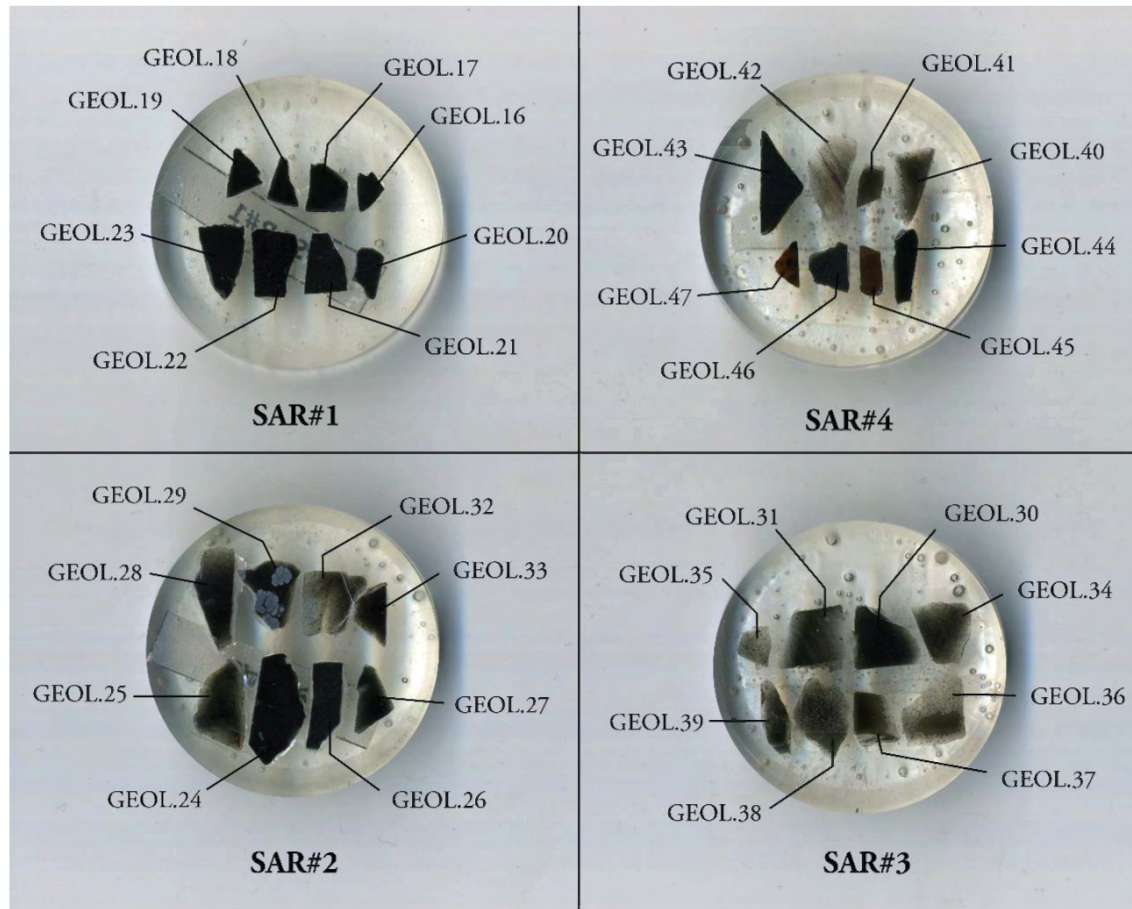
ORIGINAL ID	SCU ID	NORTH COORDINATE	EAST COORDINATE	LOCATION	SOURCE
102	SCU.GEOL.16	39°46.917'	8°42.647'	MARRUBIU	SB1
103	SCU.GEOL.17	39°46.917'	8°42.649'	MARRUBIU	SB1
105	SCU.GEOL.18	39°46.936'	8°42.659'	MARRUBIU	SB1
109	SCU.GEOL.19	39°46.936'	8°42.659'	MARRUBIU	SB1
111	SCU.GEOL.20	39°46.893'	8°42.638'	MARRUBIU	SB1
113	SCU.GEOL.21	39°46.899'	8°42.650'	MARRUBIU	SB1
115	SCU.GEOL.22	39°46.891'	8°42.644'	MARRUBIU	SB1
117	SCU.GEOL.23	39°46.915'	8°42.664'	MARRUBIU	SB1
120	SCU.GEOL.24	39°46.917'	8°42.647'	MARRUBIU	SB1
119	SCU.GEOL.25	39°46.369'	8°40.921'	MARRUBIU	SB2
124	SCU.GEOL.26	39°45.767'	8°41.347'	MARRUBIU	-
126	SCU.GEOL.27	39°45.769'	8°41.344'	MARRUBIU	SB2
128	SCU.GEOL.28	39°46.368'	8°40.924'	MARRUBIU	SB2
131	SCU.GEOL.29	39°46.361'	8°40.927'	MARRUBIU	SB2
138	SCU.GEOL.30	39°45.948'	8°41.183'	MARRUBIU	SB2
141	SCU.GEOL.31	39°46.178'	8°40.750'	MARRUBIU	SB2

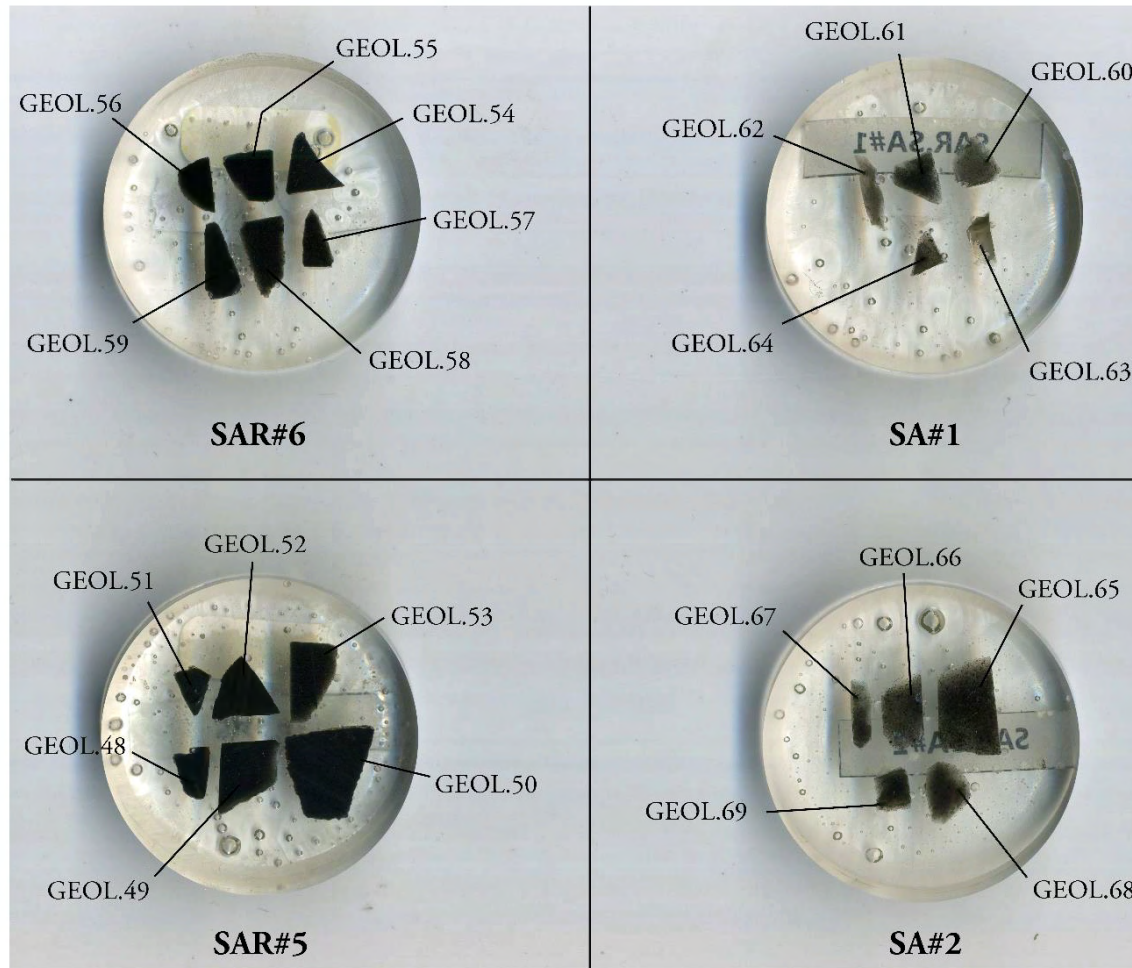
ORIGINAL ID	SCU ID	NORTH COORDINATE	EAST COORDINATE	LOCATION	SOURCE
132	SCU.GEOL.32	39°43.319'	8°43.969'	MASULLAS	SA
134	SCU.GEOL.33	39°43.315'	8°43.958'	MASULLAS	SA
136	SCU.GEOL.34	39°43.319'	8°43.950'	MASULLAS	SA
143	SCU.GEOL.35	39°43.299'	8°44.042'	MASULLAS	SA
146	SCU.GEOL.36	39°43.299'	8°44.042'	MASULLAS	SA
147	SCU.GEOL.37	39°43.269'	8°44.043'	MASULLAS	SA
149	SCU.GEOL.38	39°43.269'	8°44.040'	MASULLAS	SA
151	SCU.GEOL.39	39°43.244'	8°44.042'	MASULLAS	SA
153	SCU.GEOL.40	39°43.244'	8°44.041'	MASULLAS	SA
155	SCU.GEOL.41	39°43.230'	8°44.018'	MASULLAS	SA
157	SCU.GEOL.42	39°43.231'	8°44.020'	MASULLAS	SA
159	SCU.GEOL.43	39°48.455685'	8°45.899332'	PAU	SC
161	SCU.GEOL.44	39°48.461946'	8°46.036745'	PAU	SC
168	SCU.GEOL.45	39°48.425556'	8°46.612942'	PAU	SC
170	SCU.GEOL.46	39°48.465438'	8°46.693566'	PAU	SC
171	SCU.GEOL.47	39°48.473347'	8°46.699393'	PAU	SC
172	SCU.GEOL.48	39°48.477863'	8°46.700107'	PAU	SC
173	SCU.GEOL.49	39°48.488416'	8°46.094488'	PAU	SC
175	SCU.GEOL.50	39°48.491264'	8°47.602153'	PAU	SC
177	SCU.GEOL.51	39°48.253756'	8°47.801212'	PAU	SC

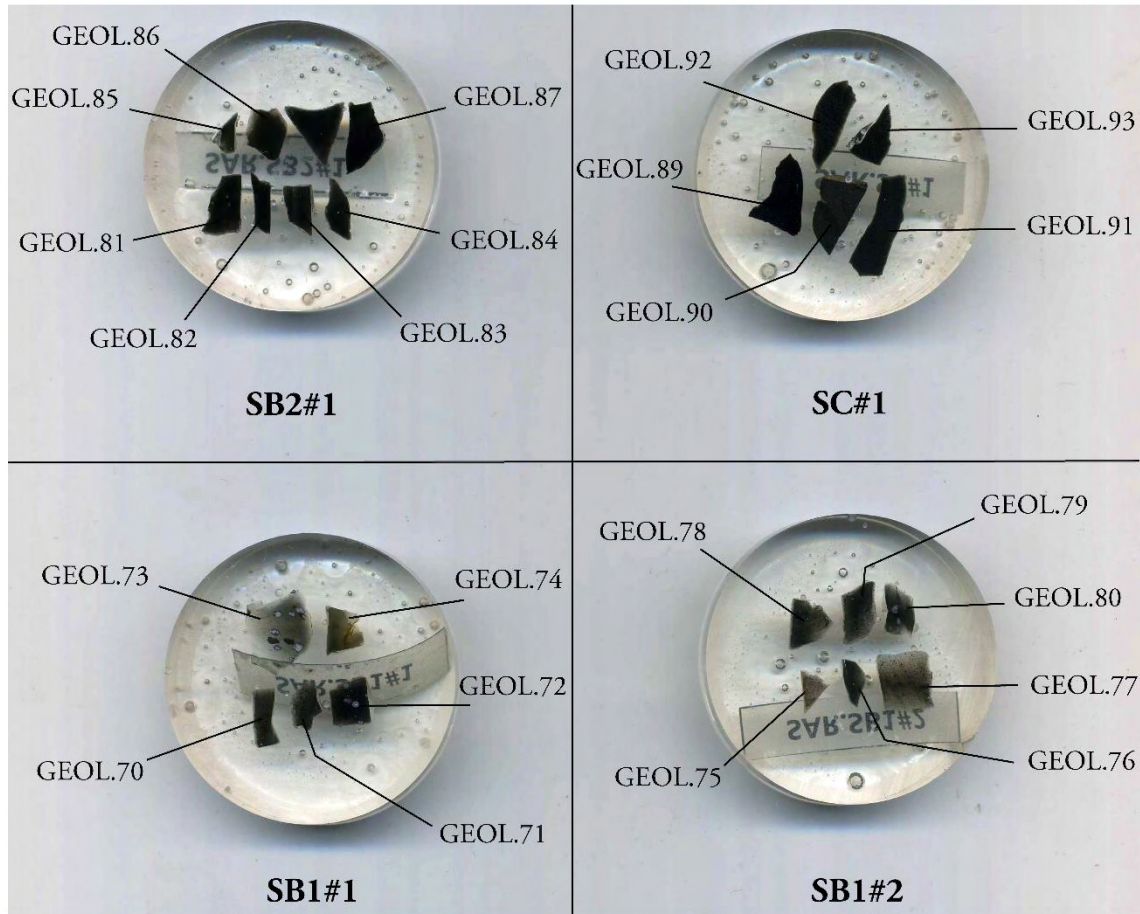
ORIGINAL ID	SCU ID	NORTH COORDINATE	EAST COORDINATE	LOCATION	SOURCE
179	SCU.GEOL.52	39°48.167722'	8°47.755909'	PAU	SC
181	SCU.GEOL.53	39°48.487966'	8°46.140049'	PAU	SC
183	SCU.GEOL.54	39°48.427364'	8°46.112216'	PAU	SC
185	SCU.GEOL.55	39°48.156352'	8°46.024115'	PAU	SC
187	SCU.GEOL.56	39°48.151504'	8°46.032542'	PAU	SC
189	SCU.GEOL.57	39°48.243081'	8°45.872433'	PAU	SC
191	SCU.GEOL.58	39°48.261782'	8°46.031469'	PAU	SC
193	SCU.GEOL.59	39°47.935154'	8°46.247022'	PAU	SC

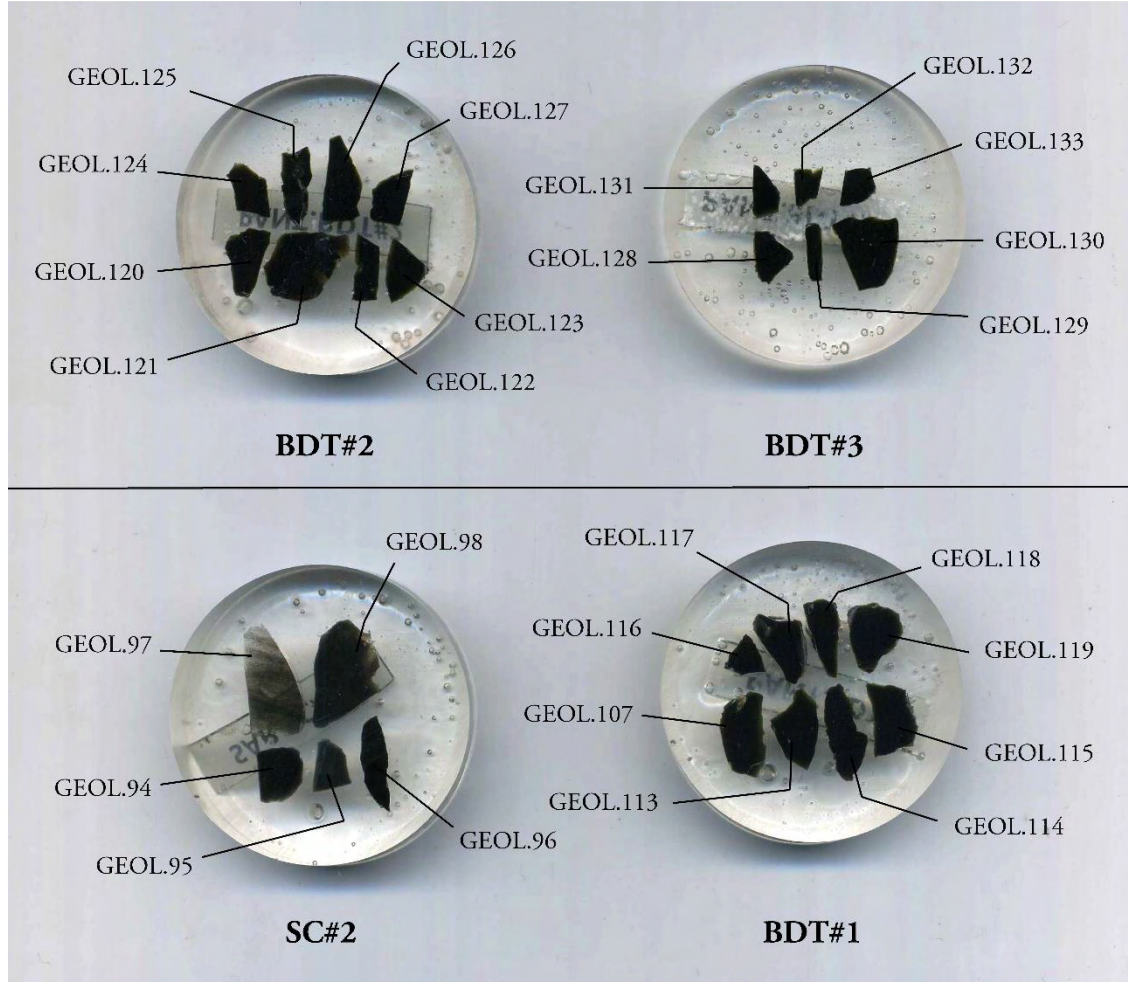
Appendix B3

Scans of the resins and identification of the geological samples embedded.

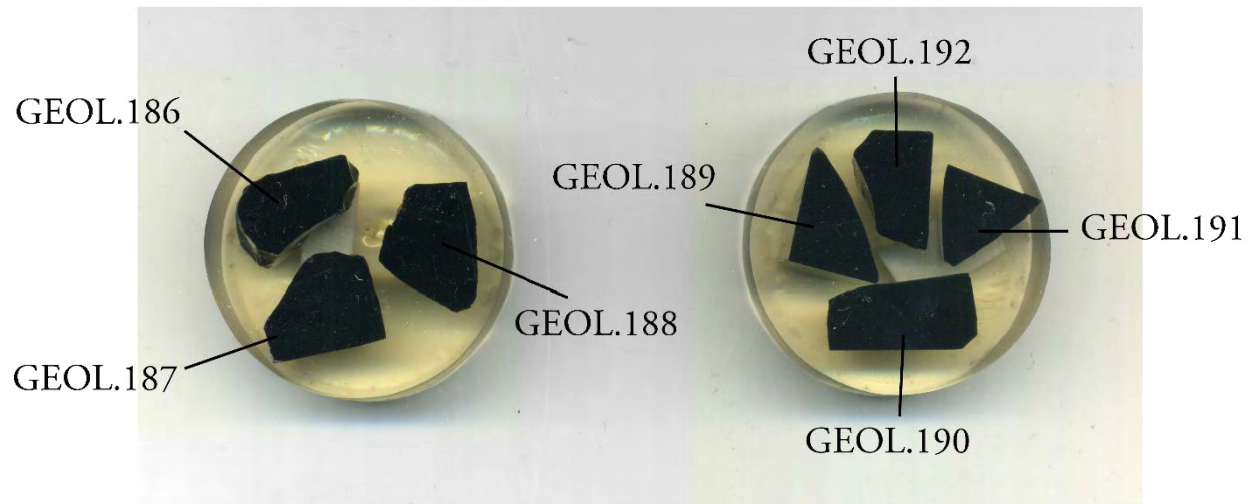






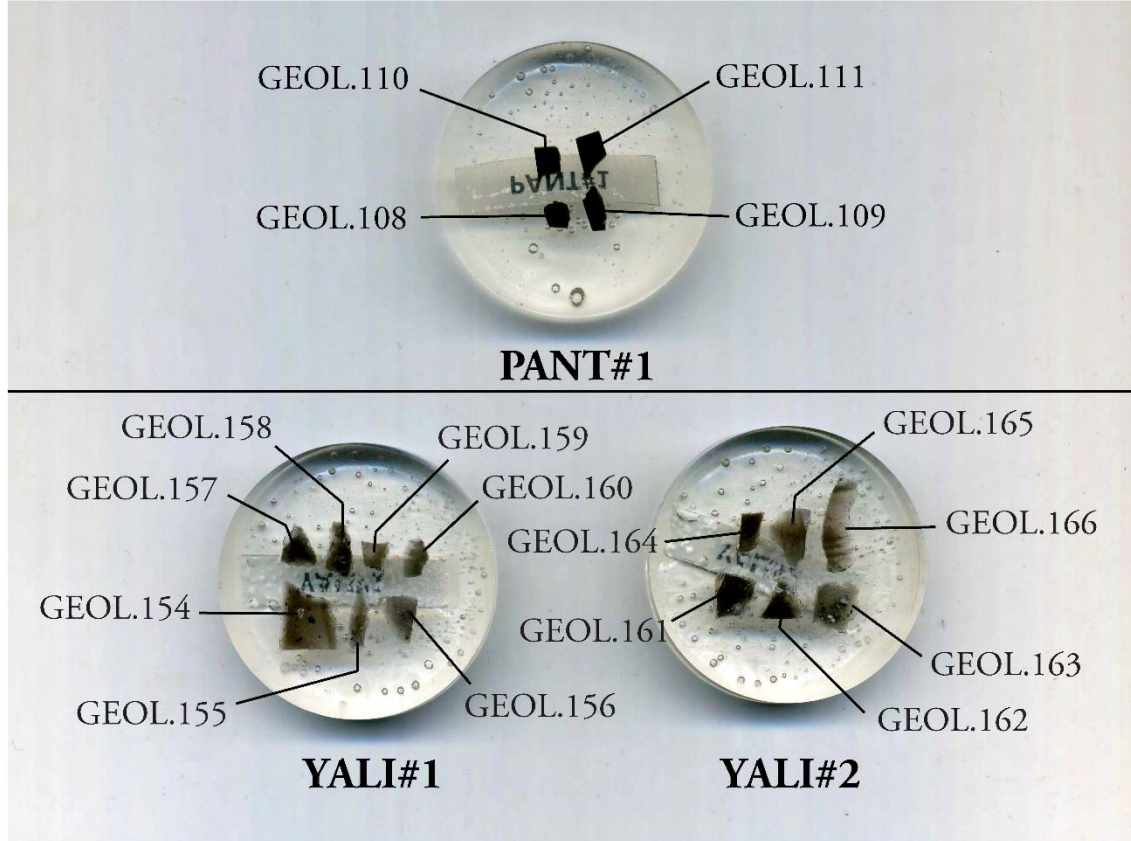


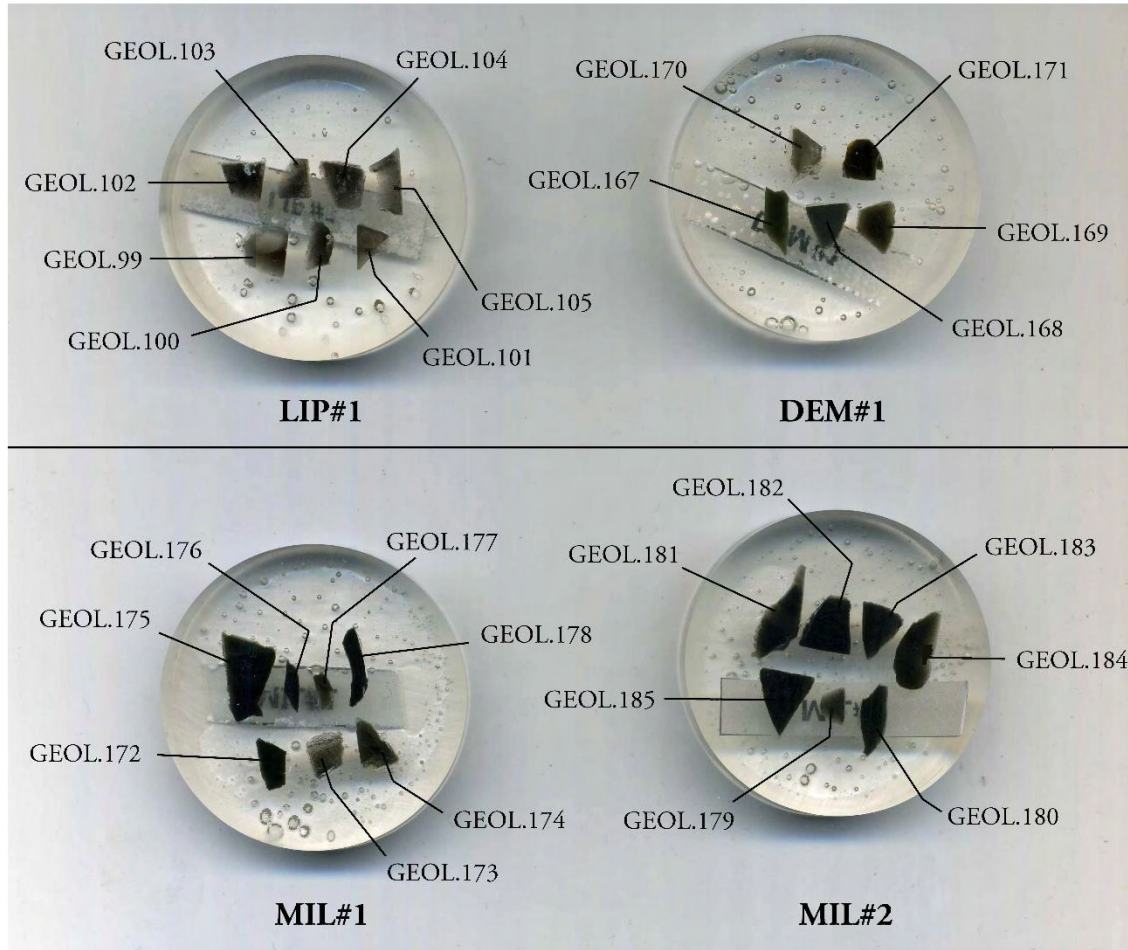


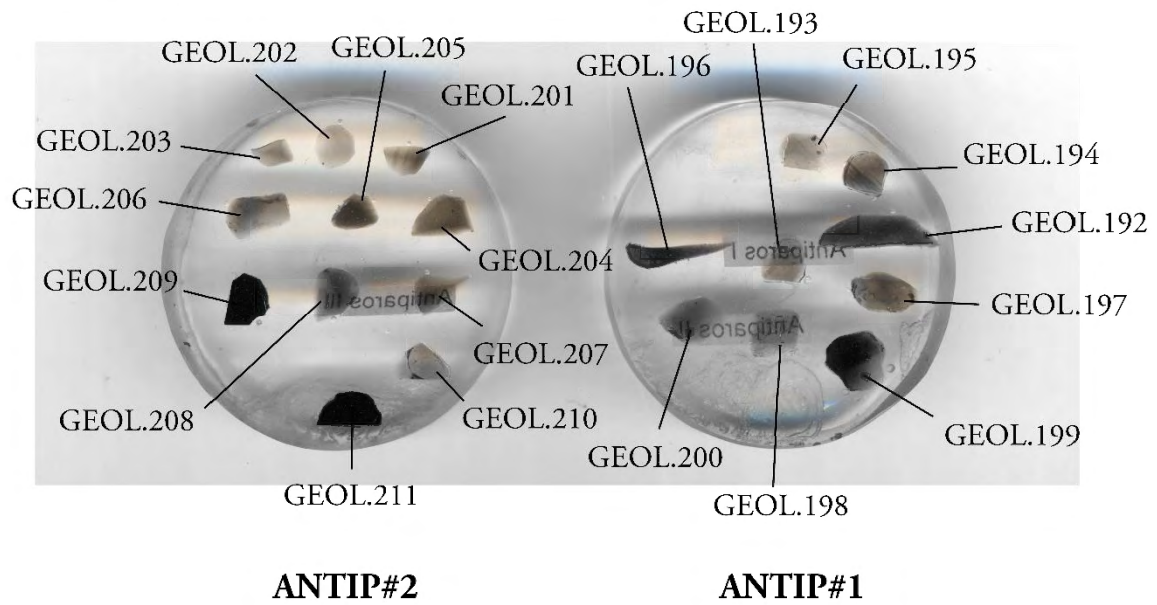


PALM#1

PALM#2







Appendix C

Polishing protocol adopted for the samples embedded in epoxy resin and scans of the resins (following pages). Protocol developed at the IRAMAT-CRP2A for automated polishing on Mecatech 334 (PRESI).

STEPS	ABRASIVE	LUBRICANT	SUPPORT	TOTAL PRESSURE	ROTATION SPEED	POLISHING DURATION	CLEANING	CONTROL
Pre1	-	Water	Resinoid grid RG2 (ESCIL) Grain 180/240 – Lubricate moderately with water	++	++++	1h-1h30	Water rinse	Binocular microscope
Pre2	-	Water	Resinoid grid RP2 (ESCIL) Grain 1000/1200 - Lubricate moderately with water	++	++++	1h30-2h	Water rinse Ultrasonic bath	Binocular microscope
Pol1	Mecaprex LD 33 E monocrystalline 6 µm (PRESI) - 0.30 ml 45 seconds	L PS (ESCIL) 0.25 mL 25 seconds	Cloth Reflex PAD-MAG RAM (PRESI)	1 DaN*	50 rpm (tray) 30 rpm (arm)	5400 seconds	Water rinse Ultrasonic bath	Metallographic microscope
Pol2	Mecaprex LD 33 E monocrystalline 3 µm (PRESI) - 0.30 ml 45 seconds	L PS (ESCIL) 0.25 mL 25 seconds	Cloth Reflex PAD-MAG RAM (PRESI)	1 DaN	40 rpm (tray) 20 rpm (arm)	5400 seconds	Water rinse Ultrasonic bath	Metallographic microscope
Pol3	Mecaprex LD 33 E monocrystalline 1 µm (PRESI) - 0.30 ml 45 seconds	L PS (ESCIL) 0.25 mL 20 seconds	Cloth Reflex PAD-MAG RAM (PRESI)	0.5 DaN	40 rpm (tray) 20 rpm (arm)	1800 seconds	Water rinse Ultrasonic bath	Metallographic microscope

STEPS	ABRASIVE	LUBRICANT	SUPPORT	TOTAL PRESSURE	ROTATION SPEED	POLISHING DURATION	CLEANING	CONTROL
Pol4	Mecaprex LD 33 E monocrystalline 1/4 μm (PRESI) - 0.30 ml 45 seconds	L PS (ESCIL) 0.25 mL 20 seconds	Cloth Reflex PAD- MAG NT (PRESI)	0.3 DaN	40 rpm (tray) 20 rpm (arm)	1800 seconds	Water rinse Ultrasonic bath	Metallographic microscope
Pol5	-	-	-	-	-	-	Ethanol and blow-drying	Metallographic microscope

*DaN: DekaNewton.

Appendix D

LA-ICP-MS results obtained on 200 geological samples from the Mediterranean area (Tyrrhenian Sea and Aegean) and the Carpathians: Sardinia (SA, SB1, SB2, and SC), Lipari, Palmarola, Pantelleria (Lago di Venere and Balata dei Turchi), Melos, Yali, Antiparos, and Carpathians. Number of rows [Nb rows] indicates the number of measurements obtained within a single ablation line, after statistical treatment with removal of the outliers with JMP statistical software (SAS); the results displayed for each isotope represent the average concentration (in ppm) for the corresponding number of 'rows'.

SOURCE	SAMPLE	Nb rows	⁴⁵ Sc	⁶⁶ Zn	⁸⁵ Rb	⁸⁸ Sr	⁸⁹ Y	⁹⁰ Zr	⁹³ Nb	¹³³ Cs	¹³⁷ Ba	¹⁴⁶ Nd	¹⁴⁷ Sm	²⁰⁸ Pb	²³² Th	²³⁸ U
Antiparos	SCU.GEOL.201	61	2	22	357	8	12	118	32	35	26	9	1	47	52	26
Antiparos	SCU.GEOL.202	59	2	21	364	8	11	105	31	35	24	8	1	48	48	27
Antiparos	SCU.GEOL.203	67	2	21	352	8	11	106	31	34	24	8	1	46	47	26
Antiparos	SCU.GEOL.204	59	2	22	349	8	11	108	30	35	24	8	1	47	48	25
Antiparos	SCU.GEOL.205	61	2	21	345	8	11	106	30	33	24	8	1	46	48	26
Antiparos	SCU.GEOL.206	59	2	21	343	8	11	108	30	34	24	8	1	46	49	26
Antiparos	SCU.GEOL.207	56	2	22	364	8	12	113	30	35	25	9	1	51	53	27
Antiparos	SCU.GEOL.208	61	2	22	356	8	12	114	31	35	25	9	1	49	51	27
Antiparos	SCU.GEOL.209	57	2	21	355	8	11	109	30	34	24	8	1	46	48	25
Antiparos	SCU.GEOL.210	68	2	22	359	8	12	113	31	35	25	9	1	49	51	27
Antiparos	SCU.GEOL.211	66	2	21	358	8	12	111	31	34	25	8	1	48	51	26
Melos	SCU.ARCH.172	59	2	27	106	76	11	78	7	3	438	11	2	10	10	3
Melos	SCU.ARCH.174	65	3	27	107	85	13	83	7	3	447	12	2	10	11	3

SOURCE	SAMPLE	<i>Nb rows</i>	⁴⁵ Sc	⁶⁶ Zn	⁸⁵ Rb	⁸⁸ Sr	⁸⁹ Y	⁹⁰ Zr	⁹³ Nb	¹³³ Cs	¹³⁷ Ba	¹⁴⁶ Nd	¹⁴⁷ Sm	²⁰⁸ Pb	²³² Th	²³⁸ U
Antiparos	SCU.GEOL.201	61	2	22	357	8	12	118	32	35	26	9	1	47	52	26
Antiparos	SCU.GEOL.202	59	2	21	364	8	11	105	31	35	24	8	1	48	48	27
Antiparos	SCU.GEOL.203	67	2	21	352	8	11	106	31	34	24	8	1	46	47	26
Melos	SCU.ARCH.175	60	3	27	107	71	11	75	7	3	433	11	2	11	10	4
Melos	SCU.ARCH.176	54	3	26	103	70	11	73	7	3	410	11	2	10	10	3
Melos	SCU.ARCH.177	67	3	26	108	83	13	86	7	3	452	12	2	10	11	4
Melos	SCU.ARCH.178	54	2	27	106	66	11	75	7	3	422	11	2	10	10	3
Melos	SCU.ARCH.179	67	2	27	105	79	12	78	7	3	435	11	2	10	10	3
Melos	SCU.ARCH.180	66	2	27	102	76	11	76	7	3	431	11	2	10	10	3
Melos	SCU.ARCH.181	56	2	26	102	80	11	74	7	3	419	11	2	10	10	3
Melos	SCU.ARCH.182	56	2	27	105	75	11	75	7	3	432	11	2	10	10	4
Melos	SCU.ARCH.183	69	2	26	102	82	11	77	7	3	431	11	2	10	10	3
Melos	SCU.ARCH.184	57	2	26	105	71	11	76	7	3	431	11	2	10	9	3
Melos	SCU.ARCH.185	62	2	27	102	79	12	78	7	3	435	11	2	10	10	3
Melos	SCU.GEOL.167	63	3	32	96	91	13	98	7	3	462	12	2	11	11	3
Melos	SCU.GEOL.168	63	3	33	101	96	13	100	7	3	463	12	2	11	11	3
Melos	SCU.GEOL.169	64	3	31	97	87	12	94	7	3	453	11	2	11	10	3
Melos	SCU.GEOL.171	58	3	33	96	96	13	101	7	3	460	12	2	11	11	3
Yali	SCU.GEOL.154	65	3	29	133	47	14	89	15	5	775	16	2	17	16	4

SOURCE	SAMPLE	<i>Nb rows</i>	⁴⁵ Sc	⁶⁶ Zn	⁸⁵ Rb	⁸⁸ Sr	⁸⁹ Y	⁹⁰ Zr	⁹³ Nb	¹³³ Cs	¹³⁷ Ba	¹⁴⁶ Nd	¹⁴⁷ Sm	²⁰⁸ Pb	²³² Th	²³⁸ U
Antiparos	SCU.GEOL.201	61	2	22	357	8	12	118	32	35	26	9	1	47	52	26
Antiparos	SCU.GEOL.202	59	2	21	364	8	11	105	31	35	24	8	1	48	48	27
Antiparos	SCU.GEOL.203	67	2	21	352	8	11	106	31	34	24	8	1	46	47	26
Yali	SCU.GEOL.155	64	3	28	135	46	13	84	15	5	767	15	2	17	15	4
Yali	SCU.GEOL.156	72	3	29	141	48	13	86	16	5	790	15	2	18	16	5
Yali	SCU.GEOL.157	63	3	28	134	48	14	87	15	5	774	15	2	17	16	4
Yali	SCU.GEOL.158	67	3	28	135	47	14	89	15	5	784	16	2	17	17	4
Yali	SCU.GEOL.159	70	3	29	138	47	13	85	15	5	773	16	2	18	16	4
Yali	SCU.GEOL.160	67	3	28	131	44	13	83	15	5	771	15	2	17	15	4
Yali	SCU.GEOL.161	64	2	29	130	47	13	81	15	5	761	15	2	17	15	4
Yali	SCU.GEOL.162	66	2	28	131	45	12	78	15	5	752	15	2	16	15	4
Yali	SCU.GEOL.163	63	2	29	132	46	13	82	14	5	773	15	2	16	15	4
Yali	SCU.GEOL.164	69	2	29	136	49	14	88	15	5	812	16	3	17	16	5
Yali	SCU.GEOL.165	65	3	31	123	57	15	93	16	4	845	17	3	16	15	4
Yali	SCU.GEOL.166	64	2	30	117	48	13	80	15	4	758	15	2	15	13	4
Carpathians	SCU.GEOL.212	59	4	28	155	53	19	43	8	8	402	16	3	27	12	8
Carpathians	SCU.GEOL.213	64	3	48	161	68	7	28	9	7	549	12	3	29	8	4
Carpathians	SCU.GEOL.214	58	3	47	158	67	7	27	9	7	540	12	3	28	7	4
Carpathians	SCU.GEOL.216	64	4	28	155	57	20	44	8	8	407	15	3	28	12	8

SOURCE	SAMPLE	<i>Nb rows</i>	⁴⁵ Sc	⁶⁶ Zn	⁸⁵ Rb	⁸⁸ Sr	⁸⁹ Y	⁹⁰ Zr	⁹³ Nb	¹³³ Cs	¹³⁷ Ba	¹⁴⁶ Nd	¹⁴⁷ Sm	²⁰⁸ Pb	²³² Th	²³⁸ U
Antiparos	SCU.GEOL.201	61	2	22	357	8	12	118	32	35	26	9	1	47	52	26
Antiparos	SCU.GEOL.202	59	2	21	364	8	11	105	31	35	24	8	1	48	48	27
Antiparos	SCU.GEOL.203	67	2	21	352	8	11	106	31	34	24	8	1	46	47	26
Carpathians	SCU.GEOL.217	57	3	27	163	41	19	37	8	9	349	13	3	29	11	9
Carpathians	SCU.GEOL.218	61	5	44	185	66	24	127	10	8	533	24	5	25	18	5
Carpathians	SCU.GEOL.219	56	5	41	186	65	23	121	10	8	515	23	5	24	17	5
Carpathians	SCU.GEOL.220	62	5	40	183	64	22	121	10	8	527	23	5	23	17	5
Carpathians	SCU.GEOL.221	57	4	29	159	49	19	41	8	9	385	15	3	30	12	8
Carpathians	SCU.ARCH.222	59	5	42	186	64	25	96	12	9	590	24	5	27	19	5
Carpathians	SCU.ARCH.223	68	6	37	206	76	27	146	11	9	593	27	5	24	19	6
Carpathians	SCU.ARCH.224	62	4	26	183	54	24	47	9	10	415	17	4	29	13	9
Carpathians	SCU.ARCH.225	63	5	43	187	66	25	96	12	9	597	24	5	28	20	5
Carpathians	SCU.ARCH.226	60	5	43	179	62	24	93	12	8	572	23	5	26	18	5
Carpathians	SCU.GEOL.215	70	3	45	161	60	7	25	8	7	495	11	3	29	7	4
Pantelleria - Balata Dei Turchi	SCU.GEOL.107	67	3	499	185	4	191	1960	378	3	24	191	38	16	36	11
Pantelleria - Balata Dei Turchi	SCU.GEOL.113	64	3	508	192	4	192	2072	391	3	25	197	38	16	36	11
Pantelleria - Balata Dei Turchi	SCU.GEOL.114	63	3	496	191	4	190	1963	382	3	24	185	38	16	37	11
Pantelleria - Balata Dei Turchi	SCU.GEOL.115	61	3	513	186	4	187	1986	375	3	23	181	37	16	36	10
Pantelleria - Balata Dei Turchi	SCU.GEOL.116	66	3	541	192	4	187	1932	383	3	24	198	37	16	36	10

SOURCE	SAMPLE	<i>Nb rows</i>	⁴⁵ Sc	⁶⁶ Zn	⁸⁵ Rb	⁸⁸ Sr	⁸⁹ Y	⁹⁰ Zr	⁹³ Nb	¹³³ Cs	¹³⁷ Ba	¹⁴⁶ Nd	¹⁴⁷ Sm	²⁰⁸ Pb	²³² Th	²³⁸ U
Antiparos	SCU.GEOL.201	61	2	22	357	8	12	118	32	35	26	9	1	47	52	26
Antiparos	SCU.GEOL.202	59	2	21	364	8	11	105	31	35	24	8	1	48	48	27
Antiparos	SCU.GEOL.203	67	2	21	352	8	11	106	31	34	24	8	1	46	47	26
Pantelleria - Balata Dei Turchi	SCU.GEOL.117	63	3	542	193	4	190	1953	382	3	24	194	38	16	36	11
Pantelleria - Balata Dei Turchi	SCU.GEOL.118	60	3	529	185	4	184	1948	370	3	24	192	37	16	36	10
Pantelleria - Balata Dei Turchi	SCU.GEOL.119	61	4	546	200	4	188	1978	379	3	24	189	37	16	37	11
Pantelleria - Balata Dei Turchi	SCU.GEOL.120	68	2	525	181	4	182	1951	370	2	22	185	37	16	36	11
Pantelleria - Balata Dei Turchi	SCU.GEOL.121	64	2	515	191	4	183	1912	364	3	23	186	37	16	36	11
Pantelleria - Balata Dei Turchi	SCU.GEOL.122	57	2	516	182	4	178	1890	361	2	23	181	36	16	36	10
Pantelleria - Balata Dei Turchi	SCU.GEOL.123	73	3	523	186	4	185	1970	379	3	24	193	38	17	37	11
Pantelleria - Balata Dei Turchi	SCU.GEOL.124	70	3	503	188	4	176	1880	377	2	24	183	37	16	37	11
Pantelleria - Balata Dei Turchi	SCU.GEOL.125	68	3	514	183	4	180	1892	369	3	23	188	37	16	37	11
Pantelleria - Balata Dei Turchi	SCU.GEOL.126	68	3	518	185	4	183	1944	369	3	23	185	36	16	37	11
Pantelleria - Balata Dei Turchi	SCU.GEOL.127	63	3	512	187	4	184	1909	375	3	24	188	37	16	36	11
Pantelleria - Balata Dei Turchi	SCU.GEOL.128	58	2	521	183	4	176	1879	379	3	23	179	36	16	35	11
Pantelleria - Balata Dei Turchi	SCU.GEOL.129	56	2	545	191	4	185	1951	380	3	24	192	39	17	38	11
Pantelleria - Balata Dei Turchi	SCU.GEOL.131	62	2	514	180	4	175	1863	377	2	23	176	36	15	34	10
Pantelleria - Balata Dei Turchi	SCU.GEOL.132	56	2	533	190	5	184	1928	379	3	24	186	37	16	35	10
Pantelleria - Balata Dei Turchi	SCU.GEOL.133	118	2	530	186	5	183	1936	378	3	24	188	38	16	36	11

SOURCE	SAMPLE	<i>Nb rows</i>	⁴⁵ Sc	⁶⁶ Zn	⁸⁵ Rb	⁸⁸ Sr	⁸⁹ Y	⁹⁰ Zr	⁹³ Nb	¹³³ Cs	¹³⁷ Ba	¹⁴⁶ Nd	¹⁴⁷ Sm	²⁰⁸ Pb	²³² Th	²³⁸ U
Antiparos	SCU.GEOL.201	61	2	22	357	8	12	118	32	35	26	9	1	47	52	26
Antiparos	SCU.GEOL.202	59	2	21	364	8	11	105	31	35	24	8	1	48	48	27
Antiparos	SCU.GEOL.203	67	2	21	352	8	11	106	31	34	24	8	1	46	47	26
Pantelleria - Balata Dei Turchi	SCU.GEOL.109	57	2	540	193	4	165	1843	376	3	23	175	35	17	34	11
Pantelleria - Balata Dei Turchi	SCU.GEOL.110	61	2	528	189	4	168	1885	375	3	24	176	35	17	34	11
Pantelleria - Balata Dei Turchi	SCU.GEOL.111	63	2	532	188	4	168	1862	373	3	23	175	35	16	34	11
Pantelleria - Lago Di Venere	SCU.ARCH.106	66	7	350	135	2	120	1509	288	1	52	118	24	11	26	8
Pantelleria - Lago Di Venere	SCU.ARCH.112	73	7	360	144	2	124	1532	301	1	55	121	24	11	27	8
Pantelleria - Lago Di Venere	SCU.ARCH.134	70	5	400	136	1	111	1192	261	2	23	116	24	10	21	6
Pantelleria - Lago Di Venere	SCU.ARCH.135	61	5	401	135	1	107	1138	250	1	23	113	23	10	20	6
Pantelleria - Lago Di Venere	SCU.ARCH.136	67	7	345	139	2	121	1503	284	1	52	118	23	11	25	8
Pantelleria - Lago Di Venere	SCU.ARCH.137	56	5	397	135	2	120	1289	263	1	24	124	25	10	22	7
Pantelleria - Lago Di Venere	SCU.ARCH.138	63	5	400	139	1	114	1196	248	1	24	120	24	10	21	7
Pantelleria - Lago Di Venere	SCU.ARCH.139	65	5	397	143	1	119	1246	273	2	24	120	25	9	21	7
Pantelleria - Lago Di Venere	SCU.ARCH.140	66	4	399	135	1	105	1145	252	1	23	113	23	10	20	6
Pantelleria - Lago Di Venere	SCU.ARCH.141	64	5	410	134	1	113	1206	260	1	23	113	23	9	20	7
Pantelleria - Lago Di Venere	SCU.ARCH.142	62	5	411	137	1	115	1249	267	1	24	120	24	10	21	7
Pantelleria - Lago Di Venere	SCU.ARCH.143	65	5	408	134	1	115	1258	270	1	24	121	24	10	21	6
Pantelleria - Lago Di Venere	SCU.ARCH.144	66	5	416	140	2	111	1209	266	1	23	112	22	9	20	7

SOURCE	SAMPLE	<i>Nb rows</i>	⁴⁵ Sc	⁶⁶ Zn	⁸⁵ Rb	⁸⁸ Sr	⁸⁹ Y	⁹⁰ Zr	⁹³ Nb	¹³³ Cs	¹³⁷ Ba	¹⁴⁶ Nd	¹⁴⁷ Sm	²⁰⁸ Pb	²³² Th	²³⁸ U
Antiparos	SCU.GEOL.201	61	2	22	357	8	12	118	32	35	26	9	1	47	52	26
Antiparos	SCU.GEOL.202	59	2	21	364	8	11	105	31	35	24	8	1	48	48	27
Antiparos	SCU.GEOL.203	67	2	21	352	8	11	106	31	34	24	8	1	46	47	26
Pantelleria - Lago Di Venere	SCU.ARCH.145	68	5	411	134	1	121	1298	261	1	23	124	25	10	21	6
Pantelleria - Lago Di Venere	SCU.ARCH.146	62	5	407	136	2	119	1282	260	1	24	124	25	10	22	7
Pantelleria - Lago Di Venere	SCU.ARCH.147	62	5	414	137	2	112	1199	266	2	24	117	24	10	21	7
Pantelleria - Lago Di Venere	SCU.GEOL.108	56	6	369	146	2	118	1466	289	1	56	121	23	12	27	8
Pantelleria - Lago Di Venere	SCU.GEOL.148	59	4	408	137	1	107	1154	248	1	24	114	23	10	20	7
Pantelleria - Lago Di Venere	SCU.GEOL.149	59	4	421	136	1	106	1170	252	1	24	116	23	10	21	7
Pantelleria - Lago Di Venere	SCU.GEOL.150	52	6	368	139	2	117	1456	281	1	55	115	23	12	26	8
Pantelleria - Lago Di Venere	SCU.GEOL.151	63	6	363	140	2	117	1441	291	1	56	119	23	12	26	8
Pantelleria - Lago Di Venere	SCU.GEOL.152	54	4	415	137	1	104	1139	250	1	23	115	23	10	20	7
Pantelleria - Lago Di Venere	SCU.GEOL.153	63	4	411	134	1	112	1202	256	2	24	119	24	10	21	7
Lipari	SCU.GEOL.100	66	2	53	290	15	35	150	32	15	14	35	7	30	45	15
Lipari	SCU.GEOL.101	61	2	58	289	16	36	164	33	15	16	39	8	30	49	15
Lipari	SCU.GEOL.102	48	2	54	285	15	36	151	32	15	14	35	7	30	44	15
Lipari	SCU.GEOL.103	64	2	54	283	15	36	154	32	15	14	36	7	30	47	15
Lipari	SCU.GEOL.104	61	2	53	286	15	35	149	32	15	14	36	7	29	45	15
Lipari	SCU.GEOL.105	58	2	54	279	15	36	153	32	15	14	35	7	28	44	14

SOURCE	SAMPLE	<i>Nb rows</i>	⁴⁵ Sc	⁶⁶ Zn	⁸⁵ Rb	⁸⁸ Sr	⁸⁹ Y	⁹⁰ Zr	⁹³ Nb	¹³³ Cs	¹³⁷ Ba	¹⁴⁶ Nd	¹⁴⁷ Sm	²⁰⁸ Pb	²³² Th	²³⁸ U
Antiparos	SCU.GEOL.201	61	2	22	357	8	12	118	32	35	26	9	1	47	52	26
Antiparos	SCU.GEOL.202	59	2	21	364	8	11	105	31	35	24	8	1	48	48	27
Antiparos	SCU.GEOL.203	67	2	21	352	8	11	106	31	34	24	8	1	46	47	26
Lipari	SCU.GEOL.99	58	2	57	285	15	35	158	33	15	16	38	8	29	47	15
Palmarola	SCU.GEOL.186	62	2	50	430	5	39	214	59	45	8	42	8	41	56	18
Palmarola	SCU.GEOL.187	60	2	51	452	5	38	213	59	46	8	42	8	42	56	18
Palmarola	SCU.GEOL.188	66	3	50	444	6	41	226	60	45	9	44	8	42	60	18
Palmarola	SCU.GEOL.189	63	2	52	441	6	49	272	64	47	9	51	10	42	68	18
Palmarola	SCU.GEOL.190	57	2	52	435	6	46	250	64	46	9	49	9	43	65	19
Palmarola	SCU.GEOL.191	62	2	51	444	5	43	238	60	44	9	46	9	42	60	18
Palmarola	SCU.GEOL.192	68	2	53	446	6	48	262	62	46	9	52	10	43	70	19
Monte Arci - SA	SCU.GEOL.170	57	4	89	231	22	28	67	43	4	111	20	6	31	15	5
Monte Arci - SA	SCU.GEOL.60	62	7	90	259	28	32	77	48	4	134	23	7	31	17	6
Monte Arci - SA	SCU.GEOL.61	60	6	89	264	25	30	70	47	4	131	22	6	31	16	6
Monte Arci - SA	SCU.GEOL.62	68	7	91	262	29	36	83	50	4	143	25	7	34	18	6
Monte Arci - SA	SCU.GEOL.63	63	7	86	252	28	35	80	48	4	135	24	7	31	17	6
Monte Arci - SA	SCU.GEOL.64	62	7	87	261	27	34	84	51	4	130	24	7	32	18	6
Monte Arci - SA	SCU.GEOL.32	61	6	86	247	24	31	73	45	4	121	22	6	31	15	5
Monte Arci - SA	SCU.GEOL.33	66	6	83	242	24	30	72	43	4	112	22	6	31	16	5

SOURCE	SAMPLE	<i>Nb rows</i>	⁴⁵ Sc	⁶⁶ Zn	⁸⁵ Rb	⁸⁸ Sr	⁸⁹ Y	⁹⁰ Zr	⁹³ Nb	¹³³ Cs	¹³⁷ Ba	¹⁴⁶ Nd	¹⁴⁷ Sm	²⁰⁸ Pb	²³² Th	²³⁸ U
Antiparos	SCU.GEOL.201	61	2	22	357	8	12	118	32	35	26	9	1	47	52	26
Antiparos	SCU.GEOL.202	59	2	21	364	8	11	105	31	35	24	8	1	48	48	27
Antiparos	SCU.GEOL.203	67	2	21	352	8	11	106	31	34	24	8	1	46	47	26
Monte Arci - SA	SCU.GEOL.34	62	5	89	250	21	28	67	46	4	103	19	6	30	14	5
Monte Arci - SA	SCU.GEOL.35	54	5	88	262	24	30	72	48	4	117	20	6	31	15	5
Monte Arci - SA	SCU.GEOL.36	64	5	89	249	25	31	72	47	4	118	21	6	31	15	5
Monte Arci - SA	SCU.GEOL.37	64	5	92	265	24	30	73	49	4	123	22	6	32	15	5
Monte Arci - SA	SCU.GEOL.38	64	5	89	261	25	29	69	47	4	118	20	6	30	14	5
Monte Arci - SA	SCU.GEOL.39	64	5	89	240	23	29	69	45	4	119	20	6	30	14	5
Monte Arci - SA	SCU.GEOL.40	59	5	84	227	24	29	67	45	4	115	19	6	29	14	5
Monte Arci - SA	SCU.GEOL.41	64	5	93	252	23	27	68	45	4	120	20	6	28	14	5
Monte Arci - SA	SCU.GEOL.42	66	5	84	235	23	28	66	43	4	114	19	6	29	14	5
Monte Arci - SA	SCU.GEOL.65	60	5	85	248	24	29	71	46	4	123	21	6	29	15	6
Monte Arci - SA	SCU.GEOL.66	61	5	86	253	26	32	78	49	4	128	22	6	30	16	6
Monte Arci - SA	SCU.GEOL.67	62	5	85	253	26	31	75	49	4	129	22	6	30	16	6
Monte Arci - SA	SCU.GEOL.68	60	5	88	254	23	32	78	49	4	120	23	7	31	16	6
Monte Arci - SA	SCU.GEOL.69	48	5	87	251	18	29	71	46	4	93	20	6	30	15	6
Monte Arci - SB1	SCU.GEOL.81	62	6	84	250	58	28	115	41	4	277	28	7	32	19	6
Monte Arci - SB1	SCU.GEOL.83	57	6	87	250	63	32	134	44	4	312	32	8	33	20	5

SOURCE	SAMPLE	<i>Nb rows</i>	⁴⁵ Sc	⁶⁶ Zn	⁸⁵ Rb	⁸⁸ Sr	⁸⁹ Y	⁹⁰ Zr	⁹³ Nb	¹³³ Cs	¹³⁷ Ba	¹⁴⁶ Nd	¹⁴⁷ Sm	²⁰⁸ Pb	²³² Th	²³⁸ U
Antiparos	SCU.GEOL.201	61	2	22	357	8	12	118	32	35	26	9	1	47	52	26
Antiparos	SCU.GEOL.202	59	2	21	364	8	11	105	31	35	24	8	1	48	48	27
Antiparos	SCU.GEOL.203	67	2	21	352	8	11	106	31	34	24	8	1	46	47	26
Monte Arci - SB1	SCU.GEOL.16	61	6	68	239	73	21	140	33	4	474	34	7	32	20	5
Monte Arci - SB1	SCU.GEOL.17	65	6	68	243	77	22	146	32	4	479	34	7	31	21	5
Monte Arci - SB1	SCU.GEOL.18	70	6	71	249	71	21	138	32	4	458	32	7	31	19	5
Monte Arci - SB1	SCU.GEOL.19	64	6	70	231	70	20	135	32	4	445	31	7	30	19	5
Monte Arci - SB1	SCU.GEOL.20	69	7	71	242	73	20	137	32	4	446	31	6	30	19	5
Monte Arci - SB1	SCU.GEOL.21	67	6	71	231	70	19	124	31	4	433	29	6	29	18	5
Monte Arci - SB1	SCU.GEOL.22	62	6	69	234	71	19	129	31	4	444	30	6	30	18	5
Monte Arci - SB1	SCU.GEOL.23	68	6	68	236	72	20	134	31	4	449	31	7	31	19	5
Monte Arci - SB1	SCU.GEOL.24	69	5	70	220	63	18	119	28	3	403	28	6	29	16	4
Monte Arci - SB1	SCU.GEOL.77	64	4	87	232	50	24	101	39	4	249	24	6	30	16	5
Monte Arci - SB1	SCU.GEOL.78	67	4	83	228	51	22	98	37	4	249	24	6	31	15	5
Monte Arci - SB1	SCU.GEOL.79	65	4	80	222	49	21	94	36	3	245	22	5	29	14	5
Monte Arci - SB1	SCU.GEOL.80	62	4	86	227	44	21	89	36	3	227	22	6	29	14	5
Monte Arci - SB1	SCU.GEOL.71	56	6	79	251	62	32	130	44	4	288	31	8	31	21	6
Monte Arci - SB1	SCU.GEOL.72	64	5	77	248	58	30	122	42	4	286	29	7	30	20	5
Monte Arci - SB2	SCU.GEOL.82	63	5	52	255	52	21	124	27	7	298	30	6	26	21	5

SOURCE	SAMPLE	<i>Nb rows</i>	⁴⁵ Sc	⁶⁶ Zn	⁸⁵ Rb	⁸⁸ Sr	⁸⁹ Y	⁹⁰ Zr	⁹³ Nb	¹³³ Cs	¹³⁷ Ba	¹⁴⁶ Nd	¹⁴⁷ Sm	²⁰⁸ Pb	²³² Th	²³⁸ U
Antiparos	SCU.GEOL.201	61	2	22	357	8	12	118	32	35	26	9	1	47	52	26
Antiparos	SCU.GEOL.202	59	2	21	364	8	11	105	31	35	24	8	1	48	48	27
Antiparos	SCU.GEOL.203	67	2	21	352	8	11	106	31	34	24	8	1	46	47	26
Monte Arci - SB2	SCU.GEOL.84	56	5	52	243	39	20	110	27	7	210	26	6	26	19	5
Monte Arci - SB2	SCU.GEOL.85	60	5	49	235	50	20	119	28	7	304	28	6	25	20	5
Monte Arci - SB2	SCU.GEOL.86	61	5	53	244	40	21	110	27	7	211	25	6	26	19	6
Monte Arci - SB2	SCU.GEOL.87	59	5	53	251	35	18	97	26	6	190	22	5	25	17	5
Monte Arci - SB2	SCU.GEOL.88	69	5	54	237	48	18	111	27	6	282	26	5	26	18	5
Monte Arci - SB2	SCU.GEOL.97	53	5	54	241	26	18	89	26	7	124	21	5	26	16	5
Monte Arci - SB2	SCU.GEOL.25	63	5	51	225	45	18	108	25	6	262	26	5	25	18	5
Monte Arci - SB2	SCU.GEOL.27	67	5	48	225	44	17	97	24	6	264	24	5	24	17	5
Monte Arci - SB2	SCU.GEOL.28	63	5	51	235	24	19	87	25	7	109	20	5	25	16	5
Monte Arci - SB2	SCU.GEOL.29	56	5	50	306	20	16	86	25	7	130	20	4	24	15	5
Monte Arci - SB2	SCU.GEOL.30	67	4	52	248	26	18	90	26	7	119	20	5	25	15	5
Monte Arci - SB2	SCU.GEOL.31	61	4	53	247	51	20	121	28	7	296	27	6	26	19	5
Monte Arci - SB2	SCU.GEOL.75	71	4	53	230	29	16	82	24	6	144	19	4	24	14	5
Monte Arci - SB2	SCU.GEOL.76	70	4	54	228	36	15	87	24	6	205	21	4	24	14	5
Monte Arci - SB2	SCU.GEOL.70	61	4	48	237	38	19	100	26	7	201	24	5	23	17	5
Monte Arci - SB2	SCU.GEOL.73	62	5	46	247	30	22	103	27	7	133	25	6	24	19	6

SOURCE	SAMPLE	<i>Nb rows</i>	⁴⁵ Sc	⁶⁶ Zn	⁸⁵ Rb	⁸⁸ Sr	⁸⁹ Y	⁹⁰ Zr	⁹³ Nb	¹³³ Cs	¹³⁷ Ba	¹⁴⁶ Nd	¹⁴⁷ Sm	²⁰⁸ Pb	²³² Th	²³⁸ U
Antiparos	SCU.GEOL.201	61	2	22	357	8	12	118	32	35	26	9	1	47	52	26
Antiparos	SCU.GEOL.202	59	2	21	364	8	11	105	31	35	24	8	1	48	48	27
Antiparos	SCU.GEOL.203	67	2	21	352	8	11	106	31	34	24	8	1	46	47	26
Monte Arci - SB2	SCU.GEOL.74	62	5	48	238	45	22	122	28	7	240	29	6	24	21	6
Monte Arci - SC	SCU.GEOL.94	59	5	71	181	104	23	233	27	2	917	53	10	33	26	4
Monte Arci - SC	SCU.GEOL.95	52	5	66	178	123	21	230	27	2	970	49	10	31	24	3
Monte Arci - SC	SCU.GEOL.96	61	5	72	172	111	21	214	27	2	908	47	9	32	23	3
Monte Arci - SC	SCU.GEOL.98	63	5	69	176	108	20	213	26	2	944	48	9	32	23	3
Monte Arci - SC	SCU.GEOL.43	62	4	65	167	102	18	197	25	2	851	42	8	29	20	3
Monte Arci - SC	SCU.GEOL.44	53	4	60	166	86	20	209	25	2	753	42	8	28	21	3
Monte Arci - SC	SCU.GEOL.45	54	4	69	163	86	18	190	25	2	770	41	8	32	19	3
Monte Arci - SC	SCU.GEOL.46	49	5	81	179	109	19	203	27	2	925	45	9	31	22	3
Monte Arci - SC	SCU.GEOL.47	64	4	62	160	89	17	174	26	2	755	40	8	30	19	3
Monte Arci - SC	SCU.GEOL.48	60	4	67	166	90	18	173	25	2	784	41	8	31	19	3
Monte Arci - SC	SCU.GEOL.49	58	4	66	170	85	20	211	25	2	721	42	8	29	21	3
Monte Arci - SC	SCU.GEOL.50	65	4	71	162	102	18	187	26	2	815	43	8	31	21	3
Monte Arci - SC	SCU.GEOL.51	59	5	66	175	94	21	212	28	2	812	46	9	31	23	3
Monte Arci - SC	SCU.GEOL.52	69	4	72	160	93	18	179	26	2	935	44	8	30	20	3
Monte Arci - SC	SCU.GEOL.53	39	4	59	172	80	21	224	24	2	672	43	8	31	22	3

SOURCE	SAMPLE	<i>Nb rows</i>	⁴⁵ Sc	⁶⁶ Zn	⁸⁵ Rb	⁸⁸ Sr	⁸⁹ Y	⁹⁰ Zr	⁹³ Nb	¹³³ Cs	¹³⁷ Ba	¹⁴⁶ Nd	¹⁴⁷ Sm	²⁰⁸ Pb	²³² Th	²³⁸ U
Antiparos	SCU.GEOL.201	61	2	22	357	8	12	118	32	35	26	9	1	47	52	26
Antiparos	SCU.GEOL.202	59	2	21	364	8	11	105	31	35	24	8	1	48	48	27
Antiparos	SCU.GEOL.203	67	2	21	352	8	11	106	31	34	24	8	1	46	47	26
Monte Arci - SC	SCU.GEOL.54	60	4	76	167	98	19	194	26	2	850	44	9	32	21	3
Monte Arci - SC	SCU.GEOL.55	48	4	68	167	84	18	190	25	2	763	41	8	29	20	3
Monte Arci - SC	SCU.GEOL.56	57	4	70	167	98	19	197	26	2	852	43	8	30	21	3
Monte Arci - SC	SCU.GEOL.57	56	4	65	174	89	19	209	25	2	754	40	8	31	21	3
Monte Arci - SC	SCU.GEOL.58	52	4	75	170	75	18	205	27	2	804	40	8	30	20	3
Monte Arci - SC	SCU.GEOL.59	59	4	71	164	86	19	192	24	2	777	43	8	31	21	3
Monte Arci - SC	SCU.GEOL.89	61	4	71	170	106	17	186	25	2	855	41	8	30	20	3
Monte Arci - SC	SCU.GEOL.90	61	4	68	169	102	17	184	25	2	860	42	8	30	19	3
Monte Arci - SC	SCU.GEOL.91	63	4	71	165	97	17	184	25	2	817	41	8	31	20	3
Monte Arci - SC	SCU.GEOL.92	53	4	63	160	75	17	180	24	2	764	38	7	29	18	3
Monte Arci - SC	SCU.GEOL.93	58	4	64	170	79	19	194	25	2	795	42	8	31	20	3

Appendix E

Proposed chronology and associated cultural facies for the Neolithic of Corsica and Sardinia. Data adapted from Soula, 2012.

		CORSICA		SARDINIA	
EARLY NEOLITHIC	<i>Proposed dates</i>	5900/5800-4900 B.C.		5900-4800 B.C.	
	<i>Facies</i>	Filiestru-Basi-Pienza (FDB) 5800-5400 B.C.	Strette-A Petra 5400-4900 B.C.	Filiestru-Basi-Pienza Filiestru-Grotta Verde	
	<i>Archaeological sites</i>	Filiestru (Sardinia) Basi-Serra-di-Ferro Pienza (Tuscany) Renaghju phase 1	Strette-Barbaghju (Corsica) A Petra-île Rousse (Corsica) Goulet-Bonifacio Longone-Bonifacio	Grotta Corbeddu-Oliena Filiestru-Mara Rio Saboccu-Gùspini Sa Punta-Terralba	
MIDDLE NEOLITHIC	<i>Proposed dates</i>	4900-3900/3800 B.C.		4800-4200/4000 B.C.	
	<i>Subdivision</i>	Middle Neolithic I 4900 – 4400/4300	Middle Neolithic II 4400/4300 – 3900/3800 B.C.	Middle Neolithic I	San Ciriaco 4500-4200/4000 B.C. ?
	<i>Facies</i>	Curasien - San Vincente 'Bonu Ighinu Corsu'	Presa	Bonu Ighinu 4800-4200 B.C.	
<i>Archaeological sites</i>	Curacchiaghju-Levie Renaghju (phase 3) I Stantari (phase 1)?	San Ciprianu-Lecci Monte Revincu-Santo-Pietro-di-Tenda Abri de la Figue	Sa 'Ucca de su Tintirriolu Su Caroppu-Sirri Grotta Ulàri-Borutta		
LATE NEOLITHIC	<i>Proposed dates</i>	3900/3800 – 3100/3000 B.C.		4200-3400 B.C.	
	<i>Facies</i>	Basien Monte Grossu		San Michele/Ozieri	
<i>Archaeological sites</i>	Basi-Serra-di-Ferro Monte Grossu-Biguglia I Sapari				
FINAL NEOLITHIC	<i>Proposed dates</i>	3100/3000 – 2200/2100 B.C.			
	<i>Facies</i>	Terrinien			
	<i>Archaeological sites</i>	Terrina Araguina-Sennola-Bonifacio Cauria XX and XXI		San Michele di Ozieri	Cucurru S'Arriu Is Arriu-Cabras

Appendix F

LA-ICP-MS data obtained on the NIST 613 international standard. 50 measurements acquired at the start and end of 25 runs. Number of rows [Nb rows] indicates the number of measurements obtained within a single ablation line, after statistical treatment with removal of the outliers with JMP statistical software (SAS); the results displayed for each isotope represent the average concentration (in ppm) for the corresponding number of 'rows'.

MEASUREMENT	<i>Nb Rows</i>	⁴⁵ Sc	⁶⁶ Zn	⁸⁵ Rb	⁸⁸ Sr	⁸⁹ Y	⁹⁰ Zr	⁹³ Nb	¹³³ Cs	¹³⁷ Ba	¹⁴⁶ Nd	¹⁴⁷ Sm	²⁰⁸ Pb	²³² Th	²³⁸ U
NIST 613 start 11-08-14-Run1	61	38	38	29	75	34	34	35	38	38	33	35	39	33	35
NIST 613 end 11-08-14-Run1	64	38	38	32	79	36	36	37	41	39	34	37	39	36	37
NIST 613 start 11-08-14-Run2	62	38	38	31	79	36	35	37	39	40	34	36	39	34	36
NIST 613 end 11-08-14-Run2	57	36	39	31	78	35	35	38	41	38	33	36	37	35	36
NIST 613 start 12-08-14-Run1	61	40	44	31	80	38	40	38	41	41	35	38	43	38	37
NIST 613 end 12-08-14-Run1	62	38	40	32	87	37	36	37	41	41	34	36	41	37	37
NIST 613 start 12-08-14-Run2	62	37	41	32	88	37	37	37	42	40	34	36	41	36	36
NIST 613 end 12-08-14-Run2	62	38	41	33	94	38	37	38	41	40	35	37	41	37	37
NIST 613 start 16-08-14-Run1	64	38	37	32	78	33	33	37	42	41	33	35	39	34	37
NIST 613 end 16-08-14-Run1	60	39	38	32	79	37	37	38	42	40	34	36	40	37	37
NIST 613 start 20-05-14-Run1	64	38	42	31	82	35	34	36	41	41	33	34	38	34	38
NIST 613 end 20-05-14-Run1	64	39	44	32	80	37	37	38	42	40	34	37	37	36	37
NIST 613 start 20-05-14-Run2	62	36	34	31	79	34	33	36	40	38	32	34	37	33	36
NIST 613 end 20-05-14-Run2	69	39	39	32	78	38	38	37	41	40	34	37	40	37	36

MEASUREMENT	<i>Nb Rows</i>	⁴⁵ Sc	⁶⁶ Zn	⁸⁵ Rb	⁸⁸ Sr	⁸⁹ Y	⁹⁰ Zr	⁹³ Nb	¹³³ Cs	¹³⁷ Ba	¹⁴⁶ Nd	¹⁴⁷ Sm	²⁰⁸ Pb	²³² Th	²³⁸ U
NIST 613 start 20-05-14-Run3	64	35	33	30	78	34	33	35	40	40	32	33	35	32	35
NIST 613 end 20-05-14-Run3	69	39	37	33	80	38	37	38	42	40	34	36	37	35	36
NIST 613 start 26-08-14-Run1	72	36	36	32	76	34	34	36	42	39	33	35	39	34	37
NIST 613 end 26-08-14-Run1	69	37	37	33	78	34	34	36	42	40	34	36	38	34	37
NIST 613 start 23-05-14-Run1	56	40	46	31	80	38	38	38	42	44	35	37	42	37	37
NIST 613 end 23-05-14-Run1	56	38	43	31	78	37	38	38	41	42	34	37	40	36	37
NIST 613 start 21-05-14-Run1	69	38	42	30	77	36	36	37	40	39	34	35	40	35	35
NIST 613 end 21-05-14-Run1	73	39	43	32	79	37	38	38	42	39	34	37	40	36	36
NIST 613 start 21-05-14-Run2	60	37	41	29	75	37	36	38	41	38	34	37	40	36	37
NIST 613 end 21-05-14-Run2	65	37	43	31	76	36	36	38	41	38	33	36	40	35	36
NIST 613 start 22-05-14-Run1	58	39	44	31	77	37	37	38	41	39	35	36	40	37	37
NIST 613 end 22-05-14-Run1	58	38	42	31	77	37	37	37	40	39	34	37	40	36	37
NIST 613 start 22-05-14-Run2	60	38	40	31	76	37	37	37	41	39	34	37	38	37	37
NIST 613 end 22-05-14-Run2	59	38	43	30	75	36	37	38	40	37	34	36	38	36	36
NIST 613 start 23-05-14-Run2	49	39	43	30	77	36	37	38	41	40	33	35	40	35	36
NIST 613 end 23-05-14-Run2	57	38	42	31	77	36	36	37	39	39	33	35	41	36	36
NIST 613 start 23-05-14-Run3	56	38	43	31	76	37	37	38	41	39	34	35	41	36	36
NIST 613 end 23-05-14-Run3	52	38	43	30	74	36	36	38	40	39	33	35	40	35	36
NIST 613 start 23-05-14-Run4	59	37	43	31	76	37	37	37	42	40	34	36	42	36	36
NIST 613 end 23-05-14-Run4	62	38	43	32	78	39	38	38	42	40	34	36	42	37	36

MEASUREMENT	<i>Nb Rows</i>	⁴⁵ Sc	⁶⁶ Zn	⁸⁵ Rb	⁸⁸ Sr	⁸⁹ Y	⁹⁰ Zr	⁹³ Nb	¹³³ Cs	¹³⁷ Ba	¹⁴⁶ Nd	¹⁴⁷ Sm	²⁰⁸ Pb	²³² Th	²³⁸ U
NIST 613 start 24-05-14-Run1	54	39	45	31	77	36	36	37	40	38	33	36	41	36	36
NIST 613 end 24-05-14-Run1	64	38	44	31	77	37	38	39	42	39	33	37	41	36	36
NIST 613 start 25-05-14-Run1	53	34	43	30	74	30	31	35	38	38	32	32	40	31	36
NIST 613 end 25-05-14-Run1	58	35	47	31	77	34	35	37	42	40	34	36	42	35	37
NIST 613 start 12-08-14-Run1	64	38	43	31	75	36	36	36	40	38	33	35	42	36	36
NIST 613 end 12-08-14-Run1	66	38	45	31	76	37	36	36	39	37	33	35	41	36	36
NIST 613 start 16-08-14-Run1	47	38	43	30	76	37	37	37	39	38	33	36	39	35	36
NIST 613 end 16-08-14-Run1	62	39	42	31	77	37	37	37	39	37	34	36	38	36	36
NIST 613 start 16-09-14-Run1	56	39	42	30	76	37	37	38	41	40	33	36	41	36	37
NIST 613 end 16-09-14-Run1	54	38	43	30	77	37	38	38	40	39	34	37	39	37	37
NIST 613 start 16-09-14-Run2	60	38	33	30	75	37	37	37	40	38	33	36	35	36	36
NIST 613 end 16-09-14-Run2	62	39	36	31	77	38	37	38	40	39	34	37	38	36	36
NIST 613 start 17-09-14-Run1	57	39	43	30	75	37	37	37	40	39	33	36	41	36	37
NIST 613 end 17-09-14-Run1	61	39	43	30	77	38	37	37	40	39	34	36	39	35	35
NIST 613 start 22-09-14-Run1	58	40	44	32	79	38	38	38	41	39	34	36	40	36	37
NIST613 end 22-09-14-Run1	58	39	45	31	76	36	37	37	40	39	33	36	39	36	36

Appendix G

LA-ICP-MS data obtained on the BCR-2G (glass) international standard; 4 measurements acquired. Number of rows [Nb rows] indicates the number of measurements obtained within a single ablation line, after statistical treatment with removal of the outliers with JMP statistical software (SAS); the results displayed for each isotope represent the average concentration (in ppm) for the corresponding number of 'rows'.

MEASUREMENT	<i>Nb Rows</i>	⁴⁵ Sc	⁶⁶ Zn	⁸⁵ Rb	⁸⁸ Sr	⁸⁹ Y	⁹⁰ Zr	⁹³ Nb	¹³³ Cs	¹³⁷ Ba	¹⁴⁶ Nd	¹⁴⁷ Sm	²⁰⁸ Pb	²³² Th	²³⁸ U
BCR-2G-1	64	35	170	46	325	33	184	11	1	685	29	7	10	6	2
BCR-2G-2	69	36	166	44	325	35	191	11	1	674	29	7	10	6	2
BCR-2G-3	70	36	174	46	329	35	192	11	1	682	29	7	11	6	2
BCR-2G-4	66	34	162	46	322	32	177	11	1	655	28	6	10	6	2

Appendix H1

LA-ICP-MS data obtained on 112 artefacts of Renaghju phase 3. Analyses conducted at the SOLARIS laboratory (Southern Cross University). Number of rows [Nb rows] indicates the number of measurements obtained within a single ablation line, after statistical treatment with removal of the outliers with JMP statistical software (SAS); the results displayed for each isotope represent the average concentration (in ppm) for the corresponding number of 'rows'.

SAMPLE	<i>Nb Rows</i>	⁴⁵ Sc	⁶⁶ Zn	⁸⁵ Rb	⁸⁸ Sr	⁸⁹ Y	⁹⁰ Zr	⁹³ Nb	¹³³ Cs	¹³⁷ Ba	¹⁴⁶ Nd	¹⁴⁷ Sm	²⁰⁸ Pb	²³² Th	²³⁸ U	PROVENANCE
SCU.ARCH.11	49	5.3	90	224	22	31	73	42	3.6	104	22	6.1	29	16	5.2	SA
SCU.ARCH.46	50	5.8	88	229	23	31	73	43	3.7	112	21	6.2	31	15	5.3	SA
SCU.ARCH.60	53	5.3	90	245	25	33	79	47	3.9	123	23	6.6	31	17	5.4	SA
SCU.ARCH.79	41	5.0	90	226	22	30	71	41	3.8	101	21	5.8	29	15	5.2	SA
SCU.ARCH.83	54	5.2	83	218	22	29	70	42	3.5	104	20	6.2	28	15	5.0	SA
SCU.ARCH.85	44	5.4	86	232	24	32	76	44	3.7	112	22	6.0	28	16	5.4	SA
SCU.ARCH.89	50	5.3	104	225	23	30	70	43	3.7	115	21	6.0	31	15	5.2	SA
SCU.ARCH.96	50	5.6	98	225	22	30	72	43	3.6	108	21	6.1	30	15	5.1	SA
SCU.ARCH.106	45	6.2	94	225	23	30	74	43	3.8	116	22	6.3	32	16	5.4	SA
SCU.ARCH.12	45	5.5	94	231	23	30	73	44	3.8	113	22	6.3	31	16	5.4	SA
SCU.ARCH.88	50	5.0	110	218	24	29	69	41	3.6	113	21	5.9	31	15	5.2	SA
SCU.ARCH.10	51	4.8	76	248	23	33	76	44	3.8	118	23	6.5	30	16	5.4	SA
SCU.ARCH.59	57	4.9	74	246	22	33	78	44	4.0	106	22	6.6	30	16	5.6	SA
SCU.ARCH.65	45	5.0	101	244	23	32	76	45	3.9	113	22	6.3	31	16	5.3	SA

SAMPLE	<i>Nb Rows</i>	⁴⁵ Sc	⁶⁶ Zn	⁸⁵ Rb	⁸⁸ Sr	⁸⁹ Y	⁹⁰ Zr	⁹³ Nb	¹³³ Cs	¹³⁷ Ba	¹⁴⁶ Nd	¹⁴⁷ Sm	²⁰⁸ Pb	²³² Th	²³⁸ U	PROVENANCE
SCU.ARCH.82	58	5.0	129	235	21	31	75	43	3.8	103	21	6.1	34	15	5.2	SA
SCU.ARCH.90	41	5.3	228	224	25	28	68	42	3.7	110	21	5.8	38	15	5.1	SA
SCU.ARCH.20	56	4.2	51	230	29	19	94	25	6.5	136	23	5.3	24	17	5.4	SB2
SCU.ARCH.32	47	4.4	68	228	25	20	96	26	6.5	116	21	5.1	25	17	5.4	SB2
SCU.ARCH.33	55	4.6	51	223	27	19	94	24	6.2	124	22	4.8	23	16	5.2	SB2
SCU.ARCH.38	48	4.9	58	218	24	18	86	24	6.2	102	20	4.7	25	16	5.2	SB2
SCU.ARCH.40	49	5.0	64	223	26	18	90	24	6.3	121	21	4.8	25	16	5.4	SB2
SCU.ARCH.55	41	4.4	83	239	25	20	99	27	6.7	104	22	5.1	25	17	5.6	SB2
SCU.ARCH.58	47	4.3	56	209	22	18	85	23	5.9	96	20	4.6	23	15	5.0	SB2
SCU.ARCH.78	50	4.6	53	224	29	20	97	25	6.3	131	22	5.1	24	17	5.3	SB2
SCU.ARCH.98	49	4.9	52	223	27	20	97	25	6.3	126	22	5.2	24	17	5.5	SB2
SCU.ARCH.103	54	5.0	66	225	31	19	96	25	6.3	152	23	5.2	27	17	5.5	SB2
SCU.ARCH.105	49	5.2	86	212	27	18	88	24	6.2	126	21	4.7	26	16	5.3	SB2
SCU.ARCH.13	51	4.2	50	218	25	20	94	24	6.2	111	22	5.1	24	17	5.6	SB2
SCU.ARCH.21	54	5.3	55	225	23	19	91	25	6.4	97	21	4.8	24	16	5.5	SB2
SCU.ARCH.28	53	4.1	45	220	25	19	92	24	6.2	108	22	5.0	23	17	5.4	SB2
SCU.ARCH.30	46	4.7	51	227	23	20	94	26	6.5	99	21	5.0	24	17	5.7	SB2
SCU.ARCH.34	48	5.1	51	222	26	20	97	25	6.5	120	22	5.3	24	17	5.6	SB2
SCU.ARCH.39	42	4.1	61	221	27	19	94	24	6.1	122	23	5.1	24	17	5.4	SB2
SCU.ARCH.49	49	5.0	134	233	45	20	109	26	6.6	235	27	5.8	29	20	6.1	SB2

SAMPLE	<i>Nb Rows</i>	⁴⁵ Sc	⁶⁶ Zn	⁸⁵ Rb	⁸⁸ Sr	⁸⁹ Y	⁹⁰ Zr	⁹³ Nb	¹³³ Cs	¹³⁷ Ba	¹⁴⁶ Nd	¹⁴⁷ Sm	²⁰⁸ Pb	²³² Th	²³⁸ U	PROVENANCE
SCU.ARCH.57	52	4.1	50	204	46	18	109	24	5.5	274	26	5.4	23	18	4.8	SB2
SCU.ARCH.62	51	4.3	52	220	26	19	93	25	6.2	117	22	5.2	24	17	5.5	SB2
SCU.ARCH.67	51	4.2	53	233	27	20	98	26	6.6	121	23	5.4	25	18	5.7	SB2
SCU.ARCH.70	53	4.2	62	209	45	18	107	24	5.6	257	26	5.4	24	18	4.9	SB2
SCU.ARCH.74	41	4.4	67	232	28	20	97	25	6.6	128	22	5.3	27	18	5.7	SB2
SCU.ARCH.75	46	4.3	65	230	30	20	100	26	6.8	142	23	5.4	26	18	5.8	SB2
SCU.ARCH.77	50	4.5	77	223	26	19	91	25	6.3	111	21	4.8	25	16	5.3	SB2
SCU.ARCH.84	53	4.3	54	225	26	20	92	25	6.4	114	22	5.1	24	17	5.5	SB2
SCU.ARCH.91	54	4.7	49	223	29	20	99	25	6.2	133	23	5.2	24	18	5.5	SB2
SCU.ARCH.92	52	4.3	94	225	29	19	92	25	6.5	132	22	5.3	26	17	5.6	SB2
SCU.ARCH.99.1	54	4.1	54	221	24	19	91	24	6.3	102	21	5.0	24	16	5.5	SB2
SCU.ARCH.99.2	49	4.2	73	220	28	18	91	25	6.2	129	22	4.9	26	17	5.4	SB2
SCU.ARCH.99.3	50	4.3	67	222	25	19	91	25	6.4	107	21	4.8	25	17	5.5	SB2
SCU.ARCH.99.4	57	4.4	48	214	50	19	116	25	5.8	293	28	5.8	25	19	5.1	SB2
SCU.ARCH.100.1	54	4.0	46	222	47	19	112	24	5.6	265	27	5.8	24	19	5.0	SB2
SCU.ARCH.100.2	53	3.7	56	219	25	18	86	24	5.9	116	20	4.7	24	15	5.1	SB2
SCU.ARCH.104	55	3.9	51	233	28	20	94	25	6.2	127	22	5.2	25	17	5.4	SB2
SCU.ARCH.22	51	4.2	52	223	43	19	106	25	6.2	236	26	5.5	26	18	5.2	SB2
SCU.ARCH.24	53	3.9	49	239	27	20	97	25	6.1	123	22	5.2	25	17	5.5	SB2
SCU.ARCH.25	51	4.1	64	239	25	21	95	25	6.4	104	22	5.1	25	17	5.5	SB2

SAMPLE	<i>Nb Rows</i>	⁴⁵ Sc	⁶⁶ Zn	⁸⁵ Rb	⁸⁸ Sr	⁸⁹ Y	⁹⁰ Zr	⁹³ Nb	¹³³ Cs	¹³⁷ Ba	¹⁴⁶ Nd	¹⁴⁷ Sm	²⁰⁸ Pb	²³² Th	²³⁸ U	PROVENANCE
SCU.ARCH.29	56	3.9	45	226	28	20	96	24	6.0	127	22	5.0	23	17	5.2	SB2
SCU.ARCH.31	50	4.0	51	236	24	20	95	25	6.7	100	21	5.0	23	17	5.7	SB2
SCU.ARCH.37	48	4.1	54	236	29	21	100	26	6.5	136	23	5.6	25	18	5.7	SB2
SCU.ARCH.42	47	4.0	46	226	39	20	104	25	6.1	209	25	5.7	24	18	5.3	SB2
SCU.ARCH.53	48	3.9	44	239	23	20	97	24	6.3	102	21	5.1	23	17	5.3	SB2
SCU.ARCH.61	56	3.9	47	236	29	20	96	25	6.2	134	23	5.1	25	17	5.3	SB2
SCU.ARCH.63	57	4.0	45	229	36	20	102	25	6.0	183	24	5.5	24	18	5.3	SB2
SCU.ARCH.76	40	4.1	64	233	27	20	94	25	6.5	117	22	5.2	25	17	5.4	SB2
SCU.ARCH.9	42	4.0	46	234	28	20	97	25	6.5	127	22	5.2	24	17	5.6	SB2
SCU.ARCH.93	50	4.0	48	235	29	21	97	25	6.5	128	23	5.5	25	18	5.4	SB2
SCU.ARCH.14	48	4.4	51	223	24	19	90	24	6.2	102	21	4.8	24	16	5.4	SB2
SCU.ARCH.15	54	4.5	57	219	26	19	92	24	6.1	116	21	4.9	24	16	5.5	SB2
SCU.ARCH.23	49	4.8	52	215	44	19	109	24	5.8	245	26	5.7	25	18	5.1	SB2
SCU.ARCH.27	52	4.1	51	226	25	20	93	25	6.3	106	22	5.0	24	17	5.4	SB2
SCU.ARCH.3	47	4.8	55	227	24	20	92	25	6.5	102	21	5.0	25	17	5.6	SB2
SCU.ARCH.35	51	4.1	51	213	39	19	104	24	5.8	206	25	5.3	25	18	5.1	SB2
SCU.ARCH.66	49	4.2	60	229	26	20	96	25	6.2	117	22	5.1	25	17	5.5	SB2
SCU.ARCH.80	45	4.1	55	217	26	19	91	24	5.9	110	21	5.0	24	16	5.0	SB2
SCU.ARCH.81	55	4.0	61	219	27	19	92	24	5.9	123	22	5.0	24	16	5.2	SB2
SCU.ARCH.110	49	6.2	63	230	27	19	94	25	6.4	121	21	5.0	25	17	5.4	SB2

SAMPLE	<i>Nb Rows</i>	⁴⁵ Sc	⁶⁶ Zn	⁸⁵ Rb	⁸⁸ Sr	⁸⁹ Y	⁹⁰ Zr	⁹³ Nb	¹³³ Cs	¹³⁷ Ba	¹⁴⁶ Nd	¹⁴⁷ Sm	²⁰⁸ Pb	²³² Th	²³⁸ U	PROVENANCE
SCU.ARCH.1	46	4.9	70	157	89	21	216	24	1.8	768	43	8.4	29	22	3.1	SC
SCU.ARCH.18	48	4.7	76	156	108	21	202	25	1.9	824	48	9.0	29	22	3.1	SC
SCU.ARCH.44	47	4.9	102	163	111	20	199	28	2.0	901	44	8.2	32	21	3.4	SC
SCU.ARCH.47	50	4.6	74	161	96	21	212	25	1.8	807	47	8.9	29	23	3.2	SC
SCU.ARCH.48	54	4.6	64	166	111	23	230	26	1.9	914	52	9.8	30	26	3.3	SC
SCU.ARCH.54	54	4.7	91	160	109	21	208	26	1.9	844	49	9.2	33	24	3.2	SC
SCU.ARCH.56	53	5.1	95	171	122	24	232	28	2.0	935	54	10.2	32	26	3.4	SC
SCU.ARCH.6	48	4.7	77	163	100	20	212	25	1.9	846	47	9.1	31	23	3.2	SC
SCU.ARCH.69	40	5.1	103	160	77	20	223	25	2.1	720	44	8.7	34	23	3.4	SC
SCU.ARCH.71	54	4.9	79	163	108	22	215	27	2.0	847	51	9.8	32	24	3.3	SC
SCU.ARCH.87	50	4.5	82	160	106	21	209	27	1.9	842	50	9.3	31	24	3.3	SC
SCU.ARCH.108	47	4.7	156	169	104	22	229	27	2.3	879	50	9.5	39	25	3.6	SC
SCU.ARCH.4	52	5.1	102	170	117	23	230	27	2.1	930	54	10.3	34	26	3.5	SC
SCU.ARCH.52	46	4.7	137	162	101	21	208	26	1.9	856	48	9.1	33	23	3.3	SC
SCU.ARCH.72	52	5.2	75	163	112	22	227	26	1.9	919	51	9.8	32	25	3.4	SC
SCU.ARCH.73	51	5.3	99	169	136	22	239	26	2.1	1027	53	10.0	33	25	3.4	SC
SCU.ARCH.8	46	6.0	92	165	95	22	232	25	2.1	821	48	9.1	31	24	3.4	SC
SCU.ARCH.94	51	4.6	85	173	102	23	237	27	2.1	915	52	10.0	33	26	3.5	SC
SCU.ARCH.95	41	6.1	104	165	100	21	220	26	2.0	872	49	9.3	32	24	3.4	SC
SCU.ARCH.97	52	4.5	91	159	106	22	221	26	1.8	880	49	9.3	32	24	3.2	SC

SAMPLE	<i>Nb Rows</i>	⁴⁵ Sc	⁶⁶ Zn	⁸⁵ Rb	⁸⁸ Sr	⁸⁹ Y	⁹⁰ Zr	⁹³ Nb	¹³³ Cs	¹³⁷ Ba	¹⁴⁶ Nd	¹⁴⁷ Sm	²⁰⁸ Pb	²³² Th	²³⁸ U	PROVENANCE
SCU.ARCH.109	48	4.6	140	159	143	21	225	25	1.7	964	50	9.6	34	24	3.2	SC
SCU.ARCH.17	57	4.5	78	164	112	23	213	27	2.0	853	51	9.8	31	25	3.4	SC
SCU.ARCH.2	50	4.4	77	171	111	23	223	26	1.7	872	53	9.9	31	25	3.2	SC
SCU.ARCH.41	50	4.4	78	167	123	22	227	26	1.9	916	50	9.8	32	25	3.3	SC
SCU.ARCH.43	52	4.5	71	168	128	22	227	26	2.0	929	49	9.5	30	24	3.3	SC
SCU.ARCH.45	52	4.6	69	168	112	24	230	27	2.1	903	54	10.3	32	26	3.4	SC
SCU.ARCH.5	52	4.3	64	170	108	22	224	25	1.9	910	50	9.7	31	25	3.4	SC
SCU.ARCH.50	50	4.2	77	166	117	21	212	25	1.7	866	48	9.3	31	23	3.2	SC
SCU.ARCH.64	47	4.3	62	175	107	23	226	26	1.9	922	53	10.0	32	25	3.3	SC
SCU.ARCH.107	52	5.2	93	164	106	22	218	26	1.9	902	48	9.3	32	24	3.3	SC
SCU.ARCH.16	47	5.3	95	166	102	22	226	26	1.9	908	51	9.7	48	24	3.3	SC
SCU.ARCH.19	42	4.7	99	168	114	23	230	26	1.9	913	53	9.9	36	25	3.4	SC
SCU.ARCH.26	51	4.5	100	166	115	22	219	25	1.9	904	51	9.2	32	24	3.3	SC
SCU.ARCH.36	46	4.4	104	175	89	23	241	26	2.1	816	48	9.4	35	25	3.6	SC
SCU.ARCH.51	53	4.3	73	161	106	21	210	25	1.7	864	49	8.9	31	23	3.1	SC
SCU.ARCH.68	51	4.5	103	162	116	22	228	26	2.0	891	51	9.6	31	24	3.3	SC
SCU.ARCH.7	51	4.1	77	161	87	21	224	24	1.9	736	45	8.7	32	23	3.3	SC
SCU.ARCH.86	29	4.2	75	128	88	15	98	11	3.4	562	18	3.5	23	12	4.2	N/A

Appendix H2

LA-ICP-MS data obtained on 99 artefacts of I Stantari phase 1. Analyses conducted at the SOLARIS laboratory (Southern Cross University). Number of rows [Nb rows] indicates the number of measurements obtained within a single ablation line, after statistical treatment with removal of the outliers with JMP statistical software (SAS); the results displayed for each isotope represent the average concentration (in ppm) for the corresponding number of 'rows'. N/A: artefacts non-attributed to a specific obsidian source.

SAMPLE	<i>Nb Rows</i>	⁴⁵ Sc	⁶⁶ Zn	⁸⁵ Rb	⁸⁸ Sr	⁸⁹ Y	⁹⁰ Zr	⁹³ Nb	¹³³ Cs	¹³⁷ Ba	¹⁴⁶ Nd	¹⁴⁷ Sm	²⁰⁸ Pb	²³² Th	²³⁸ U	PROVENANCE
SCU.ARCH.125	50	4.7	85	240	22	31	76	45	3.8	114	22	6.3	31	16	5.3	SA
SCU.ARCH.138	46	4.9	105	238	24	32	75	46	4.0	116	23	6.6	32	16	5.5	SA
SCU.ARCH.141	46	4.5	86	224	20	30	71	41	3.4	91	20	5.9	28	14	4.9	SA
SCU.ARCH.145	53	4.7	85	234	24	31	75	43	3.4	118	22	6.4	29	16	5.2	SA
SCU.ARCH.148	45	4.7	94	219	22	28	66	41	3.2	105	20	5.6	27	14	4.6	SA
SCU.ARCH.165	46	4.8	84	236	25	31	74	44	3.8	119	22	6.4	31	16	5.4	SA
SCU.ARCH.116	49	3.5	47	226	24	17	87	24	6.0	114	21	4.6	22	15	5.1	SB2
SCU.ARCH.117	56	3.5	43	212	43	17	100	24	5.6	251	25	5.3	22	17	4.8	SB2
SCU.ARCH.124	52	3.9	46	226	45	20	112	25	6.1	253	27	5.8	25	19	5.1	SB2
SCU.ARCH.137	50	3.9	59	209	26	19	88	24	5.9	108	22	5.1	22	16	5.2	SB2
SCU.ARCH.139	36	3.9	48	216	23	19	95	24	5.6	109	20	4.7	23	15	5.0	SB2
SCU.ARCH.140	53	3.9	48	211	42	19	105	24	5.3	232	25	5.3	23	17	4.7	SB2
SCU.ARCH.142	53	3.8	49	220	29	19	95	24	5.7	141	22	5.0	23	16	4.9	SB2
SCU.ARCH.143	53	3.9	50	226	28	19	93	24	6.0	124	21	5.1	22	16	5.1	SB2

SAMPLE	<i>Nb Rows</i>	⁴⁵ Sc	⁶⁶ Zn	⁸⁵ Rb	⁸⁸ Sr	⁸⁹ Y	⁹⁰ Zr	⁹³ Nb	¹³³ Cs	¹³⁷ Ba	¹⁴⁶ Nd	¹⁴⁷ Sm	²⁰⁸ Pb	²³² Th	²³⁸ U	PROVENANCE
SCU.ARCH.144	51	3.9	50	225	29	20	95	25	6.3	131	23	5.2	23	17	5.2	SB2
SCU.ARCH.146	50	3.9	50	218	25	19	88	24	5.8	106	20	4.7	22	15	4.8	SB2
SCU.ARCH.147	49	3.9	67	213	27	18	90	23	5.5	121	21	4.8	22	15	4.8	SB2
SCU.ARCH.150	53	3.9	49	207	38	18	101	23	5.4	200	23	5.2	22	16	4.6	SB2
SCU.ARCH.152	52	3.5	44	227	23	18	85	24	6.3	107	21	4.7	22	15	5.2	SB2
SCU.ARCH.153	57	3.4	46	232	22	18	85	24	6.3	95	20	4.7	23	15	5.3	SB2
SCU.ARCH.155	52	3.6	43	221	26	18	89	23	5.9	118	21	4.8	21	15	4.8	SB2
SCU.ARCH.156	51	3.4	45	214	23	16	82	23	5.8	107	19	4.5	21	14	4.8	SB2
SCU.ARCH.157	45	3.4	44	220	24	17	85	23	5.8	108	20	4.5	22	14	4.9	SB2
SCU.ARCH.160	53	3.6	45	212	45	17	104	24	5.5	263	25	5.3	22	16	4.6	SB2
SCU.ARCH.162	48	3.5	47	226	25	18	90	24	6.1	116	20	4.7	22	15	4.9	SB2
SCU.ARCH.163	56	3.5	42	224	26	18	87	24	6.0	119	21	4.7	22	15	4.9	SB2
SCU.ARCH.164	50	3.4	45	225	27	18	88	24	6.1	123	21	4.8	23	15	5.0	SB2
SCU.ARCH.166	54	3.5	45	218	38	17	98	24	5.8	212	23	5.1	23	16	4.8	SB2
SCU.ARCH.167	44	3.5	47	224	26	17	85	23	6.1	119	20	4.5	23	14	4.9	SB2
SCU.ARCH.168	57	3.7	46	213	38	17	98	23	5.7	206	23	5.3	23	16	4.6	SB2
SCU.ARCH.170	41	3.5	47	224	22	17	83	24	6.3	92	19	4.6	23	14	5.1	SB2
SCU.ARCH.175	51	3.5	47	233	26	18	93	25	6.3	119	21	4.9	24	16	5.2	SB2
SCU.ARCH.176	48	3.4	46	229	26	17	87	24	6.2	121	21	4.8	24	16	5.2	SB2
SCU.ARCH.178	44	3.5	54	216	27	18	92	24	5.7	122	21	4.9	23	15	4.9	SB2

SAMPLE	<i>Nb Rows</i>	⁴⁵ Sc	⁶⁶ Zn	⁸⁵ Rb	⁸⁸ Sr	⁸⁹ Y	⁹⁰ Zr	⁹³ Nb	¹³³ Cs	¹³⁷ Ba	¹⁴⁶ Nd	¹⁴⁷ Sm	²⁰⁸ Pb	²³² Th	²³⁸ U	PROVENANCE
SCU.ARCH.179	44	3.4	53	219	23	19	97	24	5.7	100	20	4.8	23	15	4.9	SB2
SCU.ARCH.180	48	3.7	62	220	27	18	92	24	5.7	117	21	4.8	24	15	4.9	SB2
SCU.ARCH.181	55	4.1	68	212	45	19	107	24	5.5	255	26	5.5	25	17	4.7	SB2
SCU.ARCH.185	50	3.7	56	239	28	20	96	26	6.9	122	22	5.3	25	17	5.5	SB2
SCU.ARCH.186	49	3.5	57	222	45	19	111	25	6.2	259	26	5.7	26	19	5.0	SB2
SCU.ARCH.187	52	3.5	59	223	26	18	89	25	6.1	116	21	4.9	25	15	5.1	SB2
SCU.ARCH.188	51	3.7	63	230	28	20	95	25	6.2	126	22	5.1	27	17	5.2	SB2
SCU.ARCH.190	44	3.6	54	231	27	20	99	25	6.5	120	22	5.3	24	17	5.4	SB2
SCU.ARCH.201	51	3.6	64	226	28	19	95	25	6.4	131	23	5.2	31	17	5.3	SB2
SCU.ARCH.204	52	3.3	52	221	26	17	85	25	6.2	115	19	4.6	25	15	5.2	SB2
SCU.ARCH.111	44	3.7	62	154	104	19	196	24	1.6	804	44	8.3	27	20	2.9	SC
SCU.ARCH.112	54	3.6	61	162	96	20	205	24	1.7	841	47	8.7	29	22	3.0	SC
SCU.ARCH.113	55	3.7	64	159	101	20	201	25	1.7	865	47	8.7	29	21	3.0	SC
SCU.ARCH.114	53	3.8	63	163	104	20	208	25	1.7	860	48	8.8	29	23	3.2	SC
SCU.ARCH.115	57	3.9	63	164	102	21	206	26	1.8	844	50	9.3	29	23	3.2	SC
SCU.ARCH.118	51	3.8	62	160	106	20	205	24	1.6	836	48	8.9	28	21	3.0	SC
SCU.ARCH.119	46	3.7	62	158	90	19	195	25	1.7	785	46	8.4	27	21	3.0	SC
SCU.ARCH.120	52	3.7	64	156	100	19	185	25	1.6	789	44	8.4	28	20	3.0	SC
SCU.ARCH.121	47	4.5	78	172	101	22	209	27	2.0	808	51	9.5	32	23	3.5	SC
SCU.ARCH.122	42	4.1	73	166	99	22	224	24	2.0	733	47	9.4	33	23	3.3	SC

SAMPLE	<i>Nb Rows</i>	⁴⁵ Sc	⁶⁶ Zn	⁸⁵ Rb	⁸⁸ Sr	⁸⁹ Y	⁹⁰ Zr	⁹³ Nb	¹³³ Cs	¹³⁷ Ba	¹⁴⁶ Nd	¹⁴⁷ Sm	²⁰⁸ Pb	²³² Th	²³⁸ U	PROVENANCE
SCU.ARCH.123	51	4.7	73	179	111	24	230	28	2.1	902	54	10.2	32	26	3.4	SC
SCU.ARCH.126	44	4.5	75	157	106	21	201	25	1.9	835	48	8.9	31	23	3.3	SC
SCU.ARCH.127	36	4.7	97	160	115	23	214	26	1.9	855	52	9.5	33	24	3.4	SC
SCU.ARCH.128	43	4.5	73	163	115	22	213	25	1.9	885	51	9.5	31	23	3.3	SC
SCU.ARCH.129	51	4.3	77	163	110	21	209	25	1.8	880	50	9.4	31	23	3.1	SC
SCU.ARCH.131	44	4.5	77	159	106	21	206	24	1.7	831	48	9.1	30	22	3.1	SC
SCU.ARCH.132	51	4.3	70	159	106	22	212	25	1.7	821	49	9.2	29	23	3.1	SC
SCU.ARCH.133	51	4.3	67	159	109	22	218	25	1.7	856	50	9.5	30	24	3.1	SC
SCU.ARCH.134	51	4.2	71	160	109	21	217	24	1.7	867	50	9.3	29	23	3.0	SC
SCU.ARCH.135	53	4.2	65	156	105	22	215	24	1.6	829	49	9.3	28	23	3.0	SC
SCU.ARCH.136	51	4.6	68	155	107	22	209	25	1.7	814	48	9.1	28	22	2.9	SC
SCU.ARCH.149	49	4.2	76	157	107	20	202	24	1.6	831	46	8.5	29	21	3.0	SC
SCU.ARCH.151	46	4.3	61	162	102	21	208	25	1.7	871	48	9.0	29	22	3.0	SC
SCU.ARCH.154	51	3.8	62	167	98	21	212	25	1.9	835	48	9.1	30	23	3.2	SC
SCU.ARCH.159	62	3.7	61	159	107	20	208	25	1.8	858	48	9.0	28	22	3.0	SC
SCU.ARCH.161	43	3.7	63	164	100	20	210	25	1.8	791	46	8.8	28	21	3.1	SC
SCU.ARCH.169	48	3.7	72	164	109	22	221	25	1.9	850	49	9.1	31	24	3.3	SC
SCU.ARCH.171	51	3.8	66	161	104	20	198	25	1.8	818	47	8.8	28	21	3.0	SC
SCU.ARCH.172	51	3.9	63	167	101	21	210	26	1.8	834	49	9.3	29	23	3.2	SC
SCU.ARCH.173	53	3.9	65	167	110	22	222	25	1.9	871	50	9.5	29	24	3.2	SC

SAMPLE	<i>Nb Rows</i>	⁴⁵ Sc	⁶⁶ Zn	⁸⁵ Rb	⁸⁸ Sr	⁸⁹ Y	⁹⁰ Zr	⁹³ Nb	¹³³ Cs	¹³⁷ Ba	¹⁴⁶ Nd	¹⁴⁷ Sm	²⁰⁸ Pb	²³² Th	²³⁸ U	PROVENANCE
SCU.ARCH.174	56	3.8	66	164	102	20	207	25	1.7	846	49	9.3	29	22	3.2	SC
SCU.ARCH.177	45	4.1	79	161	87	21	221	25	1.6	767	46	8.6	47	22	3.0	SC
SCU.ARCH.183	47	4.0	67	164	106	22	223	26	1.6	845	49	9.3	30	23	3.1	SC
SCU.ARCH.184	47	4.1	80	173	110	23	230	27	1.7	970	52	9.5	31	24	3.2	SC
SCU.ARCH.189	46	4.0	100	157	143	22	224	26	1.9	796	51	9.7	30	24	3.2	SC
SCU.ARCH.191	49	4.2	80	170	104	22	232	26	2.3	867	50	9.5	33	25	3.6	SC
SCU.ARCH.192	49	3.8	82	158	103	20	209	25	2.2	821	47	8.9	32	23	3.4	SC
SCU.ARCH.193	46	3.9	87	166	111	22	223	26	2.2	895	52	9.8	33	25	3.4	SC
SCU.ARCH.194	41	5.2	124	171	90	24	228	27	2.6	781	51	9.6	38	25	3.6	SC
SCU.ARCH.195	45	3.9	81	170	101	22	229	25	2.3	852	50	9.8	33	24	3.4	SC
SCU.ARCH.197	47	3.8	115	162	91	23	217	25	1.8	785	46	9.0	32	22	3.4	SC
SCU.ARCH.198	50	3.9	77	160	105	22	214	26	1.8	835	49	9.4	32	24	3.3	SC
SCU.ARCH.199	44	4.1	86	160	107	19	204	25	1.9	927	46	8.7	31	22	3.1	SC
SCU.ARCH.200	50	3.9	74	165	106	22	218	26	2.1	855	51	9.6	32	24	3.4	SC
SCU.ARCH.202	45	4.2	94	167	87	23	218	27	2.1	773	47	9.2	34	24	3.4	SC
SCU.ARCH.203	52	4.1	77	172	116	23	233	28	2.1	908	53	10.0	32	26	3.4	SC
SCU.ARCH.205	45	4.0	74	172	115	24	228	28	2.1	910	53	10.2	34	26	3.4	SC
SCU.ARCH.206	56	4.2	81	170	114	23	225	27	2.2	903	53	9.8	35	26	3.5	SC
SCU.ARCH.207	45	4.4	85	170	100	24	229	26	2.2	808	51	10.1	35	26	3.6	SC
SCU.ARCH.208	52	4.0	74	176	113	23	232	27	2.3	919	54	10.2	32	26	3.5	SC

SAMPLE	<i>Nb Rows</i>	⁴⁵ Sc	⁶⁶ Zn	⁸⁵ Rb	⁸⁸ Sr	⁸⁹ Y	⁹⁰ Zr	⁹³ Nb	¹³³ Cs	¹³⁷ Ba	¹⁴⁶ Nd	¹⁴⁷ Sm	²⁰⁸ Pb	²³² Th	²³⁸ U	PROVENANCE
SCU.ARCH.209	50	4.3	73	169	93	23	223	25	1.7	840	49	9.4	31	23	3.2	SC
SCU.ARCH.182	24	3.1	14	134	70	12	100	3	2.3	553	5	1.0	10	11	4.3	N/A
SCU.ARCH.130	52	4.3	57	204	83	19	170	24	5.5	551	32	6.4	24	19	4.4	N/A
SCU.ARCH.158	50	3.7	50	203	74	17	150	23	5.4	503	28	5.7	23	17	4.2	N/A
SCU.ARCH.196	57	4.4	84	204	92	19	188	24	5.4	591	32	6.4	28	18	4.2	N/A

Appendix I1

ED-XRF data obtained on 122 artefacts from the Abri des Castelli. Analyses conducted at the IRAMAT-CRP2A. N/A: artefacts non-attributed to a specific obsidian source. Concentrations are in ppm.

SAMPLE	TiO ₂	MnO	Fe ₂ O ₃	Zn	Ga	Rb	Sr	Y	Zr	Nb	Th	PROVENANCE
CAST.4260	901	657	12523	78	26	252	29	37	84	45	15	SA
CAST.5564	941	694	13474	87	28	268	32	37	73	37	16	SA
CAST.100198	897	672	13591	93	26	277	40	41	76	39	10	SA
CAST.5186	868	663	12497	80	25	254	31	36	74	36	9	SA
CAST.3426	911	672	13136	83	26	262	31	38	87	48	8	SA
CAST.3822	768	588	11496	75	24	233	28	35	78	42	13	SA
CAST.3337	881	647	12476	79	23	246	29	36	67	34	8	SA
CAST.3794	862	639	12252	77	24	245	31	35	73	44	15	SA
CAST.1912	918	690	12911	82	26	267	33	38	94	46	15	SA
CAST.3180	973	714	14099	88	27	286	33	39	82	47	16	SA
CAST.3614	822	590	11889	75	23	237	29	33	70	42	14	SA
CAST.3823	797	632	12352	78	24	246	30	37	81	45	8	SA
CAST.4163	815	641	12773	82	25	271	33	40	86	50	15	SA
CAST.4120	907	724	13895	90	27	315	35	40	107	50	11	SA
CAST.3825	981	745	14258	92	28	288	38	39	89	50	8	SA
CAST.2798	1260	444	13109	50	20	264	37	23	105	36	15	SB2

SAMPLE	TiO ₂	MnO	Fe ₂ O ₃	Zn	Ga	Rb	Sr	Y	Zr	Nb	Th	PROVENANCE
CAST.2941	1173	418	12259	46	20	244	37	21	99	36	7	SB2
CAST.5654	1332	456	13538	53	21	269	39	24	108	37	10	SB2
CAST.3881	1203	383	12517	49	20	260	36	25	103	40	8	SB2
CAST.5692	1364	447	13336	51	22	267	42	22	108	36	16	SB2
CAST.4561	1215	417	12568	49	20	254	36	23	114	37	9	SB2
CAST.4423	1195	435	11865	45	16	238	36	22	95	35	7	SB2
CAST.5605	1294	421	13090	48	20	248	45	21	96	34	15	SB2
CAST.4830	1493	398	13176	51	21	249	52	22	111	35	17	SB2
CAST.5169	1190	423	12974	52	20	255	37	21	99	35	15	SB2
CAST.4430	1181	405	11964	49	21	252	38	21	98	35	16	SB2
CAST.5545	1386	382	12548	46	19	234	51	22	116	35	8	SB2
CAST.100197	1578	396	13298	50	21	247	57	24	117	37	6	SB2
CAST.4174	1353	470	13369	49	20	260	38	22	116	35	10	SB2
CAST.4504	1326	503	14084	52	21	277	43	25	116	38	10	SB2
CAST.5124	1108	413	12121	46	18	244	32	22	93	34	15	SB2
CAST.4525	1212	403	12485	49	20	244	41	21	94	26	7	SB2
CAST.1339	1513	412	13355	49	20	248	51	22	112	35	9	SB2
CAST.4983	1120	419	12437	48	19	251	31	21	96	35	10	SB2
CAST.2235	1338	438	13773	52	20	266	40	23	112	37	17	SB2
CAST.2432	1584	383	13354	47	18	243	59	22	116	34	16	SB2

SAMPLE	TiO ₂	MnO	Fe ₂ O ₃	Zn	Ga	Rb	Sr	Y	Zr	Nb	Th	PROVENANCE
CAST.3261	1143	412	12510	50	21	273	35	23	104	38	9	SB2
CAST.3015	1248	403	12611	49	20	249	38	20	107	35	15	SB2
CAST.4785	1240	415	12778	48	21	252	36	22	110	34	16	SB2
CAST.4015	1163	406	12094	47	20	249	33	22	112	35	9	SB2
CAST.3958	1128	388	11946	47	19	240	33	22	95	34	9	SB2
CAST.3017	1260	426	12745	49	19	248	39	22	101	36	9	SB2
CAST.5246	1337	375	12091	45	18	236	47	23	105	34	15	SB2
CAST.5676	1233	409	12465	46	20	251	39	20	99	34	9	SB2
CAST.5374	1216	412	12222	47	20	248	37	21	96	34	16	SB2
CAST.4832	1251	406	12916	51	22	274	37	22	96	26	17	SB2
CAST.5518	1244	450	13256	51	21	264	37	24	104	38	10	SB2
CAST.2240	3378	385	16445	61	23	177	147	28	216	37	11	SC
CAST.3253	3860	419	18651	68	25	195	169	28	239	39	19	SC
CAST.1846	3694	416	18314	68	23	211	178	30	260	42	20	SC
CAST.2668	3506	372	16673	64	23	186	157	28	236	39	11	SC
CAST.2111	3474	420	17095	63	23	186	153	25	215	36	19	SC
CAST.1741	3789	397	17816	65	24	198	164	27	244	38	19	SC
CAST.3260	3700	441	18481	65	22	186	162	26	228	36	19	SC
CAST.1548	3443	399	16652	58	22	169	153	24	213	35	11	SC
CAST.1697	3439	396	17228	62	23	180	145	25	220	34	17	SC

SAMPLE	TiO ₂	MnO	Fe ₂ O ₃	Zn	Ga	Rb	Sr	Y	Zr	Nb	Th	PROVENANCE
CAST.3014	4218	400	18514	60	21	171	187	25	238	35	10	SC
CAST.2704	3678	385	17592	61	21	187	155	26	230	37	18	SC
CAST.2375	3746	395	17793	64	24	190	164	28	237	36	18	SC
CAST.3001	3436	411	17260	65	23	185	148	27	230	38	12	SC
CAST.2935	3293	392	15945	58	21	170	140	23	203	33	17	SC
CAST.3313	3395	400	16718	62	22	183	144	25	223	37	19	SC
CAST.2725	3462	353	16272	60	22	194	155	26	230	37	18	SC
CAST.1404	3498	418	17481	62	21	179	155	26	227	37	11	SC
CAST.2397	3390	427	16870	63	22	182	157	24	221	35	17	SC
CAST.3431	3465	374	16919	64	24	188	150	26	240	36	18	SC
CAST.3457	3299	409	16764	61	22	185	147	26	225	35	17	SC
CAST.2675	4362	403	18517	65	23	179	193	25	240	35	18	SC
CAST.2513	3427	402	17031	64	22	179	147	26	218	34	19	SC
CAST.3202	3434	384	16479	61	22	190	160	28	243	39	19	SC
CAST.3182	3497	374	16171	62	22	176	150	25	213	36	18	SC
CAST.2475	3380	360	16248	58	22	184	155	25	227	35	17	SC
CAST.2240	3386	388	16171	64	22	176	144	26	212	36	17	SC
CAST.2532	3753	389	18190	66	26	203	168	27	246	39	20	SC
CAST.3197	3590	385	17444	63	23	180	174	28	236	39	7	SC
CAST.3461	3674	423	17899	63	22	190	162	26	235	36	20	SC

SAMPLE	TiO ₂	MnO	Fe ₂ O ₃	Zn	Ga	Rb	Sr	Y	Zr	Nb	Th	PROVENANCE
CAST.S.313	3803	427	17861	65	23	189	162	27	233	37	19	SC
CAST.2407	3702	436	18348	67	25	190	159	26	232	37	13	SC
CAST.3425	3637	374	16935	62	23	179	154	23	216	35	18	SC
CAST.4344	3397	406	16971	65	24	180	149	26	223	37	19	SC
CAST.5140	3346	391	16411	59	22	168	145	24	205	33	11	SC
CAST.5422	3422	401	16712	58	21	174	165	26	221	35	17	SC
CAST.4258	3317	360	16138	59	20	169	141	24	208	33	16	SC
CAST.4116	3540	370	16470	59	23	176	150	24	213	33	18	SC
CAST.4162	3379	382	16516	60	21	177	146	25	214	35	18	SC
CAST.5322	3912	380	17646	58	20	163	178	23	218	33	17	SC
CAST.3872	3469	393	16987	60	22	182	157	26	227	36	19	SC
CAST.4575	3369	359	15954	56	20	164	140	23	195	32	16	SC
CAST.3424	3430	395	16921	62	22	181	153	27	225	36	19	SC
CAST.3009	3338	341	15909	57	19	168	145	24	214	34	10	SC
CAST.5012	3572	437	17847	64	24	190	159	29	236	39	12	SC
CAST.100194	3222	367	16218	59	21	171	142	24	213	34	17	SC
CAST.4098	3198	377	15002	63	22	171	137	25	196	34	12	SC
CAST.2047	3207	383	15780	63	23	178	139	26	207	35	17	SC
CAST.1911	3692	398	16766	59	22	174	156	24	216	34	11	SC
CAST.100216	3564	426	18061	65	23	186	155	26	231	38	11	SC

SAMPLE	TiO ₂	MnO	Fe ₂ O ₃	Zn	Ga	Rb	Sr	Y	Zr	Nb	Th	PROVENANCE
CAST.3355	3434	352	16123	58	22	174	144	25	213	34	17	SC
CAST.2464	3179	404	15733	58	20	168	138	24	204	33	17	SC
CAST.2118	3399	412	16556	62	22	176	157	25	226	36	11	SC
CAST.1057	3277	373	16423	60	21	176	145	25	219	35	18	SC
CAST.100217	3377	368	16298	58	21	164	148	25	212	35	17	SC
CAST.5604	3429	371	15922	56	20	170	150	26	213	34	17	SC
CAST.1904	3360	374	16811	62	24	214	157	27	234	37	20	SC
CAST.1434	3784	437	18300	69	24	207	173	27	243	39	20	SC
CAST.4096	3667	433	17734	63	22	190	159	25	229	36	19	SC
CAST.1211	3505	397	17481	61	23	182	156	26	230	36	12	SC
CAST.2624	3644	398	17476	63	23	175	154	24	214	34	19	SC
CAST.1567	3599	389	17038	62	24	177	154	23	211	33	17	SC
CAST.3002	3394	377	16247	60	21	171	144	22	197	34	11	SC
CAST.2640	3759	417	17968	61	22	172	176	25	219	38	10	SC
CAST.3456	3678	379	17987	65	23	191	163	27	233	36	19	SC
CAST.2623	3644	477	17886	63	22	179	160	26	224	35	12	SC
CAST.1968	3451	401	17141	62	21	178	151	26	222	36	12	SC
CAST.1227	3682	393	18051	67	24	193	157	28	234	37	20	SC
CAST.1700	2922	403	17186	51	21	237	125	21	195	36	9	N/A
CAST.2271	2060	527	16254	72	24	252	93	28	147	39	17	N/A

SAMPLE	TiO ₂	MnO	Fe ₂ O ₃	Zn	Ga	Rb	Sr	Y	Zr	Nb	Th	PROVENANCE
CAST.2582	1853	480	15049	66	22	236	84	26	131	37	16	N/A
CAST.4175	1553	676	15364	61	22	304	41	29	122	45	11	N/A
CAST.5626	2357	363	14795	47	20	226	101	22	168	36	8	N/A
CAST.4991	1773	460	14682	52	23	270	66	25	135	38	18	N/A
CAST.100147	1814	482	14622	64	21	237	91	26	133	39	16	N/A
CAST.2654	2574	297	14646	45	18	212	112	22	180	33	9	N/A

Appendix I2

LA-ICP-MS data obtained on 344 artefacts of the Abri des Castelli. Analyses conducted at the SOLARIS laboratory (Southern Cross University). N/A: artefacts non-attributed to a specific obsidian source. Concentrations are in ppm.

SAMPLE	⁴⁵ Sc	⁶⁶ Zn	⁸⁵ Rb	⁸⁸ Sr	⁸⁹ Y	⁹⁰ Zr	⁹³ Nb	¹³³ Cs	¹³⁷ Ba	¹⁴⁶ Nd	¹⁴⁷ Sm	²⁰⁸ Pb	²³² Th	²³⁸ U	PROVENANCE
CAST.1267	4.3	88	245	24	32	78	45	3.9	116	23	6.7	31	17	5.4	SA
CAST.3181	4.6	87	258	23	33	77	45	4.0	111	23	6.7	33	17	5.6	SA
CAST.3003	4.7	86	270	24	31	73	44	3.9	112	22	6.2	31	16	5.4	SA
CAST.2990	4.6	77	236	25	32	75	44	3.9	120	23	6.5	30	16	5.4	SA
CAST.2372	4.6	87	379	25	31	73	44	3.9	120	23	6.4	34	17	5.6	SA
CAST.2318	4.5	84	244	24	32	76	46	3.9	119	23	6.5	31	16	5.5	SA
CAST.3475	4.5	85	247	24	32	77	45	4.1	121	23	6.6	33	17	5.6	SA
CAST.4505	4.4	87	240	22	32	76	44	4.0	101	21	6.0	32	16	5.5	SA
CAST.3422	4.5	78	237	21	31	75	44	3.8	99	21	6.3	30	16	5.5	SA
CAST.3423	4.2	87	241	24	31	75	44	4.0	102	21	6.0	32	16	5.5	SA
CAST.3455	4.5	87	240	22	31	74	44	3.9	108	22	6.3	32	16	5.5	SA
CAST.3409	4.3	81	238	22	32	77	44	4.0	100	22	6.2	32	16	5.5	SA
CAST.5026	4.4	85	239	24	31	74	44	3.9	116	23	6.3	32	16	5.5	SA
CAST.3473	4.6	82	237	25	32	76	44	3.9	120	23	6.3	32	17	5.6	SA
CAST.3468	4.6	81	237	24	32	77	45	3.8	116	22	6.4	30	16	5.4	SA
CAST.3466	4.5	83	241	22	32	76	44	3.9	111	23	6.4	31	16	5.4	SA

SAMPLE	⁴⁵ Sc	⁶⁶ Zn	⁸⁵ Rb	⁸⁸ Sr	⁸⁹ Y	⁹⁰ Zr	⁹³ Nb	¹³³ Cs	¹³⁷ Ba	¹⁴⁶ Nd	¹⁴⁷ Sm	²⁰⁸ Pb	²³² Th	²³⁸ U	PROVENANCE
CAST.3467	4.5	78	239	24	32	77	45	3.9	118	23	6.6	30	16	5.5	SA
CAST.1115	4.5	84	229	23	31	74	44	3.8	116	22	6.3	30	16	5.3	SA
CAST.1940	4.6	84	236	24	31	75	44	3.8	117	22	6.4	31	16	5.4	SA
CAST.1941	4.4	84	236	24	31	74	44	3.8	119	22	6.3	31	16	5.4	SA
CAST.1380	4.6	120	238	32	31	72	44	4.0	118	21	6.0	33	17	5.8	SA
CAST.1719	4.4	89	239	24	31	74	45	4.0	113	22	6.2	33	17	5.6	SA
CAST.3419	4.3	88	242	24	32	77	45	4.1	105	22	6.4	31	16	5.5	SA
CAST.1243	4.7	86	240	23	32	76	44	3.9	112	23	6.5	32	16	5.5	SA
CAST.3459	4.6	82	239	24	31	74	43	3.8	113	22	6.3	31	17	5.4	SA
CAST.3414	4.7	85	244	22	31	74	44	3.9	111	23	6.6	32	16	5.3	SA
CAST.3447	4.9	80	235	23	31	74	45	3.8	115	22	6.4	31	16	5.5	SA
CAST.1844	4.7	82	235	24	31	75	44	3.9	118	22	6.5	31	16	5.4	SA
CAST.3465	4.6	87	236	22	32	75	44	3.8	106	22	6.3	31	16	5.4	SA
CAST.3439	4.7	86	246	24	33	77	45	4.1	116	23	6.4	32	16	5.5	SA
CAST.3404	4.7	89	237	22	32	76	45	3.8	103	22	6.3	31	16	5.4	SA
CAST.3407	4.6	83	240	20	32	77	45	4.1	91	23	6.5	30	17	5.5	SA
CAST.3420	5.2	82	243	22	32	76	44	3.9	118	23	6.7	32	17	5.7	SA
CAST.2595	4.8	86	258	25	34	81	46	4.1	123	24	7.0	34	17	5.7	SA
CAST.1382	4.8	82	239	28	32	78	45	3.9	125	22	6.4	32	16	5.5	SA
CAST.1439	4.8	86	248	23	33	79	46	4.1	111	24	6.8	33	17	5.6	SA

SAMPLE	⁴⁵ Sc	⁶⁶ Zn	⁸⁵ Rb	⁸⁸ Sr	⁸⁹ Y	⁹⁰ Zr	⁹³ Nb	¹³³ Cs	¹³⁷ Ba	¹⁴⁶ Nd	¹⁴⁷ Sm	²⁰⁸ Pb	²³² Th	²³⁸ U	PROVENANCE
CAST.1433	4.9	89	247	22	29	68	42	4.8	114	21	5.9	35	18	6.1	SA
CAST.1558	4.9	87	233	21	32	76	44	3.8	109	22	6.2	31	16	5.4	SA
CAST.1613	5.0	85	245	21	32	76	44	4.0	105	22	6.5	31	16	5.4	SA
CAST.3427	5.2	98	232	23	32	73	44	3.9	117	22	6.3	35	18	6.3	SA
CAST.4152	4.4	81	239	23	31	75	44	3.9	109	23	6.4	30	16	5.4	SA
CAST.4595	4.6	86	234	24	31	73	44	3.8	115	22	6.3	31	16	5.4	SA
CAST.4600	4.6	79	243	24	31	72	44	3.8	116	22	6.2	30	16	5.4	SA
CAST.4718	4.3	79	237	24	31	73	43	4.0	121	21	5.9	32	15	5.5	SA
CAST.3719	4.7	91	245	26	32	77	45	4.0	117	23	6.6	34	17	5.8	SA
CAST.3928	4.5	91	239	25	31	74	45	3.7	120	22	6.4	30	17	5.5	SA
CAST.3960	5.2	81	235	24	32	75	44	3.8	114	24	6.7	32	17	5.6	SA
CAST.4724	4.5	84	247	24	33	79	46	4.0	115	24	6.8	33	17	5.7	SA
CAST.4583	4.7	82	322	24	31	75	45	4.1	121	23	6.6	33	16	5.5	SA
CAST.4953	4.7	74	242	25	33	77	45	3.9	119	23	6.4	30	16	5.6	SA
CAST.4165	4.8	89	246	25	32	76	45	4.0	119	23	6.3	32	16	5.4	SA
CAST.100147	3.7	68	232	71	23	146	32	3.6	420	32	7.3	30	21	4.9	SB1
CAST.2271	3.8	77	227	71	24	137	32	3.5	394	32	7.4	30	20	4.7	SB1
CAST.2582	4.0	68	227	71	24	140	32	3.5	406	33	7.5	31	21	4.8	SB1
CAST.3408	4.0	76	230	68	23	136	33	3.6	390	31	7.0	33	20	5.0	SB1
CAST.3347	4.2	49	226	36	19	101	25	6.0	190	24	5.3	25	18	5.2	SB2

SAMPLE	⁴⁵ Sc	⁶⁶ Zn	⁸⁵ Rb	⁸⁸ Sr	⁸⁹ Y	⁹⁰ Zr	⁹³ Nb	¹³³ Cs	¹³⁷ Ba	¹⁴⁶ Nd	¹⁴⁷ Sm	²⁰⁸ Pb	²³² Th	²³⁸ U	PROVENANCE
CAST.3186	4.2	46	234	27	20	100	25	6.6	124	23	5.2	25	18	5.6	SB2
CAST.4457	3.6	53	245	28	20	98	25	6.6	125	23	5.2	26	18	5.6	SB2
CAST.5185	3.5	52	237	26	20	98	26	6.7	119	23	5.3	26	18	5.7	SB2
CAST.2332	3.6	53	246	30	20	96	26	6.6	119	22	5.1	25	18	5.6	SB2
CAST.4175	3.6	59	228	30	19	95	25	6.5	133	22	5.2	27	17	5.6	SB2
CAST.4991	3.6	47	219	47	19	118	25	6.1	268	28	5.8	25	19	5.2	SB2
CAST.3183	4.4	47	233	26	19	95	25	6.5	120	22	5.1	25	17	5.5	SB2
CAST.3062	4.3	46	277	30	19	95	25	6.5	132	23	5.2	24	17	5.5	SB2
CAST.3324	4.0	45	231	26	20	97	25	6.4	119	22	5.1	25	18	5.7	SB2
CAST.3006	3.7	54	236	27	20	98	26	6.6	124	22	5.3	28	18	5.9	SB2
CAST.2395	3.7	49	231	30	19	95	25	6.5	144	22	5.1	26	17	5.6	SB2
CAST.2297	3.6	48	227	41	19	108	25	6.4	224	25	5.5	26	18	5.3	SB2
CAST.3007	3.7	48	224	43	19	107	24	6.1	245	27	5.7	26	19	5.2	SB2
CAST.2607	3.4	50	222	25	17	87	24	6.3	114	20	4.6	25	16	5.3	SB2
CAST.1859	3.5	54	235	24	20	98	25	6.7	104	21	5.0	25	17	5.7	SB2
CAST.3469	3.7	48	223	42	20	111	25	6.2	236	26	5.4	25	19	5.3	SB2
CAST.5701	3.6	50	228	28	19	94	25	6.5	129	22	5.2	26	17	5.5	SB2
CAST.4245	3.6	47	231	28	20	97	25	6.5	129	23	5.1	25	17	5.5	SB2
CAST.4244	3.5	49	216	29	19	92	24	6.2	131	21	4.8	25	16	5.3	SB2
CAST.4247	3.6	48	232	37	19	102	24	6.4	194	25	5.5	26	18	5.4	SB2

SAMPLE	⁴⁵ Sc	⁶⁶ Zn	⁸⁵ Rb	⁸⁸ Sr	⁸⁹ Y	⁹⁰ Zr	⁹³ Nb	¹³³ Cs	¹³⁷ Ba	¹⁴⁶ Nd	¹⁴⁷ Sm	²⁰⁸ Pb	²³² Th	²³⁸ U	PROVENANCE
CAST.4456	3.5	48	230	26	19	97	25	6.3	120	22	4.9	25	17	5.5	SB2
CAST.4453	3.5	50	234	27	19	95	25	6.6	126	22	5.1	26	17	5.5	SB2
CAST.4239	3.6	48	231	26	20	98	25	6.7	120	23	5.2	26	18	5.5	SB2
CAST.4156	3.7	46	232	30	20	100	25	6.4	135	23	5.3	24	18	5.5	SB2
CAST.3460	3.8	49	228	44	20	114	25	6.2	251	27	5.6	26	19	5.1	SB2
CAST.3410	3.7	46	229	44	20	112	25	6.3	247	27	5.5	26	19	5.4	SB2
CAST.3196	3.6	51	223	47	19	111	25	6.1	270	26	5.7	26	19	5.1	SB2
CAST.3472	3.8	50	216	46	19	113	25	5.9	269	27	5.9	24	19	5.1	SB2
CAST.3471	3.7	54	231	24	20	92	25	6.6	104	21	4.8	26	17	5.7	SB2
CAST.3474	3.7	47	223	41	19	109	25	6.0	238	27	5.7	25	19	5.2	SB2
CAST.3476	3.8	58	223	47	19	113	25	6.2	277	27	5.7	27	20	5.3	SB2
CAST.1279	3.8	44	238	40	19	109	24	6.0	218	26	5.6	24	19	5.0	SB2
CAST.3413	3.8	47	234	28	20	98	25	6.5	127	23	5.1	25	18	5.4	SB2
CAST.3412	3.8	50	231	28	20	94	25	6.5	121	22	4.9	25	17	5.5	SB2
CAST.3463	3.9	48	237	29	20	97	26	6.7	132	22	5.3	25	17	5.5	SB2
CAST.3464	3.9	48	235	28	20	101	26	6.7	127	22	5.3	25	18	5.7	SB2
CAST.3438	3.6	48	220	50	18	94	24	6.1	194	20	4.6	26	16	5.2	SB2
CAST.3441	3.8	48	256	30	20	100	26	6.7	134	23	5.5	25	18	5.7	SB2
CAST.3462	5.3	47	235	26	20	100	26	6.8	121	23	5.2	26	18	5.6	SB2
CAST.2529	4.4	46	228	27	20	95	25	6.6	129	23	5.4	26	18	5.7	SB2

SAMPLE	⁴⁵ Sc	⁶⁶ Zn	⁸⁵ Rb	⁸⁸ Sr	⁸⁹ Y	⁹⁰ Zr	⁹³ Nb	¹³³ Cs	¹³⁷ Ba	¹⁴⁶ Nd	¹⁴⁷ Sm	²⁰⁸ Pb	²³² Th	²³⁸ U	PROVENANCE
CAST.1405	4.1	50	232	42	20	110	25	6.5	227	27	5.8	27	20	5.6	SB2
CAST.3012	4.0	48	242	28	21	102	26	6.8	128	24	5.4	27	18	5.7	SB2
CAST.3008	4.1	50	243	27	21	99	26	6.7	119	23	5.3	26	18	5.6	SB2
CAST.1492	4.1	47	230	48	20	117	25	6.2	276	28	6.0	27	20	5.4	SB2
CAST.3428	4.2	48	226	40	19	107	25	6.1	224	25	5.5	26	18	5.3	SB2
CAST.3886	3.7	54	219	26	18	86	24	6.2	119	20	4.8	27	16	5.6	SB2
CAST.4082	3.9	47	230	28	20	96	25	6.3	129	23	5.1	25	17	5.6	SB2
CAST.4151	3.9	48	223	48	20	115	25	6.1	277	28	5.8	26	20	5.2	SB2
CAST.4153	3.6	46	222	27	19	92	25	6.3	122	21	5.0	22	16	5.3	SB2
CAST.4343	3.7	56	218	25	19	88	25	6.1	116	21	4.8	25	16	5.5	SB2
CAST.4369	3.7	46	228	28	20	98	25	6.5	128	23	5.2	23	17	5.5	SB2
CAST.4389	3.7	51	243	27	19	96	25	6.4	123	22	5.1	26	17	5.5	SB2
CAST.4390	3.6	51	295	26	19	95	25	6.3	122	22	5.2	26	17	5.5	SB2
CAST.4440	3.7	51	234	27	20	100	26	6.7	127	22	5.2	26	17	5.4	SB2
CAST.4506	3.9	53	227	29	19	95	25	6.5	134	22	5.1	26	17	5.5	SB2
CAST.4569	3.7	49	219	45	18	111	25	6.0	260	26	5.7	24	18	5.1	SB2
CAST.4570	3.7	45	228	28	20	96	25	6.4	125	22	5.2	24	17	5.3	SB2
CAST.4571	3.8	49	209	38	18	101	24	5.8	209	24	5.3	23	17	5.1	SB2
CAST.4572	3.6	47	227	27	19	93	25	6.4	124	21	5.0	25	16	5.2	SB2
CAST.4955	3.8	45	227	26	20	98	25	6.5	121	22	5.2	24	17	5.4	SB2

SAMPLE	⁴⁵ Sc	⁶⁶ Zn	⁸⁵ Rb	⁸⁸ Sr	⁸⁹ Y	⁹⁰ Zr	⁹³ Nb	¹³³ Cs	¹³⁷ Ba	¹⁴⁶ Nd	¹⁴⁷ Sm	²⁰⁸ Pb	²³² Th	²³⁸ U	PROVENANCE
CAST.5454	3.7	44	224	27	19	94	24	6.3	122	21	4.9	24	17	5.5	SB2
CAST.5658	3.8	48	222	36	19	102	25	6.0	193	25	5.6	25	18	5.4	SB2
CAST.7164	3.7	56	229	27	20	99	25	6.6	126	23	5.3	24	17	5.6	SB2
CAST.7165	3.8	54	229	28	20	98	25	6.5	125	22	5.3	24	17	5.6	SB2
CAST.7166	3.9	57	230	29	19	93	26	6.6	134	23	5.1	26	18	5.9	SB2
CAST.4173	4.0	55	228	29	20	96	25	6.6	130	23	5.5	27	18	5.7	SB2
CAST.4397	3.8	44	238	39	20	107	25	6.3	207	26	5.7	25	19	5.5	SB2
CAST.4404	3.8	53	253	28	20	100	26	6.6	135	24	5.5	26	18	6.2	SB2
CAST.4420	4.1	57	231	52	20	118	26	6.4	297	29	6.2	29	21	5.8	SB2
CAST.4429	3.7	49	249	30	20	102	26	6.7	142	24	5.4	26	18	5.8	SB2
CAST.4639	3.7	45	226	42	20	112	25	6.1	238	26	5.7	26	20	5.5	SB2
CAST.4687	3.8	50	226	39	19	104	25	6.1	207	24	5.5	25	18	5.3	SB2
CAST.4721	3.8	132	228	29	20	96	25	6.5	123	22	5.2	27	18	5.7	SB2
CAST.4726	3.7	51	238	26	20	96	26	6.7	107	21	5.1	27	17	5.7	SB2
CAST.4933	3.8	46	226	38	20	106	25	6.2	202	26	5.7	26	19	5.5	SB2
CAST.4992	3.7	48	226	40	19	102	25	6.4	205	25	5.7	25	18	5.3	SB2
CAST.5283	4.0	45	229	29	20	99	25	6.6	132	24	5.4	26	19	5.8	SB2
CAST.5331	3.7	48	227	28	20	100	24	6.5	110	22	5.0	26	18	5.7	SB2
CAST.5653	4.3	58	228	27	20	96	25	6.5	126	23	5.4	26	18	5.6	SB2
CAST.5655	4.8	53	218	28	19	95	25	6.1	126	22	5.1	25	17	5.5	SB2

SAMPLE	⁴⁵ Sc	⁶⁶ Zn	⁸⁵ Rb	⁸⁸ Sr	⁸⁹ Y	⁹⁰ Zr	⁹³ Nb	¹³³ Cs	¹³⁷ Ba	¹⁴⁶ Nd	¹⁴⁷ Sm	²⁰⁸ Pb	²³² Th	²³⁸ U	PROVENANCE
CAST.5657	4.9	50	237	29	21	98	25	6.7	130	23	5.2	28	18	5.9	SB2
CAST.5670	3.6	55	228	28	19	97	25	6.4	121	22	5.1	25	17	5.5	SB2
CAST.7161	3.6	51	229	29	20	99	25	6.5	128	23	5.4	25	19	5.8	SB2
CAST.7163	3.7	52	233	28	20	101	26	6.7	125	23	5.4	26	18	5.7	SB2
CAST.4720	3.9	45	236	30	20	99	26	6.6	136	24	5.5	26	18	5.7	SB2
CAST.4232	4.0	46	226	27	19	94	25	6.4	126	22	5.2	26	17	5.4	SB2
CAST.4233	4.0	49	234	28	20	97	25	6.5	127	23	5.3	26	17	5.6	SB2
CAST.4234	4.1	59	248	29	20	98	26	6.7	132	23	5.4	26	18	5.7	SB2
CAST.4375	3.9	45	234	27	20	96	25	6.5	122	23	5.3	25	17	5.5	SB2
CAST.4400	3.9	47	234	26	20	100	26	6.6	115	22	5.3	25	18	5.6	SB2
CAST.4447	4.0	48	236	27	21	98	26	6.6	120	22	5.2	25	17	5.5	SB2
CAST.4606	3.8	44	237	27	20	98	26	6.7	125	23	5.4	25	17	5.6	SB2
CAST.4719	3.9	50	244	27	21	103	26	6.9	121	22	5.3	26	18	5.7	SB2
CAST.4722	3.9	47	245	27	21	95	26	6.9	114	22	5.3	25	17	5.7	SB2
CAST.4723	3.9	49	238	26	21	104	26	6.8	119	23	5.5	26	18	5.8	SB2
CAST.4725	3.8	45	237	27	21	96	26	6.7	116	22	5.5	25	17	5.8	SB2
CAST.4727	3.6	50	232	25	19	94	25	6.5	113	21	4.9	25	16	5.4	SB2
CAST.4728	3.7	46	240	27	21	100	26	6.8	125	23	5.4	26	18	5.8	SB2
CAST.4729	3.8	53	240	23	21	102	26	6.8	99	23	5.4	27	18	5.8	SB2
CAST.4833	3.8	48	244	29	20	100	27	6.8	133	23	5.4	25	17	5.6	SB2

SAMPLE	⁴⁵ Sc	⁶⁶ Zn	⁸⁵ Rb	⁸⁸ Sr	⁸⁹ Y	⁹⁰ Zr	⁹³ Nb	¹³³ Cs	¹³⁷ Ba	¹⁴⁶ Nd	¹⁴⁷ Sm	²⁰⁸ Pb	²³² Th	²³⁸ U	PROVENANCE
CAST.4886	3.8	50	241	28	20	100	26	6.9	128	23	5.3	25	17	5.6	SB2
CAST.4947	4.0	42	223	48	20	117	26	6.2	280	29	6.2	25	20	5.2	SB2
CAST.4948	3.7	43	233	30	20	98	25	6.6	125	22	5.2	25	17	5.6	SB2
CAST.4951	3.9	46	230	27	19	95	25	6.4	125	23	5.2	25	17	5.5	SB2
CAST.4952	3.8	50	225	47	19	109	26	6.3	242	26	5.6	26	18	5.3	SB2
CAST.4954	3.9	42	242	27	20	104	26	6.9	124	23	5.3	25	18	5.7	SB2
CAST.4987	4.1	45	234	33	20	100	25	6.5	161	24	5.5	25	18	5.4	SB2
CAST.4988	3.8	45	228	27	19	94	25	6.4	123	22	5.1	25	17	5.4	SB2
CAST.4989	3.8	46	227	48	20	116	25	6.1	274	28	6.0	25	20	5.2	SB2
CAST.5702	3.7	53	236	26	20	98	25	6.7	118	23	5.4	25	17	5.7	SB2
CAST.4238	4.3	46	222	27	19	95	25	6.4	127	22	5.1	25	17	5.4	SB2
CAST.4236	4.3	45	238	27	20	98	25	6.6	126	23	5.2	25	18	5.5	SB2
CAST.4342	4.2	52	239	28	19	97	26	6.7	127	22	5.0	27	17	5.4	SB2
CAST.4341	4.2	46	235	27	19	97	25	6.7	125	22	5.2	25	17	5.3	SB2
CAST.4340	4.0	44	239	27	21	102	26	6.6	126	24	5.3	25	18	5.6	SB2
CAST.4237	3.9	48	237	24	20	101	26	6.9	111	23	5.2	25	17	5.4	SB2
CAST.4154	4.7	47	221	27	20	97	25	6.3	123	22	5.0	24	17	5.3	SB2
CAST.4164	4.2	69	224	45	20	115	26	6.2	255	27	5.7	26	19	5.2	SB2
CAST.4829	4.0	56	239	28	20	101	25	6.7	128	23	5.3	26	17	5.5	SB2
CAST.4503	4.0	45	238	27	20	101	26	6.8	126	23	5.2	24	17	5.5	SB2

SAMPLE	⁴⁵ Sc	⁶⁶ Zn	⁸⁵ Rb	⁸⁸ Sr	⁸⁹ Y	⁹⁰ Zr	⁹³ Nb	¹³³ Cs	¹³⁷ Ba	¹⁴⁶ Nd	¹⁴⁷ Sm	²⁰⁸ Pb	²³² Th	²³⁸ U	PROVENANCE
CAST.5263	4.1	43	229	27	20	98	25	6.4	130	23	5.5	23	17	5.5	SB2
CAST.4990	4.4	56	233	38	20	107	26	6.5	205	26	5.8	25	19	5.4	SB2
CAST.5694	4.2	48	228	27	19	96	25	6.6	127	23	5.1	24	17	5.5	SB2
CAST.5539	4.2	51	225	27	20	96	25	6.3	122	22	5.1	24	17	5.3	SB2
CAST.4949	4.1	49	235	28	20	97	25	6.6	131	23	5.4	25	17	5.5	SB2
CAST.7162	4.6	45	227	26	20	100	25	6.6	119	23	5.2	25	17	5.4	SB2
CAST.5604	4.2	56	240	28	20	99	25	6.9	132	23	5.4	25	18	5.5	SB2
CAST.5540	4.1	51	226	26	20	93	25	6.4	109	21	4.9	23	16	5.2	SB2
CAST.5602	4.0	48	235	27	20	98	25	6.6	114	23	5.3	25	17	5.4	SB2
CAST.5603	4.0	46	228	31	19	97	25	6.5	148	23	5.3	25	17	5.4	SB2
CAST.5543	3.8	46	232	26	19	95	25	6.8	119	21	5.0	24	17	5.2	SB2
CAST.5517	4.0	44	235	27	20	101	25	6.7	126	23	5.1	24	17	5.4	SB2
CAST.5544	4.0	46	244	29	21	100	26	6.9	134	23	5.4	25	18	5.5	SB2
CAST.4374	4.6	45	228	25	19	97	24	6.4	117	22	5.0	24	17	5.3	SB2
CAST.4161	4.6	47	219	26	19	92	24	6.3	124	22	4.9	24	16	5.1	SB2
CAST.4168	4.6	48	232	27	20	93	25	6.6	120	22	5.2	26	17	5.4	SB2
CAST.3016	4.8	68	171	109	23	235	26	2.0	886	52	9.7	32	26	3.4	SC
CAST.2622	4.4	70	172	117	23	238	27	2.1	926	54	9.9	33	27	3.6	SC
CAST.1509	4.1	72	188	111	22	232	26	2.0	979	51	10.0	34	25	3.4	SC
CAST.1539	4.2	75	174	128	23	236	28	2.0	962	55	10.3	34	27	3.5	SC

SAMPLE	⁴⁵ Sc	⁶⁶ Zn	⁸⁵ Rb	⁸⁸ Sr	⁸⁹ Y	⁹⁰ Zr	⁹³ Nb	¹³³ Cs	¹³⁷ Ba	¹⁴⁶ Nd	¹⁴⁷ Sm	²⁰⁸ Pb	²³² Th	²³⁸ U	PROVENANCE
CAST.3450	4.4	71	177	119	24	232	28	2.1	922	56	10.7	33	27	3.7	SC
CAST.2374	4.1	66	178	135	22	247	27	2.1	1019	53	10.0	35	26	3.5	SC
CAST.1557	3.9	74	178	101	23	234	26	2.0	932	52	9.9	34	26	3.4	SC
CAST.3454	3.8	70	182	104	22	223	26	2.1	884	50	9.5	32	24	3.5	SC
CAST.2043	4.0	72	202	120	23	220	29	2.0	866	52	9.8	35	26	3.6	SC
CAST.1426	4.0	93	177	123	23	234	27	2.2	927	53	9.7	36	26	3.6	SC
CAST.2819	3.9	72	171	116	23	241	26	1.9	929	53	10.1	32	26	3.5	SC
CAST.2159	3.8	71	167	108	22	222	27	1.9	803	51	9.4	31	25	3.4	SC
CAST.2485	3.7	73	178	103	22	233	26	2.1	928	51	9.5	35	26	3.5	SC
CAST.3371	4.1	68	173	116	24	227	28	2.0	880	54	10.2	33	26	3.4	SC
CAST.2484	3.7	69	173	97	22	231	26	2.0	851	51	9.5	33	25	3.3	SC
CAST.1873	4.3	79	172	150	23	252	26	2.0	1058	55	10.0	33	26	3.3	SC
CAST.3418	3.8	81	181	71	21	225	26	2.0	683	44	8.6	31	23	3.3	SC
CAST.3185	4.6	65	164	116	22	221	26	1.9	903	51	9.5	31	25	3.4	SC
CAST.3021	4.4	63	168	109	21	228	25	1.9	910	52	9.9	32	25	3.4	SC
CAST.3178	4.3	63	167	112	21	213	26	2.0	869	51	9.7	33	24	3.4	SC
CAST.3300	4.4	82	171	103	22	227	26	2.1	861	52	9.9	35	26	3.7	SC
CAST.2044	4.3	71	169	110	22	213	27	2.0	849	52	9.8	32	25	3.4	SC
CAST.3179	4.1	58	179	96	22	232	25	2.0	905	51	9.6	33	25	3.4	SC
CAST.3213	4.1	63	169	104	23	230	26	1.9	882	51	9.6	32	26	3.3	SC

SAMPLE	⁴⁵ Sc	⁶⁶ Zn	⁸⁵ Rb	⁸⁸ Sr	⁸⁹ Y	⁹⁰ Zr	⁹³ Nb	¹³³ Cs	¹³⁷ Ba	¹⁴⁶ Nd	¹⁴⁷ Sm	²⁰⁸ Pb	²³² Th	²³⁸ U	PROVENANCE
CAST.3011	3.9	65	172	100	21	211	26	2.0	816	49	9.2	33	24	3.4	SC
CAST.3417	4.1	68	173	104	23	230	27	2.0	885	53	10.1	33	26	3.6	SC
CAST.3193	4.1	67	172	117	23	226	27	2.0	914	53	9.9	33	26	3.5	SC
CAST.3211	4.7	72	178	120	23	219	29	2.3	932	52	10.0	33	26	3.7	SC
CAST.3215	4.1	68	171	102	23	234	27	2.1	881	52	9.7	33	26	3.6	SC
CAST.3210	4.1	65	176	121	23	238	27	2.1	944	54	10.2	34	27	3.6	SC
CAST.3214	4.2	67	182	136	23	234	28	2.1	981	56	10.4	32	26	3.4	SC
CAST.3346	3.9	64	169	110	23	231	26	1.9	907	52	9.9	32	26	3.5	SC
CAST.2373	3.8	67	177	107	23	237	27	2.0	900	51	9.5	32	26	3.5	SC
CAST.3354	4.0	68	174	100	23	227	27	2.1	894	52	10.0	33	25	3.5	SC
CAST.3013	4.3	70	168	129	23	226	27	2.0	924	53	9.9	32	26	3.5	SC
CAST.3421	3.9	66	170	100	22	221	26	2.0	886	51	9.5	33	25	3.3	SC
CAST.3458	4.0	82	299	114	22	221	25	2.0	851	48	9.3	33	25	3.6	SC
CAST.2026	3.8	63	165	108	21	228	25	1.9	888	50	9.3	31	25	3.3	SC
CAST.2376	3.9	66	222	99	22	227	25	2.0	857	48	9.3	31	25	3.4	SC
CAST.2371	4.0	73	169	97	22	202	28	2.2	774	48	9.3	33	25	3.6	SC
CAST.2331	4.0	64	171	117	23	240	26	2.0	953	53	10.0	32	26	3.5	SC
CAST.2893	4.0	68	169	111	22	226	26	2.0	884	52	10.0	33	25	3.5	SC
CAST.4235	4.1	76	170	117	22	230	26	2.0	883	52	9.9	34	25	3.5	SC
CAST.4243	4.4	78	173	110	24	227	28	2.4	884	53	9.8	39	28	4.7	SC

SAMPLE	⁴⁵ Sc	⁶⁶ Zn	⁸⁵ Rb	⁸⁸ Sr	⁸⁹ Y	⁹⁰ Zr	⁹³ Nb	¹³³ Cs	¹³⁷ Ba	¹⁴⁶ Nd	¹⁴⁷ Sm	²⁰⁸ Pb	²³² Th	²³⁸ U	PROVENANCE
CAST.3416	4.2	65	176	121	23	240	26	2.1	947	54	9.9	32	26	3.4	SC
CAST.3453	4.0	69	179	106	23	236	26	2.0	942	49	9.5	33	24	3.4	SC
CAST.3411	4.0	71	184	96	22	244	26	2.2	830	51	9.4	34	26	3.8	SC
CAST.3452	4.5	94	178	100	23	230	27	2.2	961	50	9.5	38	27	3.8	SC
CAST.3451	4.1	74	173	119	23	236	27	2.1	952	54	10.0	34	27	3.6	SC
CAST.3429	4.0	71	173	104	23	236	27	2.0	892	51	9.6	32	25	3.7	SC
CAST.3449	4.2	68	177	119	23	237	27	2.1	940	54	10.2	33	26	3.5	SC
CAST.1364	3.9	67	178	90	23	243	26	2.1	815	50	9.6	32	25	3.5	SC
CAST.3432	3.9	67	176	104	23	230	27	2.1	899	51	9.7	34	25	3.4	SC
CAST.3405	4.2	75	174	83	21	232	27	2.1	819	46	8.9	30	23	3.3	SC
CAST.1146	4.0	67	162	94	22	225	26	1.9	813	48	9.1	31	25	3.4	SC
CAST.3434	4.0	67	167	117	23	225	27	1.9	905	52	9.8	32	25	3.4	SC
CAST.3435	4.1	69	169	115	22	223	27	2.0	894	52	9.8	32	25	3.3	SC
CAST.3436	4.0	70	174	116	22	233	26	2.0	940	52	9.8	33	25	3.4	SC
CAST.1985	4.1	68	168	103	22	234	27	2.0	897	51	9.6	33	26	3.5	SC
CAST.1742	4.0	68	173	120	22	236	26	2.1	944	52	9.8	32	26	3.5	SC
CAST.1266	4.3	66	174	124	24	234	27	2.0	939	55	10.4	32	26	3.4	SC
CAST.1277	4.1	69	171	111	22	225	26	2.1	871	50	9.5	32	25	3.4	SC
CAST.1278	4.3	74	179	108	23	223	27	2.1	890	52	9.9	34	26	3.4	SC
CAST.1331	4.1	63	174	104	23	232	26	2.0	908	50	9.5	32	25	3.3	SC

SAMPLE	⁴⁵ Sc	⁶⁶ Zn	⁸⁵ Rb	⁸⁸ Sr	⁸⁹ Y	⁹⁰ Zr	⁹³ Nb	¹³³ Cs	¹³⁷ Ba	¹⁴⁶ Nd	¹⁴⁷ Sm	²⁰⁸ Pb	²³² Th	²³⁸ U	PROVENANCE
CAST.1288	4.0	66	163	105	22	220	25	1.9	863	49	9.2	32	24	3.2	SC
CAST.1369	4.2	67	170	107	22	223	26	2.1	893	51	9.7	34	25	3.3	SC
CAST.1368	4.1	66	173	99	23	224	26	2.0	847	51	9.7	32	25	3.3	SC
CAST.3415	4.0	69	163	95	22	218	26	1.9	805	48	9.2	32	24	3.3	SC
CAST.3437	4.8	74	165	177	22	242	26	1.9	1042	51	9.5	31	24	3.2	SC
CAST.2185	4.2	62	175	71	23	245	25	2.2	667	50	9.3	30	25	3.6	SC
CAST.1143	4.4	64	170	116	23	233	27	2.0	928	53	10.0	32	25	3.4	SC
CAST.1758	4.3	67	176	107	23	227	27	2.0	863	53	9.8	32	25	3.4	SC
CAST.3440	4.2	72	201	97	23	232	27	2.0	821	50	9.6	32	25	3.6	SC
CAST.3444	4.0	69	170	101	23	233	26	2.0	858	49	9.1	32	25	3.5	SC
CAST.3443	4.3	74	188	122	24	244	28	2.0	948	54	10.3	32	27	3.5	SC
CAST.3442	4.0	66	177	97	23	246	27	2.0	861	51	9.7	32	26	3.5	SC
CAST.3446	4.6	76	174	157	23	243	28	2.1	972	53	10.1	34	25	3.5	SC
CAST.3445	4.1	66	178	107	24	239	27	2.1	856	49	9.4	33	25	3.4	SC
CAST.3433	4.1	68	172	115	23	233	26	2.0	895	52	9.9	32	25	3.4	SC
CAST.3430	4.1	76	174	103	22	226	25	2.2	859	49	9.4	36	26	3.8	SC
CAST.2488	5.6	72	164	104	21	229	26	2.0	894	49	9.5	32	24	3.3	SC
CAST.2909	5.2	61	170	119	22	229	27	2.1	937	53	9.9	34	26	3.5	SC
CAST.2255	4.9	60	171	87	22	237	25	2.0	798	48	9.1	33	25	3.6	SC
CAST.2126	5.1	66	168	119	22	236	26	2.0	902	52	9.7	33	25	3.5	SC

SAMPLE	⁴⁵ Sc	⁶⁶ Zn	⁸⁵ Rb	⁸⁸ Sr	⁸⁹ Y	⁹⁰ Zr	⁹³ Nb	¹³³ Cs	¹³⁷ Ba	¹⁴⁶ Nd	¹⁴⁷ Sm	²⁰⁸ Pb	²³² Th	²³⁸ U	PROVENANCE
CAST.2207	5.1	64	173	113	23	235	26	2.1	941	54	10.2	35	27	3.6	SC
CAST.2208	4.8	69	171	102	22	220	26	2.1	851	50	9.4	34	25	3.6	SC
CAST.2481	5.0	64	164	136	22	236	26	1.9	982	53	10.3	33	26	3.4	SC
CAST.2517	5.1	72	172	105	23	212	28	2.2	878	53	10.1	35	26	3.7	SC
CAST.2522	4.8	65	176	108	24	240	26	2.1	953	56	10.5	35	28	3.7	SC
CAST.2724	4.3	64	188	92	23	237	26	2.0	826	50	9.6	34	25	3.6	SC
CAST.2721	4.4	61	175	122	24	245	26	2.0	997	58	10.7	33	27	3.6	SC
CAST.2664	4.5	64	171	119	23	235	27	2.0	956	54	10.3	33	26	3.5	SC
CAST.2659	4.2	64	178	99	24	245	26	2.1	899	53	10.0	34	26	3.6	SC
CAST.2639	4.3	66	178	105	23	246	26	2.1	894	53	9.9	35	26	3.8	SC
CAST.3010	4.7	77	179	137	24	248	29	2.1	1032	56	10.6	36	27	3.5	SC
CAST.2535	4.4	68	180	118	24	233	29	2.2	940	57	11.0	34	26	3.6	SC
CAST.1387	4.4	72	182	119	24	246	27	2.2	986	55	10.4	35	27	3.6	SC
CAST.1432	4.4	66	174	119	22	235	26	2.0	951	54	10.3	32	26	3.4	SC
CAST.1493	4.6	70	174	115	24	238	28	2.1	948	55	10.4	34	27	3.6	SC
CAST.1478	4.4	64	175	121	23	236	27	2.0	953	55	10.3	33	27	3.4	SC
CAST.3448	4.6	67	167	107	23	217	27	2.0	852	52	9.7	32	26	3.5	SC
CAST.4257	4.0	69	167	99	22	233	25	2.1	836	50	9.4	33	24	3.5	SC
CAST.4573	4.0	73	168	97	22	228	26	2.1	857	51	9.7	32	25	3.4	SC
CAST.5407	4.0	64	163	102	22	202	27	2.0	781	50	9.5	30	23	3.4	SC

SAMPLE	⁴⁵ Sc	⁶⁶ Zn	⁸⁵ Rb	⁸⁸ Sr	⁸⁹ Y	⁹⁰ Zr	⁹³ Nb	¹³³ Cs	¹³⁷ Ba	¹⁴⁶ Nd	¹⁴⁷ Sm	²⁰⁸ Pb	²³² Th	²³⁸ U	PROVENANCE
CAST.5541	4.4	69	164	147	23	232	26	1.9	967	53	9.6	29	24	3.3	SC
CAST.100213	4.2	67	268	117	23	237	26	2.0	932	53	10.0	32	26	3.5	SC
CAST.100225	4.6	72	170	91	22	223	27	2.0	838	51	9.7	33	25	3.5	SC
CAST.3723	4.0	67	173	114	24	241	27	2.0	917	55	10.4	33	27	3.5	SC
CAST.3813	3.9	69	171	91	22	240	25	2.1	799	50	9.8	33	25	3.5	SC
CAST.3815	4.1	68	170	123	23	241	27	2.0	960	55	10.2	32	27	3.4	SC
CAST.3873	4.5	68	165	112	23	218	27	2.0	865	53	9.9	32	26	3.5	SC
CAST.3874	4.5	65	169	112	22	236	25	2.0	924	54	10.0	33	27	3.5	SC
CAST.3877	4.3	83	242	92	23	237	26	2.1	837	53	10.1	34	27	3.7	SC
CAST.3959	4.1	67	169	111	22	236	26	2.0	921	52	9.6	33	26	3.5	SC
CAST.4127	4.2	68	177	119	25	227	29	2.1	885	55	10.7	34	27	3.7	SC
CAST.4203	4.1	69	170	117	23	232	27	1.9	922	53	10.2	32	26	3.5	SC
CAST.4463	4.2	72	181	104	24	237	28	2.1	885	53	10.2	33	26	3.8	SC
CAST.5233	4.0	67	171	104	23	243	26	1.9	859	54	10.2	31	26	3.4	SC
CAST.5625	5.0	69	173	100	23	229	27	2.1	877	52	9.9	35	26	3.7	SC
CAST.5656	4.1	66	171	119	24	243	26	2.0	964	56	10.4	33	27	3.5	SC
CAST.100196	4.1	62	168	106	23	216	28	2.0	831	51	9.7	32	25	3.5	SC
CAST.100212	4.0	65	165	87	22	225	25	2.0	765	46	9.1	30	23	3.3	SC
CAST.3974	4.0	59	185	85	23	237	26	2.1	799	50	9.6	32	25	3.5	SC
CAST.4822	4.1	68	177	120	23	239	27	2.0	907	53	10.0	33	26	3.5	SC

SAMPLE	⁴⁵ Sc	⁶⁶ Zn	⁸⁵ Rb	⁸⁸ Sr	⁸⁹ Y	⁹⁰ Zr	⁹³ Nb	¹³³ Cs	¹³⁷ Ba	¹⁴⁶ Nd	¹⁴⁷ Sm	²⁰⁸ Pb	²³² Th	²³⁸ U	PROVENANCE
CAST.4946	4.3	66	169	110	22	225	26	2.0	857	52	9.9	32	25	3.4	SC
CAST.5406	4.2	69	182	107	24	237	28	2.2	880	53	10.1	33	26	3.5	SC
CAST.5433	4.4	64	170	107	23	238	26	2.0	932	54	10.1	33	26	3.4	SC
CAST.4167	4.6	59	192	108	22	234	25	2.0	873	49	9.6	32	25	3.4	SC
CAST.4246	4.6	70	172	113	23	230	27	2.0	998	53	9.9	32	25	3.3	SC
CAST.5393	4.4	63	176	132	23	240	27	2.0	968	54	9.9	33	26	3.3	SC
CAST.5659	4.4	70	168	106	22	226	26	2.0	860	49	9.1	31	24	3.3	SC
CAST.5390	4.4	66	170	96	21	214	26	2.0	834	48	9.1	31	23	3.3	SC
CAST.5542	4.4	74	168	117	23	233	26	2.0	934	53	9.8	31	25	3.3	SC
CAST.3838	4.9	65	166	101	22	231	25	1.9	888	50	9.5	31	24	3.3	SC
CAST.4157	4.8	61	167	100	23	232	25	2.1	853	51	9.6	32	25	3.4	SC
CAST.4166	4.8	65	165	114	21	222	26	1.9	900	50	9.4	32	24	3.2	SC
CAST.2430	4.4	73	226	91	20	171	24	5.9	551	33	6.6	30	21	4.7	N/A
CAST.1165	4.2	66	230	90	21	179	25	5.9	577	34	6.9	28	22	4.8	N/A
CAST.2820	4.6	64	223	94	21	220	24	5.7	641	37	7.2	28	21	4.5	N/A
CAST.1375	4.5	89	222	103	20	171	25	6.1	567	34	6.5	33	22	5.0	N/A
CAST.3184	4.8	59	213	109	19	214	24	5.6	697	34	6.7	26	19	4.4	N/A
CAST.2913	4.4	57	230	89	21	179	25	6.0	572	34	6.9	28	22	4.8	N/A
CAST.1700	4.7	60	220	99	20	201	25	5.9	644	35	6.9	28	22	4.9	N/A
CAST.5626	4.4	57	212	83	19	166	23	5.7	539	33	6.6	27	21	4.8	N/A

SAMPLE	⁴⁵ Sc	⁶⁶ Zn	⁸⁵ Rb	⁸⁸ Sr	⁸⁹ Y	⁹⁰ Zr	⁹³ Nb	¹³³ Cs	¹³⁷ Ba	¹⁴⁶ Nd	¹⁴⁷ Sm	²⁰⁸ Pb	²³² Th	²³⁸ U	PROVENANCE
CAST.2654	4.6	62	220	93	20	186	25	5.9	603	34	6.8	27	21	4.8	N/A
CAST.1328	4.5	59	216	81	19	164	23	5.8	544	32	6.2	27	20	4.6	N/A
CAST.3406	4.6	64	217	85	19	179	24	5.8	600	34	6.7	28	22	4.9	N/A
CAST.2206	4.5	63	221	81	20	173	25	6.0	556	32	6.5	28	21	4.9	N/A
CAST.S.0314	4.4	66	217	84	20	172	24	5.9	556	33	6.7	27	21	4.6	N/A
CAST.2925	4.4	56	210	81	19	169	23	5.5	528	32	6.5	26	21	4.7	N/A
CAST.3814	4.6	64	226	87	21	182	26	6.0	582	35	6.8	29	22	5.0	N/A
CAST.3975	4.6	62	230	87	21	180	26	6.2	584	34	6.6	28	22	5.0	N/A

Appendix J1

ED-XRF data obtained on 122 artefacts from A Guaita. Analyses conducted at the IRAMAT-CRP2A. Concentrations are in ppm.

SAMPLE	MEASUREMENTS	TiO ₂	MnO	Fe ₂ O ₃	Zn	Ga	Rb	Sr	Y	Zr	PROVENANCE
AG06-2b-403	3	903	706	13651	88	27	278	33	41	83	SA
AG08-2a-155	3	805	704	13137	81	27	267	35	39	84	SA
AG08-2a-232	3	929	709	13987	87	28	277	34	41	91	SA
AG08-2b-145	3	875	693	13420	86	26	278	33	40	84	SA
AG08-2b-187	3	915	679	13585	84	26	274	34	40	103	SA
AG08-2b-196	3	847	656	12901	80	25	262	32	37	92	SA
AG09-1-6	6	846	675	13104	86	27	275	34	41	84	SA
AG09-1-9b	3	857	670	13204	82	25	268	34	37	92	SA
AG09-2a-129	3	882	688	13636	84	27	277	34	41	92	SA
AG09-2a-53	3	928	709	14233	88	27	287	36	40	90	SA
AG10-2a-94	1	1044	771	15245	95	27	303	41	43	93	SA
AG10-C1-7	2	1108	757	15719	98	30	310	46	44	98	SA
AG11-2a-12b	1	1062	796	16037	101	32	324	48	47	100	SA
AG11-2b-242	1	878	730	14065	87	27	279	36	40	91	SA
AG12-2a-124	3	960	714	14142	88	26	280	33	42	85	SA
AG12-2a-136	3	871	672	13498	84	25	272	33	39	80	SA
AG12-2a-81	3	919	711	13884	88	27	281	36	41	87	SA

SAMPLE	MEASUREMENTS	TiO ₂	MnO	Fe ₂ O ₃	Zn	Ga	Rb	Sr	Y	Zr	PROVENANCE
AG12-2b-92	3	964	742	14525	93	28	289	36	40	90	SA
AG12-3-37a	1	978	793	15155	98	31	294	42	41	88	SA
AG13-2b-116	4	966	738	14542	91	28	284	35	40	88	SA
AG13-2b-13	2	865	666	13238	87	28	265	35	36	78	SA
AG13-2b-35	1	785	620	12518	79	24	255	31	37	81	SA
AG13-2b-35bis	2	857	631	12674	80	26	266	34	42	80	SA
AG13-2b-36	4	947	691	13530	84	26	269	33	39	96	SA
AG13-2b-37	1	815	689	13504	85	28	273	34	38	88	SA
AG13-2b-40	2	875	717	14098	89	28	274	34	39	85	SA
AG13-2b-68a	2	922	688	13511	87	26	268	33	40	82	SA
AG13-2b-74	3	904	702	13821	88	28	273	34	39	84	SA
AG13-3-105	4	927	689	13614	85	27	273	34	39	87	SA
AG13-3-109	3	940	697	14246	89	28	282	35	39	88	SA
AG13-3-126	3	860	646	13122	82	26	256	33	34	75	SA
AG13-3-175	2	810	655	12774	83	27	264	36	38	86	SA
AG13-3-49	3	860	677	13286	85	28	267	33	38	86	SA
AG13-3-84	3	927	695	13827	86	27	274	35	39	94	SA
AG13-3-V6remplissage-a	2	845	685	13367	88	26	280	35	40	89	SA
AG13-3-V6remplissage-b	1	832	650	12606	81	25	262	32	40	89	SA
AG08-2a-106	1	1114	398	12387	46	19	237	39	19	95	SB2

SAMPLE	MEASUREMENTS	TiO ₂	MnO	Fe ₂ O ₃	Zn	Ga	Rb	Sr	Y	Zr	PROVENANCE
AG08-2a-153	3	1369	445	13971	51	21	268	42	23	105	SB2
AG08-2b-127a	2	1397	449	14207	52	21	270	51	19	95	SB2
AG08-2b-127b	2	1228	444	14072	52	20	249	48	16	86	SB2
AG08-2b-148	3	1313	436	13680	55	21	277	43	23	110	SB2
AG09-1-9a	3	1208	426	13019	50	20	259	36	21	105	SB2
AG09-2a-114	3	1206	425	13278	51	20	274	40	23	106	SB2
AG09-2a-138	3	1226	428	13296	50	20	257	41	21	96	SB2
AG09-2a-tamisage99/100	3	1580	422	14622	53	21	273	54	25	122	SB2
AG09-2b-57	3	1427	467	14984	56	22	297	44	25	123	SB2
AG09-2b-5b	2	1780	479	15270	55	22	288	53	26	117	SB2
AG09-2b-71	3	1670	441	15052	56	23	283	64	25	134	SB2
AG11-2b-106	2	1227	433	13160	50	20	266	43	23	108	SB2
AG11-2b-256	2	1580	411	13636	50	20	253	58	22	110	SB2
AG12-2a-13	1	1660	515	15256	60	24	300	52	25	119	SB2
AG12-2a-3	4	1730	483	15304	57	22	293	45	26	117	SB2
AG12-2a-39	3	1488	412	13457	48	19	244	55	21	112	SB2
AG12-2a-96a	2	1226	430	13395	51	21	268	39	25	108	SB2
AG12-2a-96b	1	1289	455	13674	53	21	283	43	24	113	SB2
AG12-2b-77b	1	1125	389	12306	47	18	224	43	16	81	SB2
AG12-3-33	4	1717	433	14665	60	22	284	70	25	132	SB2

SAMPLE	MEASUREMENTS	TiO ₂	MnO	Fe ₂ O ₃	Zn	Ga	Rb	Sr	Y	Zr	PROVENANCE
AG12-3-37b	1	1362	468	14372	56	22	279	49	22	107	SB2
AG12-3-58	2	1360	441	14021	55	23	277	44	23	112	SB2
AG13-2a-5	4	1580	441	14318	53	21	267	55	24	120	SB2
AG13-2a-6	3	1291	449	13369	51	21	265	39	23	106	SB2
AG13-2b-11	3	1194	405	12920	49	20	261	38	23	104	SB2
AG13-2b-115	2	1581	403	13608	52	21	257	61	24	122	SB2
AG13-2b-22	4	1344	452	14242	56	23	282	43	24	112	SB2
AG13-2b-39	2	1417	454	13947	52	21	268	39	23	104	SB2
AG13-2b-50	2	1155	417	13157	48	21	251	40	19	97	SB2
AG13-2b-54	3	1347	431	13606	52	22	259	46	23	113	SB2
AG13-2b-68b	2	1457	418	13277	49	21	250	57	21	109	SB2
AG13-2b-8	2	1136	434	13714	54	24	283	44	24	113	SB2
AG13-2b-88	3	1292	412	13285	51	21	261	40	23	104	SB2
AG13-2b-tamis bande 3-4a	3	1184	410	12816	48	19	256	37	20	96	SB2
AG13-2b-tamis Z4a	2	1231	409	12905	51	20	256	40	22	100	SB2
AG13-2b-vidance foyer carre B3	2	1344	451	13599	51	20	262	39	24	108	SB2
AG13-3-123	2	1144	429	13325	51	21	266	40	21	102	SB2
AG13-3-124	2	1653	450	15435	57	23	294	69	26	137	SB2
AG13-3-154	2	1194	404	12463	47	20	237	41	20	95	SB2
AG13-3-16	1	1189	428	13659	52	22	272	42	22	111	SB2

SAMPLE	MEASUREMENTS	TiO ₂	MnO	Fe ₂ O ₃	Zn	Ga	Rb	Sr	Y	Zr	PROVENANCE
AG13-3-23(Z100)	2	1600	418	14229	51	21	268	62	23	121	SB2
AG13-3-23a(V7)	1	1283	462	14415	51	19	252	44	19	93	SB2
AG13-3-36	1	1226	438	13110	51	22	257	41	19	103	SB2
AG13-3-73	2	1175	407	12761	50	20	253	37	23	105	SB2
AG13-3-78	4	1872	499	16002	59	23	277	68	23	127	SB2
AG13-3-7b	2	1209	425	12659	47	19	255	43	24	113	SB2
AG13-3-7c	4	1383	437	13611	51	21	267	44	24	116	SB2
AG13-3-tamisage Z1/Z2a	2	1471	402	13581	48	21	253	65	22	115	SB2
AG13-3-tamisage Z1/Z2b	1	1138	395	12518	48	19	251	38	22	98	SB2
AG08-2a-194	3	3522	421	18476	66	24	195	162	27	233	SC
AG08-2a-210	2	3758	403	18420	64	24	190	179	28	251	SC
AG08-2b-195	3	3358	395	17511	64	22	193	155	28	229	SC
AG09-2a-83	3	3610	430	18923	66	24	193	167	28	234	SC
AG09-2b-5a	3	4300	435	20202	73	25	202	187	30	244	SC
AG09-2b-67	3	3997	404	19261	66	23	195	187	28	244	SC
AG10-2a-19	2	3632	415	18434	67	23	187	169	24	221	SC
AG10-2a-52	3	3932	401	19572	72	24	203	189	27	250	SC
AG10-2a-63	2	3846	427	18748	69	24	199	177	29	242	SC
AG10-2b-139	2	4385	435	20852	70	23	187	201	26	228	SC
AG10-2b-142	2	4106	445	20209	75	25	204	189	29	249	SC

SAMPLE	MEASUREMENTS	TiO ₂	MnO	Fe ₂ O ₃	Zn	Ga	Rb	Sr	Y	Zr	PROVENANCE
AG10-2b-97	2	3717	414	19914	70	24	190	178	28	227	SC
AG10-tamisage-W4	4	3732	437	19259	70	24	198	177	26	235	SC
AG11-2b-129	4	3609	391	17804	65	23	181	163	25	226	SC
AG11-2b-22	3	3701	393	18015	64	22	182	172	26	229	SC
AG11-2b-302	3	3793	450	19384	72	24	201	168	29	239	SC
AG11-2b-42	2	3629	405	17685	64	23	180	174	24	217	SC
AG11-2b-81	2	3734	412	18224	65	24	190	169	27	233	SC
AG12-2a-126	4	3533	418	18129	66	23	193	160	28	236	SC
AG12-2a-14	3	4032	443	20241	70	25	216	195	31	274	SC
AG12-2a-175	2	4241	469	20800	72	24	194	182	28	237	SC
AG12-2a-209	3	3740	437	18858	68	23	197	176	27	240	SC
AG12-2a-61	1	3623	413	18275	68	24	204	183	27	247	SC
AG12-2a-8	2	3978	453	19623	68	24	194	172	27	232	SC
AG12-2a-tamisagecarreU8a	2	3552	428	18542	67	22	192	162	27	230	SC
AG12-2a-tamisagecarreU8b	3	4220	449	20659	72	24	190	195	28	242	SC
AG12-2a-tamisV6	4	3561	410	17966	65	22	190	164	28	232	SC
AG12-2b-116	4	3494	409	17461	64	22	183	155	26	223	SC
AG12-2b-142	3	3468	402	17159	63	23	178	151	24	215	SC
AG12-2b-145	4	4027	472	20230	74	25	204	186	30	258	SC
AG12-2b-15	4	3944	451	19479	70	24	195	172	28	243	SC

SAMPLE	MEASUREMENTS	TiO ₂	MnO	Fe ₂ O ₃	Zn	Ga	Rb	Sr	Y	Zr	PROVENANCE
AG12-2b-153	4	3564	412	18413	67	22	185	171	27	231	SC
AG12-2b-77a	3	3312	394	16731	62	22	177	146	24	200	SC
AG12-2b-tamisageU6	3	4568	490	22054	78	24	203	214	27	249	SC
AG12-3-16	4	3680	417	18305	67	23	196	169	28	243	SC
AG12-3-31	3	4085	451	19594	70	23	192	181	27	239	SC
AG12-3-73	3	3622	428	18117	65	22	192	171	28	235	SC
AG12-3-79	4	3929	441	19854	71	25	197	187	28	267	SC
AG13-2a-3	4	3718	422	18308	63	21	184	167	27	236	SC
AG13-2a-42	3	3506	413	17777	63	23	183	159	25	222	SC
AG13-2a-68	4	3763	417	18460	68	24	185	161	25	224	SC
AG13-2a-81	1	3594	476	17185	64	24	190	159	27	228	SC
AG13-2b-124	3	3660	441	18502	65	23	186	166	25	226	SC
AG13-2b-20	3	3440	407	17725	65	23	187	156	26	227	SC
AG13-2b-23	4	3408	401	17770	64	22	181	166	25	227	SC
AG13-2b-39'	3	3535	399	17415	63	22	173	152	22	197	SC
AG13-2b-tamis bande 3-4b	4	3623	430	18071	68	24	193	161	28	238	SC
AG13-2b-tamis Z4c	2	3377	384	17341	66	23	181	158	24	216	SC
AG13-3-117	4	3388	432	18192	67	24	199	166	28	243	SC
AG13-3-120	3	3739	526	18769	65	23	193	171	26	237	SC
AG13-3-139	4	3359	405	17884	64	23	189	162	27	237	SC

SAMPLE	MEASUREMENTS	TiO ₂	MnO	Fe ₂ O ₃	Zn	Ga	Rb	Sr	Y	Zr	PROVENANCE
AG13-3-139bis	1	3552	417	18462	67	24	189	166	28	237	SC
AG13-3-152	3	3431	410	17842	65	22	173	152	21	194	SC
AG13-3-155	4	3637	411	18274	66	22	188	171	26	233	SC
AG13-3-165	4	4677	509	22009	75	26	207	190	31	262	SC
AG13-3-179	4	3900	430	20149	71	25	196	177	27	247	SC
AG13-3-2	2	3550	372	17276	63	24	186	160	26	226	SC
AG13-3-23b(V7)	3	3353	388	16800	59	21	174	158	25	214	SC
AG13-3-28'a	2	3616	440	18458	68	24	191	163	26	220	SC
AG13-3-28'b	3	3810	399	17968	63	22	171	176	24	205	SC
AG13-3-28'c	4	3573	416	17736	67	23	199	167	30	238	SC
AG13-3-29	4	3367	384	17149	62	22	185	159	27	226	SC
AG13-3-37	3	3954	422	19237	65	24	192	183	28	245	SC
AG13-3-42	4	3498	403	17816	64	24	183	170	27	234	SC
AG13-3-5	2	3482	431	18609	68	25	195	160	27	242	SC
AG13-3-55	3	3580	400	17891	68	23	191	160	25	220	SC
AG13-3-7a	2	3389	412	17088	65	22	190	162	29	232	SC
AG13-3-98	2	4208	520	21307	75	26	216	194	30	273	SC
AG-2a-12a	2	3577	412	17383	72	23	184	159	26	216	SC

Appendix J2

LA-ICP-MS data obtained on 6 artefacts of A Guaita. Analyses conducted at the SOLARIS laboratory (Southern Cross University). Number of rows [Nb rows] indicates the number of measurements obtained within a single ablation line, after statistical treatment with removal of the outliers with JMP statistical software (SAS); the results displayed for each isotope represent the average concentrations (in ppm) for the corresponding number of 'rows'. N/A: artefacts non-attributed to a specific obsidian source.

SAMPLE	<i>Nb Rows</i>	⁴⁵ Sc	⁶⁶ Zn	⁸⁵ Rb	⁸⁸ Sr	⁸⁹ Y	⁹⁰ Zr	⁹³ Nb	¹³³ Cs	¹³⁷ Ba	¹⁴⁶ Nd	¹⁴⁷ Sm	²⁰⁸ Pb	²³² Th	²³⁸ U	PROVENANCE
AG10-2b-131	57	2.6	64	263	14	36	150	29	14	14	35	7.2	29	46	14	Lipari
AG12-2b-14	65	2.5	58	279	15	38	160	31	15	14	38	7.7	32	50	15	Lipari
AG09-2b-22	57	2.6	57	280	15	39	162	31	15	15	37	7.6	30	50	15	Lipari
AG13-3-150	55	5.1	98	230	20	30	73	41	4	90	21	6.1	31	16	5.3	SA
AG12-2a-63	62	4.7	60	215	82	19	166	24	6	558	32	6.4	26	20	4.7	N/A
AG13-2b-tamis Z4b	58	4.8	60	212	78	19	159	23	6	517	31	6.2	27	20	4.9	N/A

